



**OPTIMUM DESIGN OF STRUCTURES WITH  
STABILITY CONSTRAINTS USING THE  
EVOLUTIONARY OPTIMISATION METHOD**



by

**Dhayanthi Manickarajah, BSc, MEngSc**

**A thesis submitted in fulfilment of the requirements for the Degree of  
DOCTOR OF PHILOSOPHY**

**Faculty Engineering and Science  
Victoria University of Technology  
Melbourne, Victoria 8001, Australia**

**March 1998**



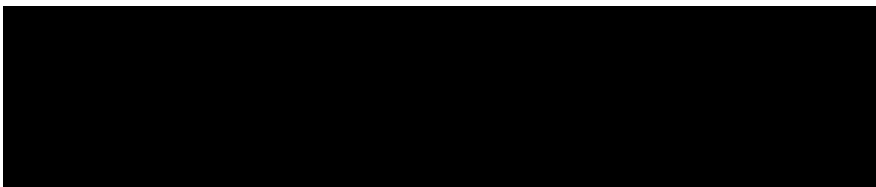
FTS THESIS  
624.17713 MAN  
30001006465613  
Manickarajah. Dhayanthi.  
1963-  
Optimum design of structures  
with stability constraints

## DECLARATION

This thesis does not contain any material, which has been previously submitted for a degree or diploma at any university. Except where due reference is made in the text, the work described in this thesis is the result of the candidate's own investigations.



Candidate



Supervisor

## **ACKNOWLEDGEMENTS**

I sincerely thank Professor Mike Xie for the supervision that he provided throughout this dissertation. His advice on technical matters, constant encouragement and motivation, ready accessibility and constructive criticism are greatly acknowledged. He made every effort to ensure that I was provided with excellent equipment and a comfortable working environment. In addition, Mike encouraged me to attend conferences and to publish our findings in international journals and sought all possible avenues to further my knowledge. Also Mike's keen interest in the topic, Evolutionary Structural Optimisation gave me inspiration to accomplish in the area of research covered.

I am also grateful to the Faculty of Engineering, Victoria University of Technology and in particular to the former Dean of Faculty of Engineering, Professor Ian Johnson for the Dean's Research Scholarship that I received, providing financial support throughout this study.

I wish to thank Professor Grant Steven from the Department of Aeronautical Engineering, University of Sydney for allowing me to get access to some source codes of STRAND6 finite element analysis software, which enabled me to carry out the research.

I wish to thank the academic and administrative staff of the Department of Civil and Building Engineering for their encouragement, support and friendship throughout my

study. I would also like to express my appreciation to the technical staff of the Department in particular to Mr. Jack Li for their help.

I thank my fellow postgraduates, Aftab, Annie, Gali, Gavin, Mahesh, Nelum, Nha, Nina, Rahman, Sujay and Sunil, for the invaluable friendship and support provided during my stay at Victoria University. I wish you all the very best in the future and hope that we will always be friends.

Finally, I should like to express my heartfelt gratitude to my parents for their love, tireless support and encouragement throughout this study and during the many years of study that preceded it. Without their support this thesis would not have been possible. It is to them I dedicate this thesis.

## **SUMMARY**

In the past most of the works on structural optimisation have been based on either mathematical programming or optimality criteria methods and have mainly concentrated on static responses of structures. These optimisation methods are mathematically complex and have limited applications. A novel approach to structural optimisation is being developed for practical applications based on the concept of slowly removing the inefficient material or gradually shifting the material from the strongest part of the structure to the weakest part until the structure evolves towards the desired optimum. From the results of finite element analysis, the contribution of each element to the required structural response may be assessed. Based on this assessment, material is gradually shifted or removed in the design domain. In doing so optimum designs can be easily achieved without resorting to any complex mathematics. This optimisation procedure is called Evolutionary Structural Optimisation (ESO). Compared to other methods for structural optimisation, ESO is overwhelmingly attractive due to its simplicity and effectiveness. ESO has been demonstrated to be capable of solving many problems of size, shape and topology optimisation.

This project examines the suitability of the ESO for the design of structures with buckling constraints. In recent years, more attention has been focused on stability and dynamic responses of structures. With the use of high strength materials and robust design methods, many structural elements are becoming thinner and more slender which makes them more susceptible to buckling. Structural optimisation for problems with buckling constraints is complicated because the calculation of buckling loads requires the solution of the prebuckling stress distribution (static analysis) and then the eigenvalue solution (buckling analysis) at each optimisation step.

In this thesis, the ESO method has been successfully applied to sizing optimisation of structures to enhance buckling resistance. This method has shown to be capable of solving multimodal structures, multiple load case structures and with multiconstraints including stress, displacement and stiffness. Some difficulties have been encountered in applying ESO method to the layout design of plate structures and these are also discussed in this thesis.

<b><u>TABLE OF CONTENTS</u></b>	<b><u>Page No.</u></b>
<b>DECLARATION</b>	<b>ii</b>
<b>ACKNOWLEDGEMENTS</b>	<b>iii</b>
<b>SUMMARY</b>	<b>v</b>
<b>TABLE OF CONTENTS</b>	<b>vi</b>
<b>PRINCIPAL NOTATIONS AND ABBREVIATIONS</b>	<b>xii</b>
<b>CHAPTER 1 - INTRODUCTION</b>	
1.1 General	1-1
1.2 Structural Optimisation	1-3
1.2.1 Classifications	1-6
1.2.2 Major approaches	1-7
1.3 Aims of the Project	1-11
1.4 Significance of the Project	1-12
1.5 Layout of the Thesis	1-14
<b>CHAPTER 2 - LITERATURE REVIEW</b>	
2.1 Introduction	2-1
2.2 Optimum Design of Columns	2-1
2.3 Optimum Design of Frames	2-4
2.4 Optimum Design of Plates	2-10
2.5 Summary	2-13

**CHAPTER 3 - EVOLUTIONARY STRUCTURAL OPTIMISATION (ESO)**

3.1	Introduction	3-1
3.2	Basic Concept and General Steps in ESO	3-2
3.2.1	ESO for structures with stress criterion	3-3
3.2.2	ESO for structures with displacements and stiffness constraints	3-7
3.2.3	ESO for problems with frequency constraints	3-12
3.3	Implementation of ESO Methods into Finite Element Codes	3-15
3.4	Discussion on Existing ESO Methods	3-16
3.5	Summary	3-19

**CHAPTER 4 - ESO FOR STRUCTURES AGAINST BUCKLING**

4.1	Introduction	4-1
4.2	Buckling Analysis of Structures	4-2
4.3	Sensitivity Number for Buckling Load - Simple Eigenvalue	4-4
4.3.1	Sensitivity number for element removal	4-5
4.3.2	Sensitivity number for element resizing	4-6
4.4	Evolutionary Procedure for Buckling Optimisation	4-8
4.5	Examples	4-13
4.5.1	Examples of column optimisation	4-13
4.5.2	Examples of frame optimisation	4-16
4.5.2.1	Optimum design of a three member portal frame	4-16
4.5.2.2	Optimum design of a 2-cell frame	4-20
4.5.2.3	Optimum design of a three storey frame	4-23
4.6	Influence of ESO Parameters on Optimum Designs	4-27

4.7	Optimality Criteria Methods Based on Uniform Strain Energy Concept	4-29
4.7.1	Optimality criterion by Khot <i>et al.</i> (1976)	4-29
4.7.2	Optimality criterion by Szyszkowski and Watson (1988)	4-32
4.8	Conclusions	4-35

## **CHAPTER 5 - OPTIMUM DESIGN OF MULTIMODAL STRUCTURES**

5.1	Introduction	5-1
5.2	Sensitivity Number for Buckling Load of Repeated Eigenvalues	5-4
5.3	Examples	5-6
5.3.1	Clamped-clamped column	5-6
5.3.2	Three member portal frame - bimodal example	5-10
5.3.3	Three member space frame - trimodal example	5-12
5.3.4	Box frame	5-14
5.4	Multimodal Optimality Criteria by Szyszkowski (1992)	5-19
5.5	Conclusions	5-21
	Appendix 5.1	5-22
	Appendix 5.2	5-24

## **CHAPTER 6 - MINIMUM WEIGHT DESIGN OF FRAME STRUCTURES**

6.1	Introduction	6-1
6.2	Uniform Scaling Factor $S_b$	6-2
6.2.1	Uniform scaling factor for 2-dimensional frames	6-3
6.2.2	Uniform scaling factor for space frames	6-5
6.3	Optimisation Procedure	6-13

6.4	Examples	6-14
6.4.1	Space frame - Example 1	6-14
6.4.2	Space frame - Example 2	6-15
6.5	Conclusions	6-17

**CHAPTER 7 - OPTIMUM DESIGN OF STRUCTURES WITH MULTIPLE  
LOAD CASES**

7.1	Introduction	7-1
7.2	Sensitivity Number	7-2
7.3	Optimisation Procedure	7-3
7.3.1	Constant weight design	7-3
7.3.2	Minimum weight design	7-4
7.4	Examples	7-8
7.4.1	Constant weight design	7-8
7.4.2	Minimum weight design	7-12
7.5	Conclusions	7-13

**CHAPTER 8 - OPTIMUM DESIGN OF STRUCTURES WITH MULTIPLE  
CONSTRAINTS**

8.1	Introduction	8-1
8.2	Multiple Constraints Problem	8-1
8.2.1	Sizing optimisation with stiffness constraints	8-3
8.2.2	Sizing optimisation with displacement constraints	8-4
8.2.3	Sizing optimisation with stress constraints	8-5

8.2.4	Uniform scaling and critical scale factors	8-7
8.3	Sensitivity Number	8-8
8.4	Optimisation Procedure	8-9
8.5	Examples	8-11
8.5.1	50-bar truss tower	8-11
8.5.2	5-Storey frame	8-17
8.6	Conclusions	8-22

## **CHAPTER 9 - OPTIMUM DESIGN OF PLATE STRUCTURES**

9.1	Introduction	9-1
9.2	Sensitivity Number and Optimisation Procedure	9-2
9.3	Examples	9-3
9.3.1	Simply supported square plate	9-4
9.3.2	Clamped square plate	9-8
9.3.3	Simply supported rectangular plate	9-11
9.4	Previously Reported Optimum Shapes	9-13
9.4.1	Optimum shapes by Pandey and Sherbourne	9-13
9.4.2	Optimum shapes by Levy and his co-workers	9-15
9.4.3	Optimum design by Folgado <i>et al.</i>	9-18
9.5	Strain Energy Distribution of Optimum Plates	9-22
9.6	Buckling Analysis of Variable-thickness Plates	9-24
9.7	Elimination of Checkerboard Patterns from 4-Node Element Designs	9-30
9.7.1	Optimum designs of plates with 4-node elements	9-31

9.7.2	Element sensitivity number re-distribution method	9-33
9.8	Layout Optimisation	9-35
9.9	Conclusions	9-42
<b>CHAPTER 10 - CONCLUSIONS AND FUTURE RESEARCH</b>		
10.1	Conclusions	10-1
10.2	Further Recommendations	10-5
<b>PUBLICATIONS DURING THIS CANDIDATURE</b>		<b>P1</b>
<b>REFERENCES</b>		<b>R1</b>

## PRINCIPAL NOTATIONS AND ABBREVIATIONS

### Principal Notations

- $A$  - cross-sectional area
- $a$  - length of a rectangular plate
- $[B]_i$  - strain-displacement relation matrix
- $b$  - breadth of a rectangular cross-section or width of a rectangular plate
- $C$  - mean compliance
- $C_{all}$  - allowable limit for the mean compliance
- $C_v$  - coefficient of variation
- $d$  - depth of the rectangular cross-section
- $d_j$  -  $j^{\text{th}}$  d.o.f displacement component
- $d_j^*$  - allowable limit for  $d_j$
- $\{d\}$  - nodal displacement vector
- $\{d_i\}$  -  $i^{\text{th}}$  element displacement vector associated with  $\{d\}$
- $\{d_{ij}\}$  -  $i^{\text{th}}$  element displacement vector associated with  $\{d_j\}$
- $\{d_j\}$  - displacement vector due to the virtual unit load vector  $\{F_j\}$
- $E$  - Young's modulus
- $[E]_i$  - element material property matrix
- $FS$  - factor of safety against buckling
- $\{F_j\}$  - virtual unit load vector at  $j^{\text{th}}$  d.o.f
- $I$  - moment of inertia
- $[K]$  - global stiffness matrix
- $[K_g]$  - global geometric stiffness matrix
- $[k_i]$  -  $i^{\text{th}}$  element stiffness matrix

- $[\Delta K]$  - change in the global stiffness matrix
- $[\Delta K_g]$  - change in the global geometric stiffness matrix
- $[\Delta k_i]$  - change in the  $i^{\text{th}}$  element stiffness matrix
- $L$  - member length
- $[M]$  - global mass matrix
- $[m_i]$  -  $i^{\text{th}}$  element mass matrix
- $nl$  - number of load cases
- $NSE$  - normalised specific strain energy
- $N_v$  - thickness distribution parameter
- $OF$  - optimum factor
- $\{P\}$  - nodal force vector
- $r$  - radius of a circular cross-section
- $S_b$  - uniform scaling factor for buckling constraint
- $S_c$  - uniform scaling factor for stiffness constraint
- $S_d$  - uniform scaling factor for displacement constraint
- $SE$  - strain energy
- $S_i$  - size of the  $i^{\text{th}}$  element (surface area or member length)
- $SPE$  - specific strain energy
- $S_s$  - uniform scaling factor for stress constraint
- $t$  - plate thickness
- $t_{max}$  - allowable maximum plate thickness
- $t_{min}$  - allowable minimum plate thickness
- $t_u$  - uniform plate thickness
- $\{u_{ij}\}$  -  $j^{\text{th}}$  eigenvector associated with the  $i^{\text{th}}$  element

- $\{u_j\}$  -  $j^{\text{th}}$  eigenvector
- $V$  - total volume of a structure
- $w$  - lateral deflection of the rectangular plate
- $\alpha_i$  -  $i^{\text{th}}$  element sensitivity number for removal
- $\alpha_i^+$  -  $i^{\text{th}}$  element sensitivity number for size increment
- $\alpha_i^-$  -  $i^{\text{th}}$  element sensitivity number for size reduction
- $\alpha_{ib}, \alpha_{ib}^+$  and  $\alpha_{ib}^-$  - sensitivity number for buckling constraint; removal, size increment and size reduction, respectively
- $\alpha_{ic}, \alpha_{ic}^+$  and  $\alpha_{ic}^-$  - sensitivity number for stiffness constraint; removal, size increment and size reduction, respectively
- $\alpha_{id}, \alpha_{id}^+$  and  $\alpha_{id}^-$  - sensitivity number for displacement constraint; removal, size increment and size reduction, respectively
- $\alpha_{if}, \alpha_{if}^+$  and  $\alpha_{if}^-$  - sensitivity number for frequency constraint; removal, size increment and size reduction, respectively
- $\alpha_{is}, \alpha_{is}^+$  and  $\alpha_{is}^-$  - sensitivity number for stress constraint; removal, size increment and size reduction, respectively
- $\alpha_{Ni}$  - nodal sensitivity number
- $\alpha_i^*$  - re- distributed modified sensitivity number
- $\varepsilon$  - eigenvalue multiplicity parameter
- $\omega_j$  -  $j^{\text{th}}$  natural frequency
- $\sigma_i^{vm}$  - maximum von Mises stress in the  $i^{\text{th}}$  element
- $\sigma_{\max}^{vm}$  - maximum von Mises stress in the whole structure
- $\sigma_{all}$  - allowable stress

- $\{\sigma\}_i$  - element stress matrix
- $\bar{\beta}$  - dimensionless minimum cross-sectional area
- $\lambda_{cr}$  - critical buckling load factor
- $\lambda_{cr}^{uni}$  - critical buckling load factor of the uniform design
- $\lambda_{cr}^{opt}$  - critical buckling load factor of the optimum design
- $\lambda_j$  -  $j^{\text{th}}$  eigenvalue
- $\rho$  - density
- $\sigma$  - normal stress
- $\nu$  - Poisson's ratio
- $\tau$  - shear stress

### **Abbreviations**

- ER* - Evolutionary Rate
- ESO* - Evolutionary Structural Optimisation
- FEA* - Finite Element Analysis
- FSD* - Fully Stressed Design
- MP* - Mathematical Programming
- OC* - Optimality Criteria
- RQA* - Rayleigh Quotient Approximation
- RR* - Rejection Ratio or Resizing Ratio

## **CHAPTER 1 - INTRODUCTION**

### **1.1 General**

The notion of an optimum solution of an engineering problem is intriguing and has been investigated for a long time. Earlier, engineering design was conceived as a kind of art that demanded great ingenuity and experience of the designer, and the development of the field was characterised by gradual evolution in terms of continual improvement of existing types of engineering designs. The design process generally was a sequential trial-and-error process where the designer's skills and experience were most important prerequisites for successful decisions for the trial phase. However, nowadays strong technological competition which requires reduction of design time and costs of products with high quality and functionality, and current emphasis on saving of energy, saving of material resources, consideration of environmental problems, etc., often involves creation of new products for which prior engineering experience is totally lacking. Development of such products must naturally resort to application of scientific methods. Hence, during recent decades, engineering design has changed from art and evolution to scientifically based methods of rational design and optimisation.

Structural optimisation deals with the optimal design of structural elements and systems employed in several engineering fields. Much research has been carried out on structural optimisation methods during the past three decades. Structural optimisation combines mathematics and mechanics with engineering and has now become a multi-disciplinary subject with applications in many fields. It was first applied in the aerospace industry, where reducing the structural weight is of utmost importance. Nowadays, use

of structural optimisation is rapidly growing in automotive, aeronautical, mechanical, civil, nuclear, naval and off-shore engineering. As the result of the growing pace of applications, research into structural optimisation methods is increasingly driven by real-life problems. This significant development has been strongly boosted by the advent of reliable and efficient general structural analysis methods such as the finite element method, design sensitivity analysis and rapid improvements in optimisation methods, along with the exponentially increasing speed and capacity of digital computers at low cost. The high performance of digital computers makes large scale structural optimisation possible and profitable in a large number of applications where thousands of design variables and constraints may need to be handled.

With the introduction of high speed computers, finite element analysis has become a very powerful tool in solving various complex structural engineering problems. After being able to determine the structural behaviour by means of finite element analysis, an important goal for engineers to achieve is to improve and optimise structural designs. In the past, the modification of a structure and the subsequent evaluation of the modified structure have been manually carried out. However, it is now possible to control repetitive modifications, re-analyses and re-evaluations automatically. Thus, a systematic improvement of structural systems may be achieved through computer simulation. In this context, structural optimisation based upon finite element method is becoming an advanced Computer Aided Design (CAD) tool.

Although there has been considerable work done on structural optimisation, the application of optimisation into practice is comparatively modest and limited to special

problems solved by optimisation experts. There is an obvious gap between the progress of the optimisation theory and its application to practical design problems. The vast majority of published work deals with the mathematical aspects of structural optimisation. It has been suggested that one major reason for the gap between the theory and practice of structural optimisation is the excessive emphasis on mathematical aspects rather than structural aspects of optimisation. Often the latter are confined to rather trivial examples, intended only to illustrate the successful application of a particular structural optimisation method.

Currently the research activity is directed towards making structural optimisation methods available to practising engineers and scientists in an easy, reliable, inexpensive and mathematically less complex form so that the optimisation techniques can be promoted as a viable tool in the design office. It is important to understand the basic concepts behind the structural optimisation methods for proper application of these methods to practical problems. The complex interactions of interdisciplinary constraints and the large number of design variables of the finite element models can severely test the limits of existing methods in this context.

## **1.2 Structural Optimisation**

The general aim of structural optimisation is to find a better design with minimum cost or weight while satisfying the safety and performance requirement(s) of the structure. The scope for structural optimisation is very wide and a particular structural optimisation problem is formulated depending on the objectives of the problem, the

constraints involved and the nature of the design variables. In general, the aim of a structural optimisation problem is formally given as:

- *minimise* (or *maximise*) objective functions *subject to* behavioural and geometrical constraints.

The following criteria can be used either as the objective function or as the behavioural constraint.

- Structural weight (volume), storage capacity
- Cost (material, manufacturing, life cycle etc.)
- Global measure of the structural performance such as stiffness, buckling load, plastic collapse load, natural vibration frequency, dynamic response etc.
- Local structural responses such as stress, strain or displacement at prescribed points; maximum stress, strain or displacement in the whole structure; stress intensity factor etc.

Single criterion optimisation is associated with only one objective function whilst multi-criterion optimisation involves several objectives. The constraints may be given in the form of equality or inequality conditions. Since these objective functions and constraints are implicit functions of design variables, most structural optimisation problems are highly non-linear.

There is another kind of constraints involved in structural optimisation called geometrical constraints or side constraints. These are restrictions imposed explicitly on the design variables due to design considerations such as manufacturing limitations,

availability of member sizes, fabrication, physical practicability, aesthetics etc. Constraints of this kind are typically inequality constraints that specify lower and/or upper bounds on the design variables. Geometrical constraints may prescribe the limit on cross-sectional dimensions, restriction on height or span of the structure etc.

The design variables, i.e. the structural parameters which are at the choice of the designer, and are required to be determined during the solution process, may be cross-sectional dimensions or member sizes, parameters controlling the geometry and layout of the structure, its material properties etc. Design variables may be continuous or discrete.

Regardless of the optimisation method used, the structural optimisation task can be mathematically stated as follows:

Find the set of design variables  $X = \{x_1, x_2, \dots, x_n\}$ , that will

Optimise  $W_k(X)$   $(k = 1, l)$

Subject to  $g_j(X) \leq 0$   $(j = 1, m)$

$x_i^L \leq x_i \leq x_i^U$   $(i = 1, n)$

where  $W_k(X)$  - Objective functions

$g_j(X)$  - Constraint functions

$x_i^L$  and  $x_i^U$  - lower and upper limits for  $x_i$ .

### **1.2.1 Classifications**

Depending on the design variables to be optimised, the structural optimisation encountered commonly in engineering practice can be classified into the following three broad categories:

**Cross-sectional or sizing optimisation** - This is a significant class of structural optimisation in which the layout of the structure is fixed. Such problems involve one- or two- dimensional systems where the centroidal axis (or middle surface) of all members is prescribed and only element stiffness properties such as cross-sectional areas or moments of inertia of bars, beams, columns and arches or thickness of membranes, plates or shells are the design variables for optimisation. Design variables for sizing may be discrete or continuous.

**Shape optimisation** - The term shape optimisation is often used in a narrow sense referring only to the optimum design of the shape of the boundary of two- and three- dimensional structural components. Shape optimisation aims at the selection of the optimum shape of external boundaries and surfaces, interior interfaces of a structure, interface between different materials and middle surfaces.

**Layout optimisation** - It aims at optimising topological design variables (such as spatial sequence, number and connectivity of members and joints of skeletal structures, location and number of holes in continuous structures) and geometrical design variables (such as the co-ordinates of the joints of skeletal structures or the centre-line or mid-

surface of continuous structures like curved beams, arches and shells) in addition to the above described shape and sizing design variables.

Both the topological and the geometrical variables define the layout of the structure. While sizing variables may be optimised under either fixed or variable layout, the layout optimisation is usually accompanied or followed by sizing optimisation. Shape and layout optimisations are typically more difficult to tackle than sizing optimisation. Even for a simple two or three member skeletal structure, simultaneous optimisations of cross sectional dimensions, nodal locations and connectivity of members are very involved. Apart from these three broad classifications, support and loading design variables such as the number, position and types of supports and external load distribution and positions and material design variables may also be changed during the optimisation process. These design variables will make the optimisation problem more complicated.

### **1.2.2 Major approaches**

Optimisation problems are highly non-linear in general. It is therefore necessary to employ iterative numerical solution schemes and determine the optimum design through a sequence of reanalyses and redesigns. The optimisation procedure generally consists of two major steps in each cycle of iteration. These are the analysis of the structure and the modification of design variables. In the past, most of the optimisation methods were based on either mathematical programming (MP) methods or optimality criteria (OC) methods. The basic concepts of MP and OC methods can be found in Morris (1982), Hafta *et al.*(1992) and Kamat (1993).

Many practical problems are so complex that their solutions cannot be found by closed form of mathematical methods, and systematic search techniques have been developed since 1960s for use in such cases. The study of these mathematical methods and search techniques is the concern of a branch of numerical analysis known as mathematical programming. The MP methods are also referred as direct optimisation methods. These methods require derivatives of objective functions and constraints with respect to all the design variables. At present, a number of MP methods compete with each other for finding the nearest local optimum in the least number of steps or in making the intervening calculations simpler by using suitable approximations. Such MP methods include feasible direction method, penalty function method, sequential linear programming, sequential convex programming, sequential quadratic programming, augmented Lagrangian multiplier method etc. (Vanderplaats 1993).

The MP methods have been applied not only to structural optimisation problems but also to several other fields of engineering, management and science etc. However, all MP methods require derivatives, whose efficient calculation can be highly problem dependent. The main disadvantage of MP methods is their limited capability in terms of the number of design variables. Although MP methods are mathematically elegant, as the number of design variables and constraints increases, the cost of computing derivatives becomes expensive and convergence to the optimum solution become erratic and unreliable. These limitations have caused serious impediments to practical applications to large scale problems. To overcome some of these difficulties, optimality criteria methods emerged during the 1960s and 1970s.

Optimality criteria are necessary and *sometimes* sufficient conditions for minimising the objective function and these can be derived by using either variational methods or extremum principles of mechanics. Initial applications were based on the intuitive criteria such as fully stressed design and uniform strain energy density methods. OC methods consist of two complementary ingredients. The first is the stipulation of the optimality criteria, which can be rigorous mathematical statements such as the Kuhn-Tucker conditions, or an intuitive one. The second ingredient is the algorithm used to re-size the structure for the purpose of satisfying the optimality criterion. Again, a rigorous mathematical method may be used or one may devise an ad hoc method which sometimes works and sometimes not. Different forms of the optimality criterion are required for different optimisation problems. A direct derivation of all potentially optimal solutions can be difficult if the number of optimality criteria is large and if they are highly non-linear. For most cases, the general optimality criteria are either not available or not tractable numerically.

In recent years these two approaches have begun to converge. The efficiency of the mathematical programming methods are improved by employing constraint approximations and faster algorithms for sensitivity calculations. Optimality criteria methods have moved from partially intuitive and ad hoc algorithms to more formal methodology. The dual methods of mathematical programming were shown to yield some of the popular optimality criteria methods.

During the last decade, stochastic search methods are also emerging as viable tool for structural optimisation. Genetic algorithms and simulated annealing are such methods

proposed in recent years (Jenkins 1991). These methods have their philosophical basis in processes found in nature, namely natural evolution. More recently the Homogenisation method (Bensoe and Kikuchi 1988) has proven to be successful in generating optimum topologies for continuum structures. In this method a material with microscale voids is introduced and the optimisation problem is defined by seeking the optimal porosity for the porous medium using one of the optimality criteria (Bendsoe 1995). Many interesting results have been produced using this method, although the model of the homogenisation method is complicated.

Realising the fact that almost all the existing structural optimisation methods usually involve complicated mathematical operations, Xie and Steven (1997) have recently presented an Evolutionary Structural Optimisation (ESO) method to avoid the use of any complicated mathematical operations. This novel approach to structural optimisation has been developed on the concept of slowly removing the unwanted material or gradually shifting the material from the strongest part of the structure to the weakest part until the structure evolves towards the desired optimum. In doing so optimum designs can be easily achieved without resorting to any complex mathematics. In the past four years the ESO methods have been demonstrated to be capable of solving the whole range of static and dynamic structural optimisation problems. The basic features of the ESO method will be described in Chapter 3. The rest of the thesis will explore the suitability of the ESO method and its application to the optimum design of structures with stability constraints.

### **1.3 Aims of the Project**

This project aims at investigating some simple, more general, computationally efficient approaches based on ESO method for the design of structures with stability constraints.

Specific aims of this project are as follows:

- To derive an efficient algorithm to determine the change in buckling eigenvalue when locally modifying an element in the finite element model of a structure under specified loading conditions.
- To develop optimisation procedures based on the concept of systematically re-sizing the elements to increase the critical buckling load factor of a structure while keeping the structural weight constant.
- To develop optimisation procedures for the minimum weight design of structures for prescribed values of buckling loads by systematic re-sizing and re-scaling of elements.
- To develop optimisation procedures for the optimum design of frame structures to resist buckling under multiple load cases.
- To develop optimisation procedures for the optimum design of frame structures subject to multiple constraints such as stress, displacement and stiffness along with stability constraints.
- To investigate the influence of the parameters pertaining to the optimisation procedures.
- And finally to develop sophisticated computer programs for the successful optimisation routines and to link these programs with the finite element analysis software STRAND6, developed by G+D Computing Pty Ltd, Australia and create

computer software which will carry out structural optimisation automatically so that it can be used as a design tool.

#### **1.4 Significance of the Project**

Since the 1960s considerable research has been carried out on structural optimisation. In the past, substantial efforts have been devoted to the associated mathematical and computational backgrounds, and the methods explored have been wide ranging and often mathematically complex. The development of commercial software for practical structural optimisation is held back by the lack of a really robust and efficient optimisation methods suitable for solving general engineering design problems. It is therefore important that simpler and computationally more efficient methods for structural optimisation should be developed.

Two major difficulties are associated with the process of interfacing a structural analysis package with an optimisation program. The first is a programming difficulty. Stand-alone optimisation packages typically expect subroutines that evaluate the values and derivatives of the objective functions and constraints. When the structural analysis program is large, or if the analyst does not have access to the source of the program, it is difficult to transform the analysis package into a subroutine called by the optimisation program. The second serious problem is the high computational cost required for many applications. For many structural optimisation problems the evaluation of derivatives of objective functions and constraints with respect to all design variables requires the execution of costly finite element analyses several hundred times. These difficulties have been avoided by the proposed ESO method. Furthermore, ESO procedures can be

easily implemented with any of the commercially available finite element analysis software packages. Even without the access to the source codes of FEA software, ESO can be carried out in batch files running FEA software and the structural modifications subroutine repeatedly.

In spite of extensive research in structural optimisation, only a small number of works have dealt with buckling optimisation. The majority of works on structural optimisation so far have concentrated on stress and displacement responses of structures. The stimulus for this project is that in recent years, more attention has been focused on stability and frequency responses of structures. With the use of high strength materials and robust design methods, many structural elements are becoming thinner and more slender which makes them more susceptible to buckling. Among a great deal of optimal structural design problems the stability factor has become one of the most important as a result of the very fast expansion of aerospace research, ship building, high-rise buildings etc.

Historically, the earliest efforts in formal structural optimisation were made by Lagrange in 1770 and later by Clausen in 1849. Coincidentally, they concerned with the stability of an elastic column. Over two centuries later, the purview of structural optimisation has widened considerably, but optimisation to enhance elastic structural stability continues to be an active area of research. Optimum structural design with stability constraints is complicated because the solution of buckling load depends on the membrane forces arising from the applied loads. Difficulties have been encountered in applying buckling optimisation methods to statically indeterminate structures including plate, shell and

solid structures. There has been some fruitful research carried out on frame structures, but the research on plate structures is very scarce. This project is expected to make a significant contribution to the optimum design of plate structures with stability constraints.

### **1.5 Layout of the Thesis**

The following is a brief outline of the material presented in this thesis. Chapter 2 presents a comprehensive review of previous research carried out on the optimum design of structures with stability constraints. In Chapter 3, basic concepts of ESO methods for problems with stress, displacement and frequency constraints are described.

Chapter 4 presents the theoretical basis of the ESO method for structures with stability constraints. Sensitivity number for the buckling load with a single eigenvalue is derived and the optimisation procedure for maximising the critical buckling load for structures of specified weight is presented. The influence of various parameters pertaining to the optimisation procedure is also investigated. Chapter 5 is devoted to the application of the proposed method to structures with repeated eigenvalues.

Chapter 6 describes the application of ESO method to the minimum weight design of frame structures for a prescribed value of buckling load. Chapter 7 outlines the ESO method for structures with multiple load cases. In Chapter 8, ESO method is extended to the optimum design of frame structures with stress, displacement and stiffness constraints in addition to the stability constraints.

As it was mentioned earlier, optimum design of plate structures with stability constraints is much more complicated than frame structures and very little research has been conducted with plate structures so far. In Chapter 9 optimum thickness distribution of plate structures with various support and loading conditions are obtained and the results are compared with previously reported designs. The validity of the uniform strain energy density optimality criteria and the buckling analysis of variable thickness plates using different approaches are discussed in detail. This chapter also investigates the problem of checkerboard patterns that is often encountered in finite element solution of distributed parameter optimisation problems, and a simple technique to effectively remove the checkerboard patterns is presented.

Chapter 10 summarises the conclusions and gives suggestions for further investigations.

A list of references is given in alphabetical order of first authors.

## **CHAPTER 2 - LITERATURE REVIEW**

### **2.1 Introduction**

The literature on structural optimisation is vast and this review is therefore focused on the works on structural optimisation with stability constraints. Most of the literature on structural optimisation with stability constraints is concerned with sizing optimisation with fixed layout. This literature review is brief, however some recent useful developments will be discussed in detail then and there in the forthcoming chapters and will be compared with the proposed method. In the following sections, the literature review is organised according to the types of structures, i.e. columns, frames/trusses (skeletal structures) and plates. This classification is not unique, however it gives an outline in chronological order of how the optimisation methods for structures with stability constraints have been developed over the years.

### **2.2 Optimum Design of Columns**

The simplest stability problem is the optimisation of Euler-buckling columns. Most of the early research was concerned with the development of optimum design of these columns with different loading and boundary conditions. Historically, one of the first optimal structural design problems addressed was treated by Lagrange in 1770 and later by Clausen in 1849. The first modern treatment of this problem, which sparked substantial interest in optimisation by the mechanics community, was presented in a paper by Keller (1960). Keller treated the problem of maximising the fundamental buckling load for a pinned-pinned column of constant volume. Keller addressed both the question of optimum tapering of the column and selection of the optimum cross-

sectional geometry. He employed a directional derivative approach to obtain necessary conditions of optimality and obtained closed form solutions.

In a subsequent paper, Tadjbakhsh and Keller (1962) dealt with a variety of boundary conditions for column optimisation, using the analytical method Keller had earlier presented. It is interesting to note that since no lower bound on cross-sectional area or upper bound on stress was specified, zero cross-sections (singularities) occurred in the designs obtained. Trahair and Booker (1970) later extended these analytical solutions with the introduction of minimum size constraints.

More general findings, based on energy considerations, were reported in a sequence of papers by Taylor (1967) and Taylor and Prager (1968), who proposed originally that an optimum structure with respect to buckling should have the configuration for which the specific strain energy of the buckling mode is uniform. Taylor and Prager developed a variational formulation of the problem of column optimisation, employing stationary of the Rayleigh quotient to obtain optimality criteria for fixed volume and maximum buckling loads, including lower bounds on cross-sectional areas. There was a subtle difference in the technical approach to developing necessary conditions of optimality by Keller and Tadjbakhsh, where a directional derivative of the buckling eigenvalue with respect to design variables was calculated, and by Taylor and Prager, where a first variation of the Rayleigh quotient was employed to calculate the derivative of the eigenvalue, which was then used with a Lagrange multiplier method to obtain necessary conditions of optimality.

The study of Olhoff and Rasmussen (1977) on clamped columns was the earliest work on bimodal buckling optimisation. In studying the optimum design of clamped column under axial load for maximum fundamental buckling load, they discovered that there was a threshold value of minimum area constraint which separated the single and bimodal buckling modes and proved that the design obtained earlier by Tadjbakhsh and Keller (1962) using single mode formulation was not optimum. Olhoff and Rasmussen (1977) established the differential equations for optimisation under the double eigenvalue formulation by using variational calculus and solved these equations by means of a numerical method. This landmark study was particularly important since it required a change in the previous mathematical formulations in order to take into account the possibility that the optimum fundamental buckling load corresponding to multiple buckling modes. This discovery led to many later publications on multiple eigenvalue buckling problems.

Simites *et al.* (1973) appear to be the first to report the use of finite element analysis and iterative procedure to optimise the shape of columns. They used the uniform strain energy density optimality criteria as the basis for their analysis. This was a major breakthrough in stability optimisation because previous methods were based on continuum theory whereas this method could be applicable to built-up structures such as frames and trusses. So far the optimum designs of columns were concerned with maximising the fundamental buckling load for columns with a specified volume. Murthy and Christiano (1973) appear to be the first to report on the minimum weight design of columns for a prescribed buckling load. They considered both linear and

quadratic size-stiffness relationships and used some iterative procedures to re-scale the optimum design to meet the specified buckling load.

### **2.3 Optimum Design of Frames**

The first systematic approach to the derivation of optimality criteria for a variety of design conditions to minimise the weight of large structural systems using finite element method and numerical iterative procedures was presented by Venkayya *et al.* (1973). However the assumption of linear size-stiffness relations in their method was a major restriction. Khot *et al.* (1976) extended this method to frame structures with stability constraints. Optimality criteria were derived using Lagrangian multiplier method and it was stated that for single load case structures, the structure would be optimum when the ratio of the strain energy density to the mass density, associated with the buckling mode was the same for all the elements. They derived the recurrence relations and scaling procedures for linear size-stiffness structures and applied to other structures with some additional modifications. However the theory proposed by Khot *et al.* (1976) is valid only for statically determinate single mode structures and under the assumption of the linear size-stiffness relationship. The recursion relation and scaling algorithm used in their paper will be discussed in detail in Chapters 4 and 6.

Later, in a sequence of papers, Szyszkowski and co-workers developed a more general method based on finite element method for the optimisation of the buckling load of columns and frames. Unlike the previously discussed method, in this method the critical buckling load was maximised for a specified weight of structure. At first Szyszkowski and Watson (1988) developed the optimisation method for single modal structures.

Using the variational approach and Lagrangian multipliers, they proposed that the optimum shape of the structure with respect to buckling should have the configuration for which the specific bending energy due to the fundamental buckling mode was uniform. A structure was divided into a number of elements and the specific bending energy of each element due to the first buckling mode was calculated. An re-sizing algorithm was formulated using the specific energy of elements based on the constant weight condition and the rule of uniform specific energy. They also pointed out that the rule of uniform specific bending energy due to the fundamental buckling load was not applicable for multimodal problems. This method is more general than the previously discussed method because the former method was more suitable for structures with linear size-stiffness relationship.

Szyszkowski *et al.* (1989) extended their method to bimodal structures. The iterative method presented here treated any frame structures from the bimodal optimisation viewpoint. The real number of modes participating in the final optimal design was determined by the numerical procedure. For a single mode optimal design the influence of the second mode was automatically eliminated by the iterative procedure. This generality was made possible because the method does not directly use the buckling load or the minimum weight of the structure as the objective function. Instead the bimodal optimality condition was used for this purpose. Szyszkowski (1992) later extended this method to general multimodal problems. Using variational calculus and Lagrangian multipliers the multimodal optimality condition was derived. The optimality condition for multimodal structures stated that a linear combination of the normalised specific energies due to the participating buckling modes must sum to unity at every

point of the structure. The whole approach was concerned only with a single load case. Resizing algorithms which use the specific energy of elements, require some arbitrary constants. The choice of these arbitrary constants sometimes hampers the convergence of optimum designs. The theory behind these methods will be discussed in detail in Chapters 4 and 5.

Canfield (1993) obtained optimum designs of frames using non-linear mathematical programming method and Rayleigh quotient approximation (RQA). RQA approximates buckling eigenvalues by separately estimating the modal strain energy due to the linear and geometric stiffness of the structure. The derivation of geometric stiffness matrix was estimated using only a first-order approximation of the internal forces. This method is suitable for small scale structures and the convergence of the optimum design is sensitive to move limits used in the process.

Lin and Liu (1989) presented a multiple criteria optimisation method for the minimum weight design for truss and frame structures with size, stress, displacement and buckling constraints. Only the first buckling mode was considered with an assumption that the internal forces acting in the structure prior to buckling are taken to be statically determinate. The optimality criterion derived for all the constraints imposed on the structure was equivalent to the Kuhn-Tucker conditions of non linear mathematical programming for a local optimum design. A general redesign equation was derived from the optimality criteria and combined with fully stressed design (FSD) formula to reduce the number of redesign iterations. They suggested that when the initial design was far away from the optimum design, the use of FSD could make the design variables

approach to the vicinity of optimum design rapidly and then applying the optimality criterion to optimise the design variables would give an economical approach. They adopted the uniform scaling of all the design variables after each iteration considering linear size-stiffness relationship. The scaling factor was obtained from the maximum of stress ratio, displacement ratio, size ratio and buckling load ratio.

Liu and Lin (1992) later proposed a method to overcome the preclusive assumption of statical indeterminacy. The optimisation method was based on the advanced primal-dual algorithm, the augmented Lagrange multipliers method (ALM). Statical indeterminacy of the structure was incorporated via an efficient gradient calculation of internal forces as obtained from the derivatives of stresses. It was shown that the statically indeterminate approach resulted in a higher computer cost per iteration than the usual statically determinate approach, but with less number of iterations. However, the indeterminate approach converged to designs no better than the determinate approach.

Barson (1994) presented another method for the optimisation of planer frames based mainly on the structural stability and dynamic behaviour of the structure. Iterative optimality criteria method was used and the strategy adopted here for searching the optimal solution had two stages. In first stage, the buckling load of the structure was taken as the objective function and the prescribed values of the fundamental frequency or the period of vibration was the only constraint, whereas in the second stage the stress, displacement and stability constraints were taken into account to verify the sizes of the cross-sections of the structural members from the first stage of analysis. If the

constraints were violated, uniform scaling procedure was applied to place the violated constraints inside the permissible domain. Barson indicated that by improving the overall elastic stability characteristics of the structure, the static, dynamic and post-elastic performances of the structure were often improved. However, in general this assertion is found to be incorrect and it will be discussed in detail in Chapter 8.

Karihaloo and Kanagasundaram published a series of papers on the minimum weight design of planar frames under multiple load systems with constraints on stress, stiffness, stability and geometry using various non-linear mathematical programming methods. The summary of all these approaches were given in Karihaloo and Kanagasundaram (1993). The solution of non-linear programming was attempted by several methods, namely Augmented Lagrangian Multiplier method (ALM), Sequential Convex Programming (SCP), Sequential Linear Programming (SLP), Sequential Quadratic Programming (SQP) and Sequential Unconstrained Minimisation Technique (SUMT) and it was concluded that both SCP and SLP were relatively more efficient methods for optimisation.

Multilevel optimisation of frames with buckling constraints as well as stress, displacement and size constraints was studied by Ding (1989). The weight of the structure, the areas of cross-sections for the independent elements and overall displacement and overall buckling were taken at the system level as objective function, design variables and constraints respectively. At the component level, the objective was to minimise the weight of each independent element subject to local stress and local buckling constraints. The hybrid approximation technique in combination with the dual

solution from mathematical programming was simultaneously used in the so-called two level optimisation processes.

Turner and Plaut (1981) discussed the optimal design of elastic structures under multiple independent loads. The iterative optimisation procedure utilised the finite element and the optimality criterion. For a constant weight structure, the critical buckling load was maximised for a given ratio of loads. This procedure was applied to variety of load ratios, and the results were plotted in the loading space in terms of stability boundaries (interaction curves or surfaces) and a stability envelope. The objective was to enlarge the stability region as much as possible by an appropriate distribution of the material of the structure. However this method is cumbersome with regard to the solution for multiple load cases as it requires the optimum solution of structure with a variety of load ratios to obtain the stability boundary.

Pezeshk and Hjelmstad (1991) suggested an optimisation based design methodology for improving the strength and stability of framed structures, the capacities of which were governed by inelastic limit-load behaviour. They also indicated that by improving the stability characteristics of the structure, the dynamic and static performance of the structure was often improved. In the companion paper by Hjelmstad and Pezeshk (1991), a novel approach to solving problems with multiple loading conditions was introduced where each eigenvalue in the objective was weighted in accordance with the degree of participation of the mode in the loading.

## **2.4 Optimum Design of Plate Structures**

Although there has been considerable amount of work carried out on optimisation of frame structures, very few papers have appeared in the literature concerning the optimum design of plates against buckling. This is because, for frame structures, the axial stress resultant in the prebuckling state is not sensitive to changes in cross-sectional areas along the length of the member. For statically determinate frame structures changes of cross-section do not have any effect on axial forces. However, this is not true for plates. The in-plane stress-resultants in the prebuckling state of plates are indeed functions of the thickness distribution. The problem of optimising plates for stability is, therefore, significantly more complicated than that for frame structures. Under the assumption of in-extensional pre-buckling deformations, which leads to thickness-independent in-plane stress-resultants in the pre-buckling state, a condition of uniform strain energy density has been established in the past as the optimality condition for plates by several researchers. However, optimisation of plates on the basis of such assumptions has led to unsatisfactory solutions. More discussion on this point will be presented in Chapter 9.

Pandey and Sherbourne (1992) carried out an extensive study on finding the optimum thickness distribution for a rectangular, isotropic plate of given volume that would maximise its uniaxial buckling load. Determination of optimum thickness distribution of uniaxially loaded rectangular plates has been an interesting and long-standing problem discussed widely in the literature. This is because the governing non-linear fourth order partial differential equations used for the solution of buckling load for rectangular plates are widely known to the mechanics community.

Pandey and Sherbourne (1992) pointed out the differences between the optimal profiles of rectangular plates previously reported. Early studies by Parsons (1955) and Mansfield (1973) reported that higher thickness near the edges than at the centre (concave profile) increased the buckling load whereas Spillers and Levy (1990) obtained convex profile for the optimum design. Pandey and Sherbourne (1992) also reported that the optimal shapes discussed in the above literature were characterised by a severely disproportionate thickness distribution resulting in very thin sections in certain regions, which indicates the possibility of local buckling at a load far lower than that predicted by the analytical methods using a limited terms of displacement function.

Pandey and Sherbourne investigated most of the previously reported optimum shapes and intuitively proposed a thickness distribution for uniaxially loaded rectangular plates based on Parsons (1955). Optimum shapes were obtained for a square plate with three boundary conditions: all edges simply supported, all edges clamped, and loaded edges simply supported and unloaded edges clamped. Rayleigh-Ritz method was used for buckling analysis. Simply supported plates were analysed with Fourier sine series whereas Gram-Schmidt orthogonal polynomials were used for plates containing clamped edges. Two prebuckling stages characterised by constant stress and constant force were considered in the analysis. Details of this analysis will be discussed in Chapter 9. Pandey and Sherbourne also highlighted that the selection of suitable displacement function, possibly with high number of terms, was crucial in the use of series solution to accurately identify the critical modes and localised effects.

Spillers and Levy (1990), Levy and Ganz (1991), Levy and Sokolinsky (1995) and Levy (1996) have carried out a series of studies to find the optimum shape of simply supported rectangular plate that would maximise its uniaxial buckling load. Originally Spillers and Levy (1990) extended the Keller's (1960) classic solution for the optimal design of columns to the case of plates. They derived an optimality condition via variational calculus which states that the plate thickness should be proportional to the strain-energy density in an optimal design. Buckling solution was obtained using Rayleigh-Ritz method and a double sine Fourier series was used to represent the lateral plate displacement.

Optimum profile for a square plate was initially obtained by Spillers and Levy (1990) with one term symmetric double sine displacement function. The buckling load of such plate was calculated to be 2.12 times that of an equivalent uniform plate. Levy and Ganz (1991) later re-analysed the above plate using a six term displacement function with a multiple of half sine waves in the direction of loading and only one half sine wave in the other direction and predicted a 44% increase in the buckling load. However, all these results were later invalidated by Pandey and Sherbourne (1992) considering the localised buckling which Spillers and Levy (1990) and Levy and Ganz (1991) failed to capture by either one term or six term displacement functions. Pandey and Sherbourne (1992) re-analysed this plate with a displacement function of half sine waves in both plate directions of total 289 terms and found a locally buckled mode. Recently Levy and Sokolinsky (1995) and Levy (1996) re-analysed the whole problem and proposed a new optimum shape which yields 32% increase in the buckling load. All these controversial optimum designs and their buckling solutions will be discussed in detail in Chapter 9.

An optimisation method for plate buckling using finite element method was recently proposed by Folgado *et al.* (1995). They extended the homogenisation method, a material based model for the layout design of plate reinforcement with a buckling load criterion. The model used a laminate theory and the optimum designs were obtained using a mathematical programming method. This method took account of repeated eigenvalues while the previously discussed techniques were solely based on the traditional energy methods and were unable to handle the multimodal behaviour. Detail analysis of optimum designs obtained by Folgado *et al.* (1995) will be discussed in Chapter 9 along with the solutions of the proposed method.

## **2.5 Summary**

Most of the early works on buckling optimisation were concerned with columns and were based on the directional derivative approach. Later more general methods based on optimality criteria were established. For single modal structures the optimality criterion stated that the optimum shape of the structure should have the configuration for which the specific bending energy due to the fundamental buckling mode is uniform. With this uniform specific energy optimality criterion and the use of finite element method, iterative procedures were set-up for the design of built-up structures such as frames and trusses. Later, multimodal optimisation methods were also established and applied to frame structures. Optimisation of frame structures with multiple constraints such as size, stress, displacement and buckling were analysed by various people using either optimality criteria methods or mathematical programming methods.

Extensive search by the candidate reveals that the literature on the optimum designs of plate buckling is very little and the available designs are mainly concerned with a particular class of problem: uniaxially loaded rectangular plates. Different controversial optimum profiles were reported for such plates by various researchers using distributed parameter optimisation methods. Buckling solutions of these plates were obtained using Rayleigh-Ritz method and assumed displacement functions. Few papers, e.g. Folgado *et al.* (1995) used the finite element method for optimisation of plate buckling.

## **CHAPTER 3 - EVOLUTIONARY STRUCTURAL OPTIMISATION (ESO)**

### **3.1 Introduction**

Recently a simple new approach to structural optimisation has been proposed by Xie and Steven (1993, 1994a) based on the concept of slowly removing the inefficient material from the structure and/or gradually shifting the material from the strongest part of the structure to the weakest part until the structure evolves to the desired optimum. This optimisation procedure is named as Evolutionary Structural Optimisation (ESO). The ESO method offers a simple way to obtain optimum designs using any of the standard finite element analysis codes. Compared to other structural optimisation methods, the ESO method is overwhelmingly attractive due to its simplicity and effectiveness. The original work on ESO involves obtaining optimum shapes and layouts of continuum structures of given loading and support conditions, by gradually removing the lowly stressed part of material from the structure (Xie and Steven 1993, 1994a). Since then during the last four years ESO has been demonstrated to be capable of solving many problems of size, shape and topology optimum designs for static and dynamic problems.

In this chapter, the basic theory behind the ESO methods for problems with stress, displacement, stiffness and frequency constraints is outlined. This chapter is kept brief and it gives only an introduction to ESO. Not all aspects of ESO methods are covered here. In the following sections, ESO method is described only for simple structural problems such as with single objective or constraint function and with single loading or single modal cases. For a wider range of applications of ESO methods, the reader is

referred to Xie and Steven (1997) and other published papers cited in the list of references.

### **3.2 Basic Concept and General Steps in ESO**

Like most other structural optimisation methods, the evolutionary structural optimisation method is iterative because of the highly non-linear nature of the structural optimisation problems. ESO methods consist of two complementary ingredients. The first is the calculation of the contribution of each element to the required structural behaviour. The second ingredient is the optimisation procedures used for resizing or gradually removing elements without violating certain requirements.

To find out the optimum locations for structural modifications, gradients (sensitivity) of structural responses are often needed. Sensitivity analysis plays a central role in structural optimisation, since virtually all the optimisation methods require the computation of the derivatives of structural response quantities and objective functions with respect to design variables. In ESO, the sensitivity of structural behaviour is expressed at each element level. Since ESO is based on the concept of slowly removing or resizing the material in the structure, each element in the design domain should have an indication whether it can be removed or resized after each cycle of analysis. From the results of finite element analysis, for shape and layout optimisation (which involves element removal) the contribution of each element to the structural behaviour such as stress, displacement, frequency, buckling load etc. is assessed. For sizing optimisation, the effects on these structural responses due to the local modification of each element need to be estimated. This contribution indication of an element with respect to the

required structural responses is referred as the *sensitivity number* of that particular element and is denoted by  $\alpha_i$  for the  $i^{\text{th}}$  element.

Based on this element sensitivity assessment, material is gradually removed or resized in the design domain. An iterative procedure needs to be set-up so that the optimisation can be done automatically. The following sections illustrate the optimisation procedures and the determination of element sensitivity numbers for various design considerations.

### **3.2.1 ESO for structures with stress criterion**

In the original application of ESO, the shape and layout of two- and three- dimensional continuum structures have been obtained by gradually removing lowly stress material (Xie and Steven 1993). Initially a design domain is chosen large enough to cover the final design and discretised into a fine mesh of elements. Static analysis is performed using a standard finite element software for the prescribed set of loading and boundary conditions. A reliable sign of potential structural failure is excessive stress or strain. Inversely a reliable sign of inefficient material use is low stress or strain. Since lowly stressed material is under-utilised it will be removed from the structure gradually and the stress level in the subsequent designs will become more and more uniform. Since the structure has been divided into many small elements, the removal of lowly stress material can be conveniently represented by deleting lowly stress elements from the structure.

The stress level at each point in a structure can be measured by some means of average of the normal and shear stress components. For this purpose the von Mises stress has

been frequently used for isotropic materials. By comparing the von Mises stress of each element  $\sigma_i^{vm}$  (where the subscript  $i$  refers the element number) with the maximum von Mises stress in the whole structure  $\sigma_{\max}^{vm}$ , a local normalised stress level  $\sigma_i^{vm} / \sigma_{\max}^{vm}$  is calculated for each element. Hence the contribution of  $i^{\text{th}}$  element for stress problem is defined as

$$\alpha_{is} = \frac{\sigma_i^{vm}}{\sigma_{\max}^{vm}} \quad (3.1)$$

where the subscript,  $s$  in  $\alpha_{is}$  refers to stress problems. Only a small amount of lowly stress material should be removed from the structure at each iteration. Thus a rejection ratio  $RR$  is introduced. After the static analysis, an element will be removed if

$$\alpha_{is} = \frac{\sigma_i^{vm}}{\sigma_{\max}^{vm}} < RR \quad (3.2)$$

The cycle of finite element analysis and element elimination is repeated for this same value of  $RR$  until a steady state is reached, i.e., no more elements or only a few elements are deleted. At this stage the current rejection ratio  $RR_{old}$  is increased to a new rejection ratio  $RR_{new}$  by adding an evolutionary rate  $ER$ .

$$RR_{new} = RR_{old} + ER \quad (3.3)$$

With this new rejection ratio, the cycle of finite element analysis and element elimination is repeated until a new steady state is reached. Such an evolutionary process is continued until a desired optimum is reached, for example, when all stress levels are within 25% of the maximum stress.

In this method two parameters, the initial rejection ratio  $RR_o$  and the evolutionary rate  $ER$  need to be given. The typical values,  $RR_o = 1\%$  and  $ER = 1\%$ , are small enough to

give satisfactory results. For certain problems where stress levels do not vary much over the whole design domain,  $RR_o$  as high as 10% and  $ER$  as large as 5% can also be used.

This evolutionary optimisation procedure for stress problems can be easily extended to structures with multiple load cases (Xie and Steven 1994a). After the static analysis, the stress distribution is obtained for each load case. The ratio of the element stress to maximum stress is calculated for each load case and an element is removed from the structure only if the ratio is less than  $RR$  for *all* the load cases present in the model. Thus, compromises are made at each iteration among these load cases. The final structure is the optimal design in the sense that every part of the remaining material has its own role to play for at least one load case and possibly for all load cases.

Initially this method has been applied to two dimensional plane stress and plane strain problems. It has also been shown to give good results for three dimensional structures. This ESO concept can also be applied to sizing optimisation of structures with fixed layout. Here again the stress ratio of each element is calculated and the cross-sectional areas of lowly stressed elements are gradually decreased and the cross-sectional areas of highly stress elements are gradually increased until a more uniform stress design is obtained. Simultaneous size and topology optimisation of discrete structures is also possible by allowing the size of the lowly stressed members to go to zero and subsequently remove them from the structure.

This ESO method for improving the strength characteristics of the structure can be made analogous to the Fully Stressed Design (FSD). FSD is the earliest intuitive optimality

criteria method used for sizing optimisation of discrete structures to improve the strength characteristics of the structure. In this method the design variables are scaled by the ratio of the element stress to the allowable stress using the formula

$$x_i^{new} = x_i^{old} \frac{\sigma_i}{\sigma_{all}} \quad (3.4)$$

where  $\sigma_{all}$  is the allowable stress. An iterative process of analysis and resizing can result in a structure where all members, except those which are at the minimum or maximum sizes, are fully stressed, i.e. their stresses are at allowable limit. However this method can give satisfactory results only for statically determinate structures under single loading condition with equal allowable stresses on tension and compression.

Both the ESO and FSD methods are based on element stress ratios and are aimed at creating lighter designs with more uniform stress distributions. The main advantage of ESO method over the FSD method is that the ESO method can be used for layout and shape optimisation. Furthermore, ESO method can be effectively used for the design of structures with multiple load cases. Since FSD is complemented by the resizing algorithm based on the assumption that the load distribution in the structure is independent of member sizes, this method may lead to non-optimum design for highly indeterminate structures. Whereas in ESO method for sizing optimisation, at each iteration only a few elements are subjected to small cross-sectional modifications. Thus the cross-sectional changes at each iteration do not cause significant changes in the element forces. This gradual evolution treats the statically indeterminate structures more effectively than the FSD method.

### 3.2.2 ESO for structures with displacement and stiffness constraints

This section describes the evolutionary procedure for the optimum design of structures with displacement and stiffness constraints. The material presented in this section derives from the work by Chu *et al.* (1996, 1997a, 1997b). The structural stiffness and displacement are major considerations when designing structures such as high-rise buildings and bridges. It is often required that the structure should be stiff enough so that the maximum deflection in the structure is within the prescribed limit satisfying serviceability requirements.

In this method, the effect of element removal on the overall stiffness of the structure or on a prescribed deflection is calculated. The direct approach to obtaining changes in the displacement field or structural stiffness is based on differentiation of the finite element discretised equilibrium equations of the structure.

#### 3.2.2.1 The sensitivity number for problems with overall stiffness constraints

The global equilibrium equation of a finite element discretised linearly elastic structure subjected to static loading is given by

$$[K]\{d\}=\{P\} \quad (3.5)$$

where  $[K]$  is the global stiffness matrix,  $\{d\}$  is the nodal displacement vector and  $\{P\}$  is the nodal force vector. If the applied load  $\{P\}$  is independent of design variables, the derivative of the displacement field with respect to any design variable  $x$  is given by

$$\frac{\partial \{d\}}{\partial x} = -[K]^{-1} \frac{\partial [K]}{\partial x} \{d\} \quad (3.6)$$

The inverse measure of the overall stiffness of a structure is known as the mean compliance,  $C$ , and is defined as

$$C = \frac{1}{2} \{P\}^T \{d\} \quad (3.7)$$

The overall stiffness of the structure is maximised by minimising its mean compliance. If the applied load  $\{P\}$  is independent of design variables, the derivative of the mean compliance with respect to any design variable  $x$  is given by

$$\frac{\partial C}{\partial x} = \frac{1}{2} \{P\}^T \frac{\partial \{d\}}{\partial x} \quad (3.8)$$

From (3.6), it leads to

$$\frac{\partial C}{\partial x} = -\frac{1}{2} \{P\}^T [K]^{-1} \frac{\partial [K]}{\partial x} \{d\} = -\frac{1}{2} \{d\}^T \frac{\partial [K]}{\partial x} \{d\} \quad (3.9)$$

The above equation is approximated to

$$\Delta C = -\frac{1}{2} \{d\}^T [\Delta K] \{d\} \quad (3.10)$$

Suppose that an element,  $i$ , is removed from the structure. Due to the removal of this element, the change in global stiffness matrix  $[\Delta K] = -[k_i]$  where  $[k_i]$  is the stiffness matrix of the  $i^{\text{th}}$  element in the global co-ordinate system. It is assumed that the removal of the element has no effect on the load vector  $\{P\}$ . Hence the change in the mean compliance due to the removal of an element  $i$ ,  $\Delta C_i$  is given by

$$\Delta C_i = \frac{1}{2} \{d_i\}^T [k_i] \{d_i\} \quad (3.11)$$

where  $\{d_i\}$  is the displacement vector associated with the element,  $i$ .  $\Delta C_i$  indicates the change in the strain energy due to the removal of  $i^{\text{th}}$  element. Both  $C$  and  $\Delta C_i$  are always positive values. The value of  $\Delta C_i$  can be calculated for each element in the structure. Hence the sensitivity number for element,  $i$ , for problems with stiffness constraint is defined as

$$\alpha_{ic} = \Delta C_i = \frac{1}{2} \{d_i\}^T [k_i] \{d_i\} \quad (3.12)$$

where the subscript,  $c$  in  $\alpha_{ic}$  refers to compliance constraint. The objective is to find the lightest structure while satisfying the stiffness constraint, typically in the form  $C \leq C_{all}$ , where  $C_{all}$  is the prescribed allowable limit for  $C$ . When an element is removed, the stiffness of the structure reduces and correspondingly the mean compliance increases. Thus it is obviously most effective to remove the element which has the lowest  $\alpha_{ic}$  so that the increase in  $C$  is minimum.

### 3.2.2.2 The sensitivity number for problems with displacement constraints

Displacement constraints may be imposed on certain degrees of freedoms (d.o.f) of the structure. The constraint imposed on the  $j^{\text{th}}$  d.o.f displacement component,  $d_j$  is given in the form,  $|d_j| \leq d_j^*$ , where  $d_j^*$  is the allowable limit for  $d_j$ . To determine the change in the  $j^{\text{th}}$  d.o.f displacement,  $\Delta d_j$ , a unit virtual load vector  $\{F_j\}$  is introduced in which only the corresponding  $j^{\text{th}}$  component is equal to unity and all the other components are equal to zero. Multiplying equation (3.6) by  $\{F_j\}^T$  gives

$$\frac{\partial d_j}{\partial x} = -\{F_j\}^T [K]^{-1} \frac{\partial [K]}{\partial x} \{d\} = -\{d_j\}^T \frac{\partial [K]}{\partial x} \{d\} \quad (3.13)$$

where  $\{d_j\}$  is the displacement vector due to the unit virtual load vector  $\{F_j\}$ . This equation is approximated to

$$\Delta d_j = -\{d_j\}^T [\Delta K] \{d\} \quad (3.14)$$

As above, if the  $i^{\text{th}}$  element is removed from the structure, the change in  $j^{\text{th}}$  d.o.f displacement component due to this element removal,  $\Delta d_{ij}$  is reduced to

$$\Delta d_{ij} = \{d_{ij}\}^T [k_i] \{d_i\} \quad (3.15)$$

where  $\{d_i\}$  and  $\{d_{ij}\}$  are the  $i^{\text{th}}$  element displacement vectors associated with  $\{d\}$  and  $\{d_j\}$  respectively. It should be noted that unlike  $\Delta C_i$  in (3.11),  $\Delta d_{ij}$  can be positive or negative. As the displacement may take positive or negative value, the aim is to reduce the absolute value of the constrained displacement. Thus it is best to remove the element which gives the lowest absolute change in displacement,  $|\Delta d_{ij}|$ . Hence the sensitivity number for the  $i^{\text{th}}$  element for problems with a displacement constraint is defined as

$$\alpha_{id} = |\Delta d_{ij}| = \left| \{d_{ij}\}^T [k_i] \{d_i\} \right| \quad (3.16)$$

where the subscript,  $d$  in  $\alpha_{id}$  refers to displacement constraint.

### 3.2.2.3 Evolutionary optimisation procedures for stiffness or displacement constraints

As discussed earlier, an iterative procedure has to be adopted and a small number of elements should be removed from the structure after each iteration depending on the element sensitivity numbers. The procedure is given as follows:

*Step 1:* Discretise the structure using a fine mesh of elements.

*Step 2:* Analyse the structure for the prescribed loading and support conditions.

*Step 3:* Calculate sensitivity number for each element.

*Step 4:* Remove a small number of elements which have the lowest sensitivity numbers.

*Step 5:* Repeat Steps 2 to 4 until the constraint reaches its limit.

For problems with displacement constraints, additional static analyses with virtual unit loads corresponding to the constrained displacements need to be included in Step 2. The

number of elements to be removed at each iteration can be prescribed by its ratio to the total number of elements of the initial or the current structure. This ratio is called the *element removal ratio*. In Step 3 the sensitivity number for each element should be calculated depending on the type of constraint involved. In Step 5 the evolutionary procedure can also be terminated when a prescribed percentage of volume has been eliminated from the structure. The influence of the element removal ratio on the final optimum design has been investigated with several examples by Chu *et al.* (1997a). In general the accuracy of the solution will improve with a smaller removal ratio but at the expense of higher computational costs.

The derivation of sensitivity numbers has been discussed here only for single constraint, single load case structures. This can be easily extended to multiple displacement constraints and multiple loading conditions by introducing weighting factors in the sensitivity number calculations to take account of the active participation of each constraint and load case appropriately. Details of this analysis can be found in Chu *et al.* (1996). This ESO method has been extended by Chu *et al.* (1997b) to the topology design of truss structures.

In this section sensitivity numbers have been derived for element removal and the optimisation procedures have been set-up for removing inefficient material which results in layout optimisation of structures. A new extension of this ESO method for resizing of frame structures has been accomplished by the candidate and this will be presented in Chapter 8.

### 3.2.3 ESO for problems with frequency constraints

The response of a structure to dynamic excitation depends, to a large extent, on the first few natural frequencies of the structure. Excessive vibration occurs when the frequency of the dynamic excitation is close to one of the natural frequency of the structure. The optimum design with frequency constraints is of great importance, particularly in the aeronautical and automotive industries. The material presented in this section derives from the work by Xie and Steven (1994a, 1996).

The dynamic behaviour of the structure is represented by the following general eigenvalue problem:

$$([K] - \omega_j^2 [M])\{u_j\} = \{0\} \quad (3.17)$$

where  $[M]$  is the global mass matrix,  $\omega_j$  is the  $j^{\text{th}}$  natural frequency and  $\{u_j\}$  is the corresponding eigenvector. The eigenvalues representing the natural frequencies can be arranged in order of magnitude as

$$0 \leq \omega_1^2 \leq \omega_2^2 \leq \dots \leq \omega_j^2 \leq \dots \leq \omega_n^2$$

Multiplying (3.17) by the transpose of the eigenvector  $\{u_j\}$  produces the following Rayleigh quotient for the squared natural frequency  $\omega_j$ .

$$\omega_j^2 = \frac{\{u_j\}^T [K] \{u_j\}}{\{u_j\}^T [M] \{u_j\}} \quad (3.18)$$

For single modal structures, the derivative of the eigenvalue with respect to any design variable  $x$  is given by

$$\frac{\partial(\omega_j^2)}{\partial x} = \frac{\{u_j\}^T \left[ \frac{\partial [K]}{\partial x} - \omega_j^2 \frac{\partial [M]}{\partial x} \right] \{u_j\}}{\{u_j\}^T [M] \{u_j\}} \quad (3.19)$$

Details of this eigenvalue derivation will be discussed in detail in Chapter 4. To determine the change in natural frequency, the above equation is approximated to

$$\Delta(\omega_j^2) \approx \frac{\{u_j\}^T ([\Delta K] - \omega_j^2 [\Delta M]) \{u_j\}}{\{u_j\}^T [M] \{u_j\}} \quad (3.20)$$

To obtain the value of  $\Delta(\omega_j^2)$  from the previous eigenvalue solution, it is assumed that the eigenvector  $\{u_j\}$  is approximately the same before and after the change in the structure. The assumption that the mode shape does not change significantly in between design cycles has been commonly used in frequency optimisation. As discussed earlier, suppose if an arbitrary element,  $i$ , is removed from the structure, the change in global mass matrix  $[\Delta M] = -[m_i]$  and the change in global stiffness matrix  $[\Delta K] = -[k_i]$ . Hence the change in the  $j^{\text{th}}$  natural frequency (squared) due to the removal of  $i^{\text{th}}$  element,  $\Delta(\omega_{ij}^2)$  is given by

$$\Delta(\omega_{ij}^2) \approx \frac{\{u_j\}^T (\omega_j^2 [m_i] - [k_i]) \{u_j\}}{\{u_j\}^T [M] \{u_j\}} \quad (3.21)$$

If only one particular frequency, say  $\omega_j$ , is considered for optimisation, the following sensitivity number need to be calculated for each element:

$$\alpha_{if} = \frac{\{u_j\}^T (\omega_j^2 [m_i] - [k_i]) \{u_j\}}{\{u_j\}^T [M] \{u_j\}} \quad (3.22)$$

where the subscript,  $f$  in  $\alpha_{if}$  refers to frequency constraint. This sensitivity number indicates which elements should be removed from the structure so that the concerned frequency will be shifted towards a desired direction. From the definition of eigenvalue problem in finite element method (equation 3.17), the summation of  $\alpha_{if}$  for all the elements in the structure should be zero. Thus the values of  $\alpha_{if}$  range from minimum negative value to maximum positive value. Hence to increase the natural frequency  $\omega_j$ ,

elements with highest  $\alpha_{if}$  values should be removed and to decrease  $\omega_j$ , elements with lowest  $\alpha_{if}$  values should be removed. It is also possible to reduce the structural weight with least change in  $\omega_j$  by removing elements with  $\alpha_{if}$  close to zero.

The denominator in equation (3.22) can be omitted in sensitivity number calculations if only one frequency is considered since it is the same for all elements. However, when multiple frequencies are considered, this term cannot be omitted unless all the concerned eigenvectors have been normalised with respect to  $[M]$ . Sensitivity numbers are also needed to be redefined according to the requirement. For example in the case of optimising the gap between two frequencies, say  $\omega_k$  and  $\omega_j$  ( $k > j$ ),  $\alpha_{if} = \Delta(\omega_{ik}^2 - \omega_{ij}^2)$ .

The evolutionary procedure for frequency optimisation is summarised as follows:

*Step 1:* Discretise the structure using a fine mesh of elements.

*Step 2:* Perform dynamic analysis and solve the eigenvalue problem.

*Step 3:* Calculate sensitivity number  $\alpha_{if}$  for each element.

*Step 4:* Remove a small number of elements to shift the concerned frequencies towards a desired direction.

*Step 5:* Repeat Steps 2 to 4 until desired optimum design is obtained.

This method has also been extended to problems with multiple frequency constraints (Xie and Steven 1996). This is very similar to the situation of optimisation with multiple static load cases. Recently Zhao *et al.* (1996c) extended this method to structures with

non-structural lumped masses. It should be noted here that the sensitivity number for frequency changes are obtained only for single modal cases. The extension of this to multimodal structures will be dealt with in detail in Chapter 5.

### **3.3 Implementation of ESO Methods into Finite Element Codes**

A batch file needs to be set up to handle the iteration cycles automatically. In each iteration, after the static or dynamic analysis, a subprogram is used for the sensitivity number calculations and subsequent element removal. From the expressions of sensitivity numbers,  $\alpha_{is}$ ,  $\alpha_{ic}$ ,  $\alpha_{id}$  and  $\alpha_{if}$ , it is seen that the computational cost involved in calculating these values, all at element level, are nominal when compared with the cost of solving the static or dynamic problem.

The element removal can be done by simply assigning the material property number of the rejected elements to zero and ignore these elements when the global stiffness matrix is assembled in the subsequent solutions. As more and more elements are eliminated, the solution time becomes less and less. When removing elements it is important to maintain the integrity of the structure. From the finite element formulation, violating the integrity of the structure may lead to a non-positive definite stiffness matrix or singular stiffness matrix. Chu *et al.* (1997b) and Zhao *et al.* (1996b) have proposed methods to overcome this problem. Symmetric nature of some structures should also be preserved during element removal and throughout the iteration cycles.

One useful feature in any structural optimisation method is the incorporation of non-design domain. For example, in stress problems some region in the structure may be at

low stress level but are essential for attachment or any other purposes and should not be removed during the iterations. The elements in the non-design domain may have the same material properties as other elements, but are assigned to a special material property number. During the optimisation process, elements with this special material property number are simply ignored for element removal.

At the end of each iteration, a picture of the remaining elements may be stored. Once the whole process is finished, the evolution history of the structure can be viewed from the stored pictures in a sequence. This option allows the designer to know every stage of the process and lets him to consider intermediate designs as well. Unlike many other FEA based structural optimisation methods, the ESO does not require re-generating new finite element meshes even when the final structure departs substantially from the initial structure. This makes the ESO methods very easy to be implemented into existing FEA codes.

### **3.4 Discussion on Existing ESO Methods**

From the previous sections, it is noted that for stiffness, displacement and frequency problems, sensitivity numbers are obtained from the first derivative of the corresponding structural response and these sensitivity numbers indicate the change in structural response due the removal of a particular element. However for stress problems the element stress level is used as an indicator for element removal. (For the sake of consistency, the notation used to define the sensitivity number of an element,  $\alpha_i$  is used to indicate the element stress ratio as well.) This is because the derivative of element

stress matrix or element stress level is computationally very expensive. In finite element method, the element stress matrix,  $\{\sigma\}_i$  can be expressed by the following equation.

$$\{\sigma\}_i = [E]_i [B]_i \{d\}_i \quad (3.23)$$

where  $[E]_i$  is the element material property matrix,  $[B]_i$  is the strain-displacement relation and  $\{d\}_i$  is the element displacement vector. The derivative of  $\{\sigma\}_i$  with respect to any design variable  $x$  is given by

$$\frac{\partial \{\sigma\}_i}{\partial x} = [E]_i [B]_i \frac{\partial \{d\}_i}{\partial x} \quad (3.24)$$

where  $[E]_i$  and  $[B]_i$  are independent of design variables. Substituting equation (3.6) for element displacement derivative, the above equation is reduced to

$$\frac{\partial \{\sigma\}_i}{\partial x} = -[E]_i [B]_i [K]^{-1} \frac{\partial [K]}{\partial x} \{d\} \quad (3.25)$$

Hence to determine element stress gradient  $[K]^{-1}$  should be known. None of the FEA packages stores or calculates  $[K]^{-1}$ . Simultaneous linear equations for static analysis are usually solved by Gaussian elimination of forward reduction and backward substitution. Even if the  $[K]^{-1}$  is available, gradient of element displacement matrix need to be established. This problem does not arise when obtaining gradient of a particular displacement component. In such case a virtual load is applied at that particular degree of freedom and the use of virtual load displacement eliminates the need of  $[K]^{-1}$  in the calculations.

Since there is no explicit stress-nodal force relations for continuum finite element models, the cost of evaluating even the approximate stresses is quite high. Much attention has been paid to solve problems with stress constraints using approximate

techniques such as the use of intermediate variables, approximations of element forces (Vanderplaats and Salajegheh 1987) or approximate displacement models (Kirsch 1992). However in all these methods either  $[K]^{-1}$  is known or decomposed matrices of  $[K]^{-1}$  are used. This high computational cost involved with stress constraints is one of the reason for the popularity of fully stressed design even it does have drawbacks.

The ESO methods described in this chapter for stress and frequency problems do not contain any clear statements for objectives or constraints. In these methods either stress distribution of the structure is brought to uniform or the concerned frequencies are optimised while reducing the weight of the structure. These ESO methods are not formulated to give minimum weight designs for a prescribed frequency or for a prescribed allowable stress or reversibly these methods cannot be used to extremise the concerned frequency or the maximum stress for a specified weight of structure. Zhao *et al.* (1996a, 1996b) attempted to solve this issue for problems with frequency constraints by providing a design chart or an evolutionary path. This design chart describes the evolutionary process of the structure and can be generated using the information associated with removing the most inefficiently used material gradually from the initial design domain until the minimum weight is met for maintaining the integrity of the structure. However ESO methods described here for stiffness and displacements constraints, can be effectively used to obtain minimum weight designs for prescribed values of displacement and compliance.

### **3.5 Summary**

In the preceding sections, concepts of ESO methods for problems with stress, stiffness, displacement and frequency constraints have been discussed. These methods have been used to solve many complex problems and validated against various classical optimum solutions. Many shape and layout designs of the existing solutions obtained by using other complex methods such as homogenisation and mathematical programming methods have been reproduced by this simple evolutionary method (Xie and Steven 1997). The rest of the thesis will be devoted to discussions on the candidate's findings in her attempt to extend the ESO method to optimum designs of structures against buckling.

## **CHAPTER 4 - ESO FOR STRUCTURES AGAINST BUCKLING**

### **4.1 Introduction**

In Chapter 3, evolutionary structural optimisation (ESO) methods for problems with stress, displacement, stiffness and frequency constraints have been discussed. This chapter describes the theoretical basis of the ESO method for structures with stability constraints. In general the instability is connected with several catastrophic failures such as buckling, overturning, sliding, collapse etc. In structural problems, the most common instability condition is buckling. Buckling occurs when the applied load reaches a critical value where a member in a structure or the whole structure converts its membrane strain energy into bending strain energy.

Optimum design against buckling may be obtained by finding the minimum weight design of a structure that satisfies the prescribed buckling load constraint. Alternatively it may be achieved by maximising the critical buckling load of the structure while keeping its weight, volume or mass constant. For the convenience of comparing the efficiency of different designs, the latter approach is generally used. In this chapter ESO method is proposed for maximising the critical buckling load of a structure of constant weight. The extension of ESO method to minimum weight design of frame structures for a prescribed buckling load is presented in Chapter 6.

In the following sections, the derivation of sensitivity number for buckling load, optimisation procedure and some criteria needed for the optimisation process are described. Two of the optimality criteria methods cited in the literature for the optimum design of frame structures against buckling are discussed and compared with the

proposed method. Illustrative examples are given to show the applicability of the ESO method for buckling optimisation. Chapters 4 to 8 focus on the optimum design of skeletal structures such as frames and trusses modelled with beam or bar elements. Optimum design of plate structures is considered in Chapter 9. This chapter applies the proposed ESO method to the optimum design of single modal frame structures only. The extension of ESO method to multimodal structures is given in Chapter 5.

## 4.2 Buckling Analysis of Structures

Buckling of bars, frames, plate and shell structures may occur as a structural response to membrane forces. Membrane forces act along member axes and tangent to plate and shell midsurfaces. The membrane force in a bar or a beam element is the axial force,  $P$ , and the membrane forces in a plate or a shell element are the in-plane forces,  $N_x$ ,  $N_y$  and  $N_{xy}$ , as shown in Figure 4.1.

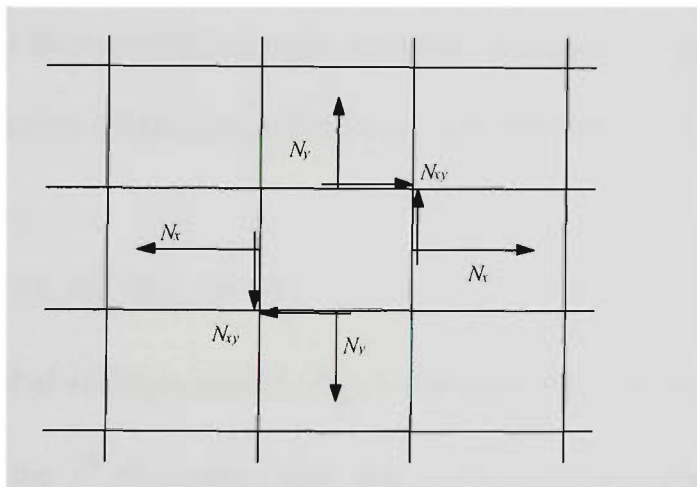


**Figure 4.1-** Membrane forces in a plate element

Small membrane deformations can store a large amount of strain energy, but comparatively large lateral deflections and rotations are needed to absorb this energy in bending deformations. Thin-walled structures and slender structures with low bending stiffness to membrane stiffness often fail as a result of buckling rather than material

yielding. There are two types of buckling that may occur in a structure. These are the local buckling of an isolated member and the overall buckling of the whole structure. Since the ESO method is based on the discrete finite element analysis, both local and global instabilities can be captured in the optimisation process.

The buckling problem may be described as determining the buckling load associated with structural instability for a prescribed loading configuration. The effects of membrane forces in an element are accounted for by an element matrix  $[k_g]$  that augments the conventional element stiffness matrix  $[k]$  in discretised system equations. The element matrix  $[k_g]$  is the non-linear element stiffness, a function of the stress state and hence of the internal element forces. Matrix  $[k_g]$  has been given various names such as element stress stiffness matrix and element geometric stiffness matrix. Assuming that the membrane forces can be obtained from the linear equations involving linear stiffness matrix only and that they remain constant during the transition to the buckled state, the linear buckling behaviour of an elastic structure is governed by the following eigenvalue problem:

$$([K] + \lambda_j [K_g]) \{u_j\} = \{0\} \quad (4.1)$$

where  $[K]$  is the global stiffness matrix,  $[K_g]$  is the global geometric stiffness matrix or stress matrix,  $\lambda_j$  is the  $j^{\text{th}}$  eigenvalue and  $\{u_j\}$  is the corresponding eigenvector. The eigenvalues from equation (4.1) are those which scale the applied load to give the buckling load. The eigenvalues are arranged in order of magnitude as

$$0 < \lambda_1 \leq \lambda_2 \leq \dots \leq \lambda_j \leq \dots \leq \lambda_n \quad (4.2)$$

The most critical buckling load is the lowest one, which is equal to the first eigenvalue  $\lambda_1$  multiplied by the applied loading. Multiplying equation (4.1) by the transpose of the eigenvector  $\{u_j\}$  produces the following Rayleigh quotient for the  $j^{\text{th}}$  eigenvalue

$$\lambda_j = -\frac{\{u_j\}^T [K] \{u_j\}}{\{u_j\}^T [K_g] \{u_j\}} \quad (4.3)$$

where the numerator represents the strain energy of the  $j^{\text{th}}$  buckling mode and the denominator represents the work done by the applied load during the transition from initial to buckled configurations.

### 4.3 Sensitivity Number for Buckling Load - Simple Eigenvalue

In ESO method, the contribution of each element to the concerned structural response needs to be assessed. For buckling optimisation, the aim is to raise the fundamental buckling load factor  $\lambda_1$ . Hence the design sensitivity (or gradient) of the eigenvalue (buckling load factor) needs to be determined. In this section sensitivity number for buckling load of simple eigenvalue is derived. A simple (or distinct or single) eigenvalue  $\lambda_j$  is associated with a unique eigenvector  $\{u_j\}$  and is differentiable with respect to any design variables. The direct approach to obtaining the eigenvalue sensitivity is to differentiate equation (4.1) with respect to a design variable  $x$  and is given below.

$$\frac{\partial ([K] + \lambda_j [K_g]) \{u_j\}}{\partial x} = 0 \quad (4.4)$$

$$\frac{\partial ([K] + \lambda_j [K_g])}{\partial x} \{u_j\} + ([K] + \lambda_j [K_g]) \frac{\partial \{u_j\}}{\partial x} = 0 \quad (4.5)$$

Multiplying equation (4.5) by  $\{u_j\}^T$  gives

$$\{u_j\}^T \frac{\partial ([K] + \lambda_j [K_g])}{\partial x} \{u_j\} + \{u_j\}^T ([K] + \lambda_j [K_g]) \frac{\partial \{u_j\}}{\partial x} = 0 \quad (4.6)$$

Since  $[K]^T = [K]$  and  $[K_g]^T = [K_g]$ , taking transpose of equation (4.1) leads to

$$([K] + \lambda_j [K_g]) \{u_j\}^T = \{u_j\}^T ([K] + \lambda_j [K_g]) = \{0\} \quad (4.7)$$

Thus the second term in equation (4.6) is reduced to zero. Therefore the eigenvector derivative is not involved in the simple eigenvalue derivative. By re-arranging equation (4.6), the eigenvalue derivative is reduced to

$$\frac{\partial \lambda_j}{\partial x} = - \frac{\{u_j\}^T \left[ \frac{\partial [K]}{\partial x} + \lambda_j \frac{\partial [K_g]}{\partial x} \right] \{u_j\}}{\{u_j\}^T [K_g] \{u_j\}} \quad (4.8)$$

By normalising the eigenvectors such that  $\{u_j\}^T [K_g] \{u_j\} = 1$ , equation (4.8) is reduced to

$$\frac{\partial \lambda_j}{\partial x} = - \{u_j\}^T \left[ \frac{\partial [K]}{\partial x} + \lambda_j \frac{\partial [K_g]}{\partial x} \right] \{u_j\} \quad (4.9)$$

Assuming that the eigenvector is approximately the same before and after a small structural modification, the change in  $j^{\text{th}}$  eigenvalue,  $\Delta \lambda_j$  due to this structural modification is approximated to

$$\Delta \lambda_j = - \{u_j\}^T ([\Delta K] + \lambda_j [\Delta K_g]) \{u_j\} \quad (4.10)$$

### 4.3.1 Sensitivity number for element removal

Consider that an element,  $i$ , is removed from the structure. As described in Chapter 3, the change in global stiffness matrix  $[\Delta K] = -[\Delta k_i]$  which can be easily calculated. However, since  $[K_g]$  depends on the current stress distribution in the structure and the removal of the  $i^{\text{th}}$  element affects the stress in its surrounding elements, it cannot be assumed that  $[\Delta K_g]$  is equal to the change in the element stress stiffness matrix of the  $i^{\text{th}}$  element only. Stress stiffness matrix of the old system (before element removal) does not provide enough information for  $[\Delta K_g]$  and a static analysis needs to be carried out after the element removal to determine the current stress distribution. If it is to be done

for each and every element it will be computationally very expensive. Therefore the change in buckling load due to element removal cannot be obtained from the finite element results of the old system unless a very computationally expensive method is employed. This difficulty does not arise in the eigenvalue optimisation of frequency problems which involve the mass matrix instead of the stress stiffness matrix.

### 4.3.2 Sensitivity number for element resizing

Now consider a small change in the cross-sectional area of an arbitrary element,  $i$ . This local cross-sectional modification of an element may be the change in plate thickness or the change in cross-sectional dimensions of bar or beam element such as width, breadth, radius etc. The change in the global stiffness matrix,  $[\Delta K]$  is equal to the change in the  $i^{\text{th}}$  element stiffness matrix,  $[\Delta k_i]$ , which can be easily calculated. The change in global stress stiffness matrix,  $[\Delta K_g]$ , is equal to zero if the axial or membrane stress resultant remains constant before and after the cross-sectional change in the elements. Such is the situation of all statically determinate structures. For a statically determinate frame, the cross sectional changes do not affect the axial forces in the members. For statically indeterminate structures,  $[\Delta K_g]$  is only negligible if the cross-sectional modifications at each iteration are so small that they do not cause significant changes in the axial or membrane stress resultants. When  $[\Delta K_g]$  is ignored, from equation (4.10) the change in the  $j^{\text{th}}$  buckling eigenvalue due to the cross-sectional change in the  $i^{\text{th}}$  element is reduced to

$$\Delta\lambda_{ij} = -\{u_{ij}\}^T [\Delta k_i] \{u_{ij}\} \quad (4.11)$$

where  $\{u_{ij}\}$  is the  $j^{\text{th}}$  eigenvector associated with the  $i^{\text{th}}$  element. The objective of buckling optimisation is to increase the fundamental eigenvalue  $\lambda_1$ . Therefore from the

above equation, the sensitivity number for buckling load of single modal structures is defined as follows:

$$\alpha_{ib} = -\{u_{i1}\}^T [\Delta k_i] \{u_{i1}\} \quad (4.12)$$

where the subscript  $b$  in  $\alpha_{ib}$  refers to buckling problem. Note that this sensitivity number is for resizing only and cannot be used for element removal.

The critical buckling load is increased when the cross-sectional area of elements with highest  $\alpha_{ib}$  is increased. If the structural weight is to be kept constant, the elements with highest  $\alpha_{ib}$  need to be strengthened and the elements with lowest  $\alpha_{ib}$  values may be weakened. In the case of an increase in the cross-sectional area  $A$  of the  $i^{\text{th}}$  element by  $\Delta A$

$$[\Delta k_i] = [\Delta k_i]^+ = [k_i(A + \Delta A)] - [k_i(A)] \quad (4.13a)$$

and in the case of a reduction in the cross-sectional area by  $\Delta A$

$$[\Delta k_i] = [\Delta k_i]^- = [k_i(A - \Delta A)] - [k_i(A)] \quad (4.13b)$$

Hence to estimate the effect of cross-sectional changes on the fundamental buckling load factor, the following two sensitivity numbers need to be calculated for each element, one for area increase

$$\alpha_{ib}^+ = -\{u_{i1}\}^T [\Delta k_i]^+ \{u_{i1}\} \quad (4.14a)$$

and the other for area reduction

$$\alpha_{ib}^- = -\{u_{i1}\}^T [\Delta k_i]^- \{u_{i1}\} \quad (4.14b)$$

So far the influence of the cross-sectional change of an element on the buckling load factor has been studied. Further if the elements in the finite element mesh are of different sizes, the element sensitivities depend also on their sizes. Here the size of the

element, say  $S_i$  for  $i^{\text{th}}$  element, is not referred to the cross-sectional dimensions. In the case of skeletal structures  $S_i$  refers to the length of the  $i^{\text{th}}$  element. In the case of plate or shell structures  $S_i$  refers to the surface area of the  $i^{\text{th}}$  element. When comparing two elements with the same  $\alpha_{ib}^+$  as defined in (4.14a), increasing the cross-sectional area of a smaller element will result in a lighter design. Similarly for elements with same  $\alpha_{ib}^-$  as defined in (4.14b), the cross-sectional area of a smaller element should be decreased. Consequently, the element sensitivity numbers for buckling load of single modal structures are redefined as follows:

$$\alpha_{ib}^+ = -\{u_{i1}\}^T [\Delta k_i]^+ \{u_{i1}\} / S_i \quad (4.15a)$$

$$\alpha_{ib}^- = -\{u_{i1}\}^T [\Delta k_i]^- \{u_{i1}\} / S_i \quad (4.15b)$$

The calculation of these sensitivity numbers only involves small matrices of individual elements. The computation cost for calculating these sensitivity numbers for all elements is nominal when compared with the cost of solving the eigenvalue problem (4.1).

#### 4.4 Evolutionary Procedure for Buckling Optimisation

Unlike the other ESO procedures described in Chapter 3, the buckling optimisation is carried out by changing the cross-sectional areas of elements for structures of fixed layout. Optimum designs against buckling may be obtained either by finding the minimum weight design for a prescribed buckling load or by maximising the buckling load of the structure while keeping its weight constant. The former approach may start with an over-designed structure with excess weight followed by gradually removing material from the structure. The latter approach involves gradually shifting material

from the strongest locations to the weakest without adding or losing any weight. The optimisation procedure for the latter approach is described below. It is obvious that the optimum solution cannot be achieved in one step. An iterative procedure has to be adopted, i.e. only a small number of elements should be resized at each iteration.

*Step 1:* Discretise the structure using a fine mesh of finite elements to adequately represent the prebuckling stress distribution and buckling modes.

*Step 2:* Solve the eigenvalue problem (4.1).

*Step 3:* Calculate the sensitivity numbers  $\alpha_{ib}^+$  and  $\alpha_{ib}^-$  for each element.

*Step 4:* Increase the cross-sectional areas of elements which have the highest  $\alpha_{ib}^+$  values and decrease the cross-sectional areas of the same number of elements which have the highest  $\alpha_{ib}^-$  values. Impose the sizing constraints, i.e. if the design variable (which represents the cross-sectional area) of an element  $x_i$  is greater than the prescribed maximum  $x_{max}$ , let  $x_i = x_{max}$  and similarly if  $x_i < x_{min}$ , let  $x_i = x_{min}$ .

*Step 5:* Calculate the total volume and if it is not equal to the original volume, scale the cross-sectional areas obtained after Step 4 to give the original volume.

*Step 6:* Repeat Steps 2 to 5 until the buckling load factor cannot be increased any further.

A batch file is set up to handle the iteration cycles automatically so that the optimisation process becomes as simple as repeated finite element analyses. In each cycle of iteration, after the static and buckling analyses using standard FEA packages, a subprogram is used to calculate sensitivity numbers and carry out subsequent element resizing. When

resizing, the cross-sectional area of elements is allowed to vary in small steps in a prescribed manner. The geometric properties of the cross-section (design variables) could be one or several from breadth or depth of a rectangular section, radius of the circular section, web or flange thickness of I or L section, thickness of plate and shell elements etc. For such simple variations  $[\Delta k_i]^+$  and  $[\Delta k_i]^-$  matrices can be easily calculated. All the other information required for the calculation of sensitivity number is readily available from the finite element solution obtained in Step 2.

At each iteration only a small number of elements should be subjected to resizing. The percentage of elements subjected to resizing is called here as the *resizing ratio*. The *resizing ratio* and the *step size* of design variables used for the cross-sectional modification at each iteration have to be given in the above evolutionary procedure. The resizing ratio and the step size are usually kept constant throughout the optimisation process. However, different values of resizing ratio and step size can be prescribed at different stages of the optimisation process. At final stages of the optimisation process these parameters can be made smaller to obtain more accurate designs. The influence of these parameters on the optimum solutions will be discussed with the examples in later sections.

When resizing the elements based on their sensitivity numbers, certain requirements of the problem need to be accommodated. They are described below.

*Non-design domain:* In certain cases some part of the structure has to be kept unchanged. In such cases it is possible to freeze this part of the structure as the non-

design domain. The elements within this non-design domain are assigned a special material property number even if they have the same material properties as other elements. During the optimisation process, elements with this special property number are not subjected to resizing.

*Sizing constraint:* If the design variables of elements reach their prescribed upper or lower bounds, these elements are not considered for resizing. However these elements are not frozen as those in non-design domain. Because in subsequent iterations design variables of these elements might vary in opposite directions. At each iteration the number of elements reached their extreme values should be monitored to calculate the actual required number of elements to be resized.

*Structural symmetry:* If the structural layout and the loadings are symmetric about any axis, the symmetric nature of the structural system should be preserved at each iteration through out the optimisation process. Unlike in static analysis, the full structure has to be considered for eigenvalue solutions even the structure has any symmetry. If the structure loses its symmetry during resizing it will lead to non-optimal design. Usually the number of elements subjected to resizing should be determined by considering the number of symmetric axes in the system. For example, if there are two symmetric axes in the system as shown in Figure 4.2a, the number of elements to be strengthened or weakened in an iteration should be equal to four or products of four so as to maintain the symmetric nature of the target structure. However if elements fall on the symmetric axes as shown in Figure 4.2b, the above rule cannot be adopted. The elements which are symmetric to each other should have the same value of sensitivity number. Hence by

using the limiting values of sensitivity numbers (which determines which element should be resized) instead of considering the number of elements directly, structural symmetry can be preserved. When determining the limiting values of sensitivity numbers, the elements which have already reached their upper or lower bounds should not be considered.

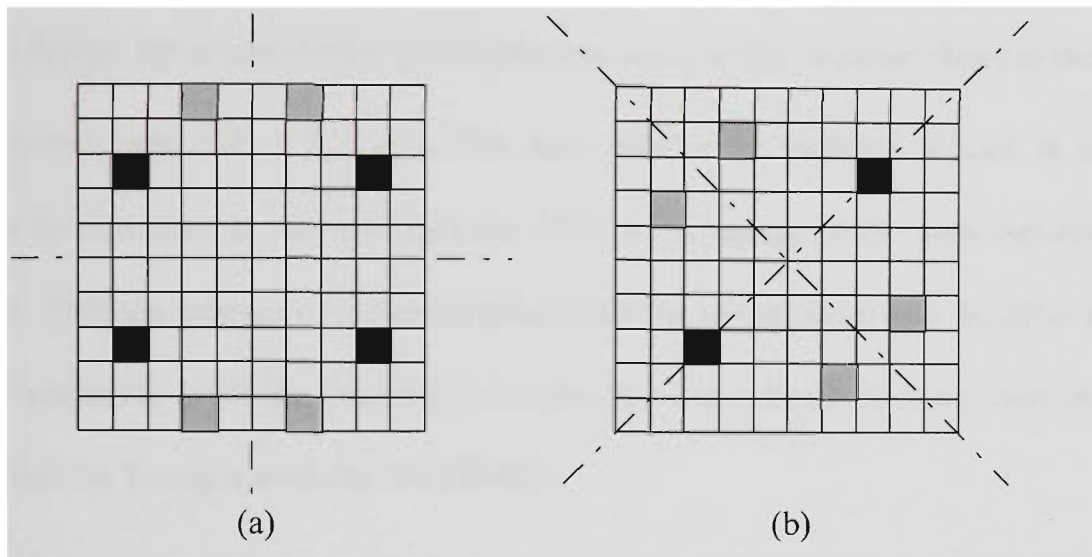


**Figure 4.2** - Symmetric elements in structures

*Constant volume/weight:* After resizing the elements, the volume of the structure has to be checked. If it is not equal to the original volume, design variables (cross-sectional dimensions) should be uniformly scaled to get the original volume. When uniformly scaling the design variables it is again necessary to impose the sizing constraints. Uniform scaling with sizing constraints need to be carried out in succession until the volume becomes equal (with tolerance) to the original volume.

## 4.5 Examples

The capability of the proposed method for cross-sectional optimisation of structures against buckling of single modal structures is illustrated with several examples. In the following sections an optimum buckling load factor,  $OF$ , defined as the ratio of the critical buckling load factor of the optimum design,  $\lambda_{cr}^{opt}$  to that of the equivalent uniform design,  $\lambda_{cr}^{uni}$  is used for comparing the efficiency of the optimum shape to that of the uniform shape ( $OF = \lambda_{cr}^{opt} / \lambda_{cr}^{uni}$ ). The total number of elements resized at each iteration is expressed as the resizing ratio ( $RR$ ), a percentage of the total number of elements. Half the number of elements resized will be strengthened and the other half will be weakened. In all the following examples the initial design is of uniform cross-section and the Young's modulus  $E = 200$  GPa.

### 4.5.1 Example of column optimisation

A slender column of variable, but geometrically similar cross-sections where the area  $A(x)$  and the moment of inertia  $I(x)$  at section  $x$  are correlated by  $I(x) = cA(x)^p$ , with the constant  $c$  given by the cross-sectional geometry is considered for optimisation. Three cases, where  $p = 1, 2$  and  $3$ , are considered. The column is simply supported at both ends and is subjected to a compressive axial load. The column is divided into 100 linear elements of equal length.

Case 1:  $p = 1$

The simplest cross-sectional shape which may satisfy the relationship  $I(x) = cA(x)$  is the rectangle with constant depth  $d$  and variable width  $b(x)$  so that  $I(x) = b(x)d^3/12 = A(x)d^2/12$ . The dimensions of the column are as follows: length  $L = 1$  m,  $d = 50$  mm,

initial value for  $b = 65$  mm. During the optimisation,  $b$  is allowed to vary in steps of 5 mm to the maximum of 125 mm and to the minimum of 5 mm. Hence 25 different cross-sectional areas are allowed in the design.

Case 2:  $p = 2$

For a circular cross-section,  $I(x) = \pi r(x)^4 / 4 = A(x)^2 / 4\pi$ , where  $r(x)$  is the radius at section  $x$ . The dimensions of the column are as follows: length  $L = 1$  m, initial value for  $r^2 = 40$  mm<sup>2</sup>. During the optimisation,  $r^2$  is allowed to vary in steps of 1 mm<sup>2</sup> to the maximum of 60 mm<sup>2</sup> and to the minimum of 10 mm<sup>2</sup>. Hence 51 different cross-sectional areas are allowed in the design.

Case 3:  $p = 3$

For the rectangular cross-section with constant width  $b$  and variable depth  $d$ , the relationship  $I(x) = cA(x)^3$  is satisfied since  $I(x) = bd(x)^3/12 = A(x)^3 / 12b^2$ . The dimensions of the column are the same as in Case 1 but in this case the depth  $d$  is allowed to change in the range of 5 mm to 125 mm in steps of 5 mm instead of the width  $b$ . Again 25 different cross-sectional areas are allowed in the design.

The optimum shapes of the column for the above three cases are obtained after between 12 and 20 iterations. For all three cases, a resizing ratio of  $RR = 40\%$  is used. These shapes are given in Figure 4.3. Due to symmetry only a quarter of each column is shown. The evolutionary histories of the buckling load factors are shown in Figure 4.4. In Table 4.1 the final optimum buckling load factors obtained by the ESO method are compared with the exact solutions obtained from variational calculus method (see Hafta

and Gurdal, 1992). Excellent agreements between the results from two methods are observed.

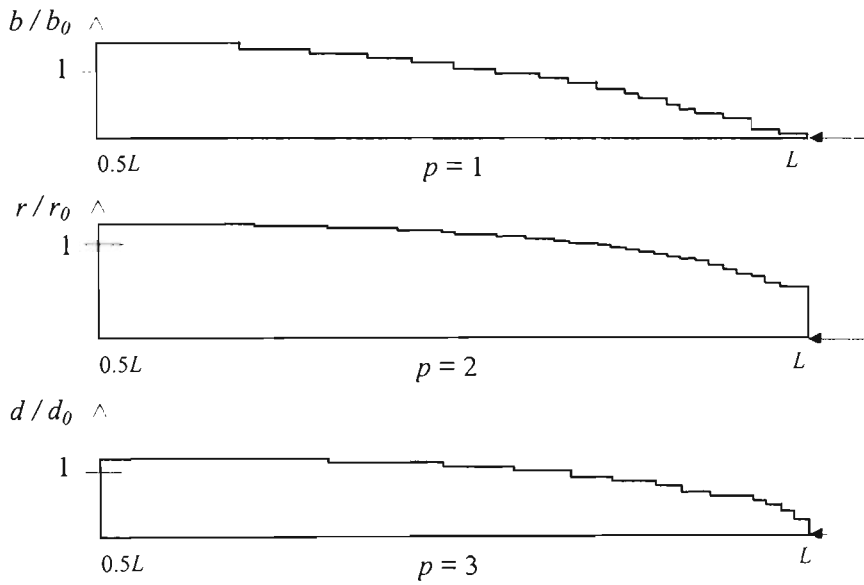


Figure 4.3 - Optimum shapes of simply supported columns

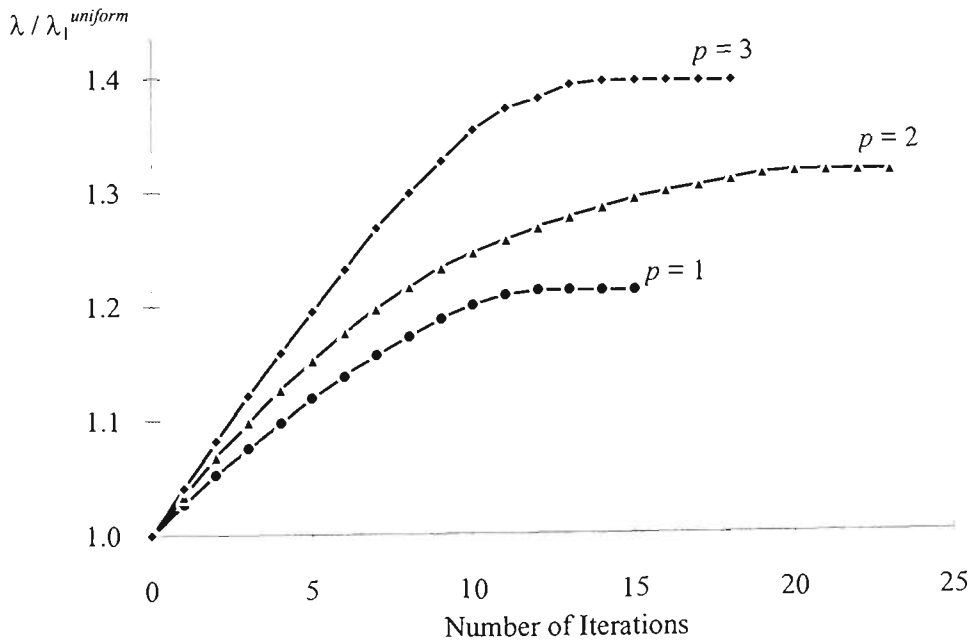


Figure 4.4 - Optimisation histories of the simply supported columns

**Table 4.1** - Optimum buckling load factors for simply supported columns

$p$	$OF = \lambda_{cr}^{opt} / \lambda_{cr}^{uni}$		% difference
	Exact	ESO	
1	$12 / \pi^2 = 1.215$	1.214	-0.1
2	$4 / 3 = 1.333$	1.328	-0.4
3	$125 / \pi^2 = 1.407$	1.400	-0.5

## 4.5.2 Examples of frame optimisation

### 4.5.2.1 Optimum design of a three member portal frame

A three member portal frame which was analysed by Szyszkowski and Watson (1988) is considered. The frame is pinned at the base and is statically indeterminate by one redundancy. The frame layout and the loading are shown in Figure 4.5. All the three members are of circular cross-sections and of equal length of 1m. Each member is divided into 10 elements of equal length. Initial uniform  $r^2$  is equal to 100 mm<sup>2</sup>. A resizing ratio of 40% is used. No maximum or minimum is specified for  $r^2$ .

The final optimum shape of the frame is shown in Figure 4.5 and the final design values are tabulated in Table 4.2 for half of the symmetric frame. The critical buckling eigenvalues of initial design and optimum design are 2.86 and 4.00 respectively. Optimum designs are obtained independently with two step sizes, 5 mm<sup>2</sup> and 2.5 mm<sup>2</sup>. The evolutionary histories of the buckling load factors of these two step sizes are shown in Figure 4.6. The history of the second buckling eigenvalue is not shown since in this case it is far from the first eigenvalue. From the uniform to the optimum design the second eigenvalue has decreased from 20.26 to 15.28.

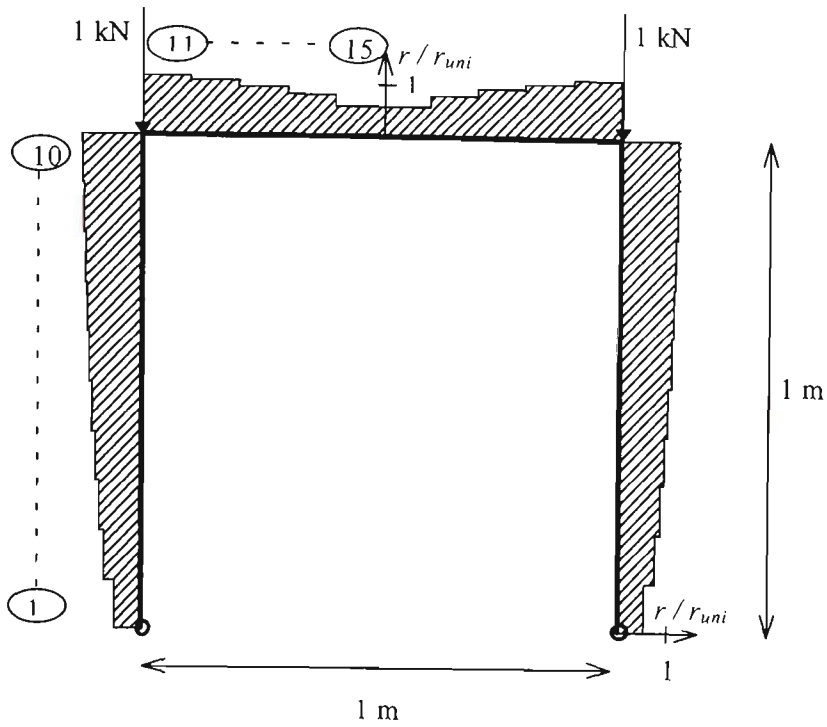


Figure 4.5 - Optimum shape of the three member frame (without sizing constraints)

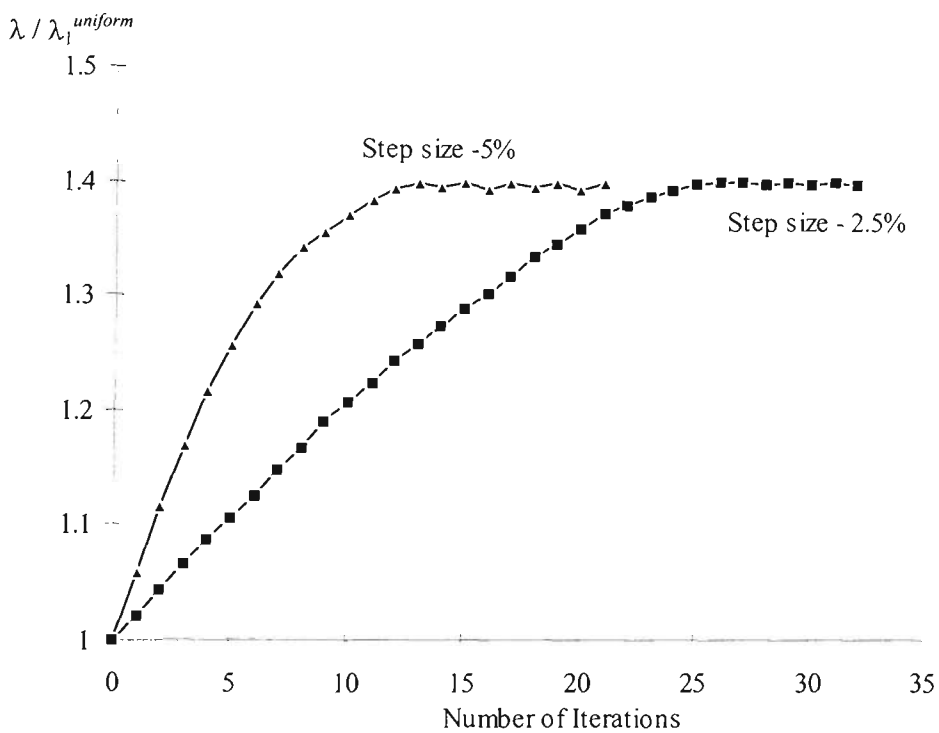


Figure 4.6 - Optimisation histories of the 3-member frame (without sizing constraints)

Obviously the smaller step size requires a high number of iterations. However the optimum designs obtained with these two step sizes are not much different although the smaller step size gives slightly better design. Optimum buckling load factors for these

designs are very close and they equal to 1.401 and 1.400 for step sizes  $2.5 \text{ mm}^2$  and  $5 \text{ mm}^2$  respectively. Szyszkowski and Watson (1988) also obtained  $OF = 1.401$  with the same number of elements.

**Table 4.2** - Optimum design values of the three member portal frame

Element number	Optimum design $r^2$ ( $\text{mm}^2$ )	
	Without sizing constraints	With sizing constraints
1	31.9	70.0
2	60.4	70.0
3	79.8	73.2
4	94.8	88.5
5	109.7	101.3
6	119.4	114.0
7	129.0	121.4
8	136.2	130.0
9	140.9	130.0
10	145.8	130.0
11	138.6	130.0
12	116.9	111.4
13	94.8	88.4
14	67.5	70.0
15	34.2	70.0

For the optimum design with no sizing constraints, the design variable  $r^2$  range from maximum  $145.8 \text{ mm}^2$  at element 10 to minimum  $31.9 \text{ mm}^2$  at element 1. This portal frame is reanalysed with sizing constraints. In this case,  $r^2$  is allowed to vary to the maximum  $130 \text{ mm}^2$  and to the minimum  $70 \text{ mm}^2$ . Again  $RR = 40\%$  is used. The final

optimum shape and the iteration histories are shown in Figure 4.7 and Figure 4.8 respectively. Again two step sizes,  $5 \text{ mm}^2$  and  $2.5 \text{ mm}^2$ , are used independently to obtain the optimum designs. No difference is observed in the final designs obtained with these two step sizes although the smaller step size obviously requires a high number of iterations. The critical buckling eigenvalue of the optimum design is equal to 3.705 ( $OF = 1.295$ ). During optimisation the second eigenvalue has decreased from 20.26 at the uniform design to 17.33 at the optimum design. The final design values are also given in Table 4.2 (column 3).

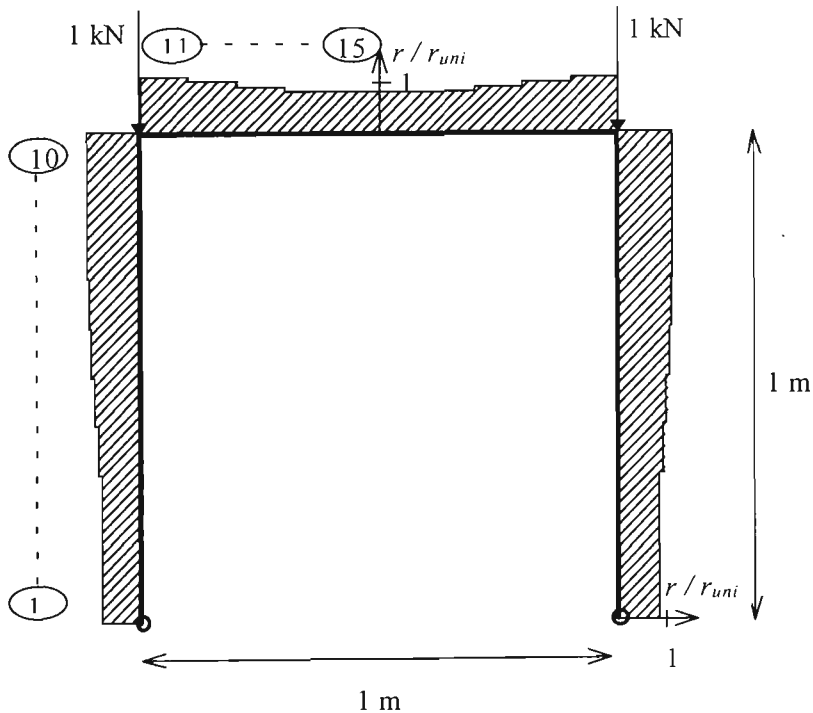


**Figure 4.7** - Optimum shape of the three member frame (with sizing constraints)

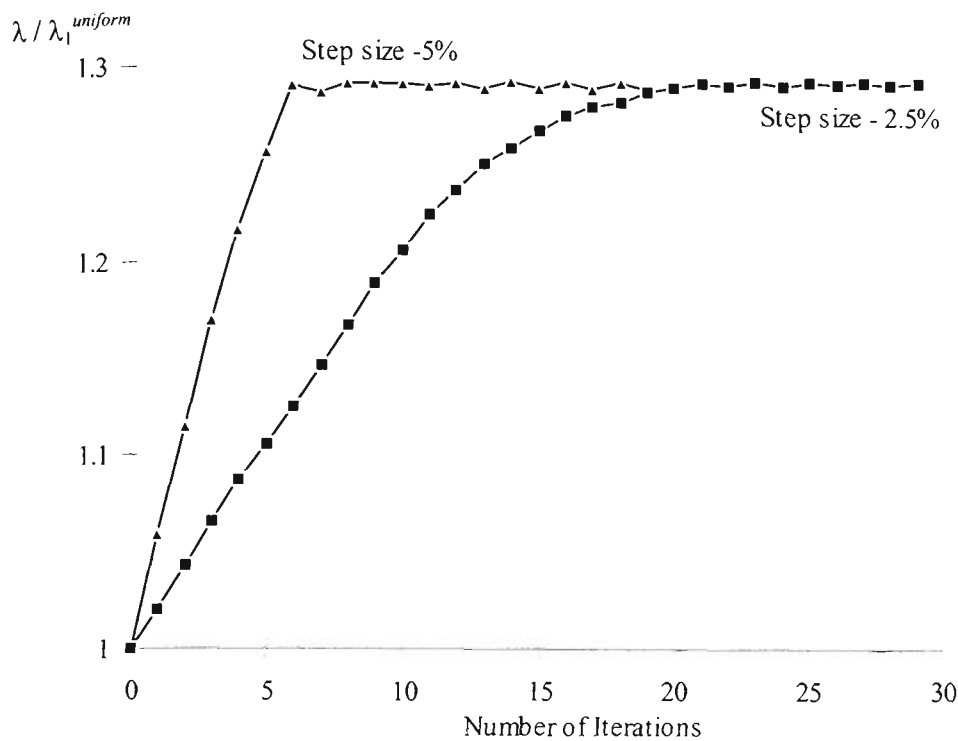


**Figure 4.8** - Optimisation histories for the 3-member frame (with sizing constraints)

#### 4.5.2.2 Optimum design of a 2-cell frame

Optimum design of a pin based 2-cell frame as shown in Figure 4.9(a) is sought using the proposed ESO method. All the members are of circular cross-sections and of equal length of 1 m. Each member is divided into three elements of equal length. Initial uniform  $r^2$  is equal to 100 mm<sup>2</sup> for all the members and  $r^2$  is allowed to vary to the maximum of 200 mm<sup>2</sup> to the minimum of 10 mm<sup>2</sup> in steps of 5 mm<sup>2</sup>.  $RR = 40\%$ .

The optimum to initial uniform area ratios (normalised areas) for half of the symmetric frame and the evolutionary histories of the first two eigenvalues are shown in Figures 4.9(a) and 4.9(b), respectively. Critical buckling eigenvalues of the uniform and the optimum designs are 2.861 and 5.602 respectively ( $OF = 1.960$ ). The maximisation of the first eigenvalue brings about some reduction of the second eigenvalue. The second

eigenvalue decreases from 9.475 at the uniform design to 6.842 at the optimum design. Szyszkowski and Watson (1988) also obtained the same optimum design for this frame.

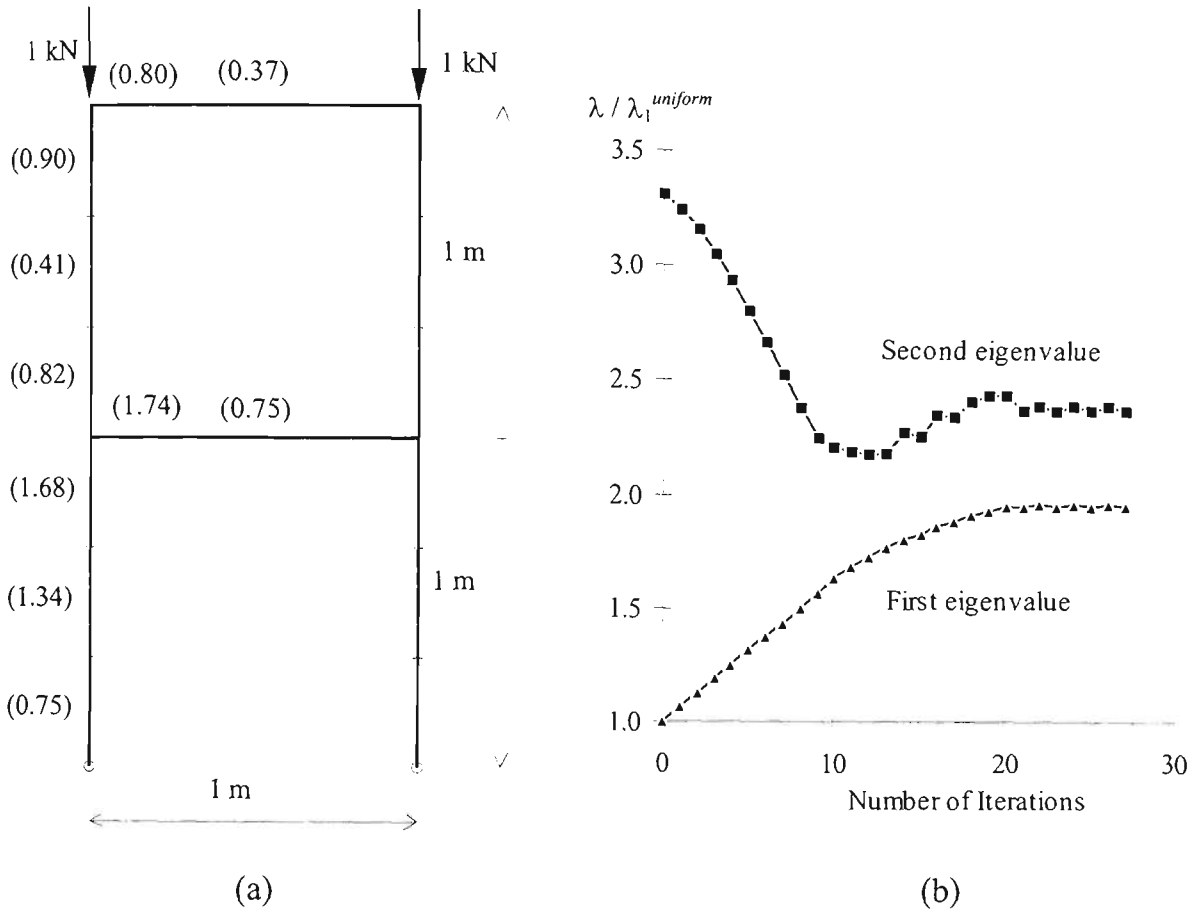


**Figure 4.9** - Optimum design and iteration history of the 2-cell frame (18 design variables)

In the above examples each member of the structure is divided into several elements. In most cases, it is not practical to have different cross-sections within a member. One might seek an optimum design by treating each member as a single segment having the same cross-sectional area. If each member in the structure is treated as a single element, finite element solutions may not be accurate enough and the final design may not be optimum. This problem can be overcome by using the finite element modelling, allowing a number of elements to model each member (as in the case of above

examples), but assigning a *modified member sensitivity number* for all the elements within a particular member. If all the elements in a member have the same sensitivity number, when resizing all the elements in that particular member will acquire a single design value. This modified member sensitivity number is obtained from the average of the element sensitivity numbers of all the elements of that particular member.

The 2-cell frame is reanalysed allowing only one design variable for each member by using the modified member sensitivity number instead of element sensitivity numbers. The final design normalised areas and the iteration histories are shown in Figure 4.10. The critical buckling eigenvalue of the final design is equal to 4.425 ( $OF = 1.546$ ) compared to the previous optimum eigenvalue 5.601. However, a more practical design is obtained with the latter approach.

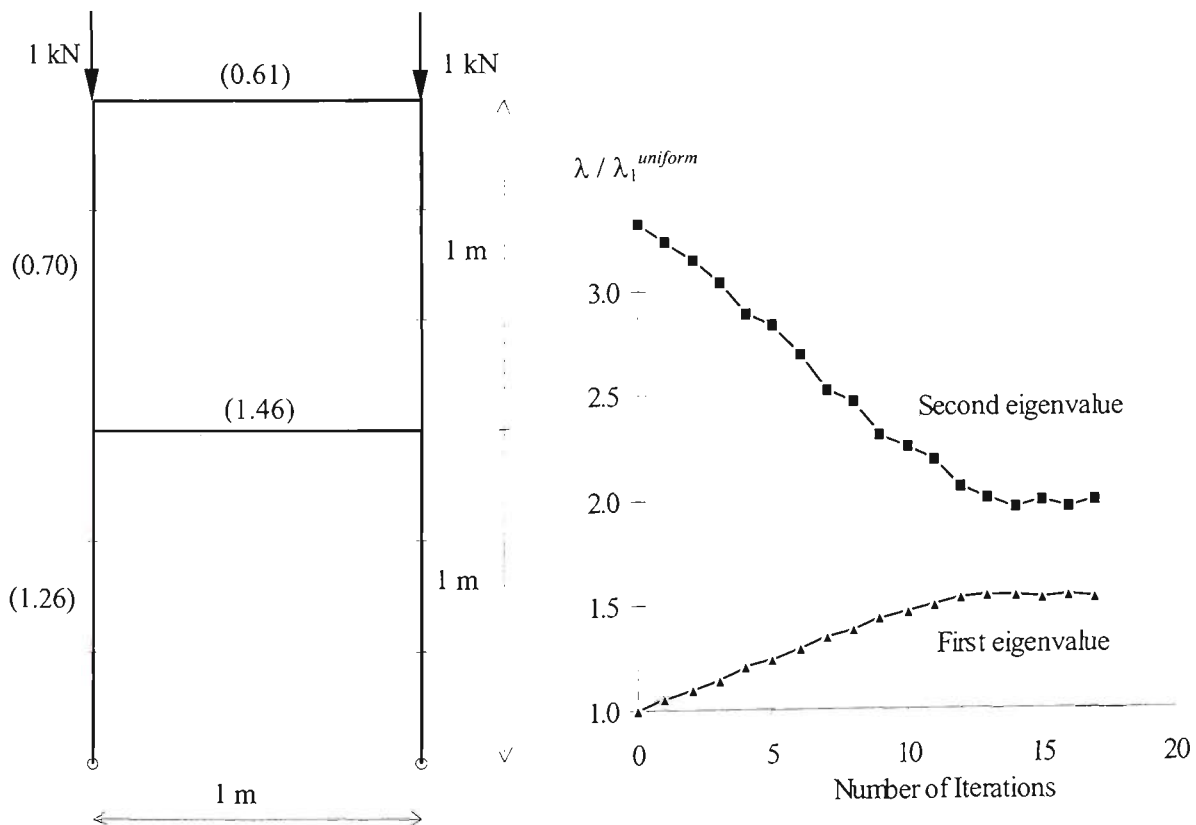


**Figure 4.10** - Optimum design and iteration history of the 2-cell frame (6 design variables)

### 4.5.2.3 Optimum design of a three storey frame

A 3-bay, 3-storey, pin based frame as shown in Figure 4.11 is considered for buckling optimisation. The frame layout, loadings and member numbering are shown in the figure. All the members are of rectangular cross-section with constant breadth,  $b = 10$  mm. Initial uniform depth  $d$  is equal to 20 mm for all members and  $d$  is allowed to change in steps of 1 mm. 20% of the total elements are subjected to resizing at each iteration. Initially the frame is optimised with no sizing constraints i.e. the design variable  $d$  can vary to any value.

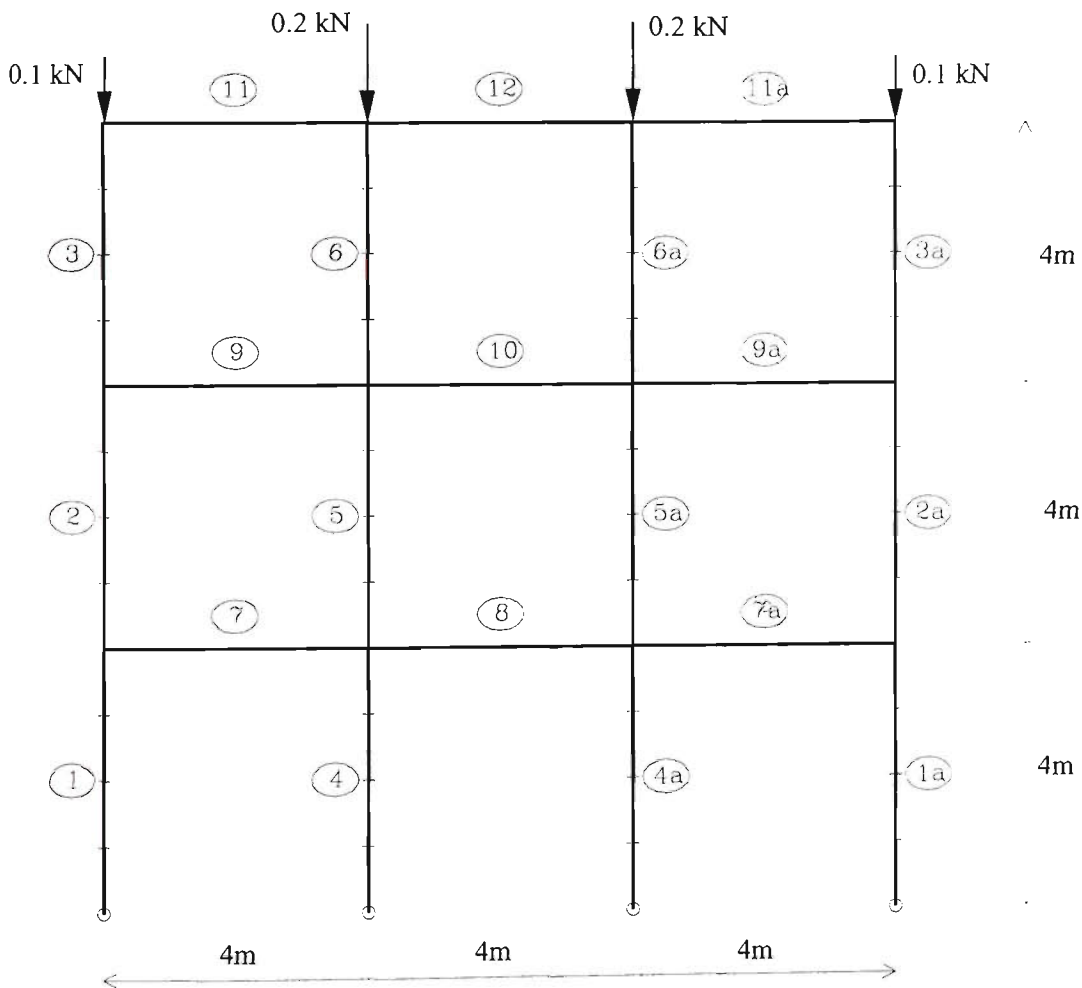


**Figure 4.11** - Structural layout of the 3-storey frame

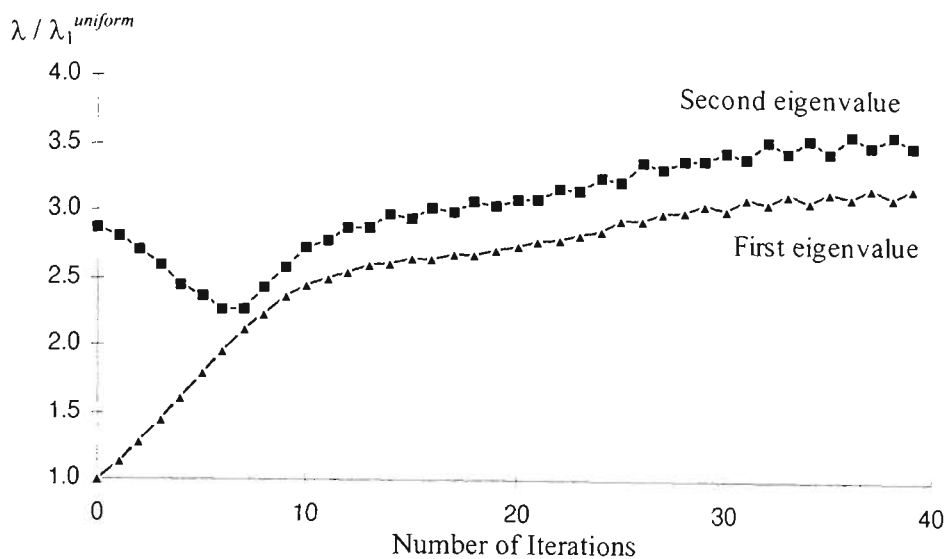
The following three cases are considered for optimisation.

*Case 1:* Each member of the frame is divided into 4 elements of equal length and allowed to have different depth for each element (optimisation using element sensitivity numbers).

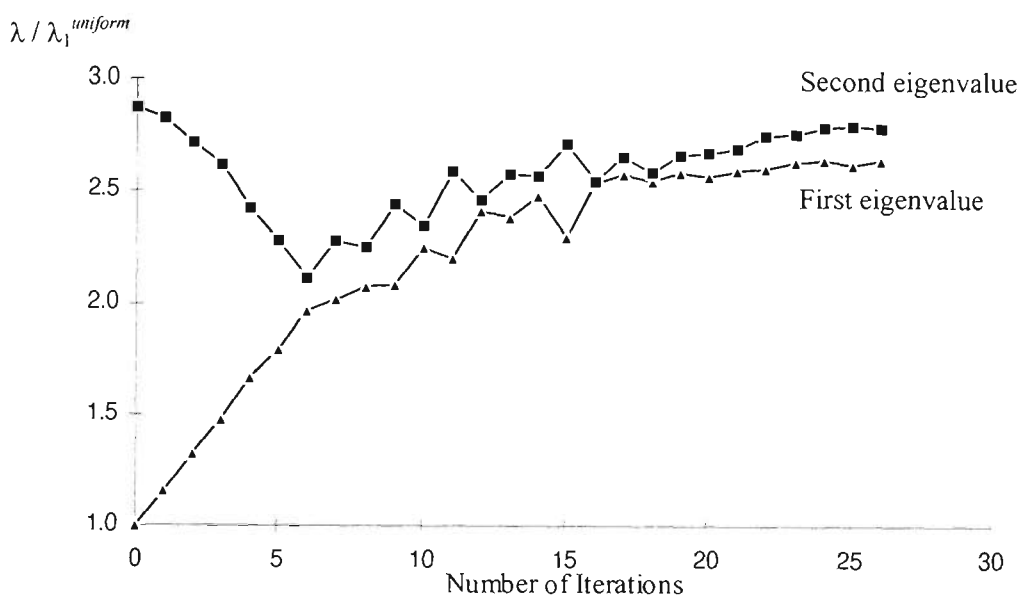
*Case 2:* Each member of the frame is divided into 4 elements of equal length, but each member is allowed to have only one design variable (optimisation using modified member sensitivity numbers).

*Case 3:* Each member of the frame is modelled with a single element.

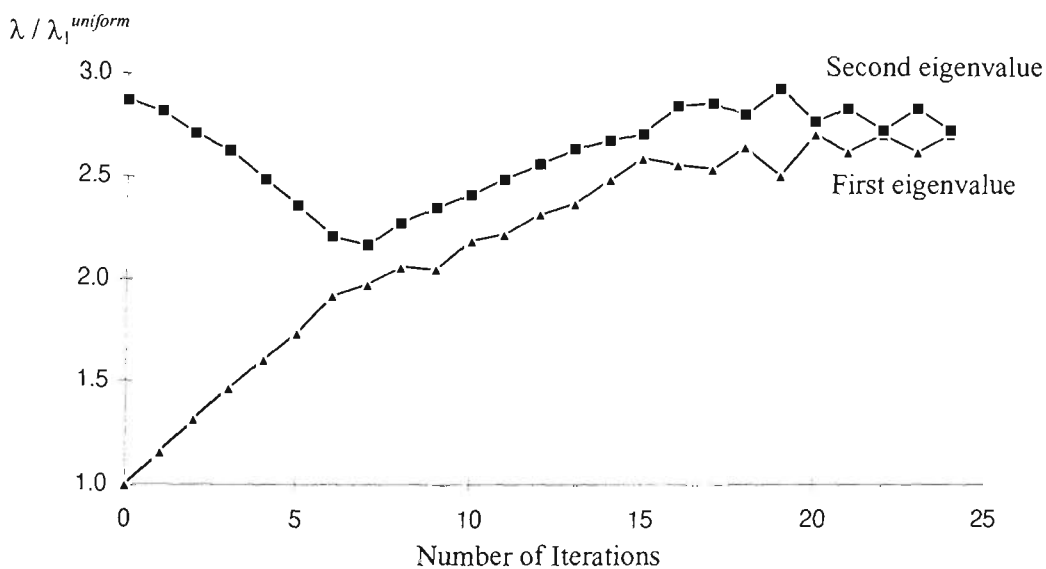
The evolutionary histories of the first two eigenvalues for all three cases are shown in Figure 4.12. The first two eigenvalues of initial and optimum designs of all three cases are tabulated in Table 4.3.



(a) Case 1



(b) Case 2



(c) Case 3

Figure 4.12 - Optimization histories of the 3-story frame

**Table 4.3** - Buckling load factors of the 3-storey frame (without sizing constraints)

	$\lambda_1$	$\lambda_2$	<i>OF</i>
Initial design	1.084	3.111	1.000
Final design - Case 1	3.440	3.780	3.173
Final design - Case 2	2.872	3.032	2.649
Final design - Case 3	2.958	2.985	2.748

Final design depths of all the members for Case 2 and Case 3 optimum designs are given in Table 4.4. However if the final design obtained in Case 3 is solved again using the finite element model of 4 elements per member,  $\lambda_1$  is dropped to 2.574 compared to the value 2.958 obtained with the finite element model of one element per member.

**Table 4.4** - Optimum member depths for the 3-storey frame

Element number	Member depths in mm			
	Without sizing constraints		With sizing constraints	
	Case 2	Case 3	Case 2	Case 3
1, 1a	13.93	11.41	23.29	25.06
2, 2a	19.81	19.26	20.27	21.09
3, 3a	12.01	11.64	10.18	10.00
4, 4a	37.49	35.54	30.00	30.00
5, 5a	19.87	19.30	16.23	15.07
6, 6a	25.65	25.09	23.30	23.09
7, 7a	17.77	21.17	30.00	30.00
8	35.56	34.85	13.21	10.00
9, 9a	17.81	19.26	20.27	21.09
10	21.82	23.21	20.28	18.11
11, 11a	4.09	5.68	10.00	10.00
12	25.75	23.25	19.26	22.09
$\lambda_1$ obtained with four elements per member	2.872	2.574	2.472	2.205

Optimum depths of Case 2, which is the most preferred case practically, range from minimum of 4.09 mm (elements 11 and 11a) to maximum of 37.49 mm (elements 4 and 4a). Optimisation of this 3-storey frame is again carried out with sizing constraints. Member depths are now allowed to vary to maximum of 30 mm and minimum of 10 mm in steps of 1 mm.  $RR = 20\%$  is used. All three cases as mentioned above are considered. The first two eigenvalues of initial and optimum designs of all three cases are tabulated in Table 4.5. The final design depths of all the members for Case 2 and Case 3 are given in Table 4.4 (columns 4 and 5). However if the final design obtained in Case 3 is solved again using the finite element model of 4 elements per member,  $\lambda_1$  is dropped to 2.205 compared to the value 2.582 obtained with the finite element model of one element per member.

**Table 4.5** - Buckling load factors of the 3-storey frame (with sizing constraints)

	$\lambda_1$	$\lambda_2$	$OF$
Initial design	1.084	3.111	1.000
Final design - Case 1	3.017	3.180	2.783
Final design - Case 2	2.472	2.565	2.280
Final design - Case 3	2.582	2.645	2.382

#### 4.6 Influence of ESO Parameters on Optimum Designs

In this section the influence of the step size and the resizing ratio  $RR$  on final optimum designs is studied with the previous examples of 3-member portal frame and 3-storey frame (Case 1, without sizing constraints). Optimum buckling eigenvalues and the numbers of iterations required to reach the optimum design are tabulated for different

step sizes and resizing ratios in Table 4.6 for the three member frame and in Table 4.7 for the 3-storey frame (Case 1).

**Table 4.6** - The influence of step size and  $RR$  on the optimum design of the portal frame

$RR$ (%)	Step size $r^2$ in $\text{mm}^2$	Number of Iterations	$\lambda_{cr}^{opt}$
10	2.5	65	4.0089
20	2.5	37	4.0089
40	2.5	26	4.0086
60	2.5	22	4.0081
10	5.0	39	4.0059
20	5.0	23	4.0048
40	5.0	14	4.0044
60	5.0	13	4.0044
10	10.0	24	4.0000
20	10.0	12	3.9975
40	10.0	9	3.9846

**Table 4.7** - The influence of step size and  $RR$  on the optimum design of the 3-storey frame

$RR$ (%)	Step size $d$ in mm	Number of Iterations	$\lambda_{cr}^{opt}$
10	0.5	103	3.5870
20	0.5	89	3.5381
40	0.5	78	3.5167
10	1.0	72	3.4557
20	1.0	62	3.4363
40	1.0	37	3.4407
10	2.0	54	3.4661
20	2.0	43	3.3890
40	2.0	27	3.3071

From Table 4.6 for the 3 member portal frame, it is observed that the optimum designs are not much affected by the choice of  $RR$  and step size. Even with the values as high as 40% for  $RR$  and step size  $10 \text{ mm}^2$  for  $r^2$ , a reasonably accurate optimum design is obtained with only 9 iterations. Since this portal frame is simple and consists of only three members, and the fundamental buckling mode is only a side sway mode, high  $RR$  values and step sizes are acceptable. However if the structural layout and the buckling mode are complex, as in the case of 3-storey frame, it is always better to use small resizing ratios and small step sizes. The optimum design also depends on the finite element mesh. If the structural members are divided into more elements, more accurate distribution of material can be obtained.

#### 4.7 Optimality Criteria Methods Based on Uniform Strain Energy Concept

Based on energy considerations, optimality criteria were established in the past for buckling optimisation of structures. The derivation of optimality condition for single modal frame structures by Khot *et al.* (1976) and Szyszkowski and Watson (1988) are described in the following sections.

##### 4.7.1 Optimality criterion by Khot *et al.* (1976)

Khot *et al.* (1976) established optimality conditions for frame structures with linear size-stiffness relations and presented a minimum weight design method using finite element analysis. In the following the derivation of optimality criteria by Khot *et al.* (1976) is described.

For linear size-stiffness structures, design variables can be represented by the cross-sectional areas of elements. Thus the optimisation problem is posed as follows: Find the

vector of design variables  $X = \{x_1, x_2, \dots, x_n\}^T$  which minimise the total structural weight of  $n$  elements

$$W(X) = \sum_{i=1}^n \rho_i x_i l_i \quad (4.16)$$

where  $\rho_i$ ,  $x_i$  and  $l_i$  are the mass density, cross-sectional area and length of the  $i^{\text{th}}$  element respectively, subject to the constraint that the fundamental eigenvalue  $\lambda_1$  should be greater than the desired buckling load factor  $\lambda^*$ .

$$\lambda_1 \geq \lambda^* \quad (4.17)$$

Hence the Lagrangian functional for the minimum weight design subject to a single constraint is formed as

$$L(X, \lambda, \mu) = \sum_{i=1}^n \rho_i x_i l_i + \mu (\lambda_1 - \lambda^*) \quad (4.18)$$

where  $\mu$  is the undetermined Lagrangian multiplier. Kuhn-Tucker optimality conditions is obtained by differentiating the Lagrangian functional with respect to any design variable,  $x_i$ .

$$\frac{\partial L(X, \lambda_1, \mu)}{\partial x_i} = \rho_i l_i + \mu \frac{\partial \lambda_1}{\partial x_i} = 0 \quad (4.19)$$

For linear size-stiffness relation

$$\frac{\partial [K]}{\partial x_i} = \frac{[k_i]}{x_i} \quad (4.20)$$

Khot *et al.* (1976) assumed

$$\frac{\partial [K_g]}{\partial x_i} = 0 \quad (4.21)$$

Substituting (4.20) and (4.21) into equation (4.8) leads to

$$\frac{\partial \lambda_1}{\partial x_i} = - \frac{\{u_{i1}\}^T [k_i] \{u_{i1}\}}{x_i \{u_{i1}\}^T [K_g] \{u_{i1}\}} \quad (4.22)$$

Substituting (4.22) into (4.19), the optimality condition is obtained as

$$-\frac{\{u_{i1}\}^T [k_i] \{u_{i1}\}}{\rho_i x_i l_i \{u_{i1}\}^T [K_g] \{u_{i1}\}} = \frac{1}{\mu} = \text{A constant} \quad (4.23)$$

Since the  $\{u_{i1}\}^T [K_g] \{u_{i1}\}$  is the same for all the elements, the optimality criterion can be interpreted as follows: “The optimum structure for stability is the one in which the ratio of the strain energy density to the mass density, associated with the buckling mode is same for all elements”. This optimality condition is valid for single modal, single load and statically determinate conditions.

The optimality criterion derived above is valid only at the optimum and has to be converted into a recurrence relation so that it can be used in an optimisation algorithm.

The following two recurrence relations are commonly used in optimality criteria methods (Morris 1982). Equation (4.23) is re-written as

$$\mu \frac{Q_i}{\rho_i x_i l_i} = 1 \quad (4.24)$$

where 
$$Q_i = -\frac{\{u_{i1}\}^T [k_i] \{u_{i1}\}}{\{u_{i1}\}^T [K_g] \{u_{i1}\}} \quad (4.25)$$

*Exponential recurrence relation:* A recurrence relation can be written by multiplying both sides of equation (4.24) by  $x_i^r$  and taking the  $r^{\text{th}}$  root. This gives

$$x_i^{v+1} = x_i^v \left( \mu \frac{Q_i}{\rho_i x_i l_i} \right)^{1/r} \quad (4.26)$$

*Linear recurrence relation:* A linear recurrence relation is given by the following equation.

$$x_i^{v+1} = x_i^v \left( 1 + \frac{1}{r} \left( \mu \frac{Q_i}{\rho_i x_i l_i} - 1 \right) \right) \quad (4.27)$$

In equation (4.27) the term  $(\mu Q_i / \rho x_i l_i - 1)$  is the error in satisfying the optimality criterion. In equations (4.26) and (4.27),  $v$  and  $v+1$  indicate the iteration numbers and the parameter  $r$  determines the step size. For most problems it has been found that  $r = 2$  is generally adequate, but it is required for some problems to increase it to reduce the step size. In addition the Lagrangian multiplier  $\mu$  has also to be found by using some iterative procedure. Note that the above recurrence relations are only for single constraint problems.

#### 4.7.2 Optimality criterion by Szyszkowski and Watson (1988)

Szyszkowski and Watson (1988) also obtained the optimality conditions using the variational approach in a slightly different way from Khot *et al.* (1976). They derived the optimality conditions and presented a resizing algorithm to maximise the critical buckling eigenvalue of structures of constant volume. In the following derivation of optimality criteria by Szyszkowski and Watson (1988) is described.

The optimisation problem is stated as follows: Find the vector of design variables  $X = \{x_1, x_2, \dots, x_n\}^T$  which would maximise the first buckling eigenvalue,  $\lambda_1$ , for the structure of a given total volume  $V_0$  which is given by

$$V_0 = \sum_{i=1}^n V_i \quad (4.28)$$

where  $V_i$  is the volume of the  $i^{\text{th}}$  element. Hence the Lagrangian functional for the optimisation problem is given as

$$L(X, \lambda, \mu) = \lambda_1 + \mu \left( V_0 - \sum_{i=1}^n V_i \right) \quad (4.29)$$

where  $\mu$  is the undetermined Lagrangian multiplier. Taking the derivative of the Lagrangian function with respect to a design variable  $x_i$  brings

$$\frac{\partial L}{\partial x_i} = \frac{\partial \lambda_1}{\partial x_i} - \mu \frac{\partial V_i}{\partial x_i} = 0 \quad (4.30)$$

The following relation between the element stiffness and the element volume was assumed instead of the linear-size stiffness relation.

$$[k_i] = [b_i] V_i^{p_i} \quad (4.31)$$

where  $[b_i]$  is the matrix containing all the information on the location and size of the element and the power  $p_i$  may vary from element to element. Thus the derivative of stiffness matrix with respect to a design variable is reduced to

$$\frac{\partial [K]}{\partial x_i} = \frac{\partial [k_i]}{\partial V_i} \frac{\partial V_i}{\partial x_i} = p_i \frac{[k_i]}{V_i} \frac{\partial V_i}{\partial x_i} \quad (4.32)$$

Szyszkowski and Watson (1988) also ignored the derivative of the stress stiffness matrix. Substituting (4.32) and (4.21) into equation (4.8) gives

$$\frac{\partial \lambda_1}{\partial x_i} = -p_i \frac{\{u_{i1}\}^T [k_i] \{u_{i1}\}}{V_i \{u_{i1}\}^T [K_g] \{u_{i1}\}} \frac{\partial V_i}{\partial x_i} \quad (4.33)$$

Thus from equation (4.30), the optimality condition is given by

$$-\frac{\{u_{i1}\}^T [k_i] \{u_{i1}\}}{V_i \{u_{i1}\}^T [K_g] \{u_{i1}\}} = \frac{\mu}{p_i} = \text{A constant} \quad (4.34)$$

The term  $\{u_{i1}\}^T [K_g] \{u_{i1}\}$  is the same for all the elements. In finite element modelling, strain energy stored in the  $i^{\text{th}}$  element due to the fundamental buckling mode is given by

$$SE_i = \frac{1}{2} \{u_{i1}\}^T [k_i] \{u_{i1}\} \quad (4.35)$$

The specific strain energy of  $i^{\text{th}}$  element is obtained by dividing the strain energy by its volume.

$$SPE_i = \frac{1}{2} \{u_{i1}\}^T [k_i] \{u_{i1}\} / V_i \quad (4.36)$$

Thus the optimality criterion given by (4.36) is stated as follows: “The optimum shape of the structure with respect to buckling should have a configuration for which the specific strain energy associated with the fundamental buckling mode is uniform”. This optimality condition is again valid only for single modal, single load structures. The extension of this optimality criteria to multimodal structures will be given in Chapter 5.

Both optimality criteria derived by Khot *et al.* (1976) and Szyszkowski and Watson (1988) are similar except the way they were derived and interpreted. In both methods, the derivative of stress stiffness matrix is ignored and the geometric constraints are not included in the Lagrangian functional. Szyszkowski and Watson (1988) assumed a relationship  $[k_i] = [b_i]V_i^{p_i}$  instead of linear size-stiffness relation. However this is true only if all the elements of  $[k_i]$  matrix are related to the volume by the same power,  $p_i$ .

Based on the specific strain energy of elements Szyszkowski and Watson (1988) proposed an algorithm for resizing the cross-sections of all the elements. For elements with  $SPE_i > SPE_{ave}$  (where  $SPE_{ave}$  is the average of  $SPE_i$  of all the elements), the cross-sectional areas are increased and for elements with  $SPE_i < SPE_{ave}$ , the cross-sectional areas are decreased. Assuming the usual relationship  $I(x) = cA(x)^p$  exists between  $I(x)$  and  $A(x)$ , the following iterative algorithm was proposed.

$$I_i^{k+1} = s\hat{I}_i^k = sI_i^k [1 + a(SE_i^k / SE_{ave}^k)] \quad (4.37)$$

where  $s$  is the scaling factor to satisfy the constant volume requirement and it is given by

$$s = \left[ \frac{\sum_{i=1}^n L_i (I_i^0)^{1/P}}{\sum_{i=1}^n L_i (\hat{I}_i^k)^{1/P}} \right]^P \quad (4.38)$$

The parameter  $a$  in (4.37) is an arbitrary constant to control convergence in the optimisation process. For most of the examples, Szyszkowski and Watson (1988) used  $a = 1$ . However in certain cases they used  $a$  as low as 0.01 and as high as 100. The analysis, specific energy calculation and resizing are carried out in cycles until the critical buckling load factor cannot be increased any further.

The ESO method and Szyszkowski and Watson (1988) method for buckling optimisation have some similarities. In ESO method at each iteration a number of elements are resized by a small cross-sectional change based on their sensitivity numbers. In Szyszkowski and Watson (1988) method all the elements are resized based on the specific energy stored in elements due to the fundamental buckling mode. If the specific energy of elements range from very small value to vary large value, the cross-sectional areas of elements also have to be changed by large values accordingly. If cross-sectional areas of elements are changed by large values, the change in stress stiffness matrix cannot be ignored. However in ESO method, since the elements are resized gradually, the change in stress stiffness matrix can be ignored. Furthermore, the resizing procedure of the ESO method is much simpler than the resizing algorithm of Szyszkowski and Watson (1988) or the recurrence relations commonly used in optimality criteria methods.

#### **4.8 Conclusions**

In this chapter ESO method for the design of structures against buckling has been described. The sensitivity number used in the optimisation process is a measure of the effect of changing the cross-sectional area on the buckling load factor and it is obtained by ignoring the change in the stress stiffness matrix. If the structure is statically

determinate and the cross-sectional change at each iteration is small, the sensitivity number gives a very accurate estimation of the change in the buckling load factor. Even for a statically indeterminate frame this sensitivity is reasonably accurate if the cross-sectional variations at each iteration in the frame results in only slight changes in the axial stress resultants. If an element is removed from the structure, because of the significant changes in the membrane or axial stress resultants in its surrounding elements, the change in the stress stiffness matrix cannot be ignored or found from the finite element solution of the old model.

The capability of the proposed ESO method has been illustrated with several examples of single modal, single load case frame structures and the results have been compared with the exact solutions and the other available results. Critical buckling load factors have been increased substantially by shifting the material from the strongest part of the structure to the weakest part. The resizing procedure used in the ESO method is much simpler than the other resizing algorithms used in optimality criteria methods. Optimum designs have been obtained with and without sizing constraints. For the design of frame structures, more practical optimum designs have been obtained by using modified member sensitivity numbers.

## **CHAPTER 5 - OPTIMUM DESIGN OF MULTIMODAL STRUCTURES**

### **5.1 Introduction**

Repeated (or multimodal) eigenvalues in the form of buckling loads and natural frequencies of vibration very often occur in complex structures that depend on many design parameters and have many degrees of freedom. For example, stiffener-reinforced thin-walled plate and shell structures have a dense spectrum of eigenvalues and repeated eigenvalues are found often. Also, symmetry of structural systems may lead to the occurrence of several linearly independent buckling modes and vibration modes with repeated eigenvalues.

Optimisation for maximum stability becomes more difficult when the lowest buckling eigenvalue of the problem, representing the critical load, is either inherently multimodal or it becomes multimodal as a result of the optimisation process. During optimisation, it is often observed that while the first eigenvalue is increasing, the subsequent eigenvalues are decreasing and gradually the first two or more eigenvalues converge to each other, although the corresponding eigenvectors may remain totally different. Some symmetrical structures are intrinsically multimodal from the outset.

One of the earliest work on multimodal buckling problem was by Olhoff and Rasmussen (1977). Olhoff and Rasmussen discovered that the optimum eigenvalue of a clamped-clamped column of given volume is bimodal. They first demonstrated that an analytical solution obtained by Tadjbaksh and Keller (1962) under the tacit assumption of a simple buckling load is not optimal and presented a bimodal formulation of the problem and obtained the correct optimum design. The discovery in 1977 of repeated

optimum eigenvalues in structural optimisation problems, and the necessity of applying a bimodal or multimodal formulation in such cases, opened a new field for theoretical investigation and development of methods for buckling optimisation.

One of the main problems related to repeated eigenvalues is that they are not continuously differentiable. This is due to the fact that the eigenvectors corresponding to the repeated eigenvalues are not unique. In fact, an infinite number of linear combinations of the eigenvectors of the repeated eigenvalues will satisfy the original eigenvalue problem (equation 4.1). The non-differentiability creates difficulties in finding sensitivities of repeated eigenvalues with respect to design changes and derivation of necessary optimality conditions in optimisation problems. The formulae derived in Chapter 4, for eigenvalue sensitivity and increment of simple eigenvalue are not applicable to multimodal problems.

Extensive research on various aspects of the problem of multimodality has been carried out in the past decade. Various approaches to design sensitivity analysis and derivation of necessary optimality conditions for multiple eigenvalues have been published. A long literature list is available in Seyranian *et al.* (1994). Although repeated eigenvalues are not continuously differentiable, Haug and Rousselet (1980) proved the existence of directional derivatives of repeated eigenvalues and obtained formulae for these directional derivatives in the design space. Bratus and Seyranian (1983) and Seyranian (1987) presented directional sensitivity analysis of repeated eigenvalues based on a perturbation technique and derived necessary optimality conditions. The reader is referred to Seyranian *et al.* (1994) for the detailed analysis of the directional derivation and sensitivity analysis of the repeated eigenvalues. The sensitivity analysis of the

repeated eigenvalues leads to the result that the increments of the repeated eigenvalues are themselves eigenvalues of a sub-eigenvalue problem. The use of directional derivatives in finding the sensitivities of repeated eigenvalues and the derivation of the necessary optimality conditions for multimodal problems are mathematically complex and computationally costly.

Szyszkowski (1992) derived optimality conditions for multimodal problems using Lagrangian functional and presented a simple approach based on the specific energy of elements due to all participating buckling modes. According to Szyszkowski (1992), the optimality criterion for multimodal structures states that a linear combination of the normalised specific energy due to the participating buckling modes must sum to unity at every point of the optimum structure. In this method Lagrangian multipliers which determine the linear combination of the participating modes need to be determined iteratively. This method is again mathematically complex and the application of this method to statically indeterminate structures may lead to non-optimum designs. In some cases convergence problems are observed. Details of this method will be discussed in Section 5.4.

In the following sections, a very simple technique to take account of multimodality in the ESO method for buckling optimisation is proposed. The application of the ESO method to multimodal problem is illustrated with several examples and compared with the available results from the literature.

## 5.2 Sensitivity Number for Buckling Load of Repeated Eigenvalues

Using a proper eigenvalue solver the solution to the problem given by equation (4.1) is obtained in the form of the set of eigenvalues  $\lambda_1 \leq \lambda_2 \leq \lambda_3 \leq \dots$  and the corresponding set of buckling eigenvectors  $\{u_1\}$ ,  $\{u_2\}$ ,  $\{u_3\}$ .... The aim is to maximise the fundamental eigenvalue,  $\lambda_1$ . However, when increasing  $\lambda_1$ , it may become close to  $\lambda_2$  and then to  $\lambda_3$  and etc..... up to  $\lambda_N$ . Consequently, the optimisation procedure finally may need to monitor the first  $N$  buckling modes simultaneously.

In the ESO method, the sensitivity number of each element is a crucial factor. In equation (4.10) only the first eigenvector is considered. When the first eigenvalue becomes close to the subsequent eigenvalues, there will be interference between the first and the subsequent eigenvectors. Therefore the effect on the fundamental eigenvalue due to all participating eigenvectors needs to be included. An eigenvalue multiplicity parameter  $\varepsilon$  is defined and the multimodality of the structure is determined by the number of eigenvalues within an  $\varepsilon$  distance of the lowest eigenvalue. If, for example, the distance between  $\lambda_1$  and  $\lambda_2$ , is within a certain limit, say  $\varepsilon = 5\%$ , and the distance between  $\lambda_1$  and  $\lambda_3$  is greater than 5% it may be assumed that the structure has now become bimodal. When  $\lambda_1$  and  $\lambda_2$  become close, the first two buckling modes may swap with each other as a result of structural modifications during the iterations. There is no point in trying to increase  $\lambda_1$  only to see  $\lambda_2$  drop its value in the next step below the previous  $\lambda_1$ . To effectively increase the buckling load factor in these circumstances, both  $\lambda_1$  and  $\lambda_2$  have to be increased. The simplest strategy for achieving this is to increase the average values of  $\lambda_1$  and  $\lambda_2$ . Therefore we redefine the sensitivity number for the bimodal case as

$$\alpha_{ib} = \frac{1}{2S_i} (\{u_{i1}\}^T [\Delta k_i] \{u_{i1}\} + \{u_{i2}\}^T [\Delta k_i] \{u_{i2}\}) \quad (5.1)$$

Similarly for a multimodal case, when the  $N^{\text{th}}$  eigenvalue  $\lambda_N$  and  $\lambda_1$  are within  $\varepsilon$  distance, the sensitivity number is defined as

$$\alpha_{ib} = \frac{1}{NS_i} (\{u_{i1}\}^T [\Delta k_i] \{u_{i1}\} + \dots + \{u_{iN}\}^T [\Delta k_i] \{u_{iN}\}) \quad (5.2)$$

For the calculation of these sensitivity numbers all the relevant eigenvectors have to be first ortho-normalised with respect to  $[K_g]$  such that  $\{u_j\}^T [K_g] \{u_j\} = 1$ . For each element two sensitivity numbers,  $\alpha_{ib}^+$  and  $\alpha_{ib}^-$ , need to be calculated by substituting  $[\Delta k_i]^+$  and  $[\Delta k_i]^-$  instead of  $[\Delta k_i]$  in the above equations.

It is not clear *a priori* whether repeated eigenvalues will occur in a specific problem. The multimodality of the optimal design of each particular problem is unknown and is rather difficult to predict. If, for example, that by steps of bimodal redesign the distance between the third eigenvalue  $\lambda_3$  and the bimodal eigenvalues  $\lambda_1$  and  $\lambda_2$  ( $\lambda_1 = \lambda_2$ ) may decrease, and if coalescence occurs, a trimodal scheme must be adopted for subsequent iterations, and so on. Thus, independent of the degree of multiplicity of the fundamental eigenvalue at a given iteration stage, it is necessary to keep track of a few of the next (higher order) eigenvalues in order to capture possible coalescence of one or more of these eigenvalues with the fundamental one, and then use an updated scheme for the subsequent iterations. The optimisation procedure for multimodal problems is the same as described in Section 4.3 except that the sensitivity numbers now need to be calculated based on equation (5.1) or (5.2).

## 5.3 Examples

### 5.3.1 Clamped - clamped column

The optimum shape of the clamped-clamped column compressed at its ends was first dealt with by Tadjbakhsh and Keller (1962). The governing differential equations were obtained using variational calculus and were solved analytically for a column with geometrically similar cross-sections satisfying  $I(x) = cA(x)^2$ . Their results stood unchallenged until 1977 when Olhoff and Rasmussen (1977) found that the optimum design should be bimodal. The study of Olhoff and Rasmussen (1977) on clamped-clamped column was the earliest work on bimodal buckling optimisation. In their landmark study, they showed that the critical load is governed by a repeated eigenvalue. They established the differential equations for optimisation under the double eigenvalue formulation by using variational calculus and solved these non-linear integro-differential equations of the continuous system by means of finite difference method.

Olhoff and Rasmussen (1977) also discovered that there was a threshold value of minimum area constraint which separated the single and bimodal buckling modes. The curve of optimum buckling load factor versus minimum area constraint  $\bar{\beta}$  for the column cross-sectional area obtained by Olhoff and Rasmussen (1977) is reproduced in Figure 5.1, where minimum dimensionless cross-sectional area  $\bar{\beta} = \bar{A}L/V$ . They found that the optimum buckling load is single for any value of  $\bar{\beta}$  in the range of  $0.280 < \bar{\beta} \leq 1$ . For  $0 \leq \bar{\beta} \leq 0.280$ , the buckling mode is bimodal and the optimum occurs at  $\bar{\beta} = 0.226$  and the corresponding optimum factor is 1.3262. The minimum cross sectional area of the column is found to be at  $x = 0.25L$  and  $0.75L$ . From the curve and the results

it is seen that the optimum design is very sensitive to the minimum area constraint and the number of buckling modes. The difference between the optimum designs obtained with single modal or bimodal optimisation is very small.

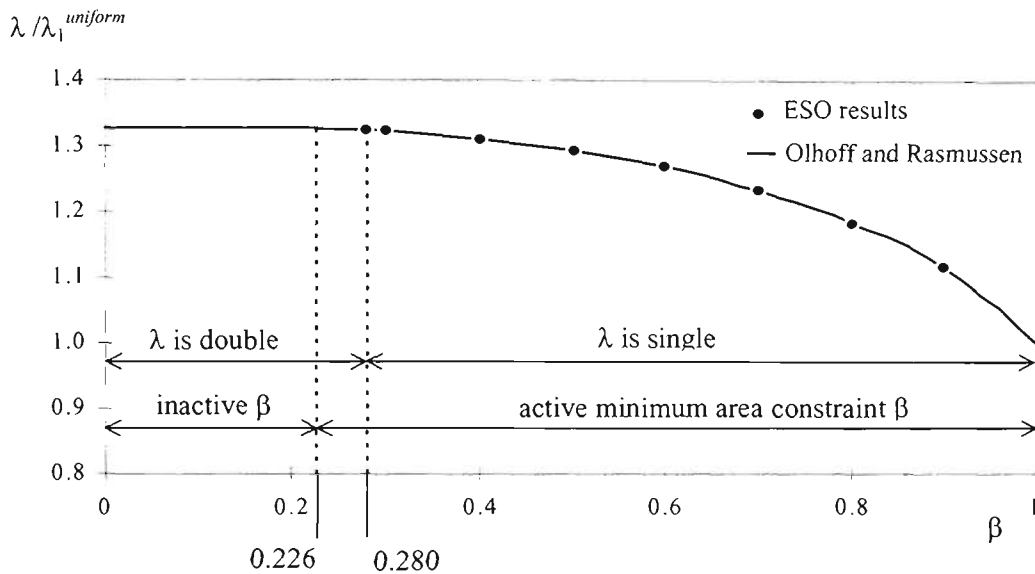


**Figure 5.1** - The curve of optimum eigenvalue vs minimum area constraint

Recently Tada and Wang (1995) re-investigated the same problem and showed the convergence of the numerical calculation is highly sensitive to the precision of the numerical calculation. Tada and Wang (1995) obtained the optimum solution using double precision computations and 6400 discrete points for the finite difference modelling to solve the differential equations. According to Tada and Wang (1995) the optimum design under single modal formulation is at  $\bar{\beta} = 0.2817$  and the optimum factor is found to be 1.32454. The minimum area  $\bar{\beta} = 0.2817$  occurs at  $x = 0.25L$  and  $x = 0.75L$ . With bimodal formulation the optimum eigenvalue increases as  $\bar{\beta}$  decreases in the region of  $0.2258 \leq \bar{\beta} \leq 0.2817$ . When  $\bar{\beta} \leq 0.2258$  the optimum eigenvalue becomes

stable with the optimum factor of 1.3262. The minimum area  $\bar{\beta} = 0.2258$  occurs at  $x = 0.247L$  and  $x = 0.753L$ .

Both Olhoff and Rasmussen (1977) and Tada and Wang (1995) obtained the optimum designs for clamped-clamped column using distributed parameter optimisation methods. With continuous design variables, high sensitivity of optimum designs with regard to minimum area constraint and the number of participating buckling modes either single or bimodal could be captured. However this extremely small difference between the single modal and bimodal designs cannot be captured with the optimisation methods based on finite element analysis due to round-off errors. Seyranian *et al.* (1994) and Szyszkowski (1992) independently tried to obtain optimum designs for clamped-clamped column using the optimality criteria method based on the finite element analysis and observed the same difficulties.

This example is reanalysed using the proposed ESO method to check the precision of the method. A circular cross-sectional column is analysed. The dimensions are as follows: length  $L = 1$  m ; uniform  $r^2 = 20$  mm<sup>2</sup> and  $r^2$  is allowed to vary to the maximum  $r^2 = 40$  mm<sup>2</sup> and to the minimum  $r^2 = 1$  mm<sup>2</sup> in steps of  $r^2 = 0.1$  mm<sup>2</sup>.  $RR = 20\%$  and  $\epsilon = 2\%$  are assumed. The column is divided into different numbers of elements and the optimum factors obtained are compared in Table 5.1. It is interesting to note that these optimum factors are only marginally less than the bimodal optimum buckling load factor 1.3262 of the continuum column determined by Olhoff and Rasmussen (1977). The optimum shape and the cross-sectional areas are shown in Figure 5.2. However, as noted from Table 5.1, there is no difference observed between the single modal and

bimodal optimum solutions. The effect of minimum area constraint on optimum design is also checked for the column divided into 200 elements. The results are tabulated in Table 5.2 and compared with the numerical results available from Olhoff and Rasmussen (1977). The points obtained by the proposed ESO method lie on the curve of Olhoff and Rasmussen (1977) as shown in Figure 5.1.

**Table 5.1** - Clamped-clamped column optimum factors

Number of elements	Optimum factors	
	Single modal	Bimodal
50	1.3200	1.3200
100	1.3233	1.3233
200	1.3242	1.3242

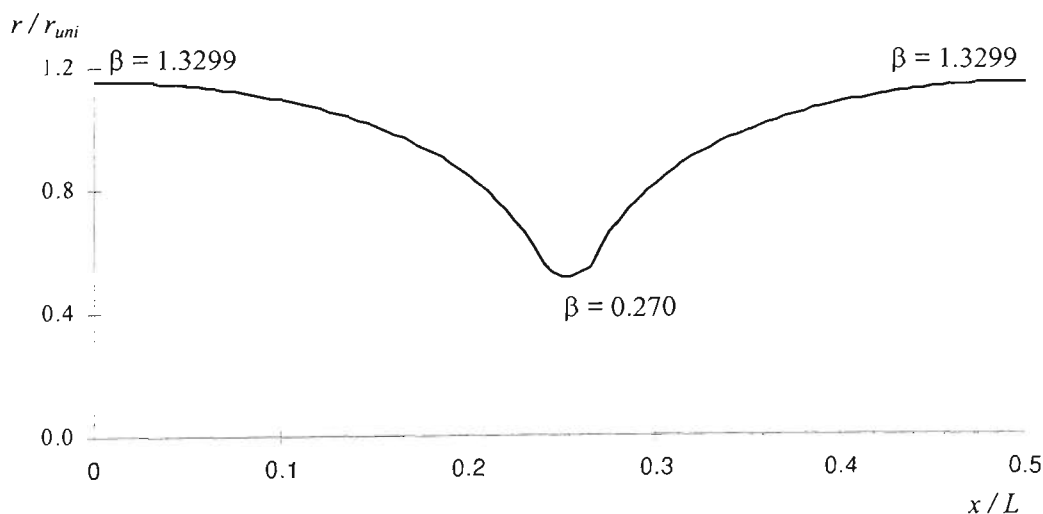


**Figure 5.2.** Optimum shape of the clamped-clamped column

**Table 5.2** - Optimum factors for different  $\bar{\beta}$  values

$\bar{\beta}$	Optimum factors	
	Olhoff and Rasmussen	ESO
0.3	-	1.3225
0.4	1.3115	1.3111
0.6	-	1.2684
0.7	1.2333	1.2332
0.8	-	1.1846
0.9	-	1.1156

### 5.3.2 Three member portal frame - bimodal example

A three member pin based frame which was analysed by Szyszkowski *et al.* (1989) for bimodal buckling is considered. The frame layout and the loading are shown in Figure 5.3. All the members are of circular cross-sections and of equal length of 1 m. Initial uniform  $r^2$  is 20 mm<sup>2</sup> and is allowed to vary to the maximum 40 mm<sup>2</sup> and to the minimum 5 mm<sup>2</sup> in steps of 1 mm<sup>2</sup>. Each member is divided into 10 elements of equal length.  $RR = 20\%$  and  $\epsilon = 5\%$  are used. For the frame with a uniform cross-section, the first buckling mode is anti-symmetric with sway and the second buckling mode is symmetric without sway. High compressive loads are applied in the horizontal direction to make the problem bimodal from the outset.

The optimum shape obtained with the bimodal method by using equation (5.1) for sensitivity number calculations is given in Figure 5.3. The corresponding buckling load is 1.247 times that of the uniform frame. This optimum design compares well with the optimum design obtained by Szyszkowski *et al.* (1989). If only the first buckling mode

is considered for optimisation and the single modal sensitivity number is used, the buckling load factor can only reach 1.125 times that of the uniform frame. The evolutionary histories of the first two eigenvalues using both single and bimodal methods are given in Figure 5.4. The above problem is analysed with different values of multiplicity parameter  $\epsilon = 1\%$ ,  $2\%$  and  $5\%$ . No difference is observed in the final design although the iteration histories of eigenvalues vary slightly in intermediate designs.

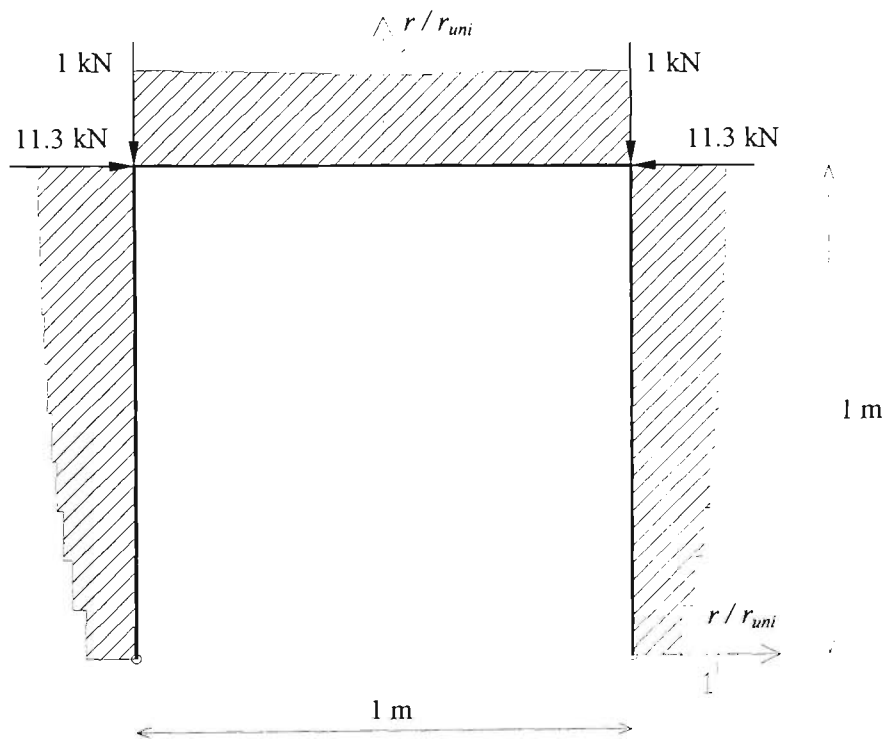


Figure 5.3 - Optimum shape of the three member portal frame

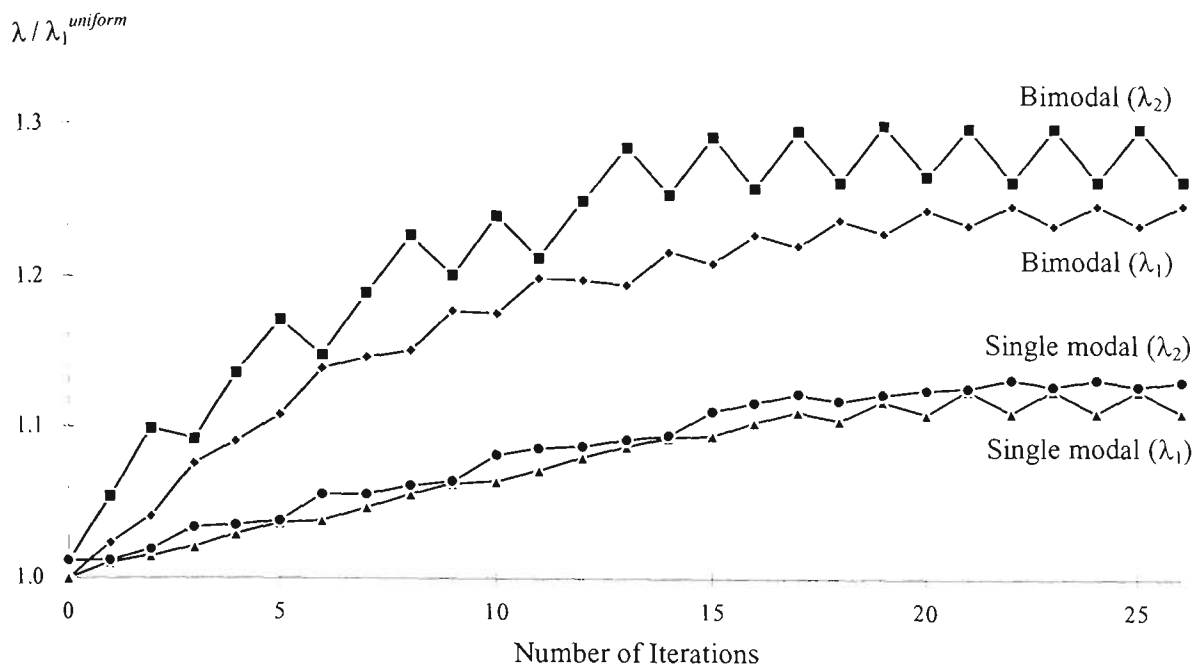


Figure 5.4 - Optimisation histories of the eigenvalues for the three member frame

### 5.3.3 Three member space frame - trimodal example

A space frame with three beams pinned at the base and clamped at the apex is considered for the trimodal optimisation. The frame layout and the loading are shown in Figure 5.5. All the members are of circular cross-sections and of length 1 m. Initial uniform  $r^2$  is  $20 \text{ mm}^2$  and it is allowed to vary to the maximum  $40 \text{ mm}^2$  and to the minimum  $5 \text{ mm}^2$  in steps of  $1 \text{ mm}^2$ . Each member is divided into 10 elements of equal length. This is a triple symmetric structure and the first three eigenvalues coincide for the uniform design and remain coincided throughout the optimisation process when the trimodal optimisation is carried out. The optimum shape obtained with the ESO method is given in Figure 5.5. The ratios of the final to initial uniform radius of the cross-section are displayed in this figure for one member as it is identical for all members. The optimum buckling load is 1.273 times that of the uniform frame and it is achieved after 10 iterations. Optimum design is also obtained by considering only the first buckling mode. The optimum factor for this is 1.251 and it is obtained after 35 iterations. Although the optimum factors obtained by trimodal and single modal

methods are differed by only 1.73%, a much higher number of iterations are required when using single modal optimisation. The iteration histories of the first three eigenvalues using both single modal and trimodal methods are given in Figure 5.6.

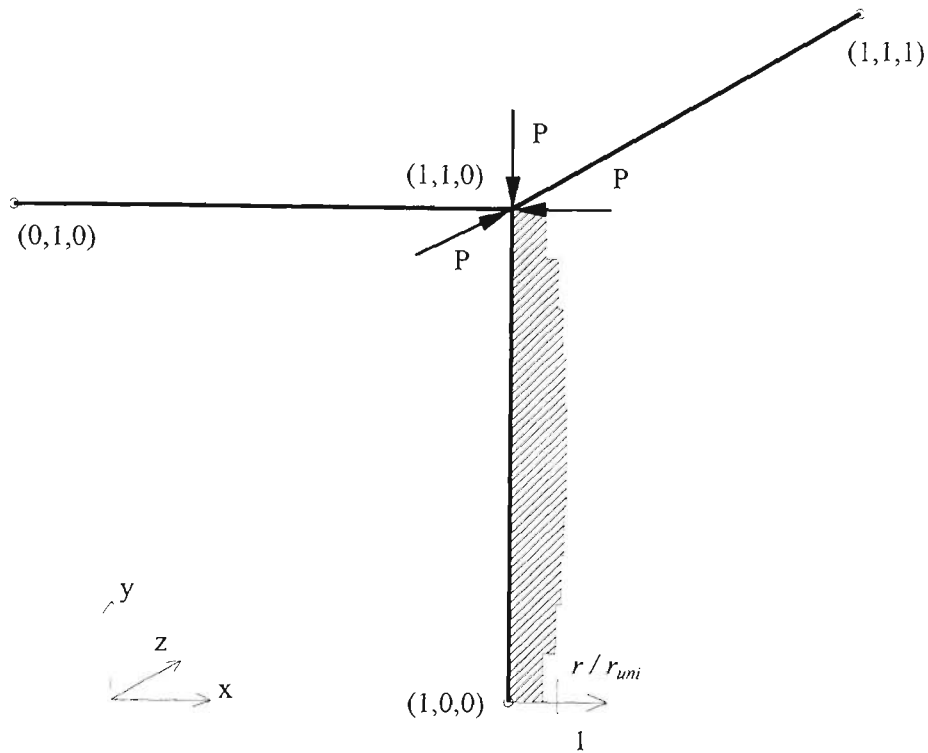


Figure 5.5 - Optimum shape of the three member space frame

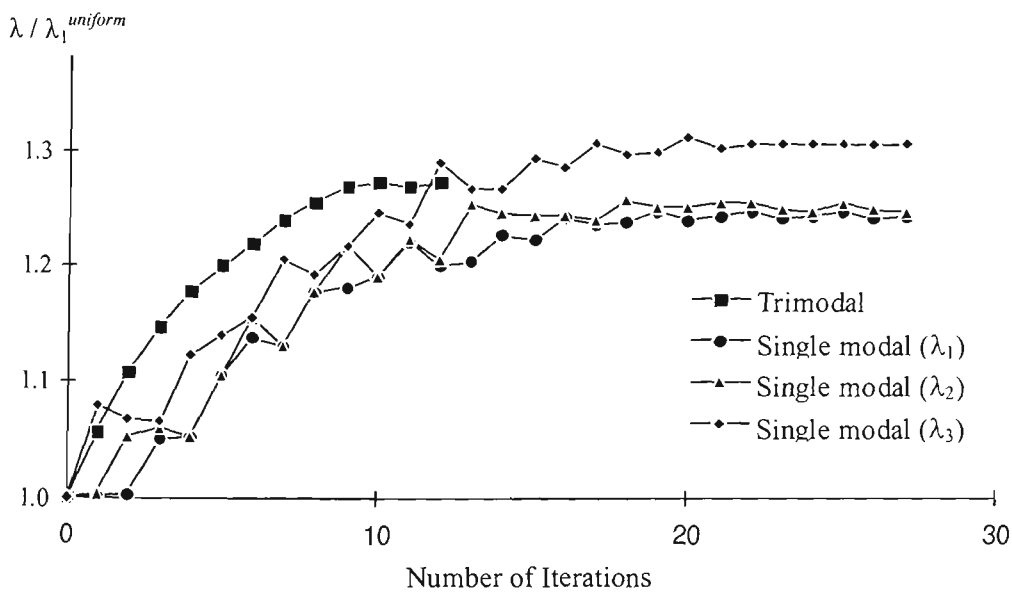


Figure 5.6 - Optimisation histories of the three member space frame

### 5.3.4 Box frame

The box frame shown in Figure 5.7 was previously considered for buckling optimisation by Szyszkowski *et al.* (1989) using optimality criteria method. This frame was later reanalysed by Canfield (1993) using non-linear mathematical programming with Rayleigh Quotient Approximation method. Buckling optimisation of this frame was considered to be one of the most difficult examples in the literature.

This box frame is optimised for buckling using ESO method and the results are compared with those from the literature. All the members are of rectangular cross-sections with constant breadth  $b = 40$  mm. Initial uniform depth  $d$  is equal to 40 mm for all the members. As shown in Figure 5.7, top and bottom horizontal members are divided into six elements of equal length and diagonal and vertical members are divided into three members of equal lengths. Since the diagonal members are under the tensile axial forces, the material of these members should probably be transferred to other members, presumably under compression. Consequently, the slender diagonal members in tension may, in the optimum design, become too thin to carry the tensile forces.

Initially the design variable, depth  $d$  is allowed without upper limit and to the minimum depth of 1 mm in steps of 1 mm.  $RR = 20\%$  is used. The optimum to the initial uniform depth ratio is shown for half of the symmetric model in Figure 5.7 (the values on the left hand half of the frame). The evolutionary histories of the first two eigenvalues using both single and multimodal methods are given in Figure 5.8. Initially for the uniform design, the fundamental eigenvalue is single. From the iteration histories of eigenvalues, it is seen, as the optimisation progresses, the first two eigenvalues converge to each

other, then they drift apart from each other and the final optimum design is single modal. The final design buckling load factor is 3.886 times that of the uniform frame. If, however, only the first buckling mode is considered using the single modal sensitivity number throughout the optimisation process, the final design buckling load factor can reach only 2.522 times that of the uniform frame. Thus even if the final optimum design is single modal, bimodal optimisation needs to be carried out to get over the intermediate bimodal situations.

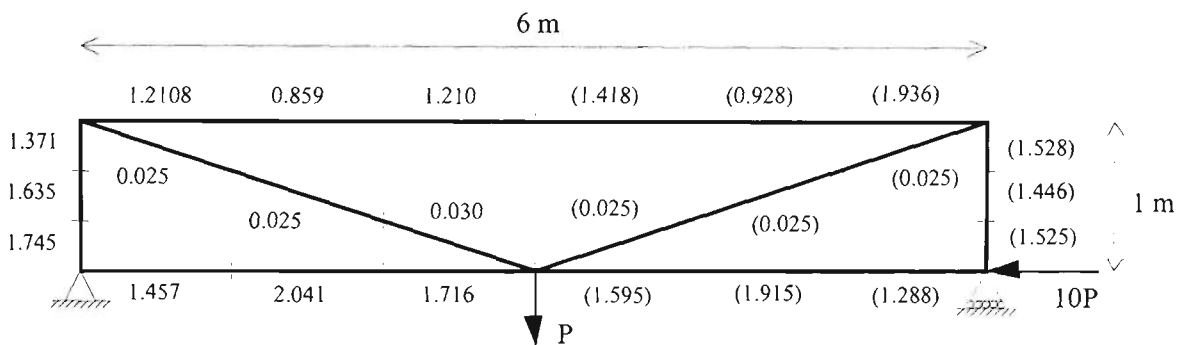


Figure 5.7 - Optimum design of the box frame (allowable minimum depth = 1 mm)

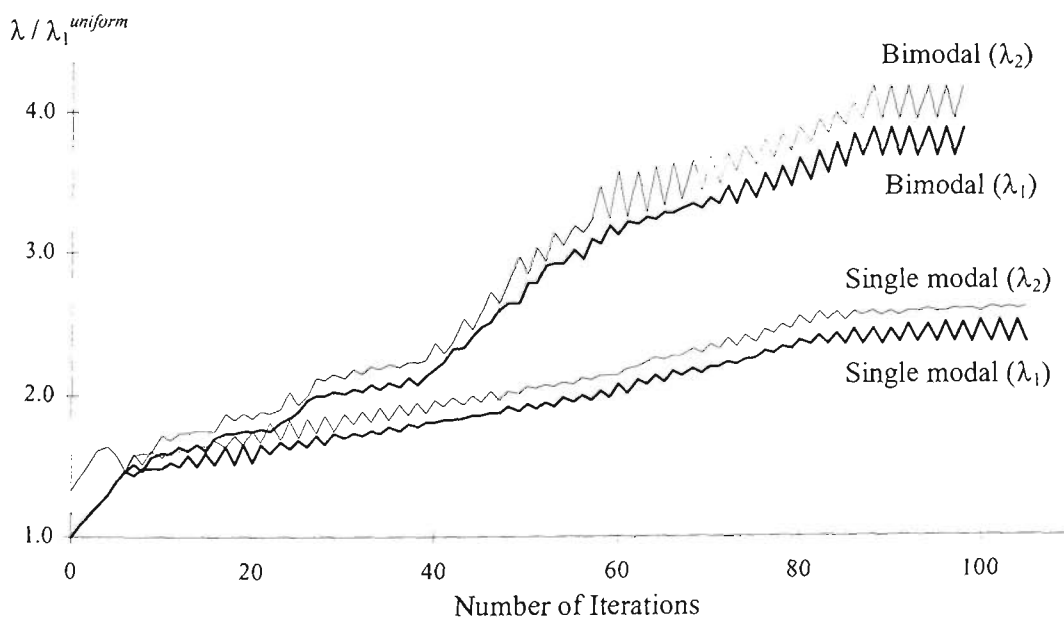


Figure 5.8 - Optimisation histories of the eigenvalues for the box frame ( $d_{min} = 1$  mm)

For this particular frame, high numbers of iterations are required to obtain optimum designs. As the optimisation progresses, the first few eigenvalues of the problem become negative, and at the final stages of the optimisation process the first eight eigenvalues are negative and the ninth and tenth eigenvalues are the first two positive eigenvalues. Hence through out the optimisation process, at least first 10 eigenvalues and eigenvectors need to be monitored to pick up the first two positive eigenvalues. The first few negative eigenvalues physically indicate that the loading direction needs to be reversed to cause the buckling in the structure. Detailed histories of the first ten eigenvalues are given in Appendix 5.1.

The optimum depth ratios obtained by Szyszkowski *et al.* (1989) are given in the parenthesis (the values on the right hand half of the frame). Optimum factor for this design reported by Szyszkowski *et al.* (1989) was only 3.018 and they claimed the final design was bimodal. Analysing this final design for buckling reproduces the same critical buckling load factor (3.018 times the load for the uniform design); however, the analysis reveals the volume of this design has increased by 5% and the design is not bimodal as claimed. ESO method produces the optimum design with much higher buckling load factor, while precisely maintaining the constant volume constraint.

This box frame is reanalysed for the minimum allowable depth  $d = 4$  mm. The optimum to initial uniform depth ratios are shown for half of the symmetric frame in Figure 5.9. The evolutionary histories of the first two eigenvalues using both single and multimodal methods are shown in Figure 5.10. The final optimum design is bimodal and the corresponding buckling load factor is 3.666 times that of the uniform design. Again at

final stages of optimisation the first eight eigenvalues are negative and the ninth and tenth eigenvalues are the first two positive values. Detailed histories of these eigenvalues are given in Appendix 5.2. The optimum depth ratios obtained by Szyszkowski *et al.* (1989) are given in the parenthesis. Buckling load factor for this design is only 2.721 times that of the uniform design.

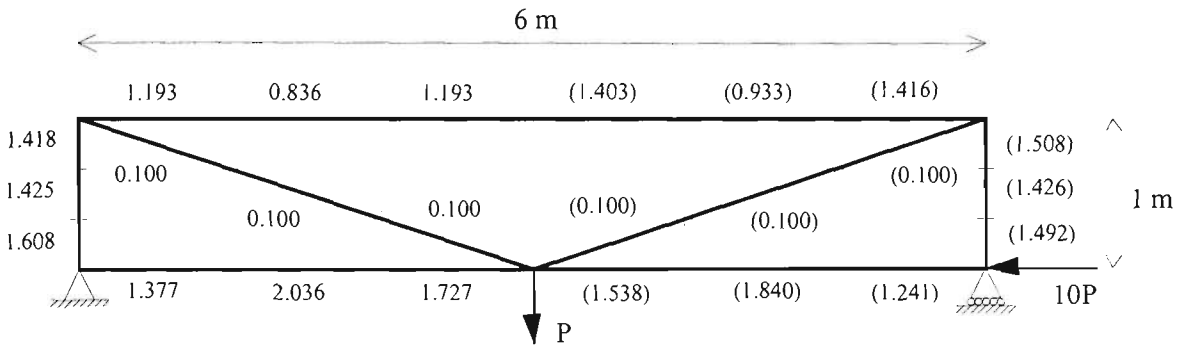


Figure 5.9 - Optimum design of the box frame (allowable minimum depth = 4 mm)

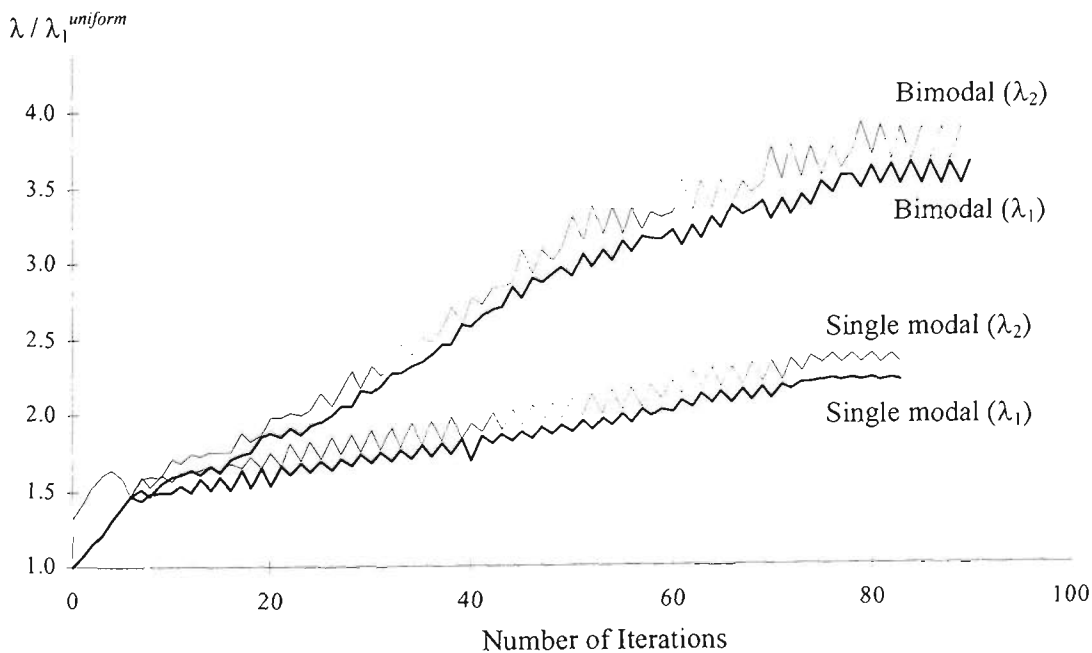
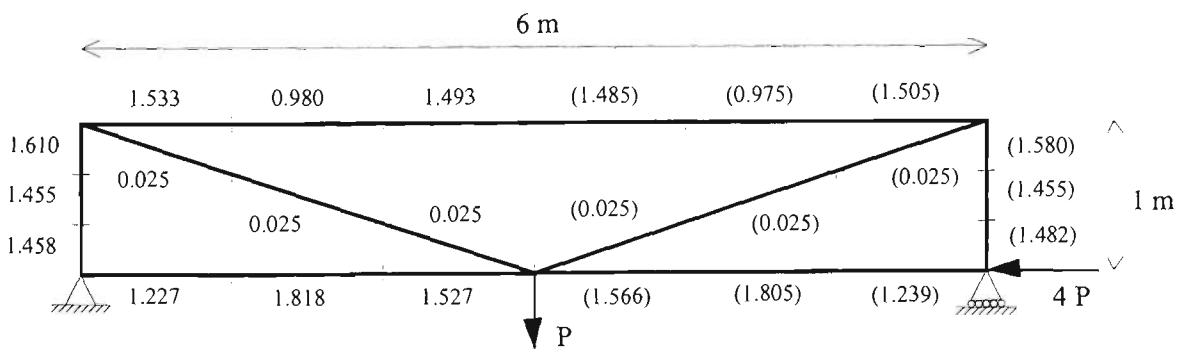


Figure 5.10 - Optimisation histories of the eigenvalues for the box frame ( $d_{min} = 4$  mm)

Szyszkowski *et al.* (1989) obtained final designs after between 25 to 30 iterations. To obtain the correct optimum designs ESO method requires between 80 to 85 iterations with  $RR = 20\%$  and step depth size = 1 mm. However, the static and buckling analyses

of this 24 element frame require only 6 seconds on a Pentium / 100 Mhz personnel computer. Hence total time requires for the whole optimisation process is only about 8 to 10 minutes. In general, for frame structures the number of iterations required to obtain the optimum designs does not really matter.

Canfield (1993) analysed this frame with a reduced ratio of horizontal to vertical load (4:1 instead of 10:1). With the allowable minimum depth  $d = 1$  mm, Canfield obtained a bimodal optimum design with the buckling load factor 3.051 times the uniform buckling load factor. ESO method also produces the same optimum buckling load factor. The optimum to initial uniform depth ratio are shown for half of the symmetric frame in Figure 5.11. The values given in parenthesis are by Canfield (1993). The evolutionary histories of the first two eigenvalues using both single and multimodal methods are shown in Figure 5.12.



**Figure 5.11** - Optimum design of the box frame (allowable minimum depth = 1 mm)  
Horizontal to vertical load ratio 4:1

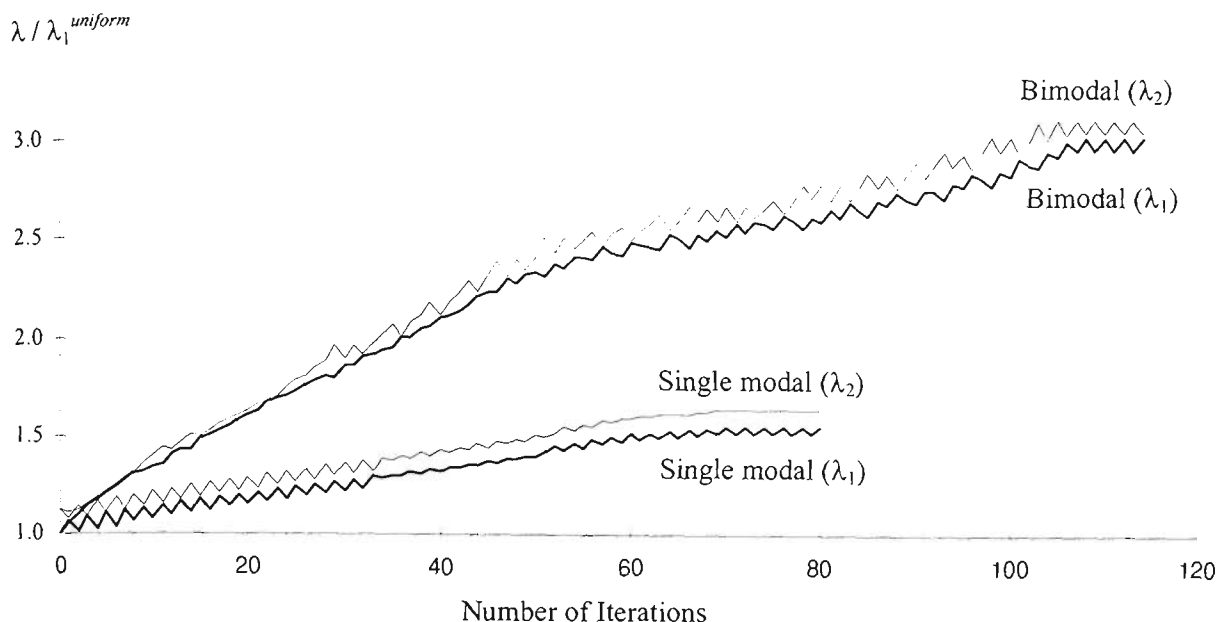


**Figure 5.12** - Optimisation histories of the eigenvalues for the box frame ( $d_{min} = 1$  mm)  
(Horizontal to vertical load ratio 4:1)

#### 5.4 Multimodal Optimality Criteria by Szyszkowski (1992)

Initially Szyszkowski *et al.* (1989) extended the single modal optimality criteria outlined in Section 4.7.2 by Szyszkowski and Watson (1988) to bimodal problems. Later Szyszkowski (1992) extended the bimodal method to general multimodal problems. Full details of the derivation of the optimality criteria can be found in their papers, but a summary of the method is given below.

In deriving the optimality criteria, Szyszkowski (1992) introduced a term  $NSE_{ij}$  which represents the *normalised specific strain energy* stored in the  $i^{\text{th}}$  element due to the  $j^{\text{th}}$  buckling mode.  $NSE_{ij}$  is defined by the following equation:

$$NSE_{ij} = \frac{SPE_{ij}}{\frac{1}{n} \sum_{i=1}^n SPE_{ij}} \quad (5.3)$$

where  $SPE_{ij}$  is the specific strain energy of the  $i^{\text{th}}$  element (as defined in equation (4.36)) and  $n$  is the total number of elements. For a multimodal problem of  $N^{\text{th}}$  order,  $\lambda_j = \lambda_1$  ( $j = 1, N$ ), Szyszkowski (1992) derived the following optimality conditions,

$$\left(1 - \sum_{j=2}^N \gamma_j\right) NSE_{i1} + \sum_{j=2}^N \gamma_j NSE_{ij} = 1 \quad (5.4)$$

for all the elements.  $\gamma_j$  ( $j = 2, N$ ) are undetermined Lagrangian multipliers and they should be within the range of

$$0 \leq \gamma_j \leq 1 \quad \text{and} \quad \sum_{j=2}^N \gamma_j \leq 1 \quad (5.5a,b)$$

These Lagrangian multipliers need to be determined iteratively during the optimisation process. The optimality condition (5.4) states that a linear combination of the normalised specific energy due to the participating buckling modes must sum to unity at every point of the structure. The actual modality of the structure is unknown in advance. If the optimum design is only  $N_R$  - modal, that is if  $\lambda_j = \lambda_1$  for  $j = 1, N_R$ , where  $N_R < N$ , equation (5.4) needs to be supplemented with the following switching conditions.

$$\gamma_j \left( \frac{\lambda_j}{\lambda_1} - 1 \right) = 0 ; \quad j = 1, N \quad (5.6)$$

For  $N_R < j \leq N$ ,  $\lambda_j \neq \lambda_1$  and all the  $\gamma_j$  must be equal to zero and equation (5.4) will involve only the first  $N_R$  participating buckling modes. The goal of the optimisation procedure is to satisfy equations (5.4) to (5.6) iteratively. Initially the values for Lagrangian multipliers  $\gamma_j$  ( $j = 2, N$ ) are assumed satisfying equation (5.5). From equation (5.4), for each element a local error,  $\xi_i$ , is calculated as

$$\xi_i = \left(1 - \sum_{j=2}^N \gamma_j\right) NSE_{i1} + \sum_{j=2}^N \gamma_j NSE_{ij} - 1 \quad (5.7)$$

If the design is optimum,  $\xi_i$  should have been zero for all the elements. Based on these local errors of elements, design variable of elements are linearly updated using

$$x_i^{k+1} = x_i^k (1 + c\xi_i) \quad (5.8)$$

where  $c$  is an arbitrary positive constant. With these new design variables,  $NSE_{ij}$  of elements are found and using a complex analysis, the initially assumed Lagrangian multipliers are updated to minimise the local errors of elements,  $\xi_i$ , in subsequent iterations. Details of the procedure can be found in Szyszkowski (1992).

## 5.5 Conclusions

The capability of the ESO method for buckling optimisation of multimodal structures has been illustrated with several examples. The proposed results compare well with exact solutions and other available results. The sensitivity number calculations and the iterative process for multimodal cases are very simple and do not involve any complex mathematical formulations such as variational calculus or Lagrangian multipliers. In many cases, using multimodal formulation results in much higher buckling load factors than using single modal formulation, if the structure has been multimodal at any stage of the optimisation. The optimality criteria method by Szyszkowski (1992) does not give optimum designs for highly statically indeterminate frames. For the same example, ESO method gives much better results than Szyszkowski (1992).

## APPENDIX 5.1

The history of the first ten eigenvalues for the box frame (minimum depth 1 mm)

$\lambda_1$	$\lambda_2$	$\lambda_3$	$\lambda_4$	$\lambda_5$	$\lambda_6$	$\lambda_7$	$\lambda_8$	$\lambda_9$	$\lambda_{10}$
12.158	16.070	27.666	27.927	34.879	58.296	71.270	84.196	-90.627	-100.211
12.963	16.988	26.387	29.133	36.645	54.880	75.276	88.194	-89.006	-99.186
13.795	18.242	24.889	31.220	39.469	51.559	80.743	-86.447	93.808	-96.234
14.656	19.462	23.509	33.371	42.461	48.357	-83.904	86.483	-93.310	93.659
15.547	20.261	22.647	35.525	45.353	45.610	-81.386	88.418	-90.423	92.480
16.493	19.554	23.072	37.179	42.564	48.532	-79.416	81.993	-88.768	98.338
17.447	18.354	24.427	37.168	42.161	51.954	76.299	-76.985	-85.984	104.588
16.943	18.447	25.781	34.792	43.859	55.055	70.289	-75.129	-84.469	106.498
18.059	18.484	25.333	37.518	42.971	53.258	-71.615	76.775	-80.432	107.203
18.532	19.847	26.385	37.817	43.949	54.650	-67.151	-75.114	77.308	109.888
18.365	19.466	27.844	35.300	45.821	57.926	-67.112	71.314	-74.786	110.605
18.989	19.883	27.367	38.035	45.072	56.585	-63.507	-70.669	77.447	113.346
19.439	21.222	28.136	37.953	45.364	56.840	-60.268	-67.321	77.788	114.761
19.693	20.399	29.630	35.355	47.376	60.130	-60.256	-67.045	71.870	113.452
20.835	20.978	30.716	35.159	48.314	-56.192	61.366	-62.270	72.322	114.964
21.189	22.254	31.666	36.148	48.933	-51.940	-57.137	62.617	74.900	-107.854
20.649	22.200	33.293	33.384	51.385	-51.925	-56.915	64.875	70.448	-107.794
21.645	22.292	32.808	36.240	-48.867	50.348	-53.470	64.542	75.172	-99.519
21.782	23.853	33.317	37.598	-45.338	-49.436	50.102	64.664	78.606	-90.845
22.195	22.813	34.811	34.968	-45.340	-49.267	52.550	67.309	73.695	-90.817
23.131	23.527	35.624	35.847	-41.736	-45.047	52.832	68.957	76.327	-82.159
23.228	25.081	35.906	37.158	-38.461	-41.378	52.289	69.454	-74.362	-77.496
23.366	24.294	34.377	37.622	-38.468	-41.257	54.888	70.171	-74.352	76.714
24.367	24.899	-35.326	35.662	37.765	-37.769	54.200	-66.983	-69.636	72.065
24.543	26.264	-32.103	-34.208	36.660	38.405	54.515	-59.696	-61.965	73.662
24.862	25.662	-30.689	-32.634	35.654	40.270	-54.218	-56.342	57.364	74.030
25.665	26.487	-28.013	-29.698	37.040	40.129	-48.160	-49.980	56.471	76.646
-25.233	25.404	-26.671	28.360	40.013	40.212	-42.103	-43.639	56.464	78.505
-24.150	-25.452	26.577	26.909	-37.489	-38.955	38.977	42.124	59.372	80.112
-21.747	-22.847	26.614	28.553	-32.451	-33.693	40.314	42.028	58.478	82.077
-20.862	-21.810	27.065	27.828	-28.459	-29.694	39.254	44.045	61.508	81.621
-18.757	-19.525	-24.293	-25.364	27.755	28.826	40.744	44.347	61.794	84.769
-16.776	-17.364	-20.524	-21.470	27.411	30.936	43.741	44.106	60.740	87.312
-16.136	-16.370	-17.613	-18.812	28.677	29.398	43.012	45.792	63.822	88.545
-14.178	-14.242	-14.744	-15.996	28.619	31.263	44.604	46.111	64.122	91.125
-11.896	-11.911	-13.703	-14.836	29.991	30.059	43.928	48.529	67.740	90.961
-9.736	-9.824	-12.140	-13.001	29.926	32.036	45.741	48.148	66.922	94.604
-7.875	-7.961	-11.460	-12.293	30.728	31.421	45.041	50.677	70.685	93.363
-6.255	-6.348	-10.099	-10.756	31.400	32.702	46.733	50.993	70.987	-85.341
-4.910	-4.995	-8.869	-9.389	31.067	35.058	50.240	50.493	69.795	-75.012
-3.888	-3.953	-8.447	-8.970	32.637	33.723	49.794	52.837	-65.728	-65.790
-3.069	-3.125	-7.509	-7.931	32.683	35.836	50.043	53.612	-57.815	-57.863
-2.456	-2.496	-7.241	-7.667	34.289	34.507	49.361	-50.027	-50.064	56.366

-1.958	-1.989	-6.374	-6.714	33.971	37.102	-42.907	-42.935	53.423	55.553
-1.731	-1.751	-6.237	-6.579	35.202	35.565	-36.463	-36.479	50.391	58.281
-1.390	-1.405	-5.498	-5.779	-30.869	-30.878	35.166	38.051	54.725	58.308
-1.188	-1.198	-5.407	-5.685	-25.671	-25.671	36.107	36.794	51.640	61.121
-0.973	-0.979	-4.840	-5.060	-21.560	-21.564	36.443	39.373	56.464	60.364
-0.814	-0.818	-4.628	-4.837	-16.869	-16.877	36.529	37.822	52.326	62.443
-0.643	-0.646	-4.172	-4.344	-13.937	-13.948	37.097	40.397	57.889	61.635
-0.529	-0.530	-3.979	-4.138	-10.529	-10.546	37.408	38.573	53.529	63.958
-0.386	-0.386	-3.526	-3.646	-8.283	-8.301	38.019	41.156	-57.705	-58.764
-0.317	-0.317	-3.307	-3.407	-6.069	-6.100	38.168	39.456	54.656	-56.158
-0.203	-0.204	-2.792	-2.856	-4.565	-4.605	39.194	41.594	-49.683	-50.503
-0.174	-0.174	-2.249	-2.270	-3.632	-3.710	38.736	40.537	-48.573	-49.369
-0.090	-0.090	-1.549	-1.554	-2.991	-3.060	40.126	42.506	-42.849	-43.458
-0.092	-0.092	-0.920	-0.921	-2.832	-2.902	39.587	41.477	-41.906	-42.498
-0.031	-0.031	-0.481	-0.482	-2.421	-2.474	-36.561	-37.018	41.227	43.248
-0.050	-0.050	-0.219	-0.219	-1.966	-2.002	-29.514	-29.842	40.556	44.740
-0.050	-0.050	-0.220	-0.220	-1.973	-2.008	-29.618	-29.936	42.146	42.163
-0.009	-0.009	-0.061	-0.061	-1.673	-1.697	-25.474	-25.703	41.785	46.350
-0.031	-0.031	-0.094	-0.094	-1.637	-1.660	-24.564	-24.781	42.498	43.177
-0.005	-0.005	-0.014	-0.014	-1.390	-1.407	-21.175	-21.331	42.708	47.168
-0.034	-0.034	-0.100	-0.100	-1.326	-1.341	-19.768	-19.915	42.466	43.596
-0.005	-0.005	-0.014	-0.014	-1.109	-1.118	-16.849	-16.948	43.175	47.347
-0.034	-0.034	-0.100	-0.100	-1.060	-1.070	-15.693	-15.790	42.534	44.044
-0.005	-0.005	-0.014	-0.014	-0.863	-0.869	-13.095	-13.158	43.647	47.403
-0.034	-0.034	-0.100	-0.100	-0.834	-0.840	-12.229	-12.288	42.649	44.516
-0.005	-0.005	-0.014	-0.014	-0.658	-0.661	-9.959	-9.996	44.124	47.495
-0.034	-0.034	-0.099	-0.099	-0.643	-0.646	-9.289	-9.324	42.697	44.997
-0.009	-0.009	-0.069	-0.069	-0.475	-0.477	-7.101	-7.122	44.163	46.613
-0.034	-0.034	-0.098	-0.098	-0.361	-0.362	-4.953	-4.963	43.398	45.584
-0.009	-0.009	-0.069	-0.069	-0.239	-0.240	-3.500	-3.505	44.735	47.395
-0.033	-0.033	-0.090	-0.090	-0.190	-0.190	-2.218	-2.220	43.930	46.318
-0.009	-0.009	-0.064	-0.064	-0.106	-0.106	-1.369	-1.370	45.440	48.000
-0.030	-0.030	-0.059	-0.059	-0.128	-0.128	-0.749	-0.750	44.728	46.968
-0.009	-0.009	-0.025	-0.025	-0.079	-0.079	-0.348	-0.348	46.060	48.942
-0.025	-0.025	-0.045	-0.045	-0.118	-0.118	-0.369	-0.369	45.134	47.365
-0.004	-0.004	-0.009	-0.009	-0.018	-0.018	-0.130	-0.130	47.228	50.328
-0.018	-0.018	-0.036	-0.036	-0.097	-0.097	-0.175	-0.175	45.214	48.215
-0.005	-0.005	-0.009	-0.009	-0.029	-0.029	-0.079	-0.079	47.272	49.954
-0.018	-0.018	-0.036	-0.036	-0.097	-0.097	-0.175	-0.175	45.219	48.212
-0.005	-0.005	-0.009	-0.009	-0.029	-0.029	-0.079	-0.079	47.272	49.954
-0.018	-0.018	-0.036	-0.036	-0.097	-0.097	-0.175	-0.175	45.219	48.212

## APPENDIX 5.2

The history of the first ten eigenvalues for the box frame (minimum depth 4 mm)

$\lambda_1$	$\lambda_2$	$\lambda_3$	$\lambda_4$	$\lambda_5$	$\lambda_6$	$\lambda_7$	$\lambda_8$	$\lambda_9$	$\lambda_{10}$
12.158	16.070	27.666	27.927	34.879	58.296	71.270	84.196	-90.627	-100.211
13.013	17.211	26.171	29.641	37.346	54.458	76.393	-88.560	89.982	-98.308
13.955	18.451	24.658	31.852	40.206	51.093	82.231	-85.857	94.920	-95.834
14.871	19.523	23.134	33.922	43.000	47.553	-83.680	87.914	92.365	-93.974
15.815	19.959	22.363	35.909	44.335	45.922	-81.486	86.219	-92.137	93.826
16.853	19.163	23.213	37.459	42.311	49.217	-78.869	80.405	-89.890	100.404
17.808	17.852	24.471	36.357	42.662	52.368	74.238	-76.800	-88.206	106.302
18.316	19.246	25.260	36.740	43.175	52.957	-72.594	75.236	-83.436	107.702
17.821	19.356	26.659	34.264	45.137	56.160	69.397	-70.719	-81.899	108.140
18.892	19.400	26.137	37.078	43.993	54.267	-67.415	75.736	-78.107	110.471
19.309	20.867	27.038	37.264	44.390	54.843	-63.702	-73.523	76.640	112.046
19.492	20.498	28.699	34.962	46.788	58.518	-61.486	71.228	-71.499	112.750
19.973	21.158	28.121	37.828	45.489	56.482	-58.402	-67.930	77.620	115.805
19.600	21.073	29.623	35.170	47.659	-58.260	59.752	-68.006	71.628	113.592
20.214	21.283	28.692	38.163	46.624	-55.302	57.960	-64.562	78.051	-111.206
19.709	21.319	30.227	35.406	48.933	-55.157	61.239	-64.570	72.084	-109.800
20.757	21.409	29.596	38.420	47.437	-52.270	59.149	-61.198	78.452	-102.560
21.132	22.931	30.473	38.463	47.648	-48.922	-56.994	59.593	79.383	-94.241
21.291	22.274	32.055	35.681	-48.770	50.021	-56.893	62.899	73.425	-93.101
22.624	22.739	32.848	35.591	-45.483	50.064	-52.756	63.301	74.352	-85.271
22.869	24.148	33.416	36.754	-42.068	-48.234	50.235	64.547	-77.208	77.489
22.594	24.077	34.161	35.371	-41.351	-47.165	53.170	67.351	73.294	-75.974
23.205	24.484	34.541	37.275	-38.912	-44.310	52.065	66.611	-70.135	-78.214
22.738	24.399	34.394	36.266	-38.702	-43.979	54.832	68.467	-69.297	74.384
23.502	24.645	35.360	-36.362	37.542	-41.203	53.636	-63.733	68.222	-72.292
23.833	26.062	-33.178	36.081	-37.076	38.658	53.908	-56.975	-64.767	69.541
24.429	25.080	-32.453	35.963	-36.087	38.131	-56.161	57.030	-63.806	72.003
25.052	26.206	-29.322	-32.298	38.173	38.912	-49.999	56.113	-57.118	73.219
25.072	-26.244	27.855	-28.510	38.148	41.737	-44.182	-50.600	55.685	74.501
-24.917	26.243	26.394	-26.627	39.037	40.273	-40.965	-47.751	58.827	77.529
-22.170	-23.487	26.155	28.250	-36.296	39.931	42.318	-42.801	57.147	77.393
-20.703	-21.527	26.604	27.521	-33.729	39.593	-40.554	42.160	60.379	79.738
-18.044	-18.539	27.659	28.192	-30.108	-36.197	40.962	41.977	60.110	82.419
-15.503	-15.810	-26.646	27.648	29.981	-32.335	42.363	42.448	59.533	82.966
-13.866	-13.979	-25.240	28.264	29.065	-30.985	39.712	44.690	62.938	82.936
-11.606	-11.653	-22.582	-27.876	28.657	30.470	43.149	43.927	60.858	-73.419
-9.523	-9.529	-21.502	-26.616	29.108	30.149	42.297	46.409	-63.489	-64.061
-7.620	-7.626	-19.506	-23.833	29.910	31.184	45.739	46.322	-54.325	-54.853
-6.042	-6.050	-17.670	-21.568	29.966	33.022	45.721	-46.645	-47.181	47.198
-4.667	-4.672	-17.165	-20.815	31.545	31.626	-39.780	-40.480	43.365	49.971
-3.481	-3.483	-15.561	-18.515	31.453	-33.190	33.739	-33.893	46.812	49.140
-2.552	-2.552	-15.108	-17.650	-28.068	-29.112	32.217	33.171	44.404	52.048

-1.808	-1.810	-13.480	-15.468	-23.277	-24.497	32.849	34.640	48.019	53.066
-1.256	-1.258	-12.654	-13.889	-20.073	-21.986	33.075	34.593	45.585	56.139
-0.974	-0.975	-10.668	-11.294	-16.948	-18.905	34.545	34.996	48.609	55.142
-0.832	-0.832	-8.726	-9.033	-14.737	-16.717	33.714	37.537	52.454	53.759
-0.708	-0.708	-6.931	-7.043	-14.154	-16.264	35.312	35.628	49.439	56.438
-0.601	-0.601	-5.136	-5.183	-12.681	-14.440	34.953	37.654	52.687	56.259
-0.520	-0.520	-3.723	-3.741	-12.621	-14.359	35.610	36.624	49.509	59.173
-0.446	-0.446	-2.540	-2.548	-11.313	-12.812	36.190	37.765	52.817	58.768
-0.386	-0.386	-1.678	-1.681	-10.322	-11.538	35.511	40.260	56.830	57.260
-0.324	-0.324	-1.080	-1.081	-10.384	-11.564	37.185	38.338	53.699	60.046
-0.258	-0.258	-0.769	-0.770	-9.434	-10.447	36.182	41.178	57.983	58.768
-0.257	-0.257	-0.765	-0.766	-9.444	-10.415	37.606	38.814	54.267	61.174
-0.256	-0.256	-0.763	-0.764	-8.447	-9.261	36.635	41.003	57.761	59.168
-0.258	-0.258	-0.767	-0.768	-7.682	-8.316	38.284	38.856	54.343	62.235
-0.256	-0.256	-0.762	-0.763	-6.794	-7.295	37.494	40.869	57.586	62.250
-0.258	-0.258	-0.766	-0.767	-6.111	-6.492	38.691	39.141	54.163	65.409
-0.257	-0.257	-0.760	-0.761	-5.345	-5.627	38.475	40.601	57.296	63.453
-0.258	-0.258	-0.764	-0.764	-4.749	-4.958	38.419	40.152	53.898	66.681
-0.256	-0.256	-0.755	-0.756	-4.122	-4.284	39.210	40.656	57.392	-60.120
-0.255	-0.255	-0.751	-0.751	-3.577	-3.702	38.023	43.211	-51.453	-52.407
-0.256	-0.256	-0.752	-0.752	-3.572	-3.692	39.503	40.754	-51.325	-52.247
-0.255	-0.255	-0.746	-0.747	-3.077	-3.161	38.542	43.081	-43.419	-44.098
-0.257	-0.257	-0.746	-0.747	-2.667	-2.724	-36.826	-37.319	40.314	40.879
-0.254	-0.254	-0.732	-0.733	-2.265	-2.306	-30.478	-30.846	39.273	43.295
-0.255	-0.255	-0.725	-0.726	-1.945	-1.972	-25.270	-25.523	41.045	41.067
-0.252	-0.252	-0.701	-0.702	-1.636	-1.653	-20.233	-20.405	40.340	43.081
-0.252	-0.252	-0.678	-0.679	-1.411	-1.421	-16.282	-16.393	40.832	42.177
-0.247	-0.247	-0.631	-0.632	-1.214	-1.220	-12.616	-12.686	41.390	42.937
-0.244	-0.244	-0.573	-0.575	-1.087	-1.090	-9.714	-9.757	40.025	45.879
-0.243	-0.244	-0.573	-0.574	-1.086	-1.089	-9.713	-9.755	41.652	43.228
-0.237	-0.237	-0.503	-0.504	-1.004	-1.005	-7.304	-7.328	40.416	46.072
-0.236	-0.236	-0.502	-0.503	-1.001	-1.002	-7.304	-7.328	42.053	43.407
-0.225	-0.225	-0.430	-0.431	-0.946	-0.946	-5.299	-5.311	41.102	45.884
-0.209	-0.209	-0.375	-0.375	-0.915	-0.915	-3.771	-3.777	43.038	43.591
-0.183	-0.183	-0.330	-0.330	-0.872	-0.872	-2.557	-2.560	42.219	45.910
-0.157	-0.157	-0.302	-0.302	-0.825	-0.825	-1.739	-1.739	43.631	44.202
-0.130	-0.130	-0.265	-0.265	-0.694	-0.694	-1.241	-1.242	43.630	45.443
-0.118	-0.118	-0.240	-0.240	-0.605	-0.605	-1.133	-1.133	42.552	47.793
-0.119	-0.119	-0.240	-0.240	-0.607	-0.607	-1.136	-1.137	44.235	45.130
-0.119	-0.119	-0.242	-0.242	-0.610	-0.610	-1.142	-1.142	42.819	47.584
-0.119	-0.119	-0.241	-0.241	-0.608	-0.609	-1.138	-1.138	44.501	44.869
-0.118	-0.118	-0.240	-0.240	-0.606	-0.606	-1.134	-1.134	42.902	47.465
-0.119	-0.119	-0.241	-0.241	-0.607	-0.607	-1.137	-1.137	44.572	44.766
-0.118	-0.118	-0.240	-0.240	-0.606	-0.606	-1.134	-1.134	42.902	47.465
-0.119	-0.119	-0.241	-0.241	-0.607	-0.607	-1.137	-1.137	44.572	44.766
-0.118	-0.118	-0.240	-0.240	-0.606	-0.606	-1.134	-1.134	42.902	47.465
-0.119	-0.119	-0.241	-0.241	-0.607	-0.607	-1.137	-1.137	44.572	44.766

## CHAPTER 6 - MINIMUM WEIGHT DESIGN OF FRAME STRUCTURES

### 6.1 Introduction

In the preceding Chapters 4 and 5, optimum designs of frame structures to enhance buckling resistance have been obtained by increasing the critical buckling load factor while keeping the weight of the structure constant. This chapter illustrates the application of ESO method to find the minimum weight design of a frame structure that satisfies the prescribed buckling load constraint. The buckling load constraint of a structure may be given in the form

$$\lambda_{cr} \geq FS \quad (6.1)$$

The critical buckling load factor,  $\lambda_{cr}$  is the first eigenvalue which scales the applied loading to give the buckling load.  $FS$  is the factor of safety against buckling. Typical values of  $FS$  for frames and trusses may be between 2 and 3 and for plates and shells, it may be even higher. From an initial over-designed structure, the excess material can be gradually removed until the buckling load constraint (6.1) is no longer met. The ESO method described in Section 4.4 can be readily extended to such minimum weight designs as follows:

*Step 1:* Discretise the structure using a fine mesh of finite elements.

*Step 2:* Solve the eigenvalue problem (4.1).

*Step 3:* Calculate the sensitivity number  $\alpha_{ib}$  for each element.

*Step 4:* Decrease the cross-sectional areas of a few number of elements which have the lowest values of  $\alpha_{ib}$ .

*Step 5:* Repeat Steps 2 to 4 until  $\lambda_{cr} = FS$ .

However this approach is not very efficient. A large over-designed structure needs to be selected at the beginning to accommodate the largest section of the optimum design. And often how large the initial design need to be selected is unknown. To avoid this lengthy process, an efficient method is proposed herein with the use of uniform scaling coupled with resizing of elements for the minimum weight design of structures. In uniform scaling, all the design variables are scaled by a single factor in order to adjust the critical buckling load factor to the factor of safety specified by the constraint ( $\lambda_{cr} = FS$ ). Since the buckling load factors are, in general, complicated functions of the design variables, uniform scaling may pose a serious challenge, particularly, for space frames.

In the following sections, uniform scaling and the ESO method for the minimum weight designs are illustrated with in-plane and space frame examples. It is assumed that the cross-sectional area at any section of these frames  $A(x)$  is related to its flexural stiffness  $I(x)$  by  $I(x) = cA(x)^p$  in which  $c$  and  $p$  are constants determined by the cross-sectional shape.

## 6.2 Uniform Scaling Factor $S_b$

In an optimisation algorithm, it is convenient to obtain a feasible design after each iteration and it can be obtained by scaling the design uniformly (all the design variables are scaled by a single factor) in order to satisfy the specified constraints. This helps keep track the reduction in the weight of the structure after each iteration and also helps to pick up the most active constraints. Uniform scaling to satisfy buckling load constraint is simple and straight forward for linear size-stiffness structures. The linear uniform scaling factor  $S_b$  is given below:

$$S_b = \frac{FS}{\lambda_{cr}} \quad (6.2)$$

The subscript  $b$  in  $S_b$  refers to buckling. In general, structural responses of frames primarily depend on the moment of inertia and for trusses these depend on the cross-sectional area. For trusses, whether they are 2- or 3-dimensional, size-stiffness relation is always linear. For 2-dimensional frames, (or even for 3-dimensional frames which displacements are constrained to in-plane movements only), size-stiffness relation is linear when  $I(x) = cA(x)$ . Khot *et al.* (1976), Morris (1982) and Berke and Khot (1988) proposed to use linear scaling factor  $S_b = FS / \lambda_{cr}$  for nonlinear size-stiffness structures as well, and claimed with a few additional iterations,  $\lambda_{cr}$  may be brought to equal to  $FS$ . However, this approach may not be efficient and for certain problems, acceptable scaling parameters cannot be obtained. In the following sections, an efficient scaling factor is proposed for nonlinear size-stiffness structures and for space frames.

### 6.2.1 Uniform scaling factor for 2-dimensional frames

The buckling load of 2-dimensional frames primarily depends on the flexural stiffness and it is proportional to the moment of inertia  $I(x)$ . The influence of axial stiffness on the buckling load may be negligible. For the relation  $I(x) = cA(x)^p$ , uniform scaling factor  $S_b$  may be taken as

$$S_b = \left( \frac{FS}{\lambda_{cr}} \right)^{1/p} \quad (6.3)$$

Uniform scaling needs to be carried out iteratively with the following resizing algorithm until convergence is achieved.

$$x_i^{v+1} = x_i^v \left( \frac{FS}{\lambda_{cr}} \right)^{1/p} \quad (6.4)$$

where  $v+1$  and  $v$  indicate the iteration numbers.

For example, consider the 3-storey frame discussed in Section 4.5.2.3 (Figure 4.11). In this case, rectangular section member depths are the design variable, hence  $p = 3$ . Initial design depths are arbitrarily chosen. The values assigned are: external columns,  $d = 20$  mm; internal columns,  $d = 30$  mm; first floor beam,  $d = 20$  mm; and second and third floor beam  $d = 10$  mm. Let  $FS = 3.0$ . No sizing constraints are imposed. The values of  $\lambda_{cr}$ ,  $S_b$  and volume of the structure at each iteration of the scaling process are given in Table 6.1.

**Table 6.1** - Uniform scaling of 3-storey frame with no sizing constraints

Iteration Number	$\lambda_{cr}$	$S_b = (FS / \lambda_{cr})^{1/3}$	Volume (m <sup>3</sup> )
0	1.276	1.330	0.0168
1	3.000	1.000	0.0223

Only one iteration is required to bring  $\lambda_{cr}$  from 1.276 to 3.0. If linear scaling factor,  $S_b = FS / \lambda_{cr}$  is used instead of  $S_b = (FS / \lambda_{cr})^{1/3}$ ,  $\lambda_{cr}$  will diverge and it cannot be brought to 3.0. The values of  $\lambda_{cr}$ ,  $S_b$  and the volume of the structure for the first few iterations for this case are given in Table 6.2.

If there are sizing constraints, they need to be imposed after uniform scaling and additional iterations may be required to make  $\lambda_{cr} = FS$ . For the above example using the nonlinear scaling factor in equation (6.3), uniform scaling with sizing constraints, 10

$mm \leq d \leq 35$  mm, is carried out. The values of  $\lambda_{cr}$ ,  $S_b$  and the volume of the structure at each iteration of the scaling process are given in Table 6.3.

**Table 6.2.** - Uniform scaling of 3-storey frame with the linear scaling factor

Iteration Number	$\lambda_{cr}$	$S_b = (FS / \lambda_{cr})$	Volume (m <sup>3</sup> )
0	1.276	2.352	0.0168
1	6.589	0.181	0.0395
2	0.098	30.576	0.0071
3	2798.2	0.0011	0.2184
4	1.36e-4	22032.3	0.0008

**Table 6.3** - Uniform scaling of 3-storey frame with sizing constraints

Iteration Number	$\lambda_{cr}$	$S_b = (FS / \lambda_{cr})^{1/3}$	Volume (m <sup>3</sup> )
0	1.276	1.330	0.0168
1	2.772	1.027	0.0212
2	2.949	1.006	0.0216
3	2.989	1.001	0.0216
4	3.000	1.000	0.0216

### 6.2.2 Uniform scaling factor for space frames

The relationship between buckling load factor and member cross-sectional properties cannot be established explicitly for space frames, unlike for 2-dimensional frames. However the following relation can be used for uniform scaling and a few additional iterations may be required to obtain an acceptable scaling parameter.

$$S_b = \left( \frac{FS}{\lambda_{cr}} \right)^{1/q} \quad (6.5)$$

Note that the value for  $q$  in this expression may not be equal to  $p$  from the relation  $I(x) = cA(x)^p$ . Besides the value for  $q$  is unknown and it may depend on the applied loads. The following examples illustrate the dependency of the value  $q$  on the convergence of uniform scaling process for different values of applied loads.

### 6.2.2.1 Example 1

Consider the space frame with inclined members shown in Figure 6.1. All the members are of rectangular cross-section with constant depth,  $d = 40$  mm. Initial uniform breadth,  $b = 40$  mm and it is allowed to vary to any (no sizing constraints are imposed). Each member is divided into 2 elements.  $E = 200$  GPa.  $G = 80$  GPa. For  $P = 1$  kN,  $\lambda_{cr} = 19.22$ . Let  $FS = 2.5$ . Uniform scaling is carried out separately with different values of  $q$  in order to bring  $\lambda_{cr} = 2.5$ . Iteration histories of the uniform scaling with different values of  $q$  for  $P = 1$  kN are given in Table 6.4.

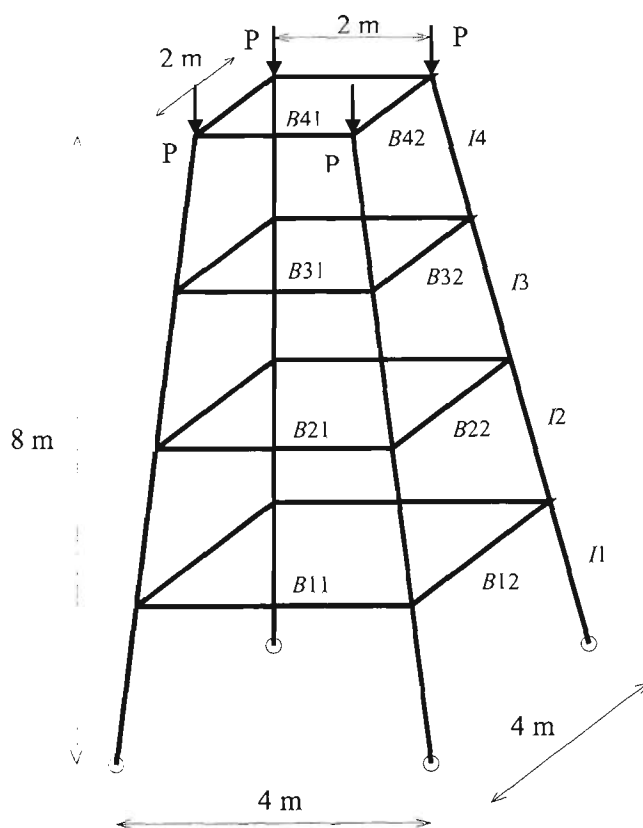


**Figure 6.1** - Layout of space frame - Example 1

**Table 6.4** - Uniform scaling of space frame - Example 1,  $P = 1$  kN

Iteration number	$q = 1$		$q = 2$		$q = 3$		$q = 4$	
	$\lambda_{cr}$	$S_b$	$\lambda_{cr}$	$S_b$	$\lambda_{cr}$	$S_b$	$\lambda_{cr}$	$S_b$
0	19.218	0.130	19.218	0.361	19.218	0.507	19.218	0.601
1	0.065	38.337	1.304	1.384	3.412	0.902	5.430	0.824
2	100.727	0.025	3.275	0.874	2.555	0.993	3.192	0.941
3	0.056	44.420	2.243	1.056	2.503	1.000	2.691	0.982
4	111.315	0.022	2.613	0.978	2.500	1.000	2.556	0.995
5	0.056	44.734	2.456	1.009			2.516	0.998
6	111.848	0.022	2.518	0.996			2.505	1.000
7	Not converged		2.493	1.001			2.501	1.000
8			2.503	0.999			2.500	1.000
9			2.499	1.000				
10			2.500	1.000				

Similar analyses (uniform scaling with different values of  $q$ ) are carried out separately for  $P = 0.1$  kN,  $P = 10$  kN and  $P = 100$  kN and the iteration histories of uniform scaling for these load cases are given in Tables 6.5, 6.6 and 6.7, respectively.

**Table 6.5** - Uniform scaling of space frame - Example 1,  $P = 0.1$  kN

Iteration number	$q = 1$		$q = 2$		$q = 3$		$q = 4$	
	$\lambda_{cr}$	$S_b$	$\lambda_{cr}$	$S_b$	$\lambda_{cr}$	$S_b$	$\lambda_{cr}$	$S_b$
0	192.18	0.013	192.18	0.114	192.18	0.235	192.18	0.338
1	1.1E-03	2379.8	0.442	2.379	3.755	0.873	10.792	0.694
2	8247.4	3.0E-04	5.712	0.662	2.519	0.998	3.713	0.906
3	4.9E-04	5137.4	1.693	1.215	2.500	1.000	2.775	0.974
4	Not converged		3.010	0.911			2.570	0.993
5			2.289	1.045			2.518	0.998
6			2.607	0.979			2.505	1.000
7			2.451	1.010			2.501	1.000
8			2.523	0.995			2.500	1.000
9			2.489	1.002				
10			2.505	0.999				
11			2.497	1.000				
12			2.501	1.000				
13			2.500	1.000				

**Table 6.6** - Uniform scaling of space frame - Example 1,  $P = 10$  kN

Iteration number	$q = 0.5$		$q = 1$		$q = 2$		$q = 3$		
	$\lambda_{cr}$	$S_b$	$\lambda_{cr}$	$S_b$	$\lambda_{cr}$	$S_b$	$\lambda_{cr}$	$S_b$	
0	1.922	1.692	1.922	1.301	1.922	1.141	1.922	1.092	
1	3.378	0.548	2.592	0.964	2.271	1.049	2.173	1.048	
2	1.656	2.279	2.499	1.000	2.383	1.024	2.278	1.032	
3	4.222	0.351	2.500	1.000	2.441	1.012	2.350	1.021	
4	0.944	7.017			2.471	1.006	2.399	1.014	
5	Not converged				2.485	1.003	2.433	1.009	
6					2.493	1.001	2.455	1.006	
7					2.496	1.001	2.470	1.004	
8					2.498	1.000	2.480	1.003	
9					2.499	1.000	2.487	1.002	
10					2.500	1.000	2.491	1.001	
11								2.494	1.001
12								2.496	1.001
13								2.497	1.000
14								2.498	1.000
15						2.500	1.000		

**Table 6.7** - Uniform scaling of space frame - Example 1,  $P = 100$  kN

Iteration number	$q = 0.75$		$q = 1$		$q = 2$		$q = 3$	
	$\lambda_{cr}$	$S_b$	$\lambda_{cr}$	$S_b$	$\lambda_{cr}$	$S_b$	$\lambda_{cr}$	$S_b$
0	0.192	30.595	0.192	13.009	0.192	3.607	0.192	2.352
1	8.110	0.208	2.784	0.898	0.724	1.858	0.471	1.745
2	1.296	2.402	2.470	1.012	1.365	1.353	0.826	1.447
3	3.352	0.676	2.503	0.999	1.876	1.154	1.205	1.276
4	2.164	1.213	2.500	1.000	2.189	1.069	1.551	1.172
5	2.674	0.914			2.354	1.031	1.835	1.109
6	2.421	1.044			2.433	1.014	2.049	1.069
7	2.538	0.980			2.470	1.006	2.201	1.043
8	2.482	1.010			2.486	1.003	2.305	1.027
9	2.509	0.995			2.494	1.001	2.375	1.017
10	2.496	1.002			2.497	1.001	2.420	1.011
11	2.502	0.999			2.499	1.000	2.449	1.007
12	2.499	1.000			2.499	1.000	2.468	1.004
13	2.500	1.000			2.500	1.000	2.479	1.003
14							2.487	1.002
15							2.492	1.001
16							2.495	1.001
17							2.497	1.000
18							2.498	1.000
19							2.500	1.000

From the above tables, it is observed, for  $P = 0.1$  kN and  $P = 1$  kN, uniform scaling is done with less number of iterations when  $q = 3$ . For  $P = 10$  kN and  $P = 100$  kN, uniform scaling is done with less number of iterations when  $q = 1$ .

### 6.2.2.2 Example 2

Consider the 3-storey, single-bay, pin-based frame shown in Figure 6.2. Torsional loads are applied at the top storey level in  $X$ - and  $Z$ -directions. All the members are of rectangular cross-section with constant depth,  $d = 20$  mm. Initial uniform breadth,  $b = 20$  mm. No sizing constraints are imposed. For  $P = 1$  kN,  $\lambda_{cr} = 3.078$ . Let  $FS = 3.0$ .

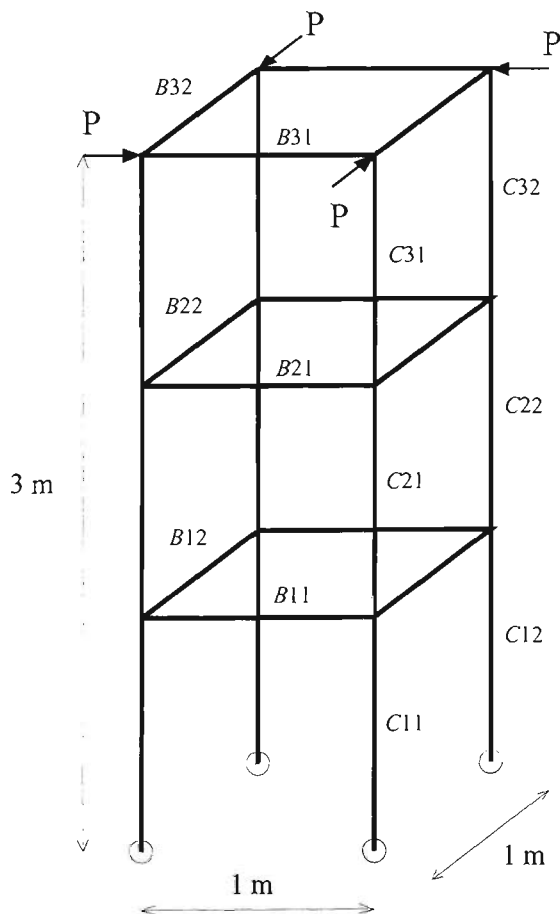


Figure 6.2 - Layout of space frame - Example 2

As described in the previous example, uniform scaling is carried out separately with different values of  $q$  for loads  $P = 0.1$  kN, 0.5 kN, 1 kN and 5 kN in order to bring  $\lambda_{cr} = 3.0$ . Iteration histories of the uniform scaling for these load cases are given in Tables 6.8, 6.9, 6.10 and 6.11, respectively.

**Table 6.8** - Uniform scaling of space frame - Example 2,  $P = 0.1$  kN

Iteration number	$q = 1$		$q = 2$		$q = 3$	
	$\lambda_{cr}$	$S_b$	$\lambda_{cr}$	$S_b$	$\lambda_{cr}$	$S_b$
0	30.778	0.097	30.778	0.312	30.778	0.460
1	0.069	43.69	1.757	1.307	4.772	0.857
2	648.3	4.6E-03	3.517	0.924	3.222	0.976
3	6.0E-04	4984.3	2.868	1.023	3.031	0.997
4	12403.2	2.4E-04	3.039	0.994	3.000	1.000
5	1.1E-03	2850.2	2.989	1.002		
6	8559.5	3.5E-04	3.003	0.999		
7			3.000	1.000		

**Table 6.9** - Uniform scaling of space frame - Example 2,  $P = 0.5$  kN

Iteration number	$q = 1$		$q = 2$		$q = 3$	
	$\lambda_{cr}$	$S_b$	$\lambda_{cr}$	$S_b$	$\lambda_{cr}$	$S_b$
0	6.156	0.487	6.156	0.698	6.156	0.787
1	1.102	2.723	2.646	1.065	3.514	0.949
2	11.83	0.254	3.072	0.988	3.103	0.989
3	0.428	7.016	2.987	1.002	3.021	0.998
4	45.25	0.066	3.002	1.000	3.004	1.000
5	0.053	56.301	3.000	1.000	3.001	1.000
6	232.62	0.013			3.000	1.000

**Table 6.10** - Uniform scaling of space frame - Example 2,  $P = 1$  kN

Iteration number	$q = 1$		$q = 2$		$q = 3$	
	$\lambda_{cr}$	$S_b$	$\lambda_{cr}$	$S_b$	$\lambda_{cr}$	$S_b$
0	3.078	0.975	3.078	0.987	3.078	0.992
1	2.899	1.035	2.987	1.002	3.017	0.998
2	3.140	0.956	3.002	1.000	3.004	1.000
3	2.824	1.062	3.000	1.000	3.001	1.000
4	3.250	0.923				
5	2.698	1.112				
6	3.452	0.869				

**Table 6.11** - Uniform scaling of space frame - Example 2,  $P = 5$  kN

Iteration number	$q = 1$		$q = 2$		$q = 3$	
	$\lambda_{cr}$	$S_b$	$\lambda_{cr}$	$S_b$	$\lambda_{cr}$	$S_b$
0	0.616	4.874	0.616	2.208	0.616	1.695
1	14.201	0.211	3.869	0.881	2.089	1.128
2	0.658	4.558	2.873	1.022	2.768	1.027
3	13.827	0.217	3.022	0.996	2.947	1.006
4	0.642	4.677	2.996	1.001	2.988	1.001
5	13.968	0.215	3.001	1.000	2.997	1.000
6			3.000	1.000	2.999	1.000

For  $P = 0.1$  kN, uniform scaling is done with a less number of iterations when  $q = 3$ . For the other loads,  $q = 2$  or  $3$  is acceptable. From the results of these two examples, the following empirical rule is proposed to obtain the appropriate  $q$  to be used in equation (6.5) for uniform scaling algorithm.

Consider the space frame example 1 with  $P = 1$  kN. Initially  $\lambda_{cr} = \lambda_0 = 19.22$ . Scale the design uniformly using the linear scaling factor  $S_b = FS / \lambda_{cr}$  and obtain the critical load factor  $\lambda_{cr} = \lambda^*$  for this design. In this case  $\lambda^* = 0.0652$  (Refer Table 6.4, column 2). Using these parameters, a value for  $q^*$  is obtained from the following relation.

$$\frac{FS}{\lambda_0} = \left( \frac{\lambda^*}{\lambda_0} \right)^{1/q^*} \quad (6.6)$$

$$\frac{2.5}{19.22} = \left( \frac{0.0652}{19.22} \right)^{1/q^*}$$

$$q^* = 2.788$$

This value is closer to 3.0. When  $q = q^* = 2.788$ , the scaled design is achieved with 3 iterations. Similarly when  $P = 100$  kN,  $\lambda_{cr} = \lambda_0 = 0.1922$ . For the scaled design obtained with  $S_b = FS / \lambda_{cr} = 2.5 / 0.1922$ ,  $\lambda^* = 2.784$  (Refer Table 6.7, column 4). Substituting  $\lambda_0$  and  $\lambda^*$  into equation (6.6),  $q^* = 1.042$  is obtained. This value is closer to 1. When  $q = q^*$

= 1.042, the scaled design is achieved with 3 iterations. Iteration histories of uniform scaling obtained with  $q = q^*$  for all the load cases are given in Table 6.12. Similar analysis is carried out for example 2 and the results are given in Table 6.13.

**Table 6.12** - Uniform scaling of space frame - Example 1 with  $q = q^*$

Iteration number	$P = 0.1 \text{ kN}; q^* = 2.791$		$P = 1 \text{ kN}; q^* = 2.788$		$P = 10 \text{ kN}; q^* = 1.137$		$P = 100 \text{ kN}; q^* = 1.042$	
	$\lambda_{cr}$	$S_b$	$\lambda_{cr}$	$S_b$	$\lambda_{cr}$	$S_b$	$\lambda_{cr}$	$S_b$
0	192.179	0.211	19.218	0.481	1.922	1.260	0.192	11.733
1	2.727	0.969	2.954	0.942	2.511	0.996	2.481	1.007
2	2.488	1.002	2.498	1.000	2.501	1.000	2.501	1.000
3	2.500	1.000	2.500	1.000	2.500	1.000	2.500	1.000

**Table 6.13** - Uniform scaling of space frame - Example 2 with  $q = q^*$

Iteration number	$P = 0.1 \text{ kN}; q^* = 2.622$		$P = 0.5 \text{ kN}; q^* = 2.394$		$P = 1 \text{ kN}; q^* = 2.338$		$P = 5 \text{ kN}; q^* = 1.982$	
	$\lambda_{cr}$	$S_b$	$\lambda_{cr}$	$S_b$	$\lambda_{cr}$	$S_b$	$\lambda_{cr}$	$S_b$
0	30.778	0.412	6.156	0.741	3.078	0.989	0.616	2.224
1	3.596	0.933	3.045	0.994	3.000	1.000	3.936	0.872
2	3.013	0.998	3.000	1.000			2.857	1.025
3	3.000	1.000					3.027	0.996
4							2.995	1.001
5							3.000	1.000

Lin and Liu (1989) proposed  $q = 2$  in general for all the complex, nonlinear size-stiffness structures. In the recurrence relations used with optimality criteria methods, described in Section 4.7.1, a step size parameter  $r$  is used (equations (4.26) and (4.27)). Again for these recurrence algorithms,  $r = 2$  is a popular number assumed in most of the works (Morris, 1982). In general,  $q = 2$  is an acceptable parameter. The results from the above examples also support it. However, in certain situations, the number of iterations required for uniform scaling is greatly reduced when  $q = q^*$  is used.

### 6.3 Optimisation Procedure

An iterative procedure is set up for uniform scaling and resizing of elements so that the weight of the structure is systematically reduced and the material is gradually shifted from the strongest to the weakest part of the structure. The optimisation process involves two steps. In the first step, the design variables are scaled uniformly to meet the buckling load constraint. In the second step, critical buckling load factor is increased while keeping the weight of the structure constant, as described in Section 4.4. These two steps are repeated in cycles until the weight of the structure cannot be reduced any further. The procedure is given as follows:

*Step 1:* Select an initial design and discretise the structure using a fine mesh of finite elements.

*Step 2:* Scale the design uniformly to bring  $\lambda_{cr}$  equal to  $FS$  using the appropriate  $q^*$  while imposing the sizing constraints.

*Step 3:* Increase the critical load factor while keeping the structural weight constant by using the evolutionary method described in Section 4.4.

*Step 4:* Repeat Steps 2 and 3 in cycles until the buckling load factor in Step 3 cannot be increased any further.

A batch file is set up to handle the iteration cycles automatically. In the above procedure, the order of Steps 2 and 3 can be interchanged. The order given above is preferred when there are sizing constraints involved. Besides, initial uniform scaling determines whether the allowable design values given are large enough to satisfy the specified buckling load constraint. In Step 3, resizing ratio  $RR$  and step size need to be

specified for resizing the elements. The values for these parameters may be reduced for the final cycles of analyses in order to get accurate designs. When there are no sizing constraints, one cycle of analysis is usually sufficient to obtain minimum weight design for 2-dimensional frames and trusses. For space frames, a few cycles of analyses may be required even if there are no sizing constraints imposed.

## **6.4 Examples**

### **6.4.1 Space frame - Example 1**

Minimum weight design is sought for the space frame described in Section 6.2.2.1 when  $P = 10$  kN.  $FS = 2.5$ . No sizing constraints are imposed. Initially  $\lambda_{cr} = 1.922$ . Optimum design is obtained in three cycles of analyses. For the first two cycles of analyses,  $RR = 25\%$  and step size = 2 mm are assumed in Step 3. In the third cycle,  $RR = 12.5\%$  and step size = 1 mm are taken for resizing. Design values of members,  $\lambda_{cr}$  and the total volume of the structure obtained at the end of uniform scaling and resizing at each cycle are given in Table 6.14 (refer Figure 6.1 for member numbering). All four inclined members have the same design values at each level. Opposite horizontal members have the same design values at each level. Iteration histories of the critical load factor and the volume of the structure are shown in Figure 6.3.

**Table 6.14** - Design values at the end of each phase of analysis for example 1

Member	Initial design	Cycle 1		Cycle 2		Cycle 3		Cycle 4
		Scaling	Resizing	Scaling	Resizing	Scaling	Resizing	Scaling
I1	40.00	50.20	85.93	64.75	72.29	61.96	60.35	58.88
I2	40.00	50.20	78.18	58.91	42.60	44.06	39.34	38.38
I3	40.00	50.20	49.90	37.60	35.37	33.88	34.10	33.27
I4	40.00	50.20	49.70	37.45	35.20	31.94	32.15	31.37
B11	40.00	50.20	83.96	63.26	62.88	57.02	53.37	52.06
B12	40.00	50.20	29.32	22.10	37.86	30.74	38.97	38.02
B21	40.00	50.20	35.46	26.72	14.64	16.87	15.97	15.58
B22	40.00	50.20	31.33	23.61	33.42	28.50	28.68	27.98
B31	40.00	50.20	41.71	31.42	21.31	21.11	22.25	21.70
B32	40.00	50.20	9.82	7.40	25.26	13.89	19.00	18.54
B41	40.00	50.20	47.76	35.99	17.87	19.80	16.91	16.50
B42	40.00	50.20	13.74	10.35	22.20	18.35	18.47	18.02
$\lambda_{cr}$	1.922	2.500	4.080	2.500	3.002	2.500	2.599	2.500
Vol. (m <sup>3</sup> )	0.12239	0.15365	0.15365	0.11574	0.11574	0.10438	0.10438	0.10186

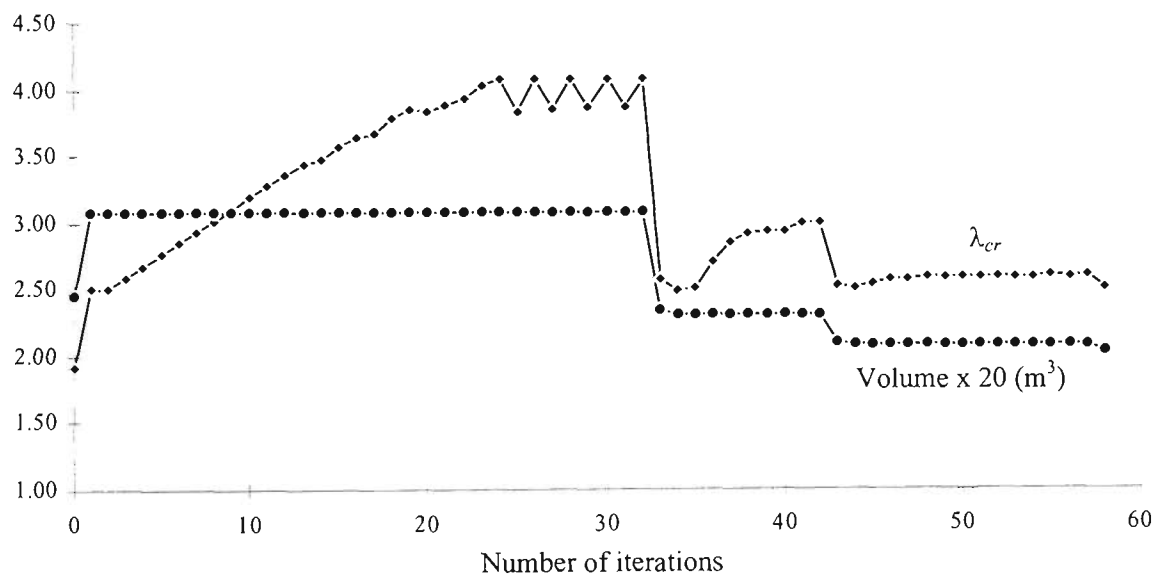


**Figure 6.3** - Iteration histories of the volume and  $\lambda_{cr}$  for the space frame, example 1

### 6.4.2 Space frame - Example 2

Minimum weight design is obtained for the 3-storey, space frame described in section 6.2.2.2. The applied load  $P = 0.4$  kN.  $FS = 3.0$ . Initially  $\lambda_{cr} = 7.695$ . Since the optimum

design is controlled by the minimum allowable depth, the following two cases are considered. Case 1: minimum allowable depth  $d_{min} = 5$  mm and Case 2: minimum allowable depth  $d_{min} = 10$  mm.  $RR = 25\%$  and step size = 1 mm are assumed for resizing. The iteration histories of the critical load factor and the volume of the structure are shown in Figures 6.4 for Case 1 design. The volume of the structure and the critical buckling load factor at the end of each phase of the analysis for the two cases are given in Table 6.15. Final design depths obtained for these two cases are given in Table 6.16 (refer Figure 6.2 for member numbering). At each level, opposite members, either column or beam, have the same design values.

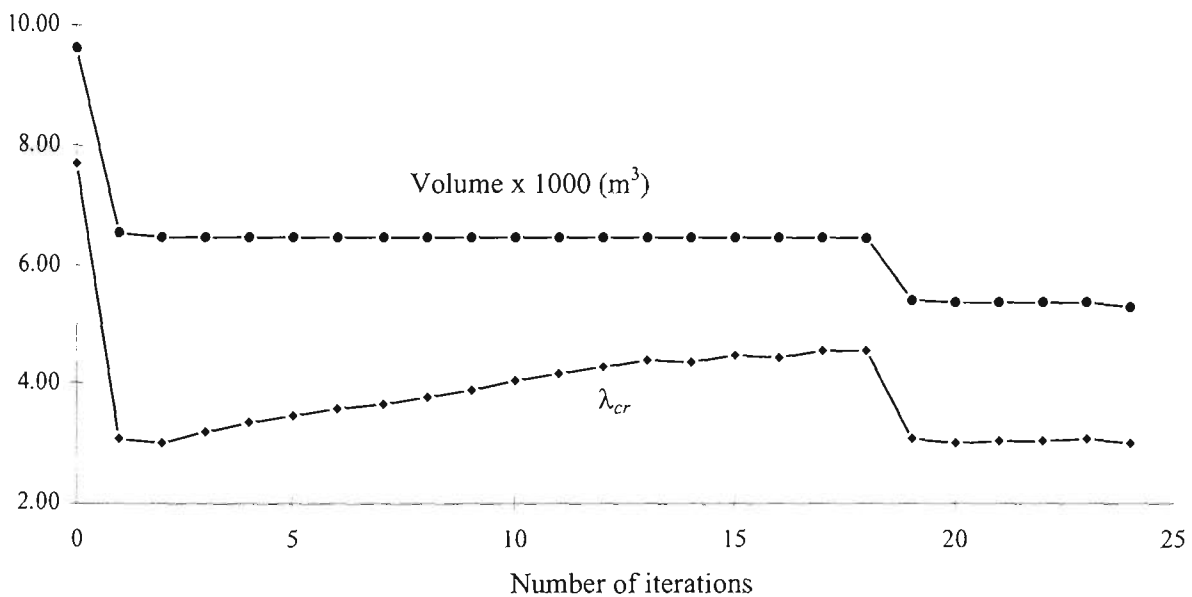


**Figure 6.4** - Iteration histories of the volume and  $\lambda_{cr}$  for Case 1 of example 2

**Table 6.15** - Buckling load factors at the end of each phase of analysis for example 2

Cycle number		Case 1- $d_{min} = 5$ mm		Case 2- $d_{min} = 10$ mm	
		$\lambda_{cr}$	Vol x 1000 (m³)	$\lambda_{cr}$	Vol x 1000 (m³)
0	Initial	7.695	9.60	7.695	9.60
1	Scaling	3.000	6.34	3.000	6.34
	Resizing	4.527	6.34	3.974	6.34
2	Scaling	3.000	5.35	3.000	5.77
	Resizing	3.068	5.35		
3	Scaling	3.000	5.30		

**Table 6.16** - Final design depths for the two cases of example 2

Member	Final depth in mm	
	Case 1	Case 2
<i>B11</i>	5.00	10.00
<i>B12</i>	23.45	20.29
<i>B21</i>	5.00	10.00
<i>B22</i>	16.53	14.11
<i>B31</i>	5.00	10.00
<i>B32</i>	11.21	10.00
<i>C11</i>	16.28	16.44
<i>C12</i>	10.84	10.00
<i>C21</i>	8.67	10.00
<i>C22</i>	14.03	13.29
<i>C31</i>	6.00	10.00
<i>C32</i>	10.46	10.00

## 6.5 Conclusions

The ESO method has been extended to the minimum weight design of frame structures with prescribed buckling constraints. Uniform scaling has been introduced to bring the critical buckling load factor  $\lambda_{cr}$  close to the factor of safety. Minimum weight design of single load case structures has been obtained by repeating the steps of uniform scaling and maximising the critical load factor with constant volume in cycles until no further reduction in the structural volume. Uniform scaling of nonlinear size-stiffness structures and space structures are complicated. An empirical rule has been proposed for the uniform scaling of space frames and has been tested with the examples. This empirical rule greatly reduces the number of iterations required for uniform scaling and ensures convergence.

## CHAPTER 7 - OPTIMUM DESIGN OF STRUCTURES WITH MULTIPLE LOAD CASES

### 7.1 Introduction

In the preceding Chapters 4, 5 and 6, optimum designs of frame structures with enhanced buckling resistance have been obtained for single load case conditions. Many structures in the real environment are subjected to a variety of load cases such as self weight, snow loads, wind loads and earthquake loads. A similar situation occurs when a structure is subjected to a traffic load, where the force is moving from one part of the structure to the other. Each independent load case may cause instability when acting alone. In this chapter, the ESO method is extended to the optimum design of structures against buckling with multiple load cases.

In mathematical programming (MP) methods, multiple load cases are treated as additional objective and constraint functions. The derivatives of objective and constraint functions with respect to design variables need to be calculated separately for each load case. Thus the size of the problem (which is very crucial in MP methods) increases multiple folds compared to the single load case problems. In optimality criteria (OC) methods, a multiple load case problem is treated as a multi constraint problem and the active participation of each load case is determined by the Lagrangian multipliers which are estimated by some iterative procedures. For example, Khot *et al.* (1976) extended the uniform strain energy density to the mass density optimality criterion which was derived for the single load case structures to the multiple load conditions as follows:

$$\sum_{k=1}^{nl} \frac{e_{ik}}{\mu_k} = 1 \quad (7.1)$$

where  $nl$  is the number of loading conditions. The quantity  $e_{ik}$  is the ratio of strain energy density to mass density associated with the critical buckling mode of the  $i^{\text{th}}$  element in the  $k^{\text{th}}$  loading condition. The Lagrangian multipliers,  $\mu_k$  ( $k = 1, nl$ ), have to be determined by some iterative procedure.

There is not much literature available on the optimum design of structures to resist buckling under multiple load cases. Turner and Plaut (1981) obtained the optimum design with multiple load cases by maximising the critical load factor for a given ratio of loads. This procedure was applied to a variety of load ratios, and the results were plotted in the loading space in terms of stability boundaries (interaction curves or surfaces) and a stability envelope. The objective was to enlarge the stability region as much as possible by an appropriate distribution of the material of the structure. A novel approach to solving problems with multiple loading conditions was introduced by Hjelmstad and Pezeshk (1991) where each eigenvalue in the objective was weighted in accordance with the degree of participation of the mode in the loading.

## 7.2 Sensitivity Number

For each load case, sensitivity numbers  $\alpha_{ib}^+$  and  $\alpha_{ib}^-$  as defined in Section 4.3 can be calculated for each element. Let the sensitivity numbers for the  $k^{\text{th}}$  load case be renamed as  $\alpha_{ibk}^+$  and  $\alpha_{ibk}^-$ . Therefore for  $nl$  number of load cases,  $\alpha_{ibk}^+$  ( $k = 1, nl$ ) and  $\alpha_{ibk}^-$  ( $k = 1, nl$ ) need to be calculated for each element. Ideally the cross-sectional area of the element of which all  $\alpha_{ibk}^+$  ( $k = 1, nl$ ) are highest should be increased and the cross-sectional area of the element of which all  $\alpha_{ibk}^-$  ( $k = 1, nl$ ) are highest should be decreased. However this situation generally does not exist. To overcome this difficulty the element

sensitivity is evaluated by the sum of its relative sensitiveness with regard to each load case. Further it is necessary to treat each load case separately depending on how active it is in the current design. If the critical load factor of a particular load case is much higher than its limit ( $FS$ ), this load case may not affect the optimum shape. Thus to measure the influence of each load case, uniform scaling factors of the load cases (as defined in Chapter 6, equation (6.2) or (6.3) or (6.5)) are used as weighting parameters. When obtaining these scaling factors, different values of factor of safety may be assumed for each load case. Let  $S_{bk}$  be the  $k^{\text{th}}$  load case uniform scaling factor. Hence the following two new sensitivity numbers are defined for multiple load case structures.

$$\alpha_{ib}^+ = \sum_{k=1}^{nl} S_{bk} \frac{\alpha_{ibk}^+}{\alpha_{bk,av}^+} \quad (7.2a)$$

$$\alpha_{ib}^- = \sum_{k=1}^{nl} S_{bk} \frac{\alpha_{ibk}^-}{\alpha_{bk,av}^-} \quad (7.2b)$$

where  $\alpha_{bk,av}^+$  is the average of the  $\alpha_{ibk}^+$  values of all elements of the  $k^{\text{th}}$  load case and  $\alpha_{bk,av}^-$  is the average of the  $\alpha_{ibk}^-$  values of all elements.

### 7.3 Optimisation Procedure

Optimum procedures are given for the design with constant volume constraint; and for the minimum weight design that satisfies the prescribed buckling load constraints.

#### 7.3.1 Constant weight design

The objective is to raise the critical buckling load factors  $\lambda_{cr,k}$  ( $k = 1, nl$ ) for all load cases as much as possible while satisfying the constant volume constraint and the sizing constraints. The scaling factor of each load case,  $S_{bk}$  will be minimised and roughly brought equal to a single value. The procedure is given as follows.

*Step 1:* Discretise the structure using a fine mesh of finite elements to represent the stress distribution and buckling modes adequately for all the load cases.

*Step 2:* Carry out the static analysis and buckling analysis for each load case.

*Step 3:* Calculate the uniform scaling factor,  $S_{bk}$  for each load case.

*Step 4:* Calculate the sensitivity numbers  $\alpha_{ib}^+$  and  $\alpha_{ib}^-$  for each element according to equation (7.2).

*Step 5:* Increase the cross-sectional areas of elements with the highest values of  $\alpha_{ib}^+$  and decrease the cross-sectional areas of the same number of elements with the highest values of  $\alpha_{ib}^-$ . Impose the sizing constraints.

*Step 6:* Calculate the total volume and if it is not equal to the original volume, scale down the cross-sectional areas obtained after Step 5 to give the original volume.

*Step 7:* Repeat Steps 2 to 6 until the critical load factors of each load case cannot be increased any further.

### **7.3.2 Minimum weight design**

The objective is to minimise the structural weight while satisfying the buckling constraint,  $\lambda_{cr,k} \geq FS_k$  ( $k = 1, n_l$ ) for all load cases. In Chapter 6, ESO method for the minimum weight design has been described. For single load case structures, uniform scaling and maximising the  $\lambda_{cr}$  with constant volume are repeated in cycles until no further reduction in the structural volume. The flowchart for this method is given in Figure 7.1.

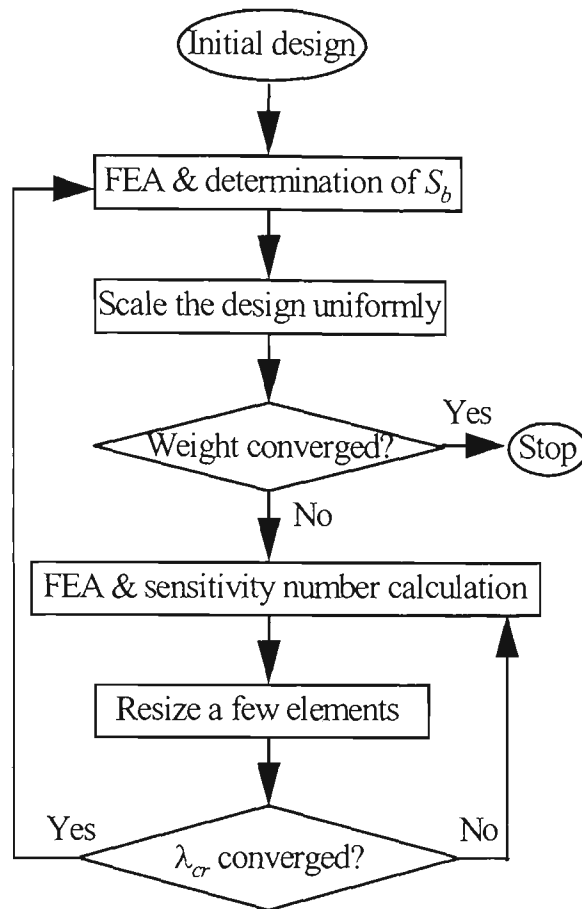


**Figure 7.1** - ESO for the minimum weight design - Method 1

The minimum weight design can also be obtained in a slightly different way as described by the flowchart given in Figure 7.2. Obviously in this method, additional uniform scaling needs to be done after each step of resizing unlike in the former approach. For multiple load cases, the influence of each load case on the current design needs to be considered simultaneously during the optimisation process. There is no point of optimising the structure for one load case and let the design violates the other loading conditions. Thus Method 2 for the minimum weight design is more suited for the multiple load case structures. This method allows for calculating the scaling factors after each step of resizing and these updated scaling factors can be used as weighting parameters in the subsequent sensitivity number calculations.

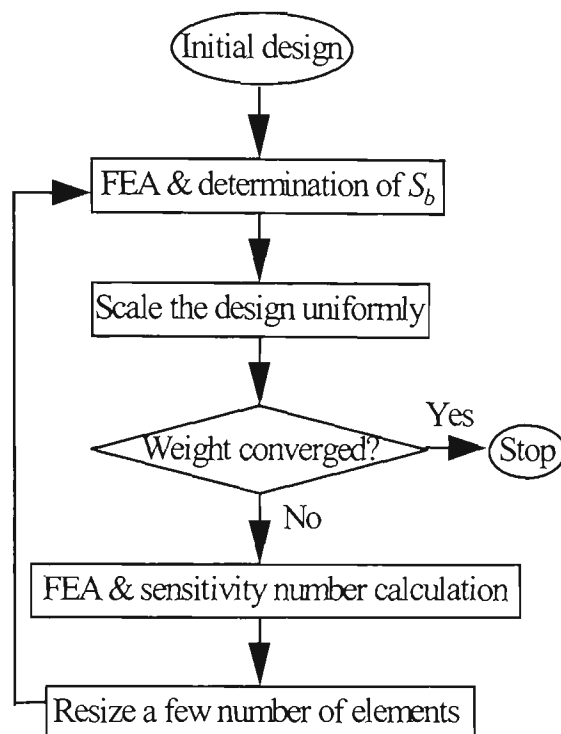


**Figure 7.2** - ESO for the minimum weight design - Method 2

The iterative procedure for the multiple load cases design involves two steps. In the first step, the design variables are scaled uniformly in order to satisfy the most critical load case. In the second step, the elements are resized according to their sensitivity numbers. These two steps are repeated in cycles until the desired optimum design is obtained. A batch file is set up for uniform scaling and element resizing so that the weight of the structure is systematically reduced and the material is gradually shifted from the strongest to the weakest part of the structure. The detailed steps of the optimisation procedure is given below and it is also described by the flowchart given in Figure 7.3.

*Step 1:* Discretise the structure by using a fine mesh of finite elements to represent the stress distributions and buckling modes adequately.

*Step 2:* Perform static and buckling analyses for each load case.

*Step 3:* Determine the uniform scaling factors  $S_{bk}$  ( $k = 1, nl$ ).

*Step 4:* Scale the design variables uniformly using the most critical scaling factor, i.e. maximum of  $S_{bk}$  ( $k = 1, nl$ ). Impose the sizing constraint.

*Step 5:* Carry out static and buckling analyses for each load case.

*Step 6:* Calculate the sensitivity numbers  $\alpha_{ib}^+$  and  $\alpha_{ib}^-$  for each element.

*Step 7:* Increase the cross-sectional area of elements with the highest values of  $\alpha_{ib}^+$  and decrease the cross-sectional area of the same number of elements with the highest values of  $\alpha_{ib}^-$  while imposing the sizing constraints.

*Step 8:* Repeat Steps 2 to 7 until the weight of the structure cannot be reduced any further.

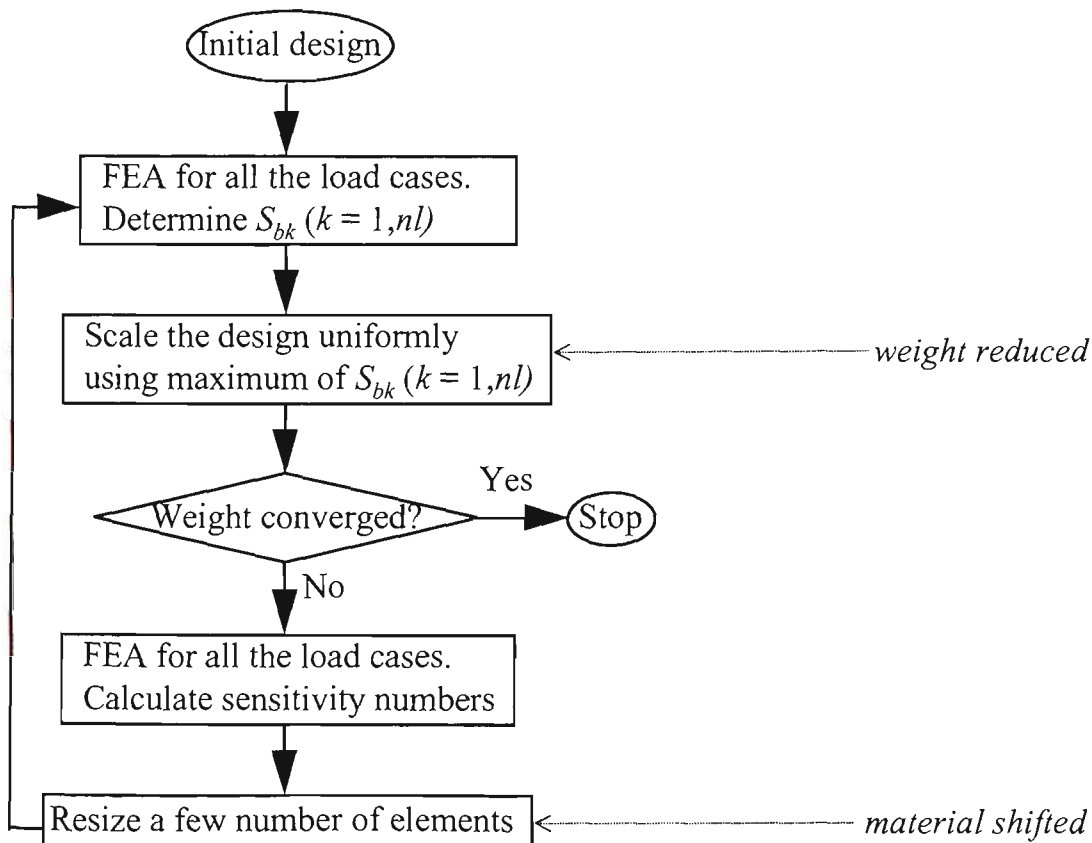


**Figure 7.3** - ESO for the minimum weight design with multiple load cases

## 7.4 Examples

### 7.4.1 Two-bay frame - Constant weight design

Consider the single story, two-bay frame shown in Figure 7.4. All the members are of rectangular cross-section with constant breadth,  $b = 20$  mm and the initial uniform depth,  $d = 20$  mm. The supports are pinned. Each member is divided into six elements of equal length. The frame is exposed to three possible loading conditions as shown in the figure. For each load case,  $FS$  is assumed to be 3.0. Optimum designs are obtained while keeping the structural volume constant. Member depths are the design variables ( $p = 3$ ) and they are allowed to vary to the maximum 60 mm and to the minimum 5 mm in steps of 1 mm. 20% of the elements are resized at each iteration. The optimum shape of the frame obtained by considering all the load cases simultaneously (i.e, by using the multiple load case sensitivity numbers and the procedure described in section 7.3.1) is shown in Figure 7.5a. The evolution of the critical buckling load factor of each load case during the optimisation process is given in Figure 7.5b.

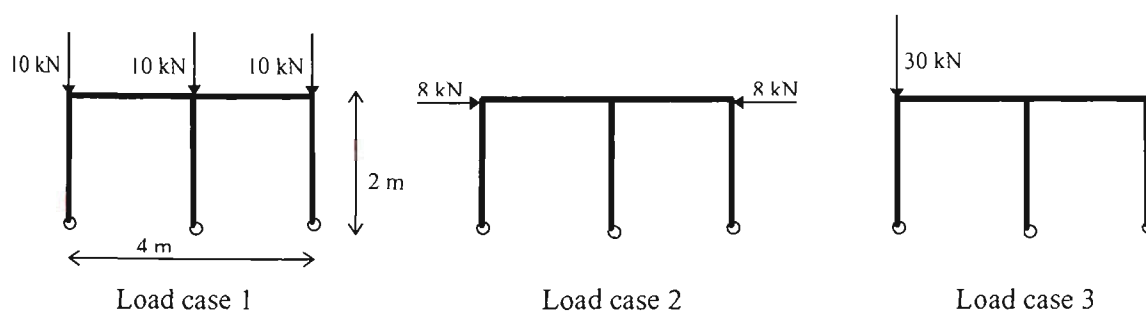


**Figure 7.4** - Structural layout and load cases of the two-bay frame

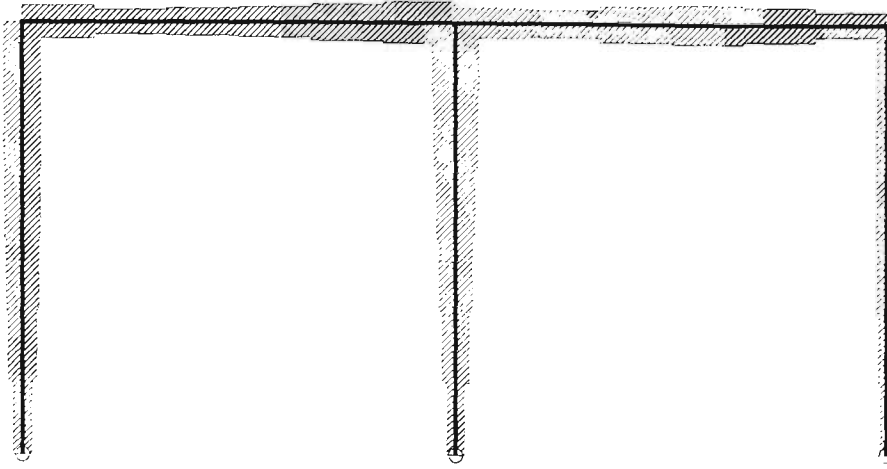


**Figure 7.5a** - Optimum shape with all three load cases

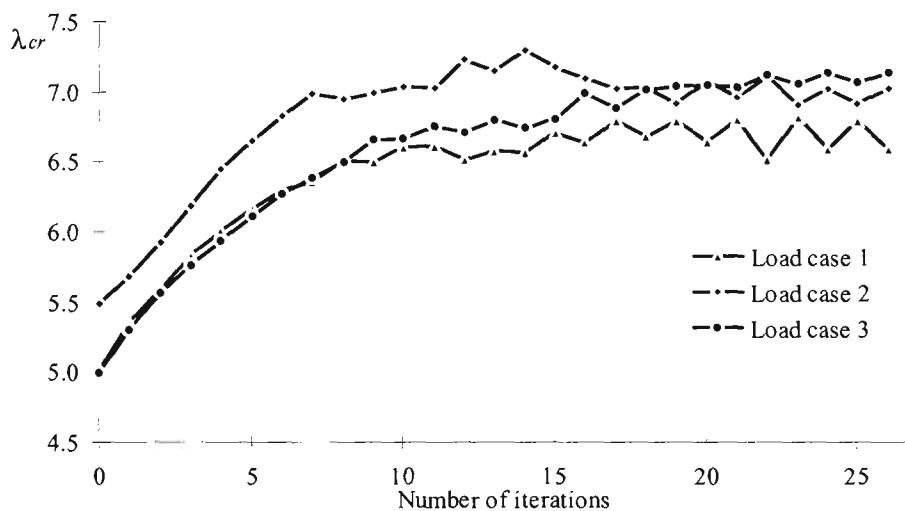


**Figure 7.5b** - Iteration history with all three load cases.

Optimum designs are also obtained for each load case separately by using the respective single load case sensitivity numbers and the single load case optimisation procedure. During the optimisation process, buckling load factors of the other load cases are also obtained. The optimum shapes and the iteration histories for load case 1, load case 2 and load case 3 are given in Figures 7.6, 7.7 and 7.8, respectively. The optimum shapes of each load case show a clear preference for the loading direction. For the load case 2 optimum design, column dimensions are at their lower limit ( $d = 5$  mm), indicating that

the columns contribute little to the structural stability under this loading condition. Similarly for the load case 3 optimum design, the right hand side beam and column dimensions are at their lower limit. The critical load factors of each load case for the initial design and the optimum designs are compared in Table 7.1. These results indicate that if a structure is optimised under any single loading condition, critical load factors of other load cases will be greatly reduced. When all the load cases are considered simultaneously during the optimisation, the buckling load factor of each load case is concurrently increased.

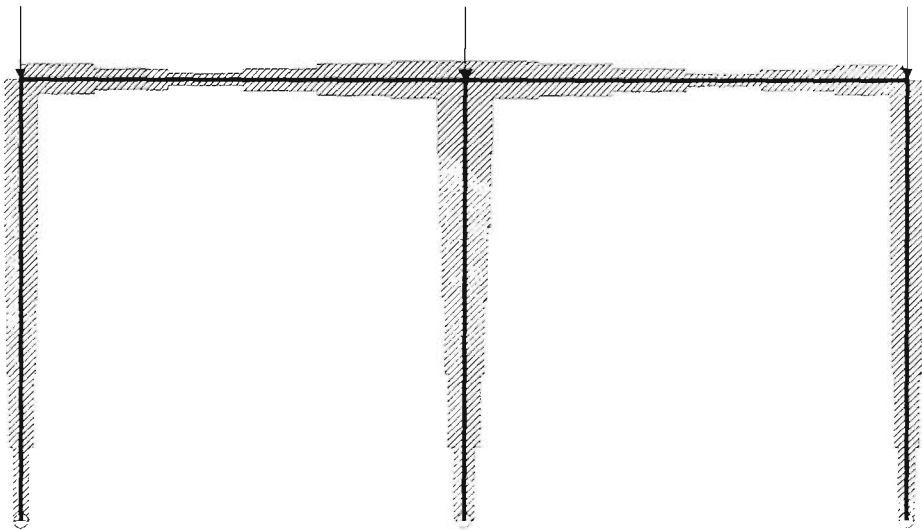


Figure 7.6a - Optimum shape - load case 1 alone

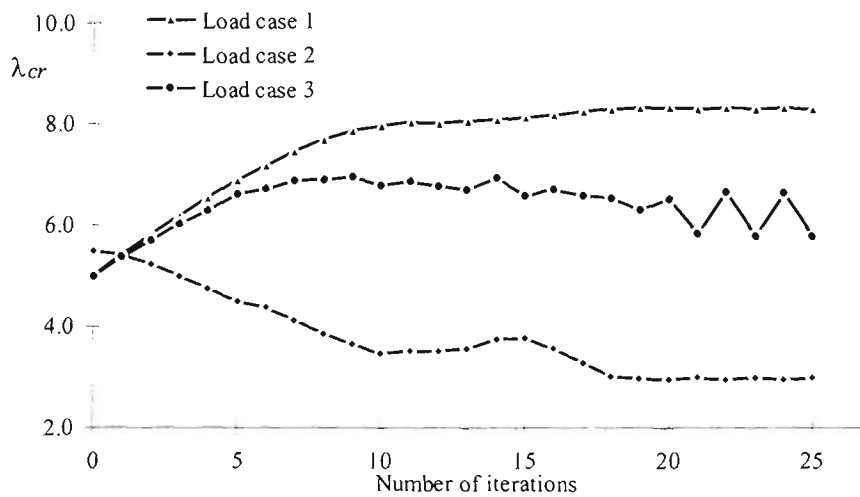


Figure 7.6b - Iteration history - load case 1 alone

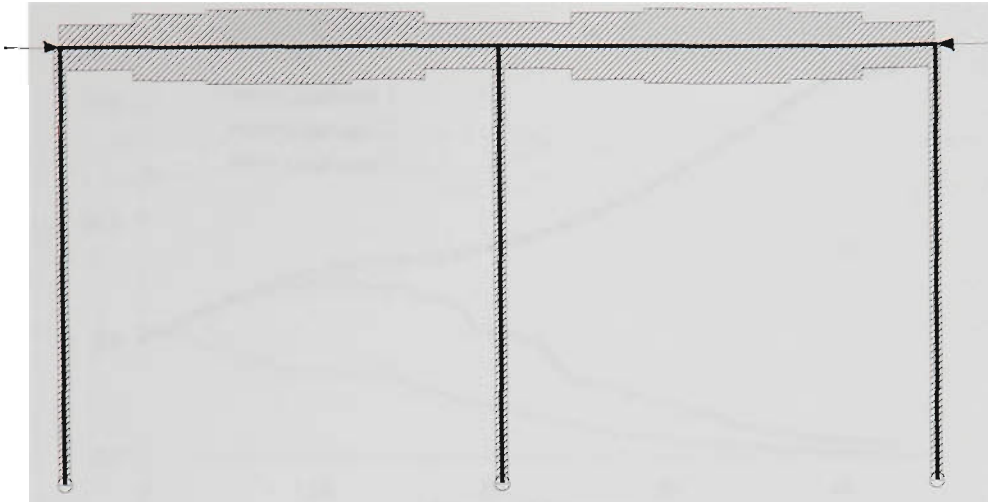


Figure 7.7a - Optimum shape - load case 2 alone

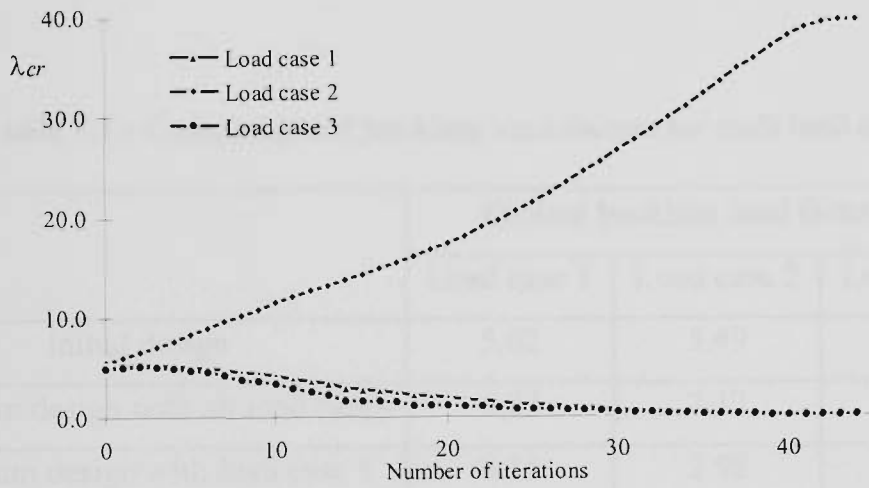


Figure 7.7b - Iteration history - load case 2 alone

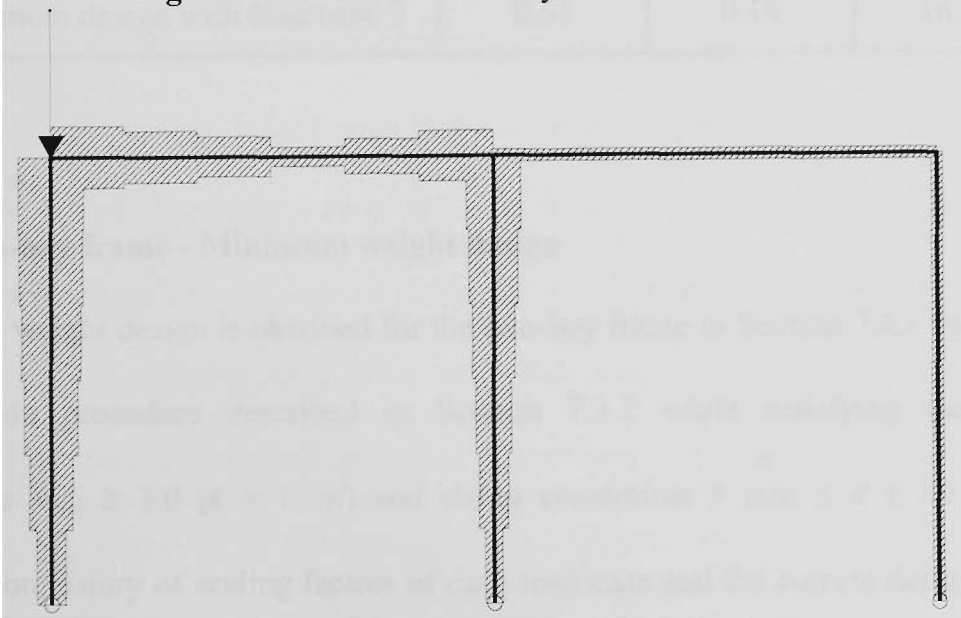
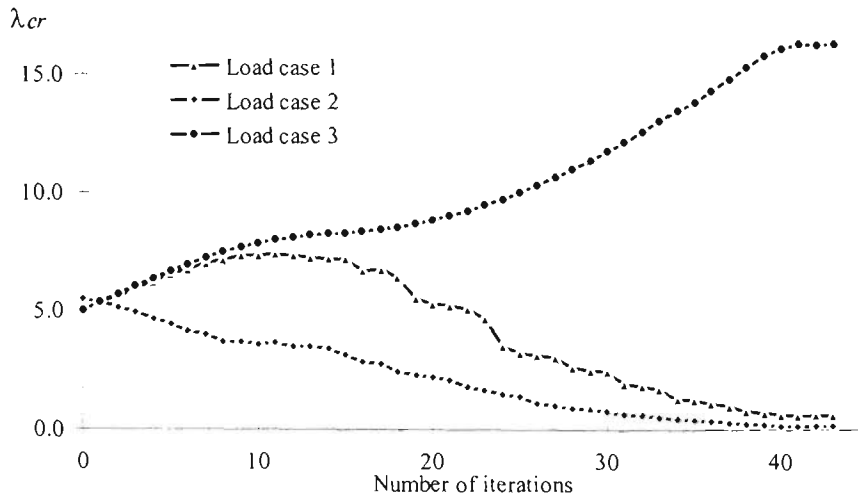


Figure 7.8a - Optimum shape - load case 3 alone



**Figure 7.8b** - Iteration history - load case 3 alone

**Table 7.1** - Comparison of buckling load factors for each load case

	Critical buckling load factor ( $\lambda_{cr}$ )		
	Load case 1	Load case 2	Load case 3
Initial design	5.02	5.49	5.00
Optimum design with all load cases	6.83	7.12	7.14
Optimum design with load case 1	8.31	2.98	6.28
Optimum design with load case 2	0.10	39.70	0.10
Optimum design with load case 3	0.61	0.14	16.39

#### 7.4.2 Two-bay frame - Minimum weight design

Minimum weight design is obtained for the two-bay frame in Section 7.4.1 by using the optimisation procedure described in Section 7.3.2 while satisfying the stability constraints  $\lambda_{cr,k} \geq 3.0$  ( $k = 1, nI$ ) and sizing constraints  $5 \text{ mm} \leq d \leq 60 \text{ mm}$ . The optimisation history of scaling factors of each load case and the current design to initial design weight ratio  $w/w_o$  is given in Figure 7.9. For the optimum design,  $S_{b1} = 1.0$ ,  $S_{b2} = 1.0$ ,  $S_{b3} = 0.97$  and  $w/w_o = 0.76$ .

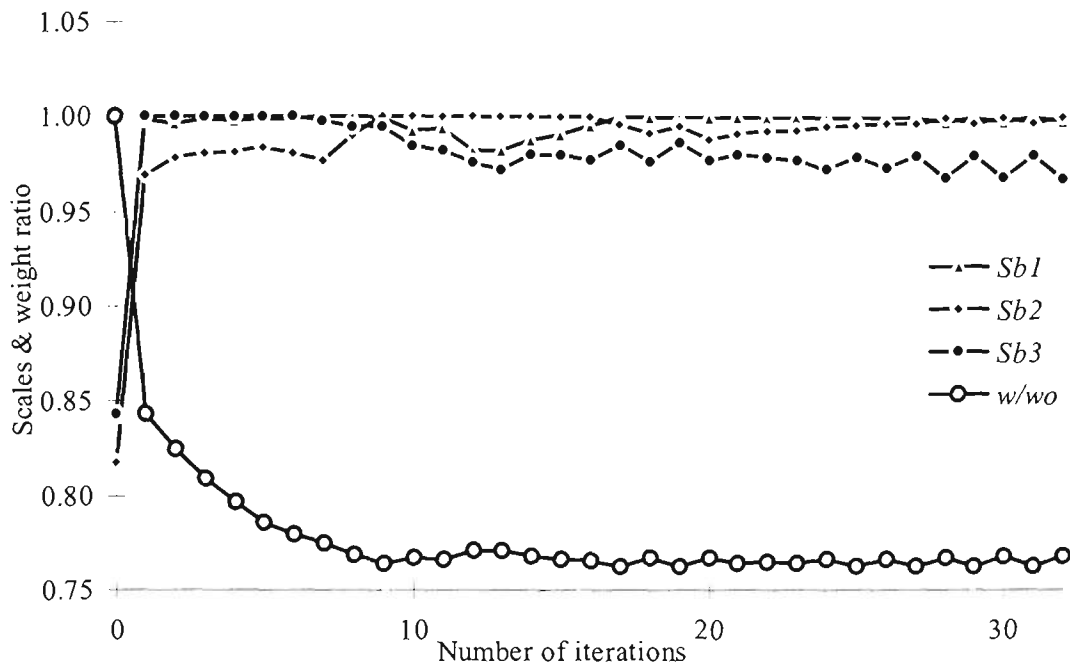


**Figure 7.9** - Iteration history of the minimum weight design

## 7.5 Conclusions

The ESO method has been easily extended to enhancing the buckling resistance of multiple load case frame structures. Sensitivity numbers for resizing are calculated by considering the influence of all the load cases. Thus compromises are made at each iteration of the evolutionary process among these load cases. The uniform scaling factors which are used as weighting parameters to define the sensitivity numbers play a similar role as the Lagrangian multipliers in optimality criteria methods. These uniform scaling factors determine the active participation of each load case on the optimum design. When the buckling load factor of a particular load case is far more than the corresponding factor of safety of that load case, influence of that load case in the current design becomes less important. From the examples it has been shown that optimising a structure under any single load case may violate the other load case buckling constraints. When all the load cases are considered simultaneously, each load case buckling load factor is increased.

## CHAPTER 8 - OPTIMUM DESIGN OF STRUCTURES WITH MULTIPLE CONSTRAINTS

### 8.1 Introduction

Although there has been considerable amount of work carried out on the optimum design of frame structures, most of these studies do not treat the stability constraint in parallel with other common constraints such as strength and displacement limits. The optimum design of structures including stability constraint is of great importance because with high strength materials many structural elements are becoming thinner and modern frame structures are more slender than their forerunners. Optimum design of frame structures including stability constraint along with stress and displacement constraints has been reported by Lin and Liu (1989), Pezeshk and Hjelmstad (1991) and Barson (1994) using optimality criteria methods and by Karihaloo and Kanagasundaram (1993) using non-linear mathematical programming method. This chapter extends the ESO method to the cross-sectional optimisation of frames and trusses considering stress, stiffness, displacement and stability constraints simultaneously.

### 8.2 Multiple Constraints Problem

The optimisation problem here is to minimise the weight of a structure in such a way that the normal and shear stresses and the deflection at any point of the frame, the critical buckling load factor and the sizing parameters do not violate respective prescribed limits under any load system. The following constraints are considered in addition to the buckling constraint  $\lambda_{cr} \geq FS$ .

*Stiffness constraint:* The inverse measure of the overall stiffness of a structure, known as the mean compliance  $C$ , should not exceed the prescribed limit  $C_{all}$ .

$$C \leq C_{all} \quad (8.1)$$

*Displacement constraint:* Displacement constraints may be imposed on certain degrees of freedom (d.o.f) of the structure. Constraint imposed on the  $j^{\text{th}}$  d.o.f displacement component,  $d_j$  is given in the form,

$$|d_j| \leq d_j^* \quad (8.2)$$

where  $d_j^*$  is the allowable limit for  $d_j$ .

*Stress constraint:* The equivalent stress at any point in a structure is expressed by some means of average of the normal and shear components of stress. For this purpose, the von Mises stress,  $\sigma_{vm}$  has been frequently used for isotropic materials. Thus the stress constraint is given in the form that the von Mises stress at any point of the structure should not exceed the allowable stress  $\sigma_{all}$ :

$$\sigma_{vm} \leq \sigma_{all} \quad (8.3)$$

In Chapter 3, ESO for shape and layout optimisation of structures separately with stiffness, displacement or stress constraints has been described. Element sensitivity numbers for these constraints,  $\alpha_{ic}$  (Eq. 3.12),  $\alpha_{id}$  (Eq. 3.16) and  $\alpha_{is}$  (Eq. 3.1), indicate the change in corresponding structural response due to the removal of a particular element and they are used for shape and layout optimisation which involves gradual removal of elements. In the following sections, sensitivity numbers are derived for cross-sectional

optimisation for which the change on all these structural responses due to the local modification of each element needs to be estimated.

### 8.2.1 Sizing optimisation with stiffness constraints

From equation (3.10) (Chapter 3, Section 3.2.2.1), the change in mean compliance due to the cross-sectional change in the  $i^{\text{th}}$  element,  $\Delta C_i$ , is given by

$$\Delta C_i = -\frac{1}{2} \{d_i\} [\Delta k_i] \{d_i\} \quad (8.4)$$

The aim is to minimise the mean compliance  $C$ , so that the overall stiffness of the structure can be maximised. Therefore the cross-sectional area of elements with lowest values of  $\Delta C_i$  (or highest values of  $-\Delta C_i$ ) has to be increased to minimise  $C$ . Hence the following two sensitivity numbers are defined for each element for sizing optimisation.

$$\alpha_{ic}^+ = -\Delta C_i = \{d_i\}^T [\Delta k_i]^+ \{d_i\} \quad (8.5a)$$

$$\alpha_{ic}^- = -\Delta C_i = \{d_i\}^T [\Delta k_i]^- \{d_i\} \quad (8.5b)$$

To be consistent with the buckling optimisation (in which the cross-sectional areas of elements with highest values of  $\alpha_{ib}^+$  and  $\alpha_{ib}^-$  are increased or decreased),  $-\Delta C_i$  value is taken to define the sensitivity numbers. As discussed in Section 4.3, when elements are of different lengths, the element sensitivities depend also on their lengths. When comparing two elements with the same  $\alpha_{ic}^+$ , increasing the cross-sectional area of shorter element will result in a lighter design. Consequently, the element sensitivities for stiffness constraint are redefined below.

$$\alpha_{ic}^+ = \{d_i\}^T [\Delta k_i]^+ \{d_i\} / l_i \quad (8.6a)$$

$$\alpha_{ic}^- = \{d_i\}^T [\Delta k_i]^- \{d_i\} / l_i \quad (8.6b)$$

Thus to increase the overall stiffness of the structure, the cross-sectional areas of elements with the highest values of  $\alpha_{ic}^+$  are increased and those with the highest values of  $\alpha_{ic}^-$  are reduced.

### 8.2.2 Sizing optimisation with displacement constraints

From equation (3.14) (Chapter 3, Section 3.2.2.2), the change in the  $j^{\text{th}}$  d.o.f displacement,  $d_j$  due to the cross-sectional change in the  $i^{\text{th}}$  element,  $\Delta d_{ij}$  is given by

$$\Delta d_{ij} = -\{d_{ij}\}[\Delta k_i]\{d_i\} \quad (8.7)$$

As the displacement may take positive or negative value, the aim is to reduce the absolute value of  $d_j$ ,  $|d_j|$ . If  $d_j > 0$ , the cross-sectional area of elements with highest value of  $\{d_{ij}\}^T[\Delta k_i]\{d_i\}$  needs to be increased to minimise  $|d_j|$ . Similarly if  $d_j < 0$ , the cross-sectional area of elements with lowest value of  $\{d_{ij}\}^T[\Delta k_i]\{d_i\}$  needs to be increased to minimise  $|d_j|$ . Hence the following sensitivity numbers are defined for  $j^{\text{th}}$  d.o.f displacement constraint:

$$\alpha_{id}^+ = \frac{d_j}{|d_j|} \{d_{ij}\}^T[\Delta k_i]^+ \{d_i\} / l_i \quad (8.8a)$$

$$\alpha_{id}^- = \frac{d_j}{|d_j|} \{d_{ij}\}^T[\Delta k_i]^- \{d_i\} / l_i \quad (8.8b)$$

If there are several displacement constraints, sensitivity numbers need to be calculated for each displacement constraint.

### 8.2.3 Sizing optimisation with stress constraints

The normal and shear stresses at any point in an element can be computed from element displacements (equation 3.23) or from element forces. The von Mises equivalent stress at a point can then be calculated from the following relationship.

$$\sigma_{vm} = \frac{1}{\sqrt{2}} [(\sigma_x - \sigma_y)^2 + (\sigma_y - \sigma_z)^2 + (\sigma_z - \sigma_x)^2 + 6(\tau_{xy}^2 + \tau_{yz}^2 + \tau_{zx}^2)]^{\frac{1}{2}} \quad (8.9)$$

The critical stress of an element in a frame or truss can be determined by examining the stress levels at certain preselected extreme points at different section of the element. If the element is not subjected to distributed forces, evaluation of stresses at both ends of the element and at mid-section would be sufficient. For planar structures, the von Mises stress is reduced to  $\sigma_{vm} = (\sigma^2 + 3\tau^2)^{1/2}$  where  $\sigma$  and  $\tau$  are normal and shear stresses respectively. For example, von Mises stress at a point on a rectangular cross-section of a beam element of a planar structure (no bi-axial bending or torsional forces) as shown in Figure 8.1 is given by

$$\sigma_{vm} = \sqrt{\left(\frac{12My}{bd^3} + \frac{P}{bd}\right)^2 + \frac{108S^2}{b^2d^6} \left(\frac{d^2}{4} - y^2\right)^2} \quad (8.10)$$

The stress recovery points considered should be sufficient to identify the critical stress in the section under combined normal and shear stress conditions.

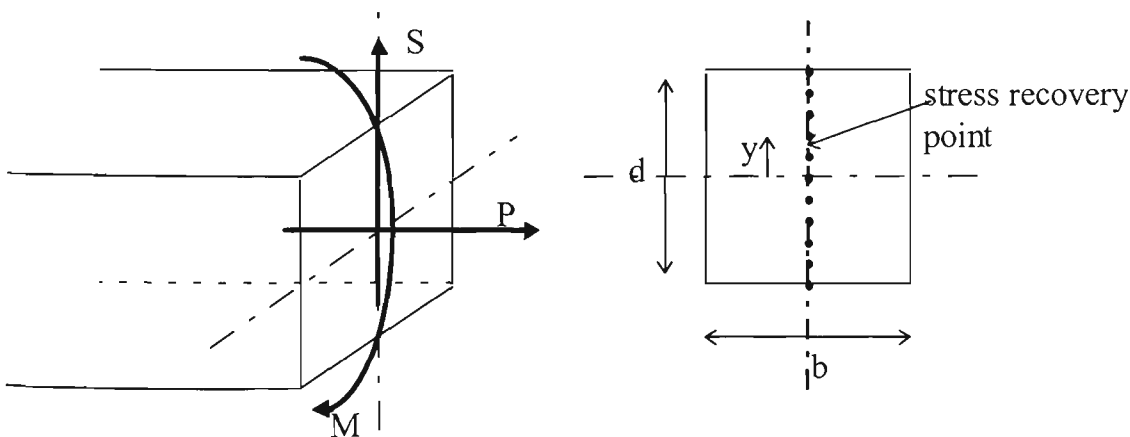


**Figure 8.1** - Rectangular cross-section of a beam element in a planar structure

An element library may be created in which the details of typical beam and bar cross-sections can be provided. The necessary information such as relations between the geometrical properties and locations to calculate stress levels are given in the library. Some of the beam cross-sections and their stress recovery points are shown in Figure 8.2. The number of stress recovery points and their locations are fixed for each section. The equations for calculating the von Mises stress from the forces and moments in the section such as equation (8.10) are also given in the library.

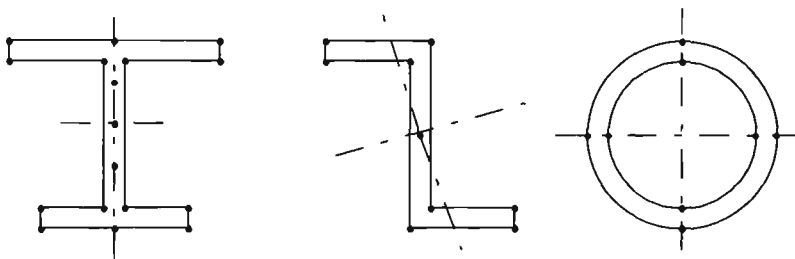


**Figure 8.2** - Typical beam cross-sections and stress recovery points

As discussed in Chapter 3, the evaluation of change in stress due to structural modifications is computationally very expensive. However, if the cross-sectional modifications of elements at each iteration are kept small, they do not cause significant changes in the element forces. For frames and trusses this assumption is reasonably accurate. Hence the new approximate stresses in an element after the cross-sectional changes can be directly calculated from the element forces and new cross-sectional dimensions.

In practice, the strength criterion is satisfied by using the fully stressed design (FSD) concept which is one of the early optimality criteria. If the stress distribution of a structure is to be brought to uniform, highly stressed elements need to be strengthened

and lowly stressed elements need to be weakened. Hence the following element sensitivity numbers are defined for stress constraint.

$$\alpha_{is}^+ = \sigma_{ivm}^+ / l_i = \sigma_{ivm} (A + \Delta A) / l_i \quad (8.11a)$$

$$\alpha_{is}^- = -\sigma_{ivm}^- / l_i = -\sigma_{ivm} (A - \Delta A) / l_i \quad (8.11b)$$

where  $\sigma_{ivm}^+$  is the maximum stress in the element  $i$ , when the area is increased by  $\Delta A$  and  $\sigma_{ivm}^-$  is the maximum stress in the element  $i$ , when the area is reduced by  $\Delta A$ . Thus to bring the stress distribution uniform, the cross-sectional areas of elements with highest values of  $\alpha_{is}^+$  are increased and those with the highest values of  $\alpha_{is}^-$  are reduced. For the expression  $\alpha_{is}^-$ , a negative sign is introduced to be consistent with other sensitivity numbers  $\alpha_{ic}^-$ ,  $\alpha_{id}^-$  and  $\alpha_{ib}^-$ .

### 8.2.4 Uniform scaling and critical scale factors

As discussed in Chapters 6 and 7, during the optimisation process, it is convenient to obtain a feasible design after each iteration by scaling the design uniformly in order to satisfy the most critical constraint. This helps keep track the reduction in the weight of the structure after each iteration and also helps to pick up the most active constraints. Determination of uniform scaling factor for stability constraint,  $S_b$  has been discussed in detail in Chapter 6. Similarly, uniform scaling factors for stiffness constraint,  $S_c$  and displacement constraint,  $S_d$  can be obtained. For the structures with linear size-stiffness relationship ( $p = 1$ ),  $S_c = C/C_{all}$  and  $S_d = |d_j|/d_j^*$ . For structures with other values of  $p$ ,  $S_c \approx (C/C_{all})^{1/p}$  and  $S_d \approx (|d_j|/d_j^*)^{1/p}$ . When the von Mises stress at any point in a section is linearly related to the design variable of that section (for example in equation 8.10,  $\sigma$

$\propto 1/b$ ), uniform scaling factor for stress constraint,  $S_s = \sigma_{vm}^{max} / \sigma_{all}$ . If the von Mises stress is not linearly related to the design variable,  $S_s \approx (\sigma_{vm}^{max} / \sigma_{all})^{\frac{1}{2}}$  can be used in general and additional iterations are needed to resolve  $S_s$ . The scaled design should be critical to the most active constraint. Hence the critical scale factor is determined from the maximum of uniform scaling factors among  $S_b$ ,  $S_c$ ,  $S_d$ , and  $S_s$ .

In the preceding chapters, sizing sensitivity numbers and uniform scaling factors are given separately for stiffness, displacement and stress constraints. Optimum designs separately with each constraint (either with constant volume constraint or minimum weight design) can be obtained by using the appropriate sensitivity numbers and uniform scaling factors in the optimisation procedures described for buckling optimisation in Chapters 4 to 7. In the following sections, sensitivity numbers and the optimisation procedure for the multiple constraints problem are proposed.

### 8.3 Sensitivity Number

Ideally the cross-sectional area of the element of which all  $\alpha_{ic}^+$ ,  $\alpha_{ib}^+$ ,  $\alpha_{id}^+$  and  $\alpha_{is}^+$  are highest should be increased and the cross-sectional area of the element of which all  $\alpha_{ic}^-$ ,  $\alpha_{ib}^-$ ,  $\alpha_{id}^-$  and  $\alpha_{is}^-$  are highest should be decreased to improve the design with all the constraints. However this situation generally does not exist. To overcome this difficulty the element sensitivity is evaluated by the sum of its relative sensitiveness with regard to each constraint. Further it is necessary to treat each constraint separately depending on how active it is in the current design. To measure the influence of each constraint, the uniform scaling factors  $S_b$ ,  $S_c$ ,  $S_d$ , and  $S_s$  are used as weighting parameters. Taking all

these into account, finally for each element the following two new sensitivity numbers are defined.

$$\alpha_i^+ = S_b \frac{\alpha_{ib}^+}{\alpha_{b,av}^+} + S_c \frac{\alpha_{ic}^+}{\alpha_{c,av}^+} + S_d \frac{\alpha_{id}^+}{\alpha_{d,av}^+} + S_s \frac{\alpha_{is}^+}{\alpha_{s,av}^+} \quad (8.12a)$$

$$\alpha_i^- = S_b \frac{\alpha_{ib}^-}{\alpha_{b,av}^-} + S_c \frac{\alpha_{ic}^-}{\alpha_{c,av}^-} + S_d \frac{\alpha_{id}^-}{\alpha_{d,av}^-} + S_s \frac{\alpha_{is}^-}{\alpha_{s,av}^-} \quad (8.12b)$$

where  $\alpha_{b,av}^+$  is the average of the  $\alpha_{ib}^+$  values of all elements and other average values are similarly defined. If any of these constraints is not considered in the optimum design, corresponding term can be simply omitted in the final sensitivity numbers. There can be several displacement constraints and for each displacement constraint the corresponding term needs to be added in the final sensitivity numbers.

The above sensitivity numbers are defined for single load case structures. They can be easily extended to sensitivity numbers for multiple load cases as follows:

$$\alpha_i^+ = \sum_{k=1}^{nl} S_{bk} \frac{\alpha_{ibk}^+}{\alpha_{bk,av}^+} + S_{ck} \frac{\alpha_{ick}^+}{\alpha_{ck,av}^+} + S_{dk} \frac{\alpha_{idk}^+}{\alpha_{dk,av}^+} + S_{sk} \frac{\alpha_{isk}^+}{\alpha_{sk,av}^+} \quad (8.13a)$$

$$\alpha_i^- = \sum_{k=1}^{nl} S_{bk} \frac{\alpha_{ibk}^-}{\alpha_{bk,av}^-} + S_{ck} \frac{\alpha_{ick}^-}{\alpha_{ck,av}^-} + S_{dk} \frac{\alpha_{idk}^-}{\alpha_{dk,av}^-} + S_{sk} \frac{\alpha_{isk}^-}{\alpha_{sk,av}^-} \quad (8.13b)$$

#### 8.4 Optimisation Procedure

An iterative procedure is set up for uniform scaling and resizing the elements so that the weight of the structure is systematically reduced and the material is gradually shifted from the strongest to the weakest part of the structure. The procedure is given as follows:

*Step 1:* Select an initial design and discretise the structure using a finite number of elements.

*Step 2:* Perform fully stressed design two or three times.

*Step 3:* Solve static and buckling analyses and determine the uniform scaling factors  $S_b$ ,  $S_c$ ,  $S_d$  and  $S_s$ .

*Step 4:* Scale the design variables uniformly by using the most critical scale factor, i.e. maximum of  $S_b$ ,  $S_c$ ,  $S_d$  and  $S_s$ . Impose the sizing constraint.

*Step 5:* Solve the static and buckling analyses and calculate the sensitivity numbers  $\alpha_i^+$  and  $\alpha_i^-$  for each element.

*Step 6:* Increase the cross-sectional area of elements which have the highest values of  $\alpha_i^+$  and decrease the cross-sectional area of the same number of elements which have the highest values of  $\alpha_i^-$ .

*Step 7:* Repeat Steps 3 to 6 until the weight of the structure cannot be reduced any further.

For the problems with displacement constraints, additional static analyses for unit loads corresponding to the constrained displacements need to be included in Step 5. In some problems, with initial design, some part of the structure may be highly stressed. Thus the uniform scaling in Step 4 using  $S_s = \sigma_{vm}^{\max} / \sigma_{all}$  may bring all the cross-sectional areas of elements to exceed the maximum limit and further optimisation cannot be done. To prevent this problem initially fully stress design is performed two or three times to bring the stress distribution roughly uniform. In some problems FSD also helps to bring the design closer to the optimum design since most of the problems are critical to stress constraint.

## 8.5 Examples

The examples reported by Barson (1994), Lin and Liu (1992), Pezeshk and Hjelmstad (1991) and by Karihaloo and Kanagasundaram (1993) for multiple constraint optimisation were governed by either stress or displacement or stability constraint at optimum designs. These examples did not show the effectiveness of the multi constraint optimisation method. The capability of the proposed method is illustrated with the following examples. Note that the loads and dimensions are intentionally chosen to be critical to all the constraints.

### 8.5.1 50-Bar truss tower

A minimum weight design for a 50-bar planar truss tower as shown in Figure 8.3 is sought using the ESO method. The truss tower is 40 m high and 2 m wide subjected to a vertical load of 200 kN at each corner of the top storey. A similar structure has been analysed previously by Lin and Liu (1992) and Khot *et al.* (1976) with different dimensions and loadings. However in both examples, the final optimum design was governed by only buckling and minimum size constraints.

The constraints taken into account are:  $\sigma_{vm} \leq \sigma_{all} = 150$  MPa;  $C \leq C_{all} = 10$  kNm; and  $\lambda_{cr} \geq FS = 2.0$ . Young's modulus  $E = 200$  GPa. The initial cross-sectional areas of all members are uniform and equal to  $15.625$  cm<sup>2</sup>. This initial area is chosen so that the uniform design just satisfies the most critical constraint. For this example it is the buckling constraint and for the initial design  $\lambda_{cr} = 2.0$  ( $S_b = 1$ ). The cross-sectional areas are allowed to vary to maximum  $20$  cm<sup>2</sup> and to minimum  $1$  cm<sup>2</sup>. The step size used for resizing is equal to  $0.5$  cm<sup>2</sup> and 20% of the elements are resized at each iteration.

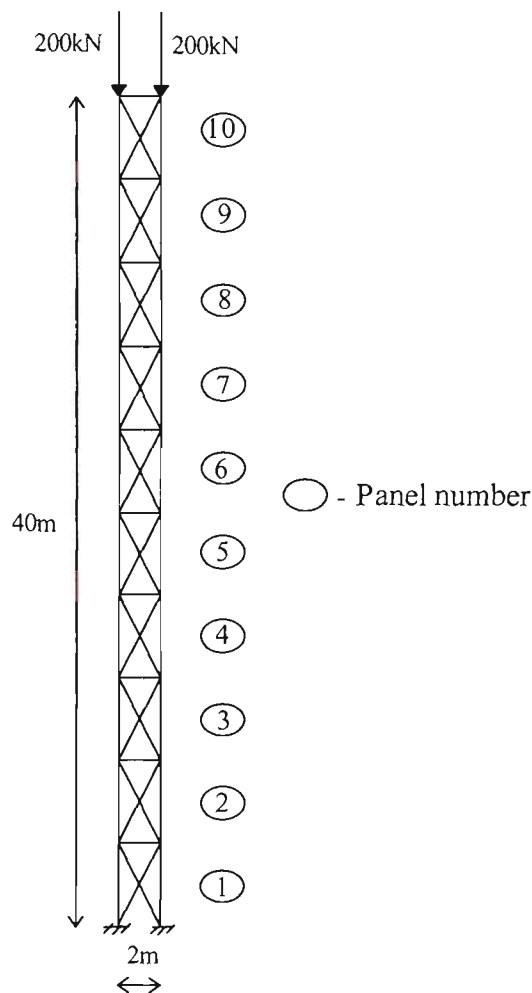


**Figure 8.3** - The 50-bar truss tower

The optimum design is obtained after 11 iterations and the final design areas are given in Table 8.1 (columns 2 and 3). The symmetry of structural layout and loadings results in a material distribution that is also symmetric, i.e. the two vertical members in each panel are equal and so are the diagonal members. The cross-sectional area of all the horizontal members are at the minimum value of  $1.0 \text{ cm}^2$  except for the panel 9 horizontal member cross-sectional area being equal to  $1.63 \text{ cm}^2$ . The optimisation history of scaling factors and the current design to initial design weight ratio,  $w/w_o$  are given in Figure 8.4. Initially FSD is carried out to bring the variables closer to the optimum design. The optimum design is governed by all the constraints and at optimum,

$S_b = S_S = S_c = 1$ . It indicates that all the constraints are equally active at the optimum design. The volume of the optimum design with all the constraints is reduced to 46.9% of the initial design volume.

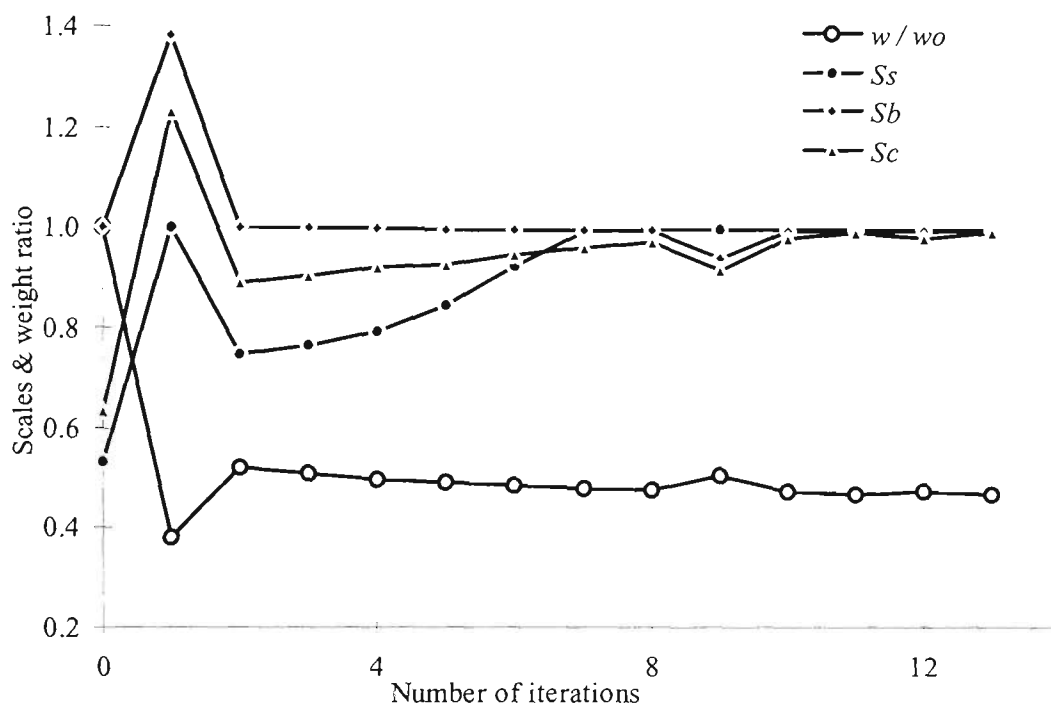


**Figure 8.4** - Iteration history of the 50-bar truss tower with all the constraints

Optimum designs are also obtained considering each constraint separately. Optimisation histories of these designs are shown in Figures 8.5, 8.6 and 8.7 respectively for stability, stress and stiffness constraints. Cross-sectional areas obtained for these designs are given in Table 8.1 (columns 4-9). Cross-sectional area of all the horizontal members are at the minimum value of  $1.0 \text{ cm}^2$ . The volume of the optimum design with stability constraint alone is reduced to 42.6% of the initial design volume and for stress constraint alone and stiffness constraint alone, it is reduced to 38.1% and 45.3% respectively. Optimum design volumes and scaling factors of all these designs are compared in Table 8.2. The scaling factors corresponding to the volume of optimum

design with all the constraints ( $0.139 \text{ m}^3$ ) are also obtained from the single constraint design iteration histories and are compared in Table 8.2.

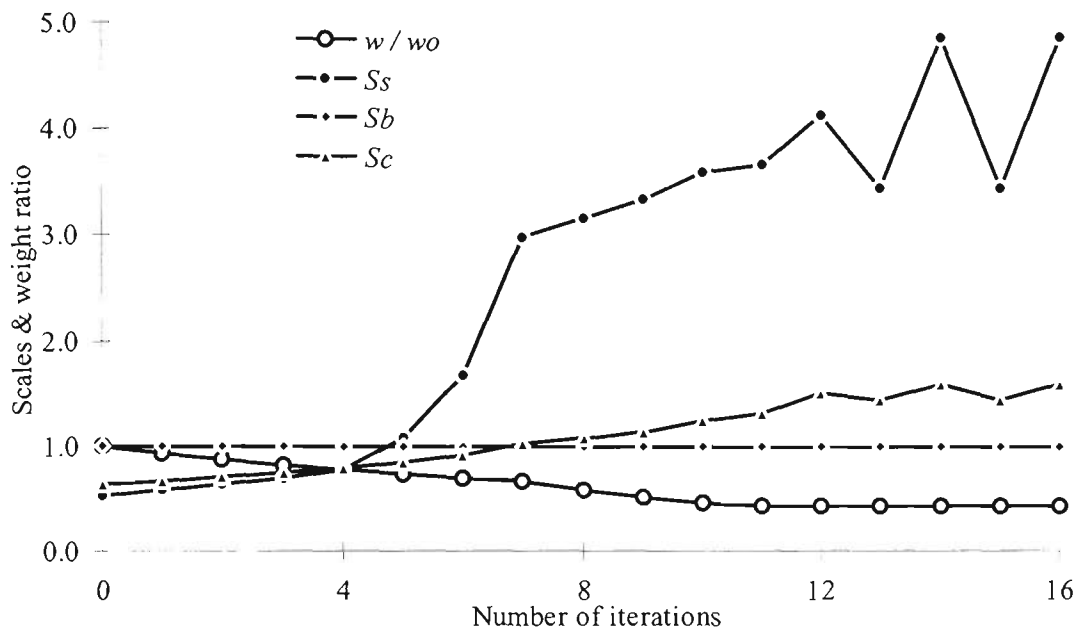


Figure 8.5 - Iteration history of the 50-bar truss tower with stability constraint alone

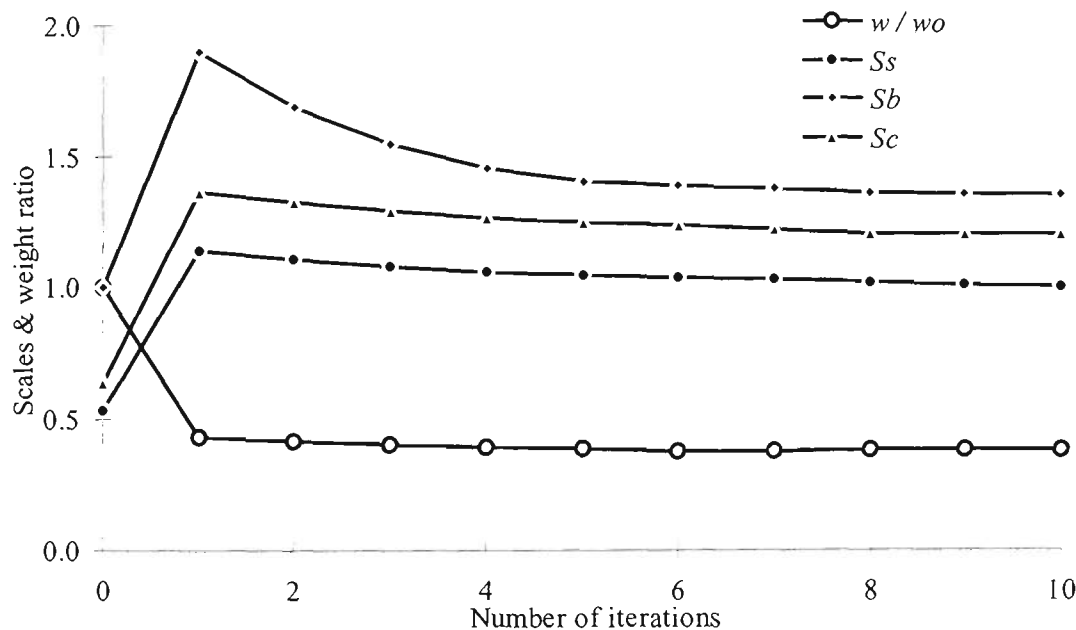


Figure 8.6 - Iteration history of the 50-bar truss tower with stress constraint alone

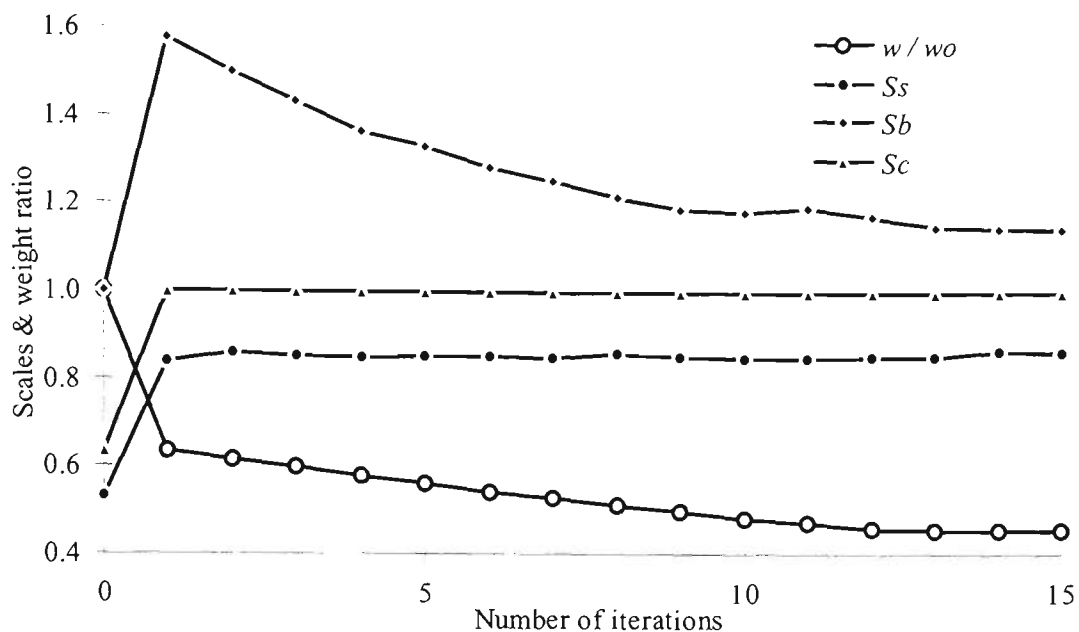


Figure 8.7 - Iteration history of the 50-bar truss tower with stiffness constraint alone

Table 8.1 - Optimum design cross-sectional areas of the 50-bar truss tower

Panel number	Cross-sectional areas in cm <sup>2</sup>							
	All constraints		Stability alone		Stress alone		Stiffness alone	
	Vertical	Diagonal	Vertical	Diagonal	Vertical	Diagonal	Vertical	Diagonal
1	19.17	1.00	19.66	1.00	12.74	1.00	15.39	1.00
2	18.43	1.00	19.66	1.00	12.73	1.00	15.39	1.00
3	18.43	1.00	19.66	1.00	12.73	1.00	15.39	1.00
4	17.63	1.00	18.61	1.00	12.73	1.00	15.39	1.00
5	17.43	1.00	16.85	1.10	12.73	1.00	15.39	1.00
6	15.31	1.00	14.40	1.78	12.73	1.00	15.39	1.00
7	14.77	1.00	12.00	1.58	12.73	1.00	15.39	1.00
8	13.20	1.63	9.30	2.19	12.73	1.00	15.39	1.00
9	12.55	1.51	5.85	2.18	12.73	1.00	15.39	1.00
10	11.31	1.45	2.16	2.14	12.73	1.00	15.39	1.00

**Table 8.2** - Comparison of optimum design parameters for the 50-bar truss tower

	Volume (m <sup>3</sup> )	$S_b$	$S_s$	$S_c$
Initial uniform design	0.296	1.00	0.53	0.63
Optimum design with all constraints	0.139	1.00	1.00	1.00
Optimum design with stability constraint alone	0.126	1.00	3.98	1.49
	0.139**	1.00	3.36	1.24
Optimum design with stress constraint alone	0.113	1.35	1.00	1.20
	0.139**	1.46	1.00	1.18
Optimum design with compliance constraint alone	0.134	1.14	0.85	1.00
	0.139**	1.18	0.86	1.00

\*\* Scaling factors corresponding to the optimum design volume with all constraints are obtained from the iteration histories.

These results indicate that if a structure is optimised with a single constraint, the other constraints will be adversely affected at the optimum design. For example if the structure is optimised with stability constraint alone, at optimum design (corresponding to the optimum volume with all constraints) the maximum stress will be 3.36 times the allowable limit and the mean compliance of the structure will be 1.24 times the allowable limit. This observation contradicts the notion suggested by Barson (1994) and Pezeshk and Hjelmstad (1991) which states that by improving the overall elastic stability characteristic of a structure, the static, dynamic and post elastic performance of the structure will be also improved.

### 8.5.2 5-Storey frame

A 2-bay, 5-storey frame, as shown in Figure 8.8 is analysed. The loading on the structure consisted of dead loads of 40 kN/m for roof level and 80 kN/m for typical floor level and wind loads as shown in the figure. The following values are taken for the analysis:  $\sigma_{all} = 400$  MPa;  $FS = 2.5$ ; and  $E = 200$  GPa. In this problem the horizontal displacement at the top storey is controlled. According to the design requirements the horizontal drift should not exceed 1/500 times the height of the building. Hence the horizontal displacement at top storey should not exceed 30 mm. All the members are of rectangular cross-section with constant depth  $d = 120$  mm ( $p = 1$ ). Initial uniform breadth,  $b = 234$  mm for all the members and  $b$  is allowed to vary to maximum 400 mm and to minimum 40 mm. This initial uniform design rightly satisfies the most critical displacement constraint ( $S_d = 1$ ). The step size used for resizing is equal to 5 mm and 20% of the elements are resized at each iteration.

Since the beams are subjected to uniformly distributed loads, each beam is divided into 10 elements for the analysis. Each column is divided into 3 elements. However optimum designs are obtained by treating each member (either beam or column) as a single segment, thus avoiding stiffness jump within the member. The stress levels are evaluated at both ends of each element within the member and the maximum stress value of all the elements is taken to calculate the stress sensitivity number for that member. Other stiffness, displacement and stability constraints sensitivity numbers of the member are calculated from the average value of the respective sensitivity numbers of elements within that member.

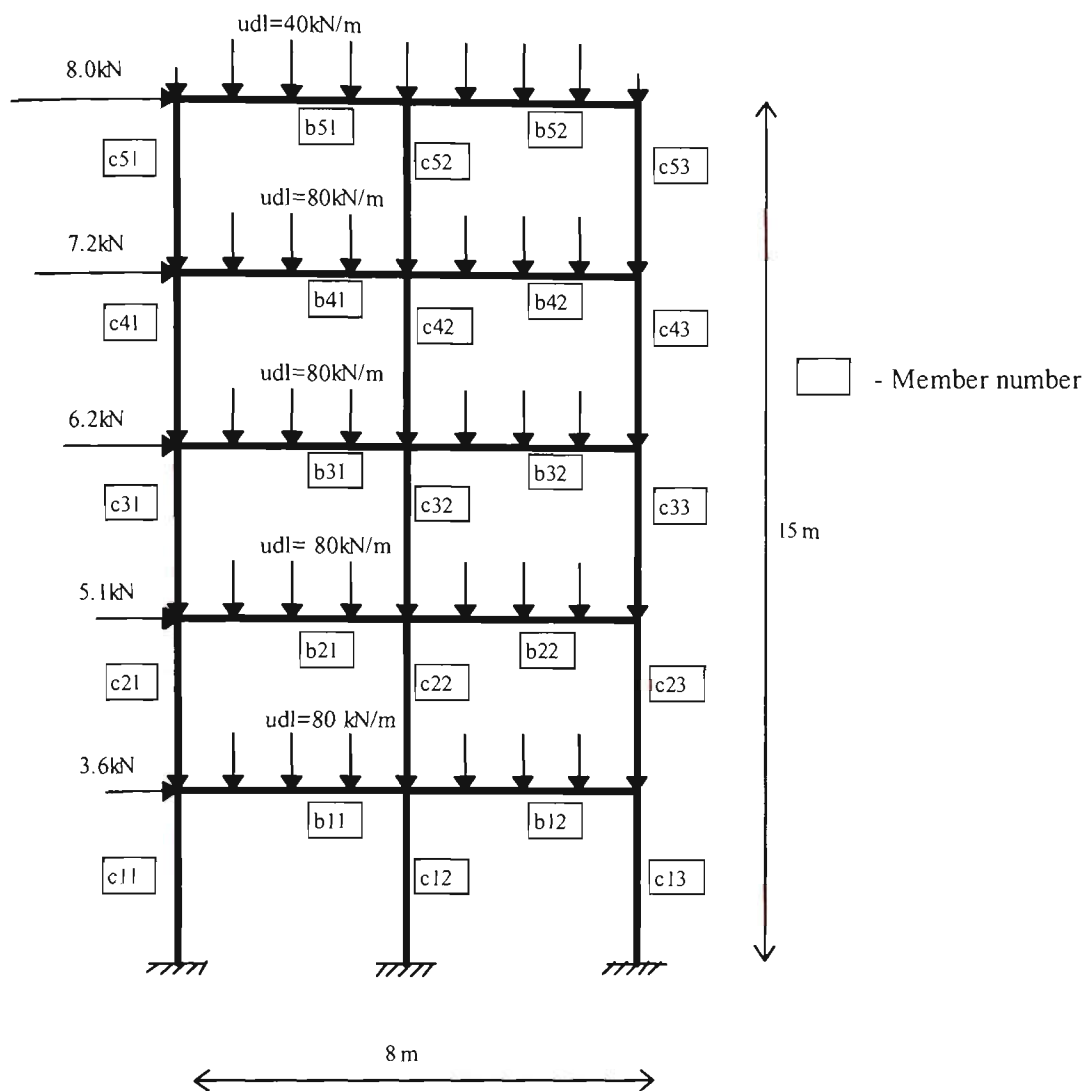


**Figure 8.8** - Layout of the 5-storey frame

The iteration history of the design with all constraints is given in Figure 8.9. At optimum  $S_d = S_s = 1$  and  $S_b = 0.95$ . The volume of the optimum design with all the constraints is reduced to 62.6% of the initial design volume. Optimum designs are also obtained considering each constraint separately and the optimisation histories are given in Figures 8.10, 8.11 and 8.12 respectively for stability, stress and displacement constraints. Optimum design values of members for all these designs are tabulated in Table 8.3. The optimum scaling factors and the volume for these designs are compared in Table 8.4.

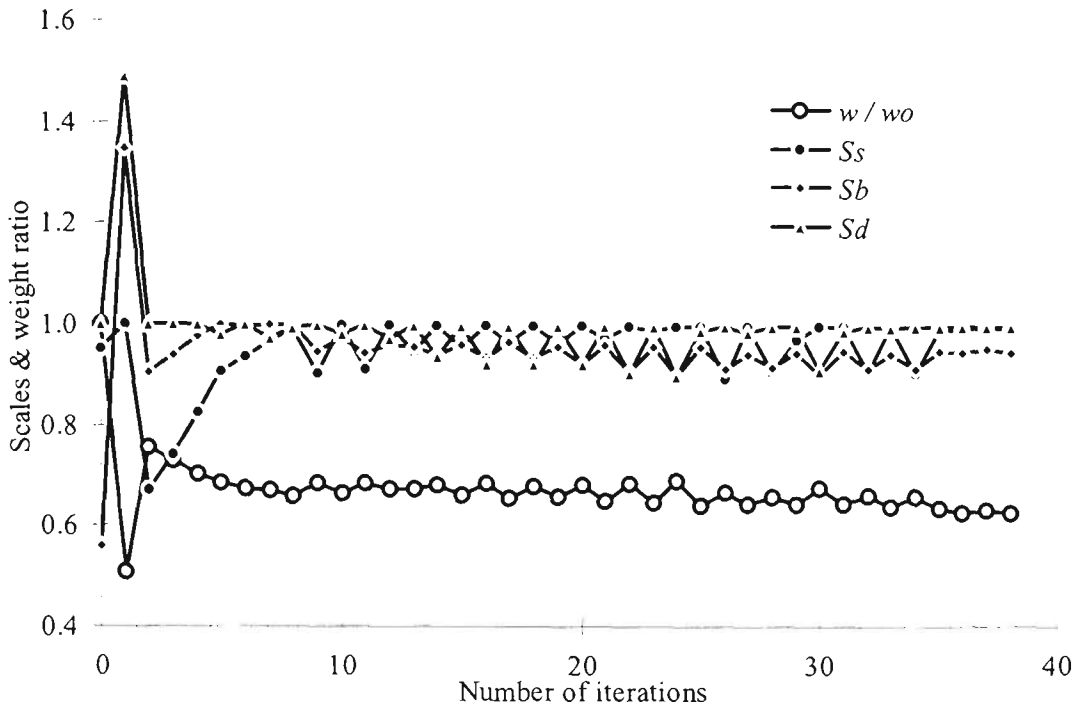


Figure 8.9 - Iteration history of the 5-storey frame with all the constraints

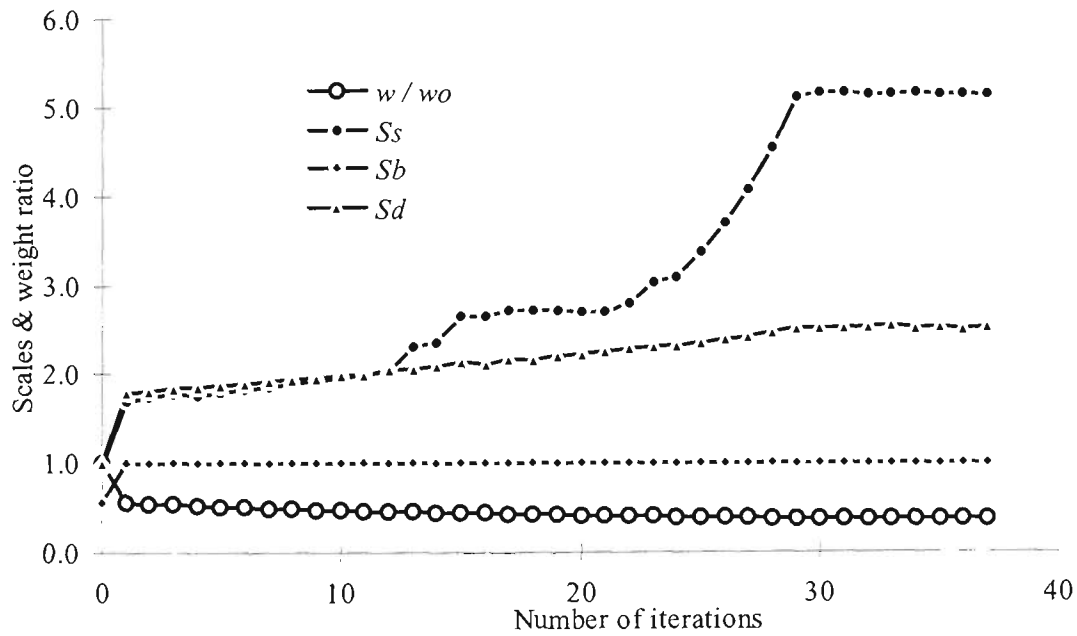


Figure 8.10 - Iteration history of the 5-storey frame with the stability constraint alone

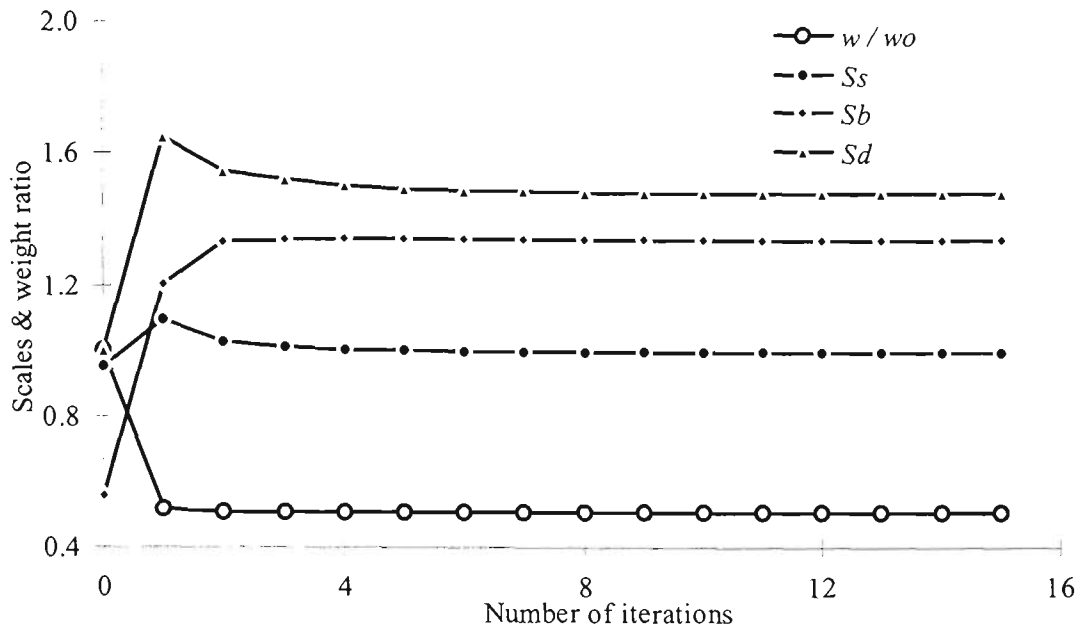


Figure 8.11 - Iteration history of the 5-storey frame with the stress constraint alone

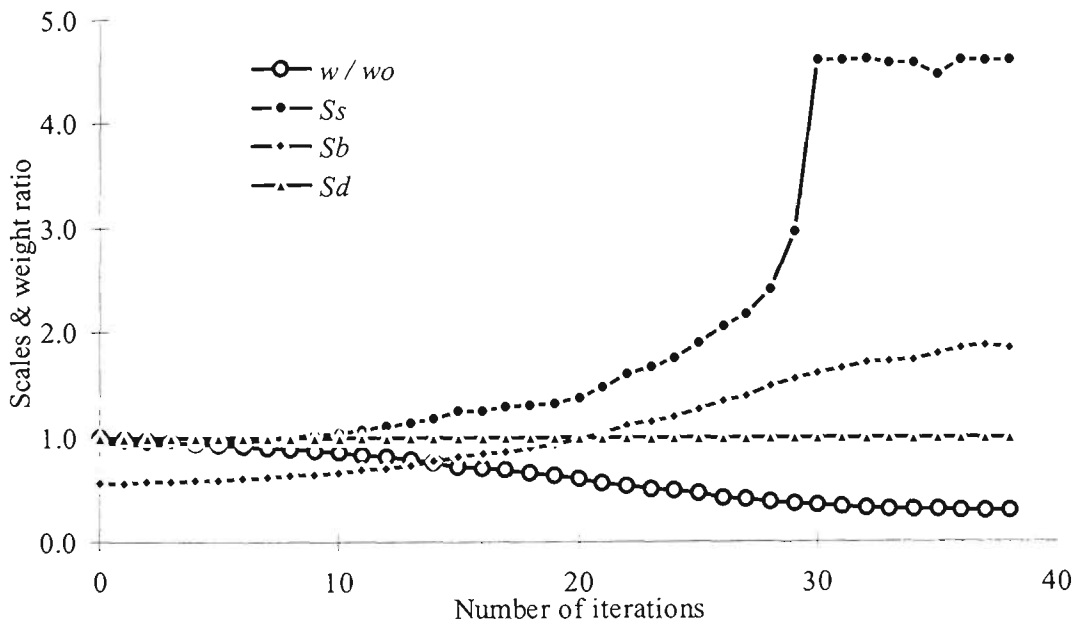


Figure 8.12 - Iteration history of the 5-storey frame with displacement constraint alone

**Table 8.3** - Optimum design values of the 5-Storey frame

Element number	Breadth of the member in mm			
	All constraints	Stability	Stress	Displacement
C11	56.7	93.2	40.0	40.0
C12	123.0	179.1	84.7	104.8
C13	130.0	88.5	78.2	60.5
C21	95.3	94.5	51.2	40.0
C22	99.4	183.5	63.4	60.7
C23	158.7	94.9	97.8	98.5
C31	73.5	68.2	43.4	40.0
C32	67.6	138.1	46.0	84.7
C33	142.6	63.1	82.8	55.5
C41	95.0	40.0	47.6	40.0
C42	70.6	71.5	40.0	40.0
C43	130.8	40.0	77.6	87.2
C51	44.4	40.0	42.1	40.0
C52	40.0	40.0	40.0	40.0
C53	129.7	40.0	56.9	82.7
B11	263.4	152.8	241.9	130.4
B12	206.8	148.0	190.0	40.0
B21	245.1	150.4	225.2	130.2
B22	202.7	141.0	186.2	40.0
B31	232.1	99.1	217.0	130.1
B32	202.2	94.1	189.5	40.0
B41	230.7	40.0	211.4	106.8
B42	211.4	40.0	194.2	40.0
B51	117.7	40.0	106.6	51.1
B52	114.5	40.0	100.0	40.0

**Table 8.4** - Comparison of optimum design parameters for the 5-storey frame

	Volume (m <sup>3</sup> )	$S_b$	$S_s$	$S_d$
Initial uniform design	2.391	0.56	0.95	1.00
Optimum design with all constraints	1.497	0.95	1.00	1.00
Optimum design with stability constraint alone	0.912	1.00	5.17	2.53
	1.497**	0.89	1.52	1.60
Optimum design with stress constraint alone	1.215	1.35	1.00	1.49
	1.497**	0.87	1.00	1.32
Optimum design with displacement constraint alone	0.698	1.87	4.63	1.00
	1.497**	0.93	1.30	1.00

\*\* Scaling factors corresponding to the optimum design volume with all constraints are obtained from the iteration histories.

## 8.6 Conclusions

The proposed ESO method for multiple constraints problem systematically reduces the weight by uniform scaling and shifting the material from strongest part to the weakest part through the use of sensitivity numbers. The uniform scaling factor of each constraint determines the active participation of that constraint in the current design and serves as weighting parameter when defining the sensitivity numbers. Unlike in other optimisation methods, the number of design variables and the number of constraints are not a restriction in the proposed evolutionary method. Hence this method is suitable for designing practical structures with a large number of design variables. The optimum designs obtained for the 50-bar truss and the 5-storey frame result in significant volume

reductions. At optimum designs all the constraints are equally active. It is also shown with the examples that the optimum designs obtained with a single constraint alone significantly violate the other constraints.

## **CHAPTER 9 - OPTIMUM DESIGN OF PLATE STRUCTURES**

### **9.1 Introduction**

Optimisation for plate buckling resistance is complicated, because the in-plane stress resultants in the prebuckled state of a plate are functions of thickness distribution. Although there has been a considerable amount of work done on optimisation of frame structures to enhance buckling resistance, very little research has been reported for plate structures. This is because the axial stress resultant in the prebuckling state of a frame structure is approximately independent of change to member cross-sections imposed by the optimisation process. However, such an approximation is not valid for plates and shells. For example, once the thickness distribution of a plate becomes variable, the distribution of the prebuckling stress resultants becomes non-uniform and statically indeterminate. The problem of optimising plates for stability is, therefore, significantly more complicated than that for frame structures.

The main part of this chapter discusses the problem of finding the optimum thickness distribution of isotropic plate structures, with a given volume and layout, that would maximise the buckling load. Thin plates of variable thickness are not commonly used, yet they exhibit properties that are worth considering especially in weight sensitive industries. Of particular interest are the variable thickness plates that are required to withstand compressive loads. When properly shaped, they possess much higher buckling loads for a given volume of material. Optimum thickness profiles of compression-loaded rectangular plates with different boundary conditions and plate aspect ratios are obtained by using the ESO method.

Optimum designs from earlier studies and the methods for buckling analysis used to attain these results are discussed in detail in the following sections and compared with the designs from the ESO method. The reliability of the buckling solutions of variable-thickness plates are analysed. It is also investigated the validity of the optimality criterion frequently used for plate buckling optimisation by other researchers, which is based on the uniform strain energy density.

## 9.2 Sensitivity Number and Optimisation Procedure

To increase the buckling resistance of a plate by redistributing its thickness, the change in the critical buckling load factor due to an increase or a decrease in the thickness of elements need to be calculated. The change in the stiffness matrix for an increase in thickness by  $\Delta t$  in the  $i^{\text{th}}$  element is given by

$$[\Delta k_i] = [\Delta k_i]^+ = [k_i(t + \Delta t)] - [k_i(t)] \quad (9.1a)$$

Similarly, for a reduction in thickness by  $\Delta t$  in the  $i^{\text{th}}$  element,

$$[\Delta k_i] = [\Delta k_i]^- = [k_i(t - \Delta t)] - [k_i(t)] \quad (9.1b)$$

As discussed in Chapter 4, the change in stress stiffness matrix  $[\Delta K_g]$  can be neglected if the modification to the thickness distribution done at each optimisation step is kept sufficiently small. Thus the sensitivity numbers of elements,  $\alpha_{ib}^+$  and  $\alpha_{ib}^-$  are obtained by using the change of stiffness matrix only. An iterative procedure, as described in Section 4.4, is set up for resizing the plate thickness so that the material is gradually shifted from the strongest, oversized part of the structure to the weakest part while keeping the structural volume constant. In the evolutionary procedure, the plate element thickness is allowed to vary in small steps in a prescribed manner. The sizing constraint,

$t_{min} \leq t \leq t_{max}$  is imposed on plate thickness during element resizing, where  $t_{max}$  and  $t_{min}$  are the allowable maximum and minimum thicknesses, respectively.

### 9.3 Examples

Determination of optimum thickness distribution for uniaxial-compression-loaded rectangular plates (Figure 9.1) has been an interesting problem widely discussed in the literature. This is because the governing non-linear fourth order partial differential equations used for the solution of buckling loads of rectangular plates are well known. Optimum thickness distribution of three such plates with different boundary conditions and plate aspect ratios have been obtained by the candidate using the ESO method. The plates are made of an isotropic material with a Young's modulus  $E = 200$  GPa and a Poisson's ratio  $\nu = 0.3$ . The objective is to find the optimum thickness distribution that would maximise the critical value of the applied stress resultant  $Nx_{cr}$  (Figure 9.1). For these plates, a uniaxial-compression distributed load of 1 kN/m is applied. Thus, the first eigenvalue,  $\lambda_1$  is equal to the critical load per unit length,  $Nx_{cr}$ . For these examples, an optimum load factor,  $OF$ , which is defined as the ratio of the buckling load of an optimised plate to that of an equivalent uniform thickness plate, is used to measure the efficiency of the optimised plate.

Optimisation procedures that are based on discrete models often generate anomalies. In particular, the problem of getting patches of checkerboard-like patterns in optimum plate designs is encountered quite often. Jog and Haber (1995) have addressed the problem of checkerboard-like patterns that have appeared in finite-element solutions for distributed-parameter optimisation and variable-topology shape design problems and

have shown that the cause of the problem is numerical instability. Usually, but not always, with the higher order displacement elements this numerical instability can be eliminated, and stable and smoothly varying designs can be obtained. Therefore in the following examples eight-node isoparametric elements are used to model the plate structures to minimise the formation of checkerboard-like patterns. The problem and remedy for numerical instability and the formation of checkerboard-like patterns will be further discussed in Section 9.7.

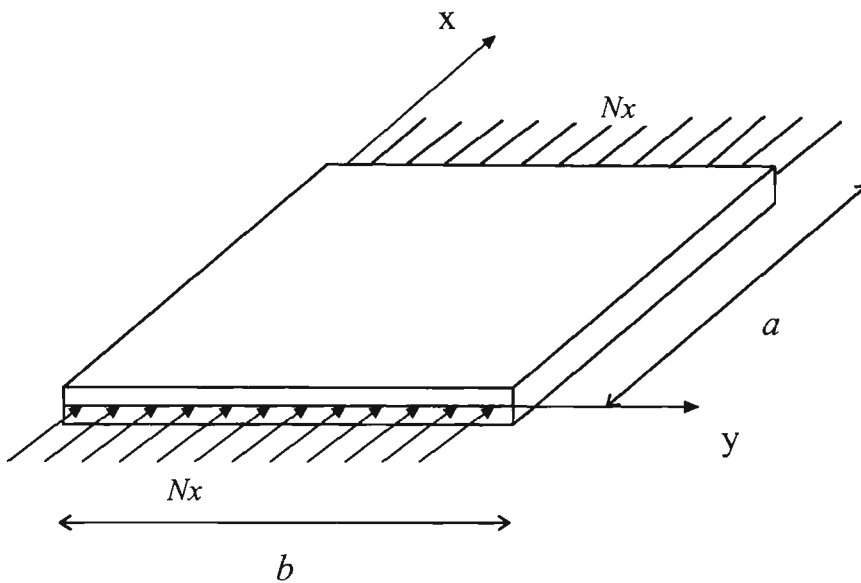


**Figure 9.1** - Uniaxial-compression-loaded rectangular plate.

### 9.3.1 Simply supported square plate

The optimum thickness distribution is sought for a uniaxial-compression-loaded square plate that is simply supported on all sides. This example is considered as a benchmark problem because it has been analysed extensively in the past by using different optimisation methods. A series of studies were carried out independently by Parsons (1955), Capey (1956), Mansfield (1973), Spillers and Levy (1990), Levy and Ganz (1991), Pandey and Sherbourne (1992), Levy and Sokolinsky (1995) and Levy (1996) to

find the optimum thickness profile for a square plate. Some of these optimum shapes will be examined in the following sections.

A square plate with a side-width  $a = 2$  m and an initial uniform thickness  $t_u = 15$  mm is considered. The following two cases are examined:

Case 1:  $t_{max} = 20$  mm and  $t_{min} = 10$  mm

Case 2:  $t_{max} = 25$  mm and  $t_{min} = 5$  mm

The plate is discretised into  $20 \times 20$  square elements and 16% of the elements are resized at each iteration (i.e., the thicknesses of 32 elements increased and the thicknesses of 32 elements decreased at each iteration). Plate thicknesses are allowed to change in steps of 1 mm. The resizing ratio and the step size are kept constant throughout the optimisation process.

The optimum element thicknesses for the two cases that are obtained with the 8-node isoparametric elements are given in Figure 9.2 for one quarter of the plate. The optimum thickness distributions for the whole plate are shown in Figure 9.3. The value of  $Nx_{cr}$  for the uniform-thickness plate and the optimum designs for Cases 1 and 2 are 608.31 kN/m, 826.08 kN/m (OF = 1.36), and 894.08 kN/m (OF = 1.47), respectively. The evolutionary histories of the first two eigenvalues for both cases are shown in Figure 9.4 and the results indicate that there is not any modal interaction present. The results in Figure 9.3 indicate that optimum designs are obtained at between 30 and 35 iterations.

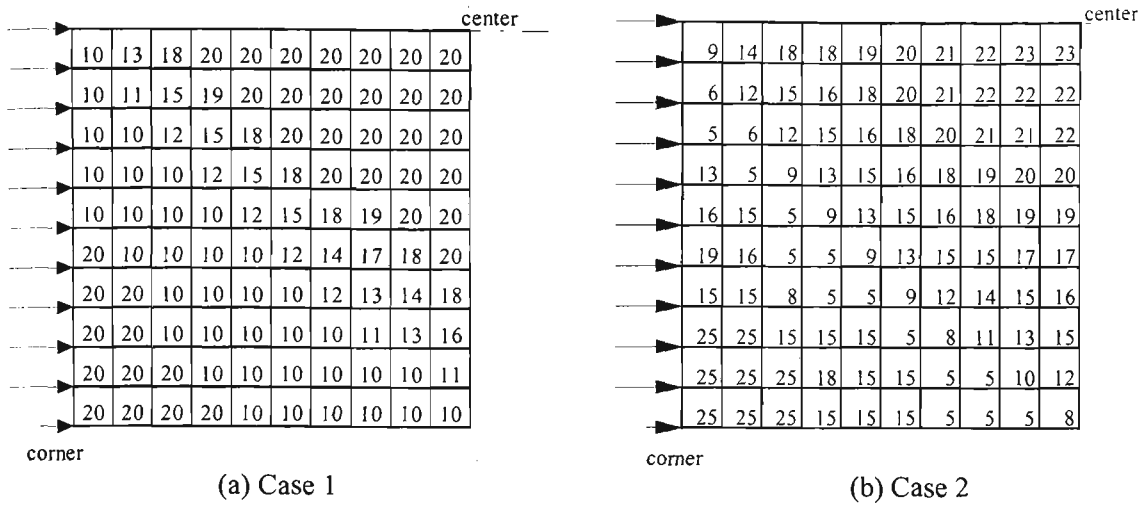


Figure 9.2 - Optimum element thicknesses of the simply supported square plate for one quarter of the plate

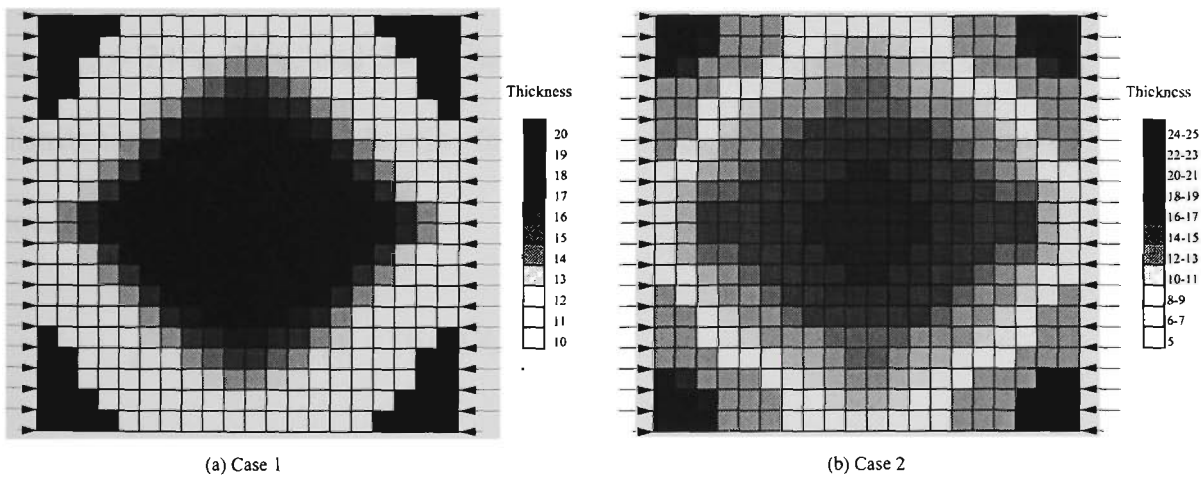
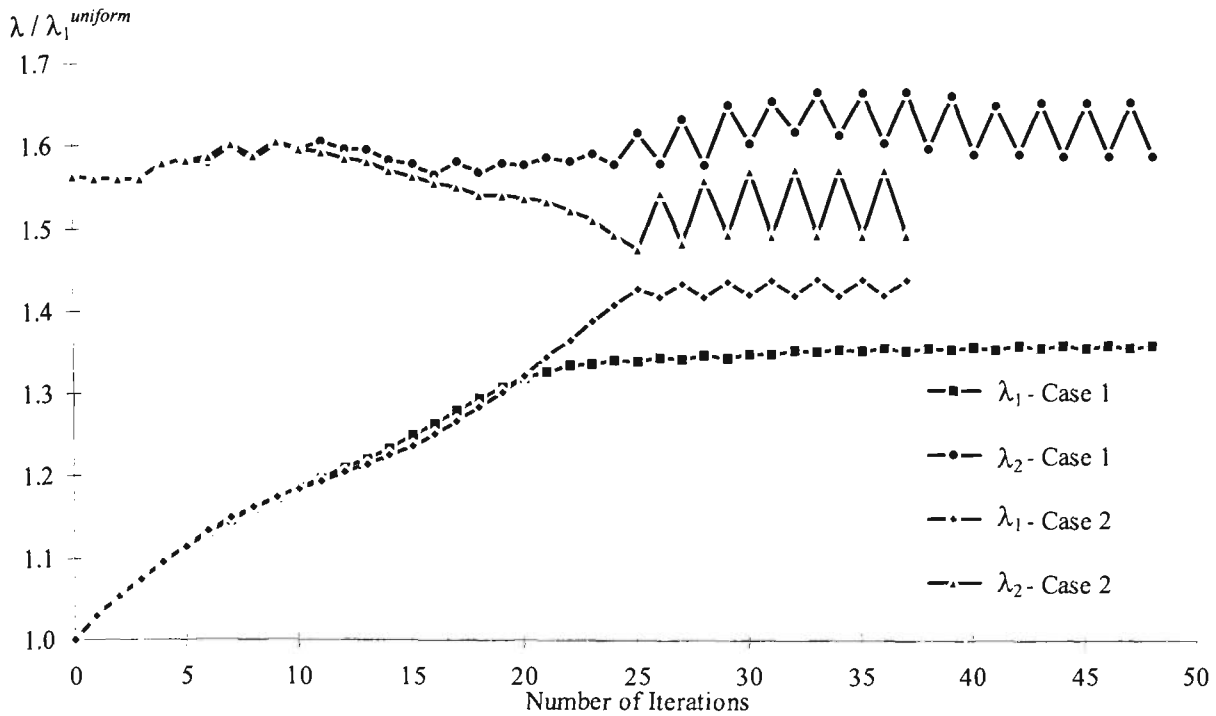


Figure 9.3 - Optimum designs of the simply supported square plate



**Figure 9.4** - Iteration histories of the simply supported square plate

For both Cases 1 and 2 optimum designs, the plate material is redistributed to thicken the center and the four corners. Similar designs were obtained for the thickness ratios  $t_{max}/t_{min} = 24/8, 24/6,$  and  $24/4$ . Based on these results, a smooth optimum thickness distribution is proposed herein for this square plate with the following quadratic equations:

$$t(r) = kt_{min} - (k-1)t_{min} \left( \frac{r}{a/2} \right)^2 \quad \text{when } r \leq a/2, \quad (9.2a)$$

$$t(r) = kt_{min} - (k-1)t_{min} \left( \frac{\sqrt{2} - 2r/a}{\sqrt{2} - 1} \right)^2 \quad \text{when } r > a/2, \quad (9.2b)$$

where  $r$  is the radius measured from the center of the plate and  $k = t_{max}/t_{min}$ . Values of  $N_{xcr}$  were obtained for plates with this thickness distribution for values of  $k = 3, 3.5, 4, 4.5,$  and  $5$  from  $40 \times 40$  finite element models (8-node isoparametric elements). These results are tabulated in Table 9.1. The results predict a small variation in the enhancement to buckling resistance for the values of  $k$  used, with the highest

enhancement to buckling resistance occurring for  $k = 4$ . A 37% higher value of  $Nx_{cr}$  is obtained for the plate with  $k = 4$  than for the corresponding plate with the uniform thickness. An exaggerated plot of the thickness distribution of the plate with  $k = 4$  is shown in Figure 9.5.

**Table 9.1** - Buckling load factors for the plate as defined by equation (9.2)

$k$	3.0	3.5	4.0	4.5	5.0
$OF = Nx_{cr} / Nx_{cr}^{uniform}$	1.355	1.369	1.370	1.358	1.331

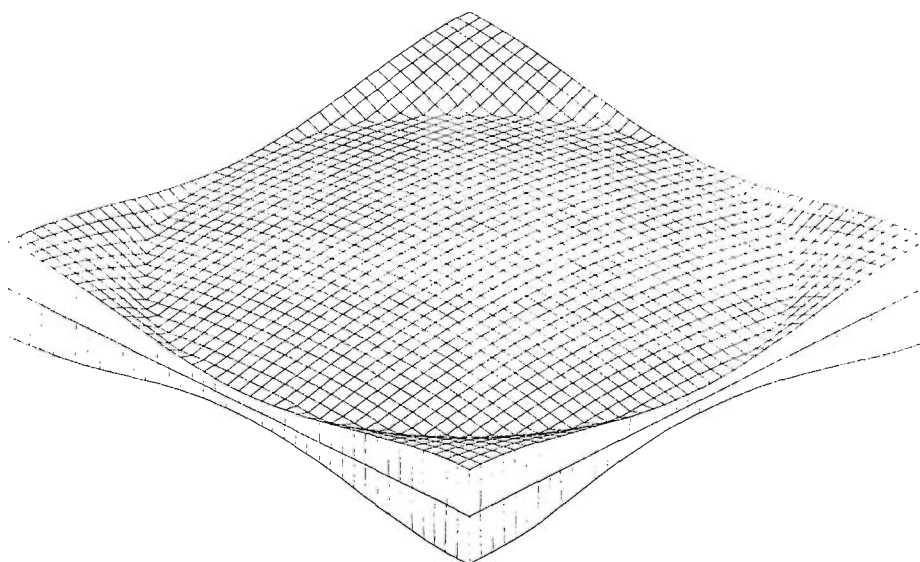


**Figure 9.5** - Proposed smooth profile for the simply supported square plate ( $k = 4$ ).

### 9.3.2 Clamped square plate

Optimum thickness profile is sought for a uniaxial-compression loaded square plate that is clamped on all sides. Plate dimensions and design parameters are the same as those of simply supported plate in Section 9.3.1. Again, the two cases (Case 1 with  $t_{max}/t_{min} = 20/10$  and Case 2 with  $t_{max}/t_{min} = 25/5$ ) are considered. The plate is discretised into 20 x 20 square elements and 8% of the elements are resized at each iteration (i.e., thickness

of 16 elements increased and thickness of 16 elements decreased at each iteration). Plate thicknesses are allowed to change in steps of 1 mm at each iteration.

Final designs that are obtained with 8-node isoparametric elements are shown in Figure 9.6. The first and second eigenvalues of the uniform plate and the optimum designs for Case 1 and Case 2 are given in Table 9.2. For Case 1, the plate has become bimodal as a result of optimisation. For Case 2, although the intermediate designs exhibit bimodal behaviour, the final design is single mode. Optimum designs are also obtained by considering only the first buckling mode by using single mode sensitivity numbers. Buckling loads of these designs are lower than those of the optimum designs obtained by using the sensitivity numbers which consider modal interaction. The evolutionary histories of the first two eigenvalues for Cases 1 and 2 that are obtained by using both single and bimodal methods are given in Figures 9.7 and 9.8, respectively.

**Table 9.2** - The first two eigenvalues of the square clamped plate designs

		$\lambda_1 = Nx_{cr}$ (kN/m)	$\lambda_2$	$OF$
Uniform design		1534.3	1767.3	1.00
Case 1 designs	Bimodal	2383.7	2408.6	1.55
	Unimodal	2242.7	2263.9	1.46
Case 2 designs	Bimodal	2850.3	3416.6	1.86
	Unimodal	2539.0	2625.2	1.65

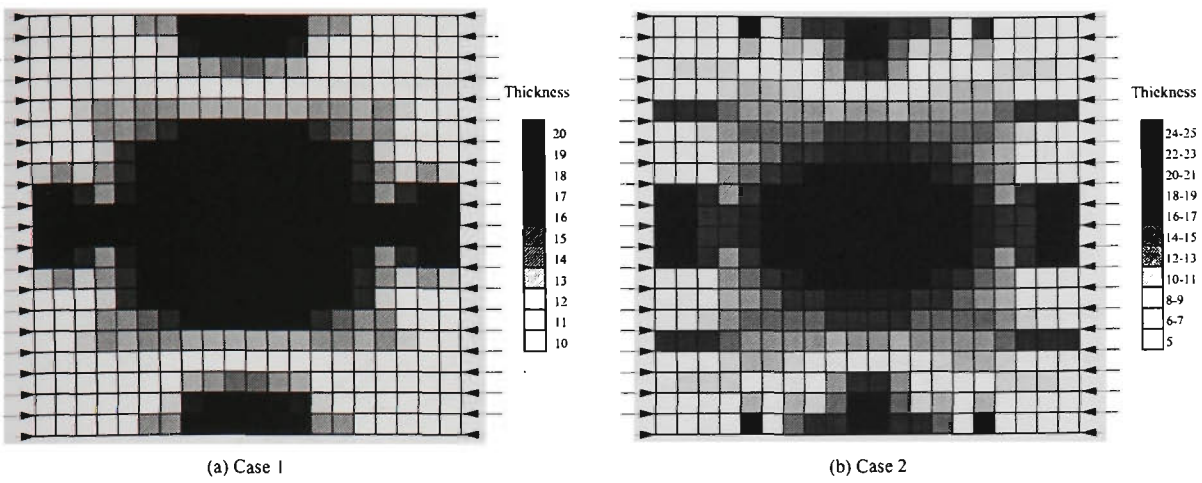


Figure 9.6 - Optimum designs of square clamped plate

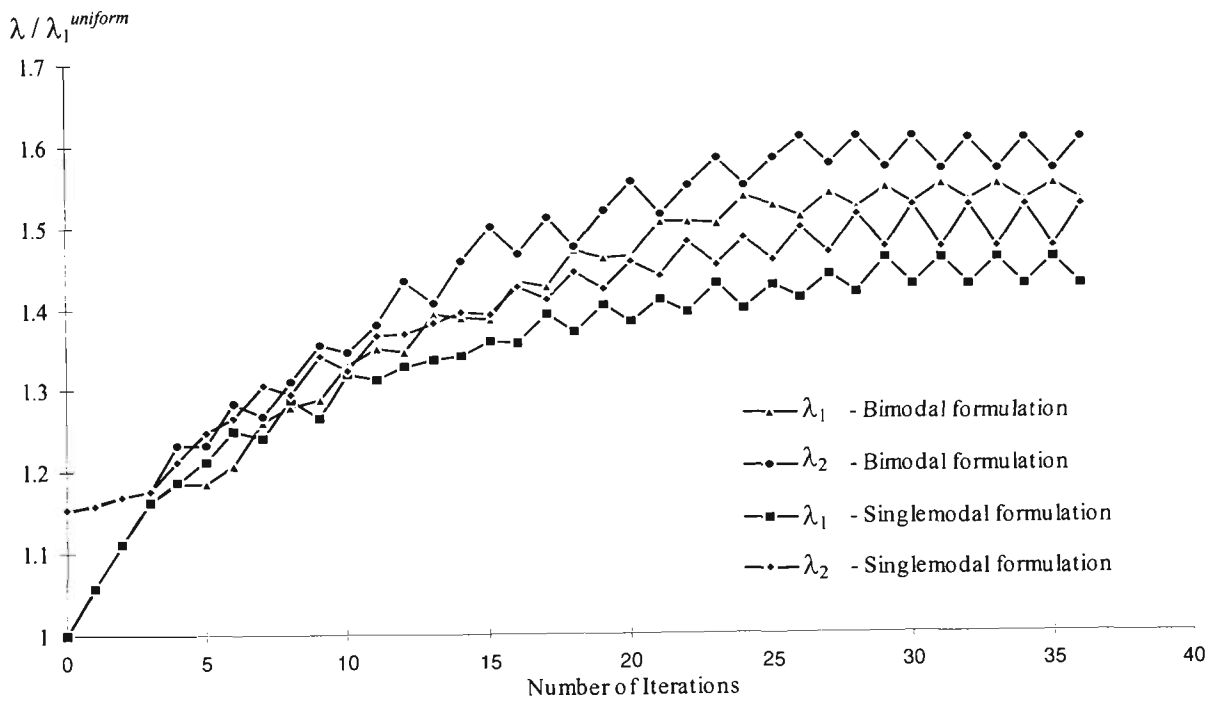
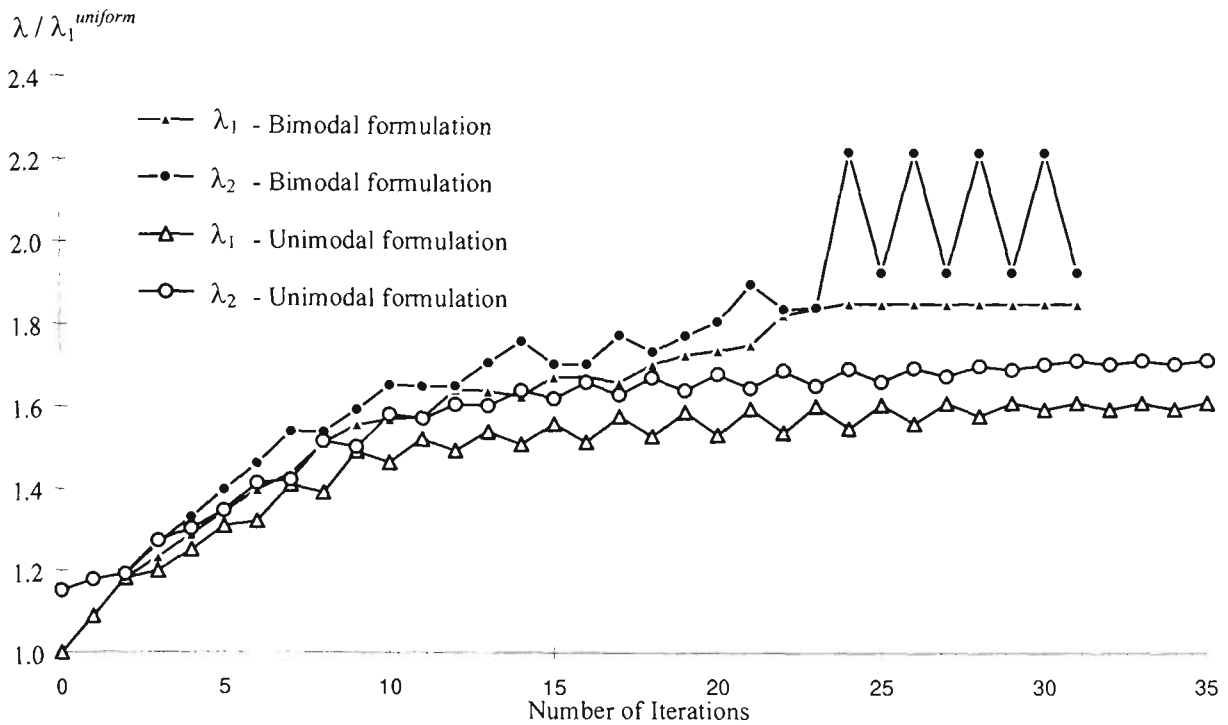


Figure 9.7 - Iteration histories of the square clamped plate (Case 1)



**Figure 9.8** - Iterations histories of the square clamped plate (Case 2)

### 9.3.3 Simply supported rectangular plate

A simply supported rectangular plate of dimensions 3.2 m by 2.4 m is analysed. Uniform uniaxial-compression load is applied on the shorter edge of the plate. The initial uniform thickness of the plate is 15 mm and the thickness is allowed to vary to the maximum of 20 mm and to the minimum of 10 mm in steps of 1 mm. The plate is discretised into 32 x 24 square elements. At each iteration, 64 elements are subjected to thickness resizing. The first and second eigenvalues of the uniform plate are 458.82 kN/m and 496.19 kN/m, respectively. The final design (Figure 9.9) is bimodal and it is obtained after 31 iterations. The first and second eigenvalues of this optimum design are very closely spaced and are equal to 573.96 kN/m ( $OF = 1.25$ ) and 574.17 kN/m, respectively. The plate is also optimised with the single mode sensitivity numbers and the value of  $N_{xcr}$  for the final design is 530.86 kN/m ( $OF = 1.15$ ). The evolutionary histories of the first two eigenvalues that are obtained by using both single and bimodal methods are given in Figure 9.10.

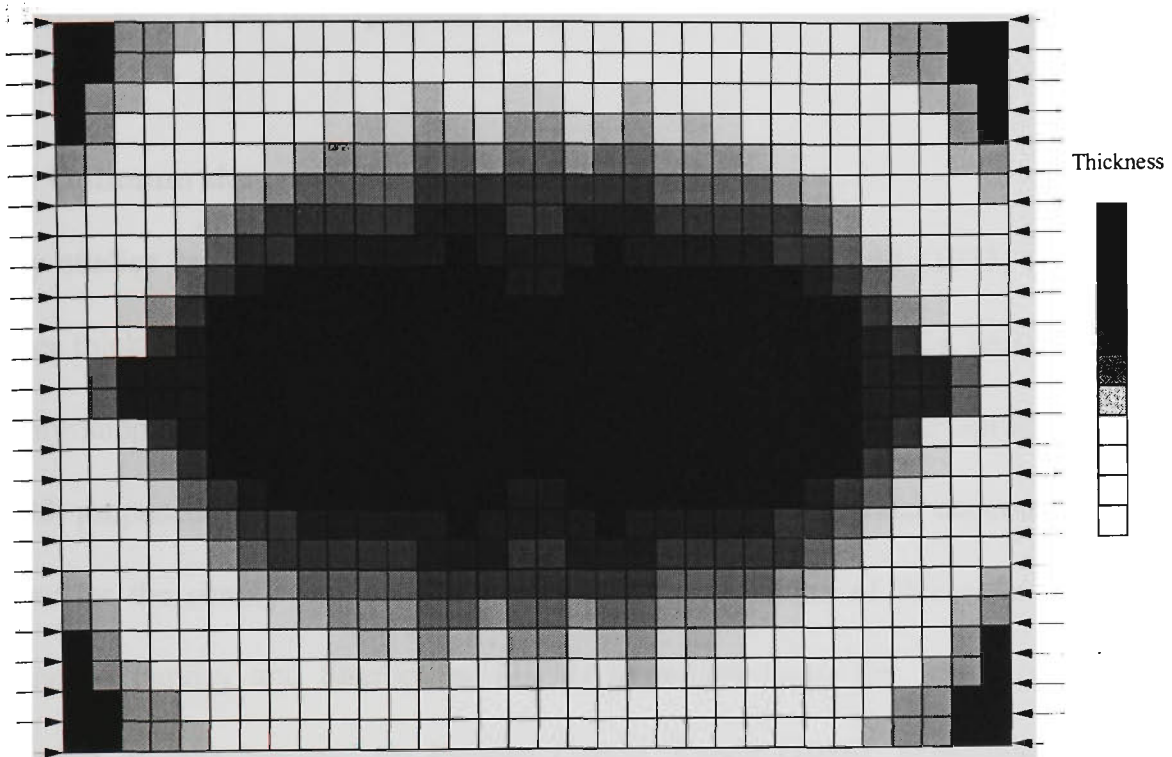


Figure 9.9 - Optimum design of the rectangular plate ( $t_u = 15$  mm)

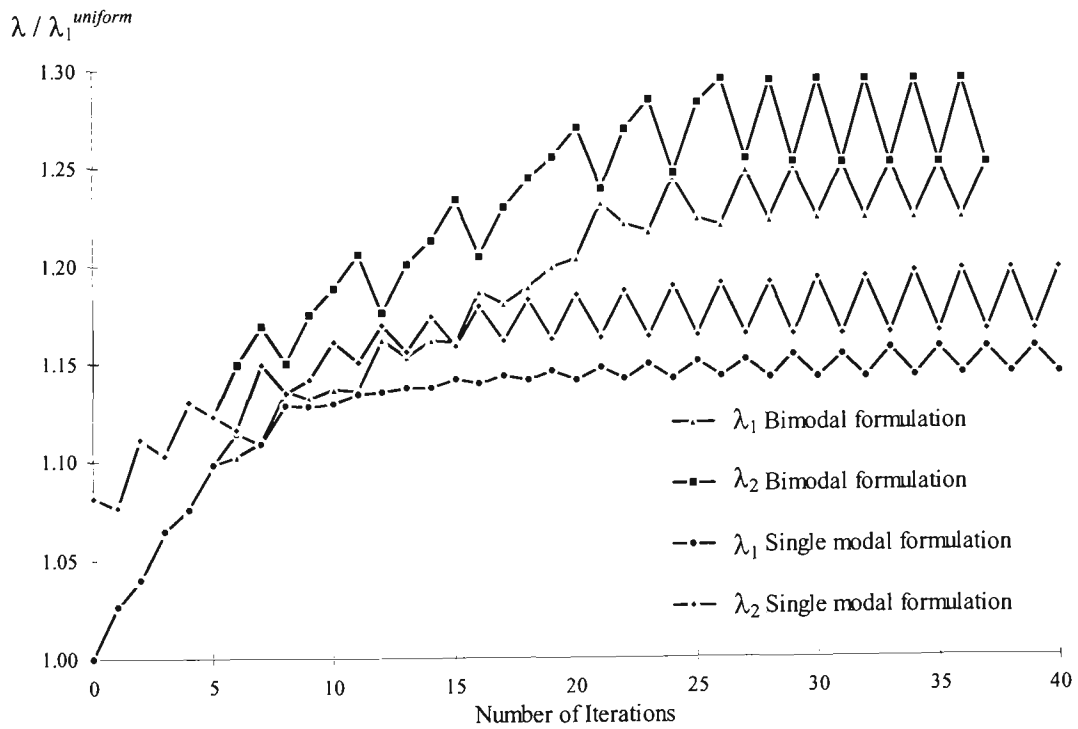


Figure 9.10 - Optimisation histories of the rectangular plate ( $t_u = 15$  mm)

## 9.4 Previously Reported Optimum Shapes

### 9.4.1 Optimum shapes by Pandey and Sherbourne

Early studies by Parsons (1955), Capey (1956), and Mansfield (1973) reported that higher thickness near the edges versus center (concave profile) of a uniaxially loaded simply supported square plate increased its buckling resistance. Spillers and Levy (1990) proposed a convex thickness profile with very high material concentration in the center for the simply supported square plate. This paradox of thickness distributions motivated Pandey and Sherbourne (1992) to re-investigate the whole problem. The optimum designs reported by Parsons (1955), Capey (1956), Mansfield (1973) and Spillers and Levy (1990) are characterised by a severely disproportionate thickness distribution resulting in very thin sections in certain regions. Pandey and Sherbourne (1992) found that these plates actually buckled locally at a load far lower than what have predicted by those authors. Buckling solutions of these plates were obtained by using the Raleigh-Ritz method with assumed displacement functions. The number of terms used in the series to represent the plate lateral displacement was not big enough to capture the local buckling.

Pandey and Sherbourne (1992) proposed a thickness distribution for uniaxially loaded rectangular plates based on Parson's (1955) sinusoidal thickness variation and it is given by the following equation.

$$t(x, y) = \frac{t_u}{k_1^2} \left( 1 + (N_v - 1) \sin \frac{\pi x}{a} \right) \left( 1 + (N_v - 1) \sin \frac{\pi y}{b} \right) \quad (9.3)$$

where  $k_1 = 1 + 2(N_v - 1) / \pi$ ,  $N_v$  is a variable called thickness distribution shape parameter,  $t_u$  is the uniform plate thickness, and  $a$  and  $b$  are length and width of the

plate. Optimum shapes were obtained for a square plate with three sets of boundary conditions; that is, a) all edges simply supported, denoted by SSSS; b) all edges clamped, denoted by CCCC and c) loaded edges simply supported and unloaded edges clamped, denoted by SSCC.

The Rayleigh-Ritz method was used for the buckling analyses. The following Fourier sine series of half sine waves in both plate directions was used to represent the lateral deflection,  $w(x,y)$  of the simply supported plate.

$$w(x,y) = \sum_{m=1}^N \sum_{n=1}^N A_{mn} \sin \frac{m\pi x}{a} \sin \frac{n\pi y}{b} \quad (9.4)$$

where  $A_{mn}$  is a constant. The following Gram-Schmidt-type orthogonal polynomials were used for the plates with clamped edges.

$$w(x,y) = \sum_{m=1}^N \sum_{n=1}^N A_{mn} \phi_m \left( \frac{x}{a} \right) \psi_n \left( \frac{y}{b} \right) \quad (9.5)$$

where  $\phi_m$  and  $\psi_n$  are orthogonal polynomial sequences that at least satisfy the geometrical boundary conditions in  $X$ - and  $Y$ - directions, respectively. The total number of terms used in the both displacement functions was 81 ( $N = 9$ ).

Buckling loads were obtained for plates with various values of thickness distribution parameter,  $N_v$ . Poisson's ratio  $\nu = 0.3$  was used in this analysis. For the simply supported square plate the maximum buckling was obtained when  $N_v = 2$  (convex profile as shown in Figure 9.11) and the buckling load was 28.4% higher than that of the uniform plate load ( $OF = 1.284$ ). The ratio of the plate thickness at the centre to corner for this convex plate is 4. For CCCC and SSCC plates, optimum buckling loads were obtained when  $N_v = 0.25$  (concave profile as shown in Figure 9.12). Reported optimum

factors of these CCCC and SSCC plates are 2.046 and 2.359, respectively. However, the buckling solutions reported for these concave profiles appear to be in error, as shall be discussed later in Section 9.6.

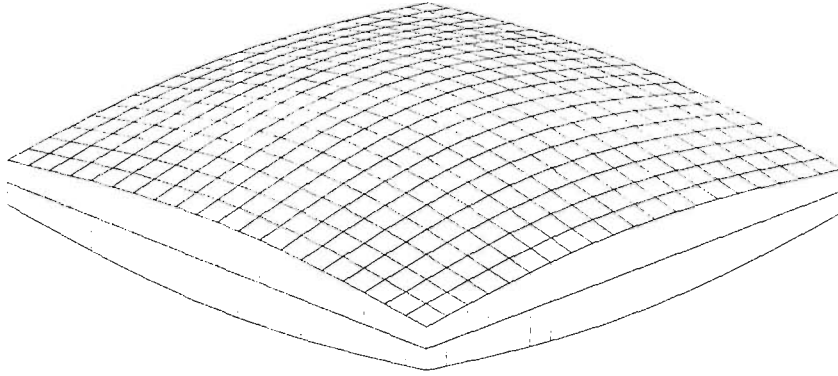


**Figure 9.11** - Optimum Shape by Pandey & Sherbourne for SSSS plate ( $N_v = 2.0$ )

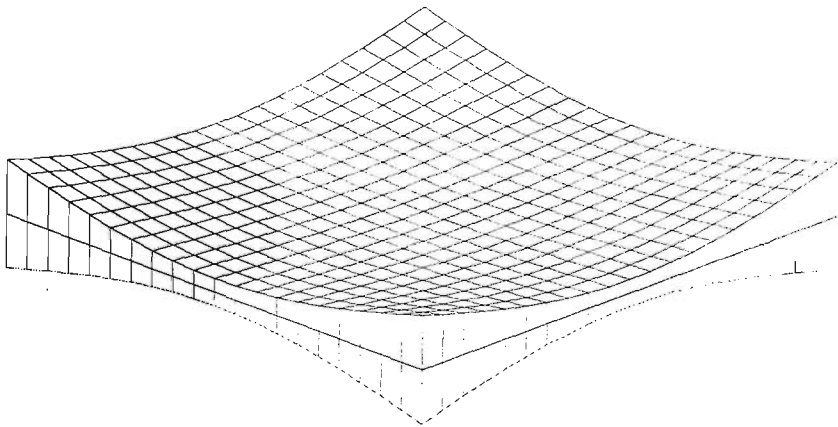


**Figure 9.12** - Optimum shape by Pandey & Sherbourne for CCCC and SSCC plates

$$(N_v = 0.25)$$

#### 9.4.2 Optimum shapes by Levy and his co-workers

Originally, Spillers and Levy (1990) extended Keller's (1960) classic solution for the optimal design of columns to the case of plates and derived an optimality condition via variational calculus which states that the plate thickness distribution should be proportional to the strain-energy density distribution in an optimal design. They

proposed the following thickness profile for the uniaxially loaded simply supported rectangular plate.

$$t(x, y) = t_u \left( 1 - 0.586 \cos \frac{2\pi x}{a} \right) \left( 1 - 0.586 \cos \frac{2\pi y}{b} \right) \quad (9.6)$$

The optimum shape according to equation (9.6) for a square plate is shown in Figure 9.13. Buckling solution was obtained by using the Rayleigh-Ritz method with the following one-term symmetric double sine series representation for the plate lateral displacement.

$$w(x, y) = A \sin \frac{\pi x}{a} \sin \frac{\pi y}{b} \quad (9.7)$$

The buckling load for this plate was calculated to be 2.12 times that of an equivalent uniform plate ( $OF = 2.12$ ). Levy and Ganz (1991) later re-analysed this problem by using a six term displacement function with a multiple of half sine waves in the direction of loading and only one half sine wave in the other direction (equation. 9.8) and predicted a 44% increase in the buckling load ( $OF = 1.44$ ).

$$w(x, y) = \sum_{n=1,3,5,\dots}^{11} A_n \sin \frac{n\pi x}{a} \sin \frac{\pi y}{b} \quad (9.8)$$

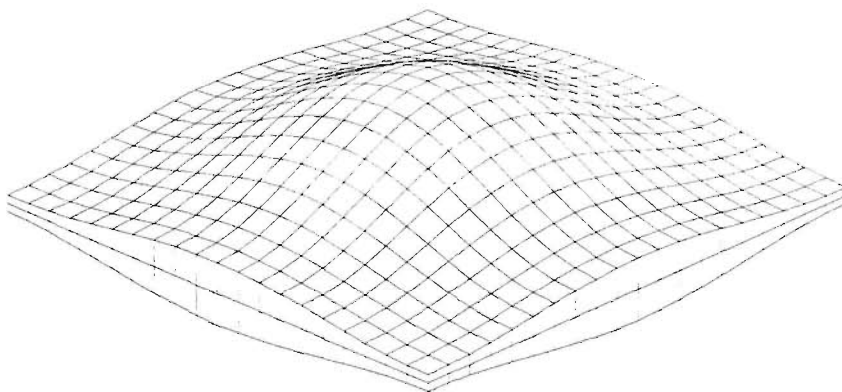


**Figure 9.13** - Optimum shape by Spillers & Levy (1990)

Pandey and Sherbourne (1992) found that the displacement functions given by equations (9.7) and (9.8) could encapsulate a critical mode of global nature only and could not capture the complex localised buckling modes. They re-analysed Levy's plate with a displacement function of half sine waves in both plate directions of a total of 289 terms:

$$w(x, y) = \sum_{m=1}^N \sum_{n=1}^N A_{mn} \sin \frac{m\pi x}{a} \sin \frac{n\pi y}{b} \quad \text{where } N = 17 \quad (9.9)$$

They reported, that Levy's plate locally buckles at corners for a load far lower than that predicted and also less than the buckling load of uniform thickness plate ( $OF = 0.44$ ).

Recently Levy and Sokolinsky (1995) and Levy (1996) re-analysed the whole problem and proposed the following two thickness distributions as optimum shapes.

(a) Double cosine symmetric plate given by

$$t(x, y) = t_u \left( 1 - 0.295 \cos \frac{2\pi x}{a} \right) \left( 1 - 0.295 \cos \frac{2\pi y}{b} \right) \quad (9.10)$$

(b) Hybrid double sine symmetric plate given by

$$t(x, y) = c_1 \left( 1 + c_2 \sin \frac{\pi x}{a} \right) \left( 1 + c_2 \sin \frac{\pi y}{b} \right) \quad (9.11)$$

where  $c_1$  and  $c_2$  depend on  $t_u$ . For  $t_u = 0.05$ ,  $c_1 = 0.0135$  and  $c_2 = 1.452$ . Shapes of a square plate given by equations (9.10) and (9.11) are shown in Figures 9.14 and 9.15. Rayleigh-Ritz method was used with a sufficiently accurate displacement function to obtain the buckling loads of these plates. For the Poisson's ratio  $\nu = 0.32$ , optimum buckling load factors reported for cosine and sine plates are 1.234 and 1.323, respectively.

example, the initial outer layers (reinforced layers) have a uniform material distribution with volume fraction  $\mu = 0.4$ . The plate is discretised into  $32 \times 24$  eight-node isoparametric elements.

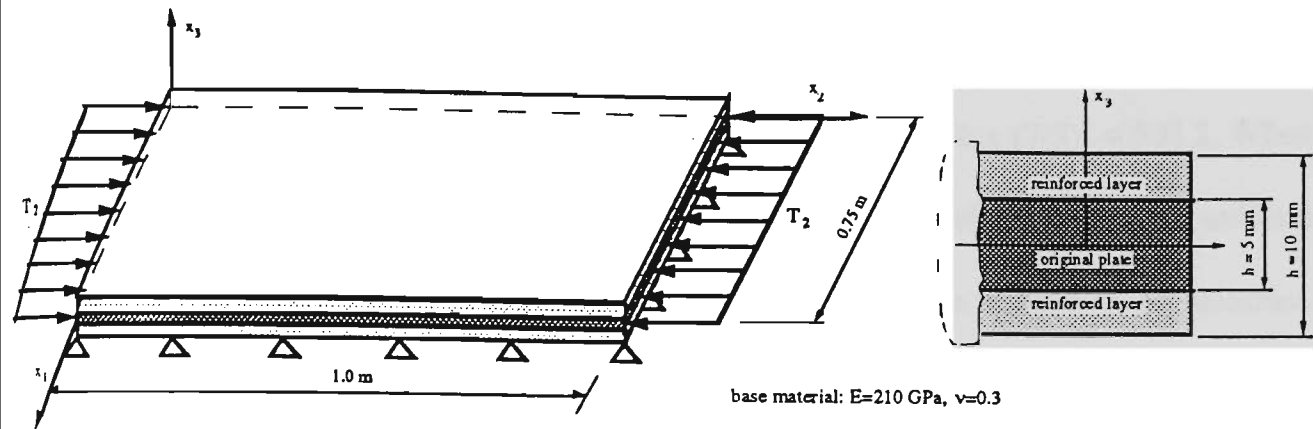


Figure 9.16 - Loads and geometry of the plate by Folgado *et al.* (1995)

The final design obtained and the iteration history of the first three eigenvalues are given in Figure 9.17. The final design was bimodal and was obtained after 112 iterations. The buckling loads reported by Folgado *et al.* were: a) for internal solid layer of 5 mm thickness (without reinforced layers) -  $N_{x_{cr}} = 183.0$ ; b) for initial design with uniform reinforced layers (increase the plate thickness to 10 mm with 40% volume increment) -  $N_{x_{cr}} = 409.1$ ; c) for the final design -  $N_{x_{cr}} = 589.0$ .

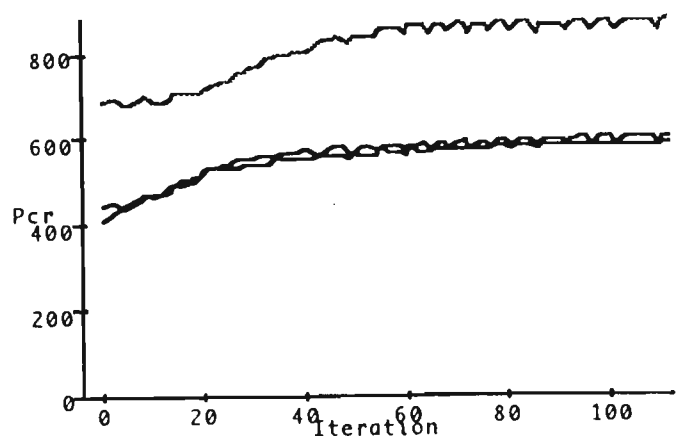
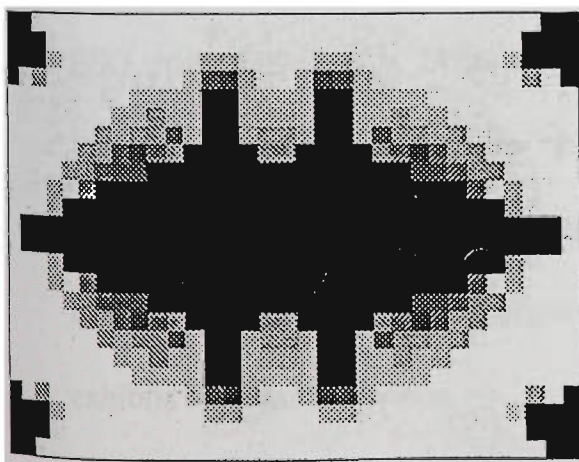


Figure 9.17 - Optimum solution of the plate by Folgado *et al.* (1995)

This problem can be made analogous to the plate with solid material having variable thickness distribution. If the initial design with uniform reinforced layers of  $\mu = 0.4$  is made to a solid layer, the thickness of the initial plate would be  $5 + 5 \times 0.4 = 7$  mm. Hence the buckling load of solid uniform plate would be  $183.0 \times (7/5)^3 = 502.2$ . When comparing the buckling load of solid plate (502.2) and that of the plate with uniform reinforced layers (409.1), the buckling load of the latter plate appears to be incorrect. Because the plate with uniform reinforced layers (which has the material further away from the neutral axis than the solid plate) should be more efficient than the solid plate. Based on the buckling load of solid plate, the optimum load factor of final design would be  $589.0/502.2 = 1.173$ .

This problem can be well compared with Example 9.3.3. The aspect ratio of the plate, the ratio of  $t_{max}/t_{min}$  and the Poisson's ratio are the same for both problems. However, in Example 9.3.3, the uniform plate thickness  $t_u$  was 15 mm. To match the exact conditions of Folgado's plate the uniform plate thickness should have been taken as 14 mm (40% volume increase of minimum thickness 10 mm). Example 9.3.3 is re-analysed using the ESO method with  $t_u = 14$  mm. The final design (Figure 9.18) is obtained after 30 iterations. Buckling loads of the uniform plate and the optimum plate are 373.12 and 458.44 kN/m respectively. Optimum load factor of this design is 1.229. The iteration histories of first and second eigenvalues are shown in Figure 9.19. This plate also exhibits bimodal behaviour.

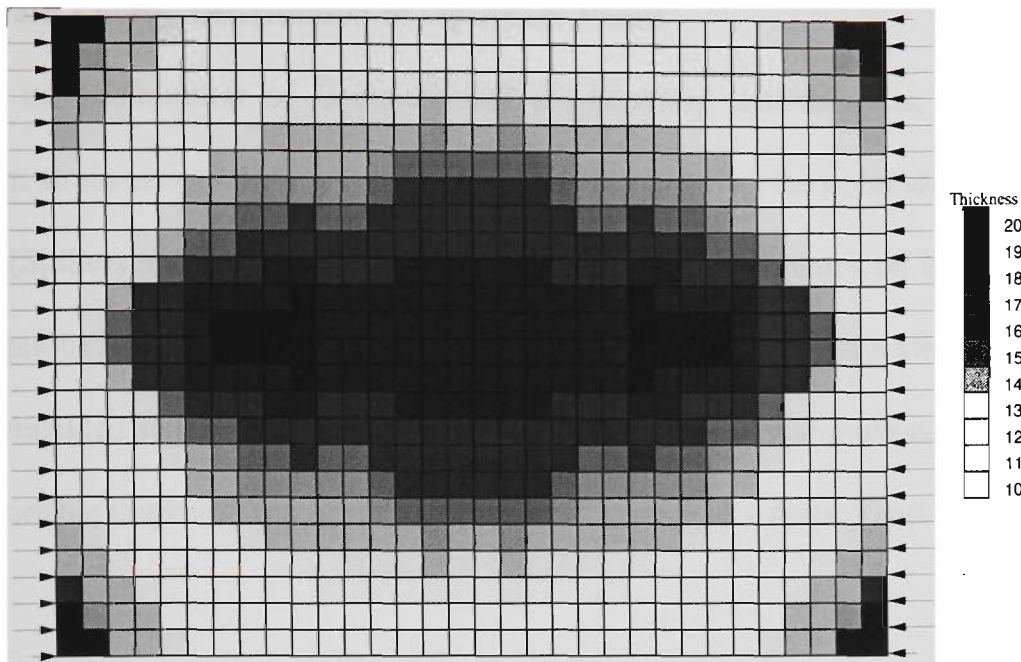


Figure 9.18 - Optimum design of the rectangular plate by ESO method ( $t_u = 14$  mm)

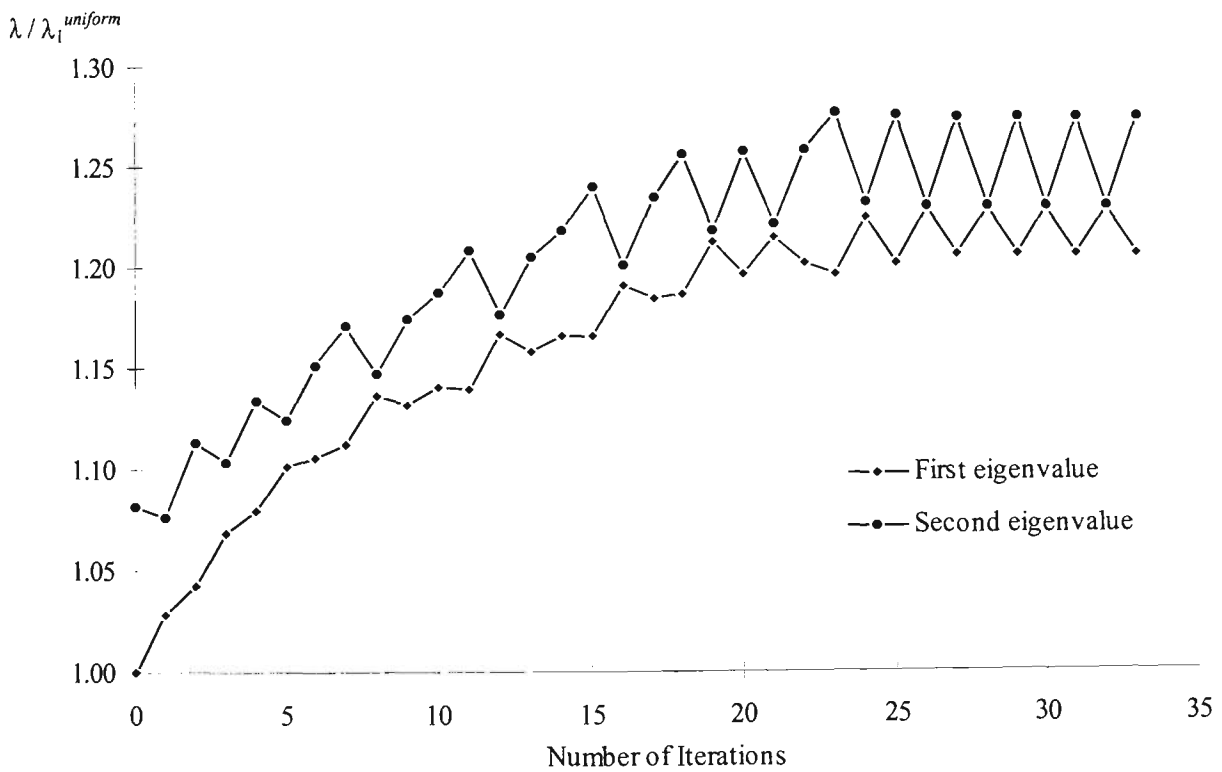
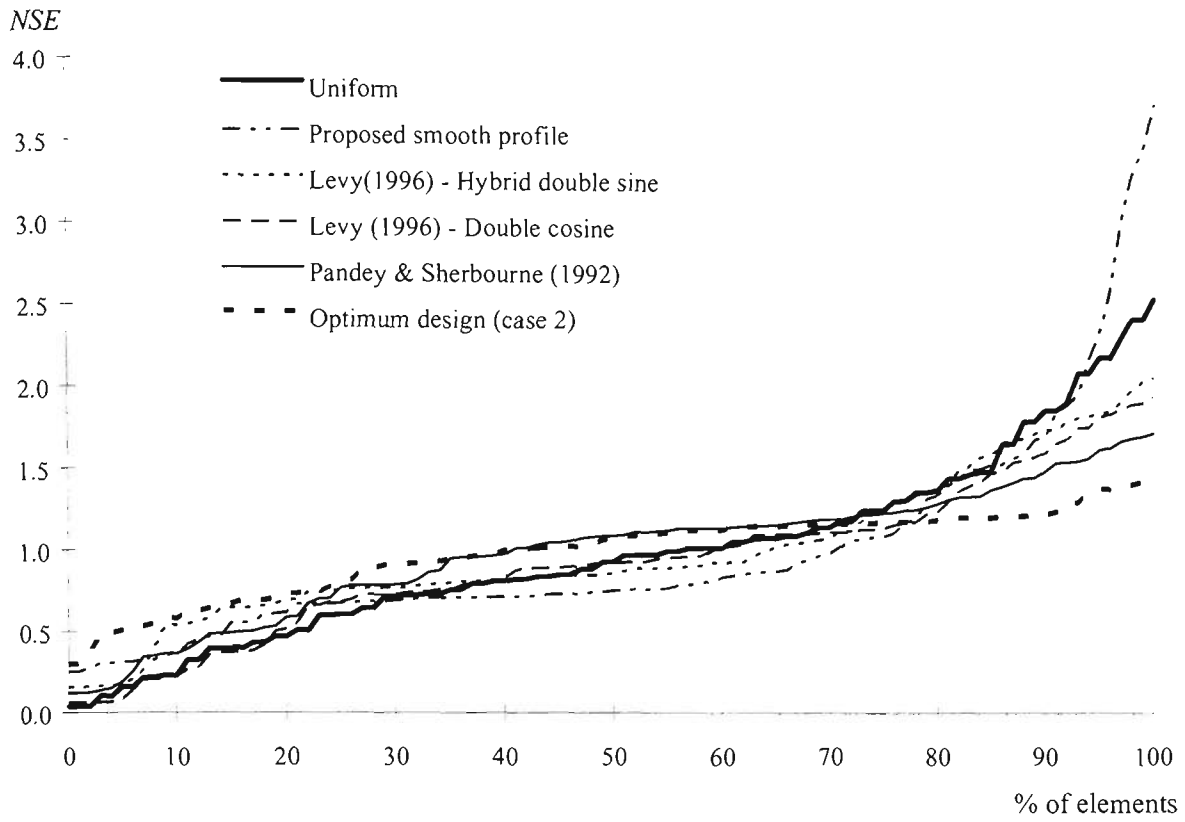


Figure 9.19 - Iteration histories of the rectangular plate by ESO method ( $t_u = 14$  mm)

## 9.5 Strain Energy Distribution of Optimum Plates

Under the assumption of in-extensional pre-buckling deformations, a condition of uniform strain energy density has been established as being the optimality condition for plates (Spillers and Levy (1990)). However, optimisation of plates on the basis of such assumptions have led to unsatisfactory solutions. Since the in-plane stress resultants in the prebuckled state of plates are functions of the thickness distribution, plate structures with variable thickness can never be considered as statically determinate structures.

According to the uniform strain energy density optimality criterion, at optimum design the normalised specific energy of each element  $NSE_i$  (defined in Chapter 5, equation (5.3)) is constant and equals unity. The distributions of normalised specific energy of uniform and optimum shapes of the simply supported square plate are compared in Figure 9.20. The horizontal axis of the Figure 9.20 gives the percentage of elements which have the normalised specific energy below the corresponding  $NSE$  value at the vertical axis. Uniformity of specific energy distribution is not observed in any of these designs. There is no particular difference noticed between the uniform plate and other optimum shapes.



**Figure 9.20** - Comparison of normalised specific energy distribution of the optimum designs of the simply supported square plate

## 9.6 Buckling Solutions of Variable-thickness Plates

Traditionally, special purpose energy-based methods such as the Raleigh-Ritz and the Bubnov-Galerkin methods have been preferred to general purpose finite-element methods because of the excessive cost, storage and data preparation that usually accompany finite-element analysis. However, with the advent of powerful computers and advances in finite-element methods, numerical techniques are becoming more popular for structural analysis, and they can be readily applied to any shapes, boundary and loading conditions. Moreover, the accuracy of results obtained from energy-based methods depends on the number of terms used to describe the displacement function.

Since Rayleigh-Ritz method was used by Pandey and Sherbourne (1992) and Levy (1996) for the buckling analysis of their optimum shapes, it is now important to check the reliability of their results. Buckling solutions of these optimum plates are obtained by using the finite element method. Eight-node isoparametric elements are used to model these variable thickness plates. Buckling loads of SSSS, CCCC and SSCC plates with thickness distribution according to equation (9.3) for various values of  $N_v$  are obtained. Buckling loads of Levy's shapes are obtained for both  $\nu = 0.32$  and  $\nu = 0.3$ . For all the other plates  $\nu = 0.3$  is used. It is found that finite element solutions and the corresponding reported results by Rayleigh-Ritz method are compared in Table 9.3. Finite element solutions of simply supported plates are reasonably close to the reported results (Levy's results differed by 2% and Pandey's results differed by 4-5%).

**Table 9.3** - Comparison of finite-element solutions with Levy and Pandey and Sherbourne results.

Plate type* and reference	Rayleigh-Ritz method		Finite Element Method	
	Parameter	<i>OF</i>	Modelling	<i>OF</i>
SSSS plate Levy (1996)	Sin ( $\nu = 0.32$ )	1.323	80 x 80 8-node isoparametric elements	1.296
	Cosine ( $\nu = 0.32$ )	1.234		1.212
	Sin ( $\nu = 0.30$ )	-		1.286
	Cosine ( $\nu = 0.30$ )	-		1.162
SSSS plate Pandey and Sherbourne (1992)	$N_\nu = 0.5$	0.789	80 x 80 8-node isoparametric elements	0.851
	$N_\nu = 2.0$	1.284		1.238
	$N_\nu = 3.0$	1.278		1.230
	$N_\nu = 4.0$	-		0.858
	$N_\nu = 5.0$	0.700		0.569
CCCC plate Pandey and Sherbourne (1992)	$N_\nu = 0.25$	2.046	40 x 40 8-node isoparametric elements	0.128
	$N_\nu = 0.5$	1.451		0.501
	$N_\nu = 1.5$	-		1.175
	$N_\nu = 2.0$	0.727		1.216
	$N_\nu = 2.5$	-		1.211
	$N_\nu = 3.0$	-		1.190
	$N_\nu = 4.0$	0.600		1.014
SSCC plate Pandey and Sherbourne (1992)	$N_\nu = 0.25$	2.359	40 x 40 8-node isoparametric elements	0.162
	$N_\nu = 0.5$	1.438		0.628
	$N_\nu = 1.5$	-		1.067
	$N_\nu = 2.0$	0.652		1.035
	$N_\nu = 2.5$	-		0.954
	$N_\nu = 3.0$	-		0.852
	$N_\nu = 4.0$	0.448		0.601

\* The first two letters denote the loaded edge support conditions

Buckling loads of uniform thickness plate with clamped edges reported by Pandey and Sherbourne ( $99.43 D_u/b^2$  for CCCC plate and  $75.91 D_u/b^2$  for SSCC plate, where  $D_u = Et_u / (1-\nu^2)$ ) are very close to the finite element solutions ( $99.29 D_u/b^2$  for CCCC plate and  $75.83 D_u/b^2$  for SSCC plate). However, buckling loads of variable thickness plates with clamped edges reported by Pandey and Sherbourne and finite element solutions are totally different. Pandey and Sherbourne's results give higher buckling loads for concave profiles ( $N_v < 1$  as shown in Figure 9.12) whereas FEM gives higher buckling loads for convex profiles ( $N_v > 1$  as shown in Figure 9.11). Finite element solutions reveal that for the concave plate with  $N_v = 0.25$ , local buckling occurs at the middle of the plate for all boundary conditions. Apparently this local buckling has not been captured by Pandey and Sherbourne even with 81 terms displacement function. For the convex plate with  $N_v = 4.0$ , local buckling is found by FEM at corners of the plate. Critical buckling modes of plates for  $N_v = 0.25$  and  $N_v = 4.0$  obtained with FEM for the boundary conditions CCCC and SSCC are shown in Figures 9.21 and 9.22, respectively. Buckling modes of CCCC plates with  $N_v = 0.25$  and  $N_v = 4.0$  reported by Pandey and Sherbourne are given in Figure 9.23. These buckling modes did not show local buckling around the corners or at the centre of the plate.

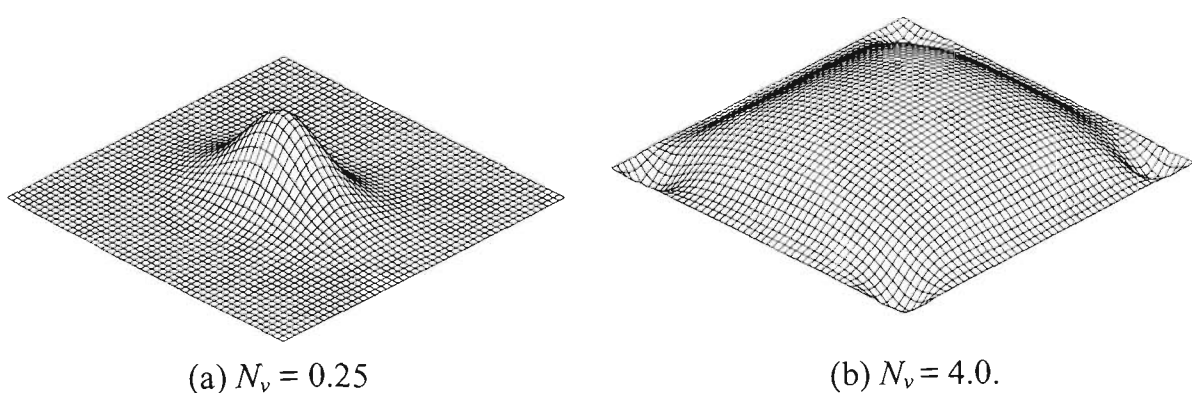


**Figure 9.21** - Fundamental buckling mode of CCCC plates from FEA

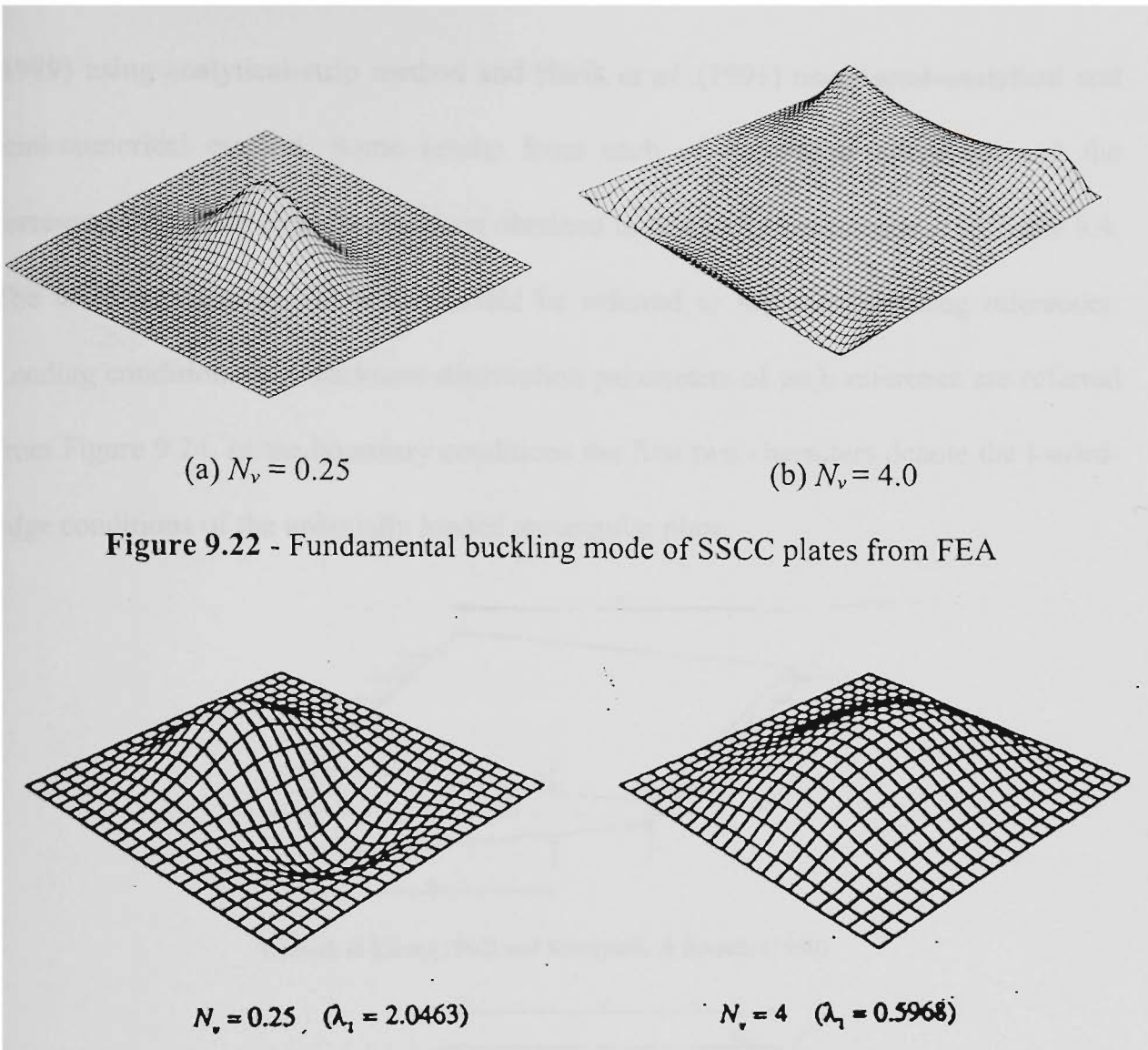
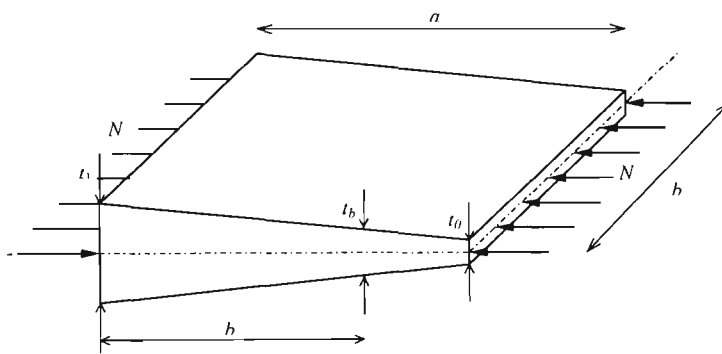


**Figure 9.22** - Fundamental buckling mode of SSCC plates from FEA

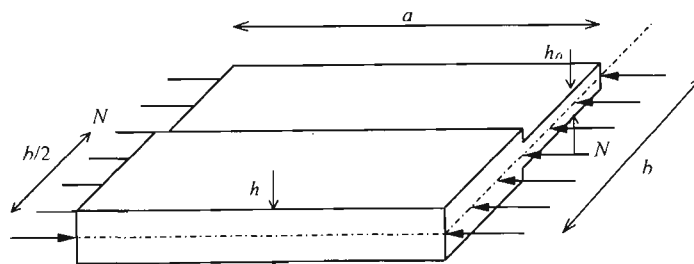
**Figure 9.23** - Fundamental buckling mode of CCCC plates by Pandey and Sherbourne

The contradiction, regarding the buckling solutions of plates with clamped edges by FEA and by Pandey and Sherbourne has motivated the candidate to check the reliability of the finite-element software when applied to the buckling analysis of variable-thickness plates. Considerable amount of research has been carried out on the buckling analysis of variable thickness plates (such as exponential, linear tapered, sinusoidal, step variation etc.) with different boundary conditions, aspect ratios and various loading conditions using energy methods and numerical methods. Some of the noted studies are by Wittrick and Ellen (1962) and Ng and Araar (1989) using Galerkin method; Kobayashi and Sonoda (1990) using exact power series method; Harik and Andrade

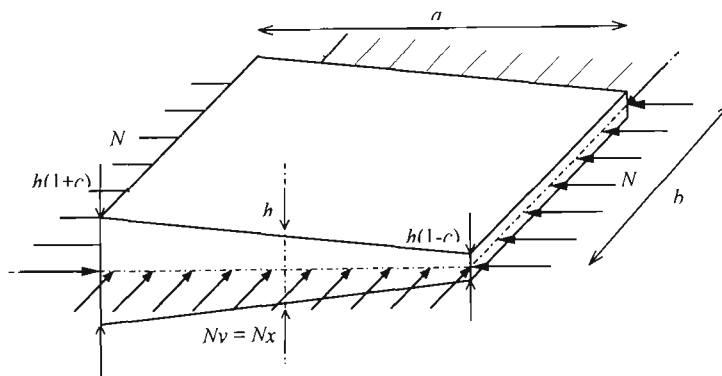
(1989) using analytical strip method and Harik *et al.* (1991) using semi-analytical and semi-numerical method. Some results from each of the above references and the corresponding finite element solutions obtained in this study are compared in Table 9.4. The table numbers in Table 9.4 should be referred to the corresponding references. Loading conditions and thickness distribution parameters of each reference are referred from Figure 9.24. In the boundary conditions the first two characters denote the loaded-edge conditions of the uniaxially loaded rectangular plate.



Wittrick & Ellen (1962) and Kobayashi & Sonada (1990)



Harik & Andrade (1989)



Ng & Araar (1989)

**Figure 9.24** - Thickness distribution parameters of the variable-thickness plates

**Table 9.4** - Comparison of finite-element buckling solutions with reported results for variable-thickness plates.

Boundary conditions *	Reference	Aspect ratio	Thickness variation and parameter	Reported results	FEM mesh **	FEM results
SSSS	Wittrick	0.5	Exponential - $t_1/t_0 = 1.5$	6.049	10 x 20	6.039
	Tables II & III	2.0	Linear taper - $t_1/t_0 = 2.0$	2.236	20 x 10	2.242
SSCC	Wittrick	1.0	Exponential - $t_b/t_0 = 2.0$	16.58	20 x 20	16.61
	Tables IV & V	1.5	Exponential - $t_b/t_0 = 1.5$	10.90	30 x 20	10.93
		0.5	Linear taper - $t_b/t_0 = 2.0$	33.64	40x 20	33.68
		3.0	Linear taper - $t_b/t_0 = 1.5$	11.24	30 x 10	11.29
SSSS	Kobayashi	3.0	Linear taper - $t_1/t_0 = 2.0$	1.922	20 x 20	1.920
	Table 1	1.5	Linear taper - $t_1/t_0 = 1.5$	3.339	30 x 20	3.341
SSCS	Harik	1.8	Step variation - $h/h_0=1.5$	8.295	18 x 10	8.304
SSCS	Table 1 & 2	2.0	Step variation - $h/h_0=1.5$	8.762	20 x 10	8.547
SSCF		2.0	Step variation - $h/h_0=1.5$	2.348	20 x 10	2.343
SSCF		2.0	Step variation - $h/h_0=1.5$	2.348	20 x 10	2.357
SSCC		1.2	Step variation - $h/h_0=1.5$	10.705	12 x 10	10.916
SSCC		1.8	Step variation - $h/h_0=1.5$	11.665	18 x 10	11.844
SSCC		2.0	Step variation - $h/h_0=1.5$	10.542	20 x 10	10.616
CCCC		Ng & Araar	2.0	Linear taper - $c = 0.0$	15.696	40 x 20
CCCC	Table 1	2.0	Linear taper - $c = 0.2$	15.891	40 x 20	13.330
CCCC		2.0	Linear taper - $c = 0.4$	16.429	40 x 20	9.325
CCCC		2.0	Linear taper - $c = 0.6$	17.238	40 x 20	5.333
CCCC		2.0	Linear taper - $c = 0.8$	18.285	40 x 20	1.069

\* The first two letters denote the loaded edge support conditions.

\*\* 8-node isoparametric elements are used.

Comparison of the results indicates that the finite element solutions are in excellent agreement with the results reported by Wittrick and Ellen (1962), Kobayashi and Sonoda (1990) and Harik and Andrade (1989) and differ by only 0.3% maximum. Again the buckling solutions obtained by and Ng and Araar (1989) for the bi-axially loaded all edges clamped plates using Galerkin method with six term displacement function considerably differ from the finite element solutions.

## **9.7 Elimination of Checkerboard Patterns from 4-node Element Optimum**

### **Solutions**

Numerical instability problems are often encountered in finite element solutions to distributed-parameter and variable-topology shape design problems. Although the physics of a given problem might imply a regular solution, optimisation procedures that are based on discrete models often generate irregularities in the design field at the length scale of the numerical grid. These anomalies can take the form of checkerboard patterns and rib like formations in the design of solid plates, internal boundaries in shape optimisation of continua and corrugations in thin shells of constant thickness, wherein the finite element solution for the design field alternately overestimates and underestimates the expected continuum solution in adjacent elements. These instabilities are strictly a numerical artifact and do not have any physical significance. The origin of checkerboard patterns and other irregularities are related to features of the finite element approximations. When 4-node linear elements are used in ESO for plate buckling, checkerboard like patterns are often observed in the optimum designs. It is illustrated with the following examples.

### 9.7.1 Optimum designs of plates with 4-node elements

The optimum designs of the simply supported square plate for the two cases ( Example 9.3.1) that are obtained with the 4-node isoparametric elements are shown in Figure 9.25. Values of  $Nx_{cr}$  for the final designs for Cases 1 and 2 are 872.9 kN/m and 1257.8 kN/m, respectively. Checkerboard-like patterns are observed in these final designs and most of the elements reach extreme thickness, either  $t_{max}$  or  $t_{min}$  in the final designs. Numerically the designs with checkerboard-like patterns represent stiffer structure. These final designs are re-analysed with 8-node isoparametric elements and the values of  $Nx_{cr}$  obtained are only 790.0 kN/m for Case 1 design and 672.0 kN/m for Case 2 design. Simply supported rectangular plate (Example 9.3.3) is re-analysed with the 4-node isoparametric elements and the final design obtained is shown in Figure 9.26. Again checkerboard-like patterns exist in the final design and most of the elements reach extreme thicknesses.

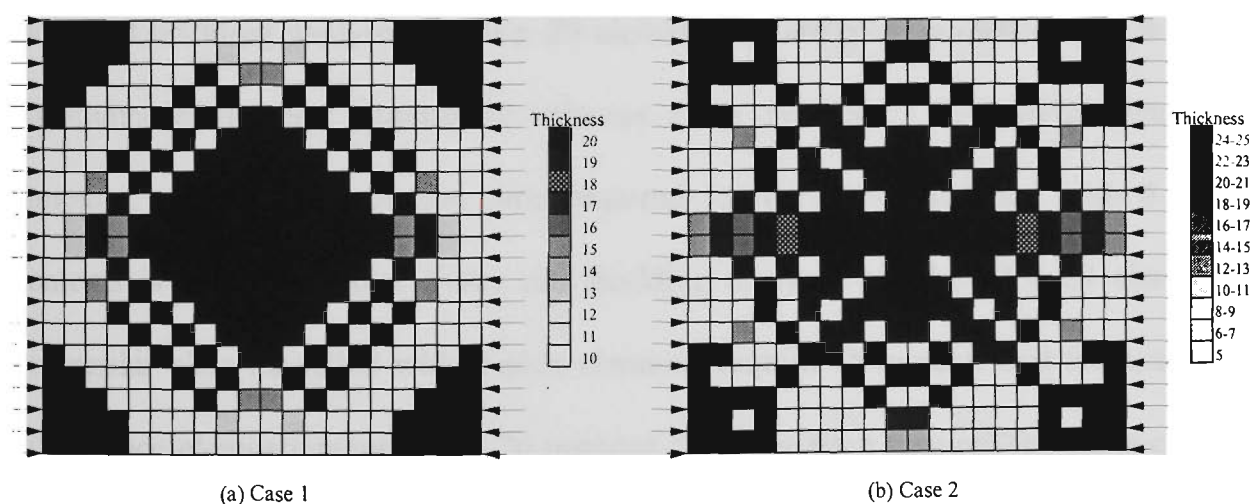


**Figure 9.25** - Final designs of SSSS square plate obtained with 4-node elements

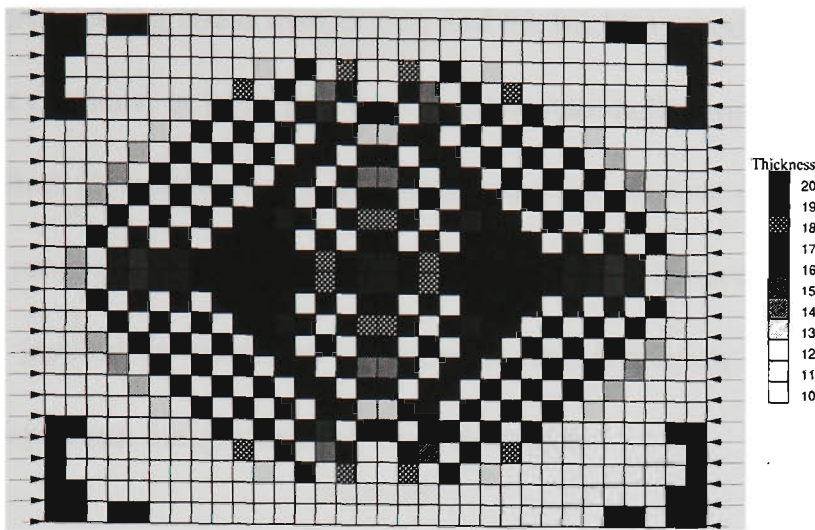


**Figure 9.26** - Final design of SSSS rectangular plate obtained with 4-node elements

Usually, the higher the order of the displacement element, the greater the numerical stability. Thus in general 8-node elements are used for plate optimisation problems. Both the ESO method and the Folgado's method use 8-node isoparametric elements to model the plate structures. However the size of the finite element model and the computational time are significantly increased with higher order elements. For example, static and buckling analyses of 20 x 20 elements square plate modelled with 8-node isoparametric elements require 30 minutes on a Pentium / 120 MHz personnel computer, whereas the solution time required for the plate modelled with 4-node elements is only 6 minutes. Static and buckling analyses of the 32 x 24 elements rectangular plate modelled with 8-node elements require 75 minutes and the analyses with 4-node elements require only 20 minutes. Thus the time required for the buckling solution of a structure modelled with 8-node elements is four to five times higher than the time required by the same structure modelled with 4-node elements. The number of elements used in the above examples is small since the critical buckling mode of these plates are not complicated. In real problems, a fine mesh of elements is needed to

represent the prebuckling stress distribution and the buckling mode adequately. The use of higher order elements in large problems is computationally expensive. Therefore it is important to find alternative ways to improve the use of low order elements in the optimisation process. In the following section, an element sensitivity number redistribution method is proposed to suppress the formation of checkerboard-like patterns from optimum designs using 4-node elements.

### 9.7.2 Element sensitivity number re-distribution method

In this method element sensitivity numbers are re-calculated by considering the influence of elements in the neighbourhood. The *modified sensitivity numbers* are calculated for each element as follows:

- Calculate the initial sensitivity numbers for each element as defined by the equations (4.15) or (5.2).
- Compute the nodal sensitivity numbers,  $\alpha_{Ni}$  at each node by taking the average of the sensitivity number of elements connected to that particular node. For example, nodal sensitivity numbers of nodes 1, 2, 3, 5 and 6 in the Figure 9.27 given below are calculated as follows:

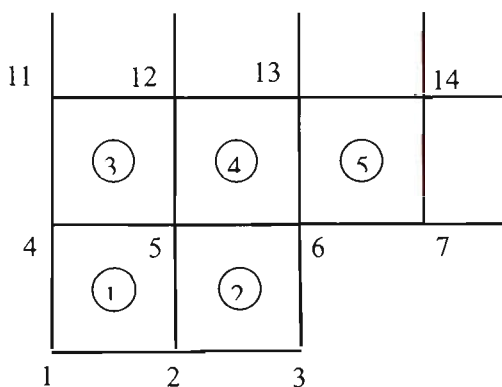


Figure 9.27

$$\alpha_{N1} = \alpha_1$$

$$\alpha_{N2} = (\alpha_1 + \alpha_2) / 2$$

$$\alpha_{N3} = \alpha_2$$

$$\alpha_{N5} = (\alpha_1 + \alpha_2 + \alpha_3 + \alpha_4) / 4$$

$$\alpha_{N6} = (\alpha_2 + \alpha_4 + \alpha_5) / 3$$

- Re-calculate the *modified sensitivity numbers*,  $\alpha'_i$  for each element by taking the average of the nodal sensitivity numbers of that particular element. For example the *modified sensitivity numbers* of elements 1 and 5 in the above figure are

$$\alpha'_1 = (\alpha_{N1} + \alpha_{N2} + \alpha_{N4} + \alpha_{N5}) / 4 \quad \text{and}$$

$$\alpha'_5 = (\alpha_{N6} + \alpha_{N7} + \alpha_{N13} + \alpha_{N14}) / 4.$$

The above two examples are re-analysed with the 4-node linear elements using the *modified sensitivity numbers*. Final designs obtained are shown in Figures 9.28 and 9.29 for the square plate and the rectangular plate, respectively. Patches of checkerboards are eliminated from these designs to a large extent. This method works well when the ratio between the maximum and minimum allowable thicknesses is small.

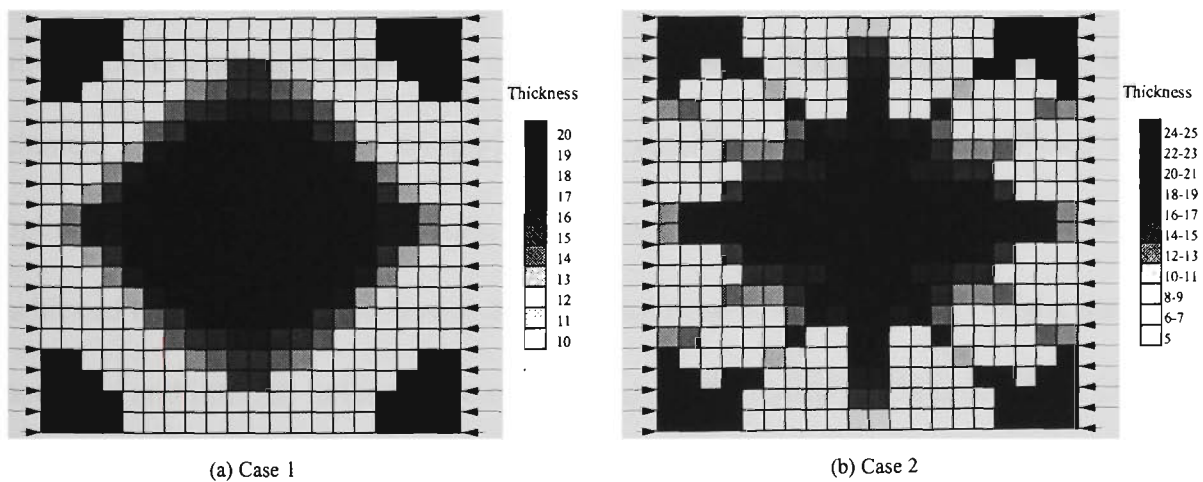


**Figure 9.28** - Optimum designs of the square plate obtained with the re-distributed sensitivity numbers for 4-node elements

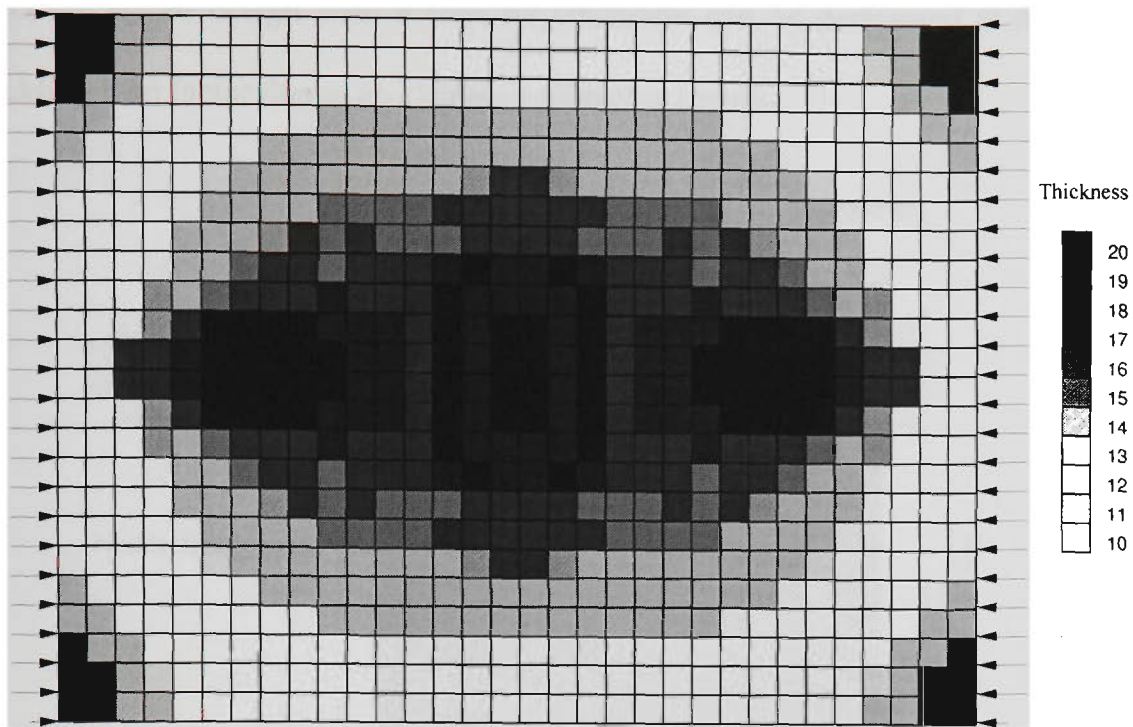


**Figure 9.29** - Optimum design of the rectangular plate obtained with the re-distributed sensitivity numbers for 4-node elements

### 9.8 Layout Optimisation

Buckling optimisation sensitivity numbers are calculated by ignoring the change in stress matrix and these sensitivity numbers are not applicable to optimisation involving element removal. For this reason ESO for stability constraints is restricted to sizing optimisation with fixed topology. However, a significant weight reduction can be achieved by optimising the layout of the structure where the topology of the structure is not fixed and internal holes can be created during the optimisation process. In Chapter 3, ESO for shape and layout optimisation of structures with stiffness, displacement, stress and frequency constraints have been briefly described. ESO for layout designs with stability constraints can be achieved by gradually removing the inefficient elements from the design domain so that the decrease in critical buckling load factor is kept as small as possible. In the following section an example is presented to illustrate how the

ESO for layout design with a stability constraint can be performed if the change in buckling load factor due to an element removal is known.

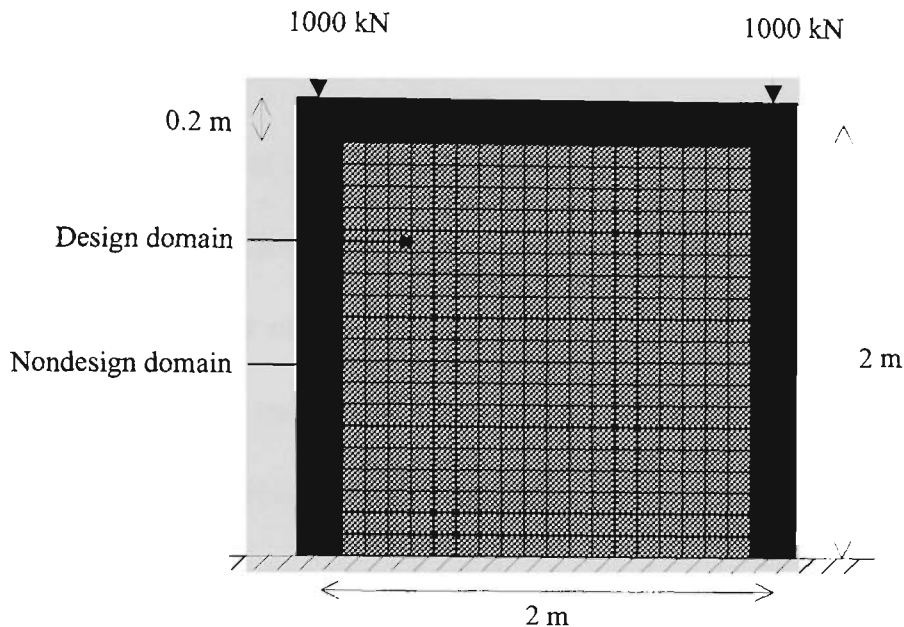
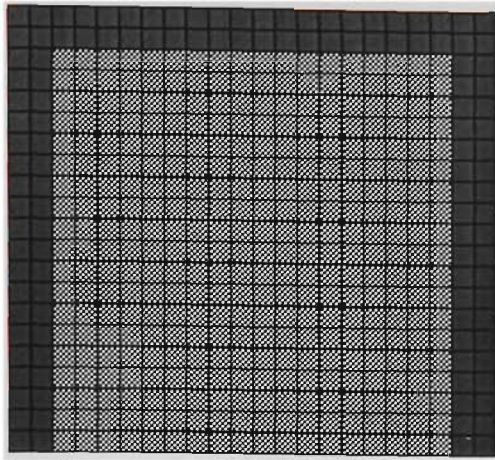


**Figure 9.30** - Initial structure of the 2-dimensional portal frame for layout optimisation

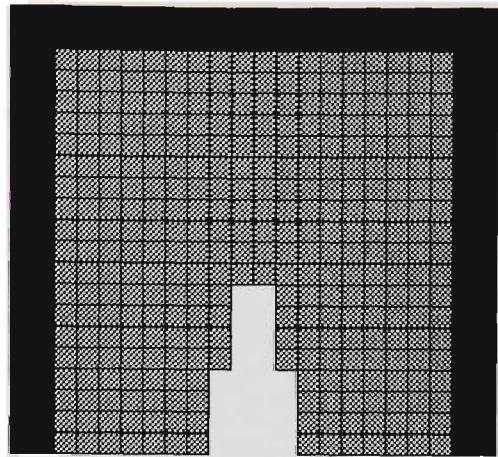
Consider a portal frame, clamped at base as shown in Figure 9.30. It is required to find the optimum topology of material within the design domain. External columns and beam which are represented by nondesign domain are fixed. This is a two dimensional problem and the structure is modelled with  $22 \times 21$  square 8-node isoparametric elements. The material is isotropic with Young's modulus  $E = 200$  GPa and Poisson's ratio  $\nu = 0.3$ . Both the design and nondesign domain plate thickness is equal to 10 mm and it is kept constant. Since the change in buckling load factor due to the removal of an element cannot be obtained from the results of finite element analysis of the previous structure, a buckling analysis with the removal of the element has to be carried out to obtain the change in buckling load factor. This analysis is repeated for each and every element in the design domain to assess the influence of the removal of each element to the critical buckling load. This is done by assigning the plate property number zero to

the removed element. Once the buckling analysis is performed that particular element is re-assigned with the correct plate property number and the plate property number of the next element to be removed is assigned to zero and so on.

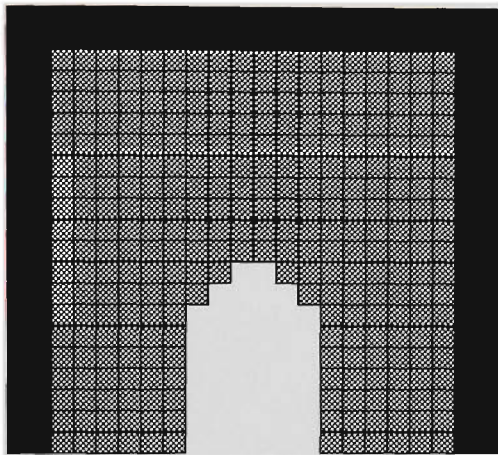
When removing the elements, symmetry of the structure should be preserved. Therefore at each analysis 1 x 2 (since there is one symmetric axis) elements are removed. Once the buckling load factors of the structure with the removal of each set of symmetric elements are found, the most inefficient set of symmetric elements is removed. By repeating this whole procedure the inefficient elements are gradually removed (one symmetric set of elements at a time) from the design domain. The evolving shapes (after removing every 12 x 2 elements) are given in Figure 9.31. Buckling load factors of the original structure (with and without the design domain) and the evolving shapes are also given in Figure 9.31. Figure 9.32 shows the evolutionary history of the critical load factor after each set of symmetric elements is removed. Initially  $\lambda_{cr}$  is almost unchanged with the removal of elements.  $\lambda_{cr}$  is reduced by only 1.26% after 92 x 2 elements are removed, i.e, the design domain weight is reduced to 46.2%. Then  $\lambda_{cr}$  is decreased gradually with the removal of elements. At intermediate stages, some irregular designs such as with checkerboard like patterns are observed. This may be due to the reason that the finite element mesh used in this problem is very coarse. Final designs show the potential locations of diagonal members for the portal frame. Layout optimisation of this structure is also obtained with 4-node linear elements and the evolving shapes are shown in Figure 9.33. Very irregular checkerboard like patterns are observed even at early stages of the designs.



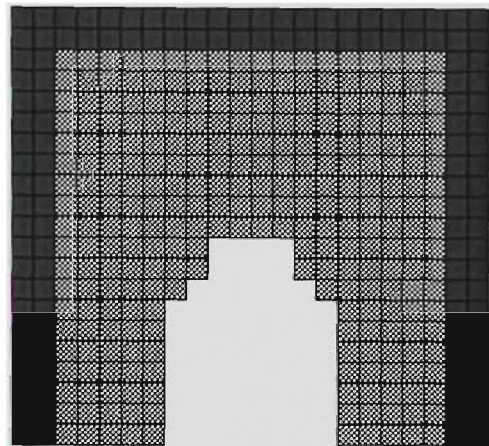
$\lambda_1 = 5769.99$   
Initial design



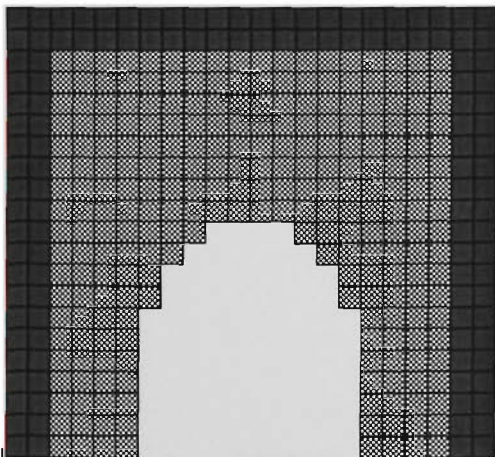
$\lambda_1 = 5769.59$   
12 x 2 elements removed



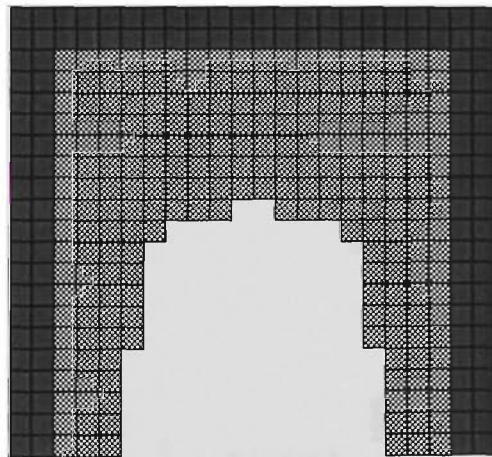
$\lambda_1 = 5768.65$   
24 x 2 elements removed



$\lambda_1 = 5767.07$   
36 x 2 elements removed

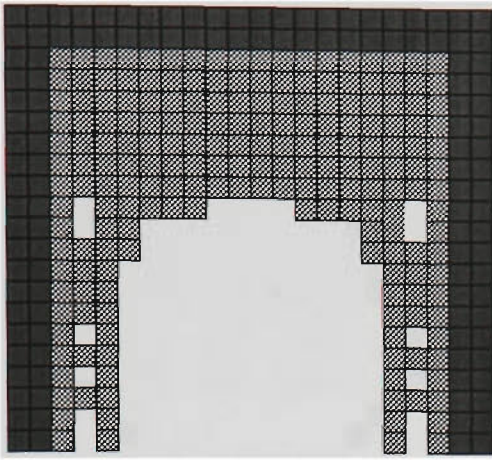


$\lambda_1 = 5764.48$   
48 x 2 elements removed

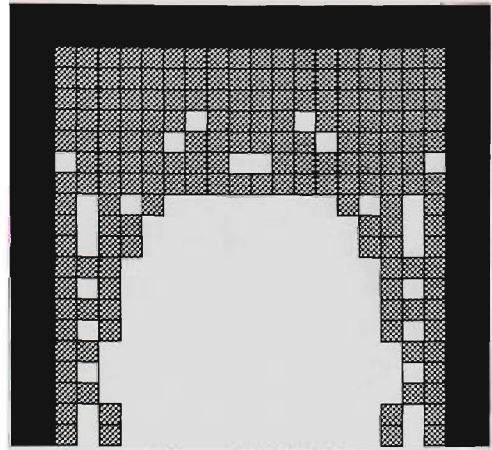


$\lambda_1 = 5760.57$   
60 x 2 elements removed

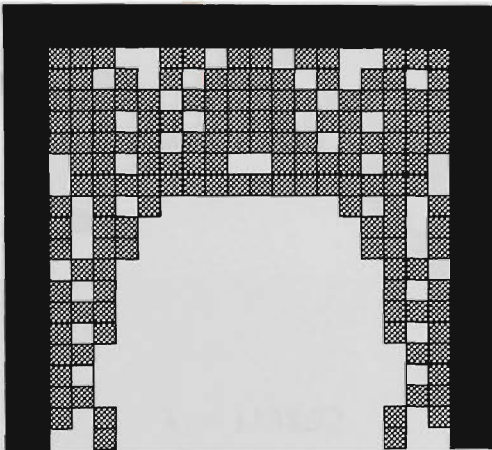
Figure 9.31 - Evolving layouts and corresponding buckling load factors of the portal frame (continued)



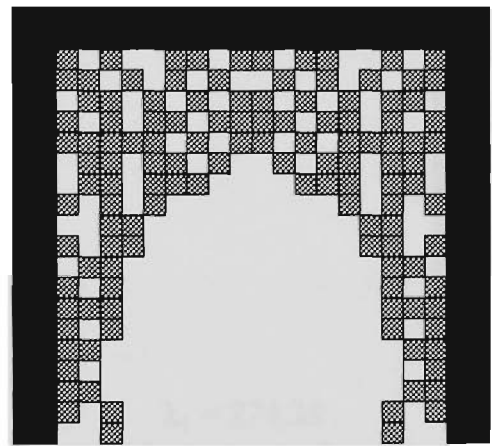
$\lambda_1 = 5750.17$   
72 x 2 elements removed



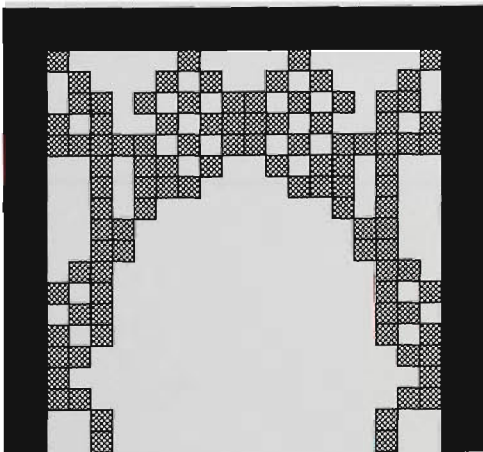
$\lambda_1 = 5727.45$   
84 x 2 elements removed



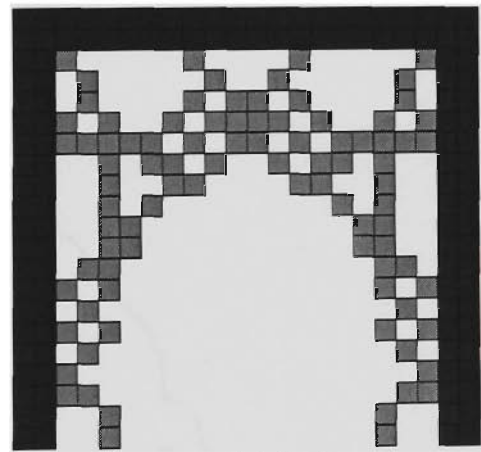
$\lambda_1 = 5628.13$   
96 x 2 elements removed



$\lambda_1 = 5337.41$   
108 x 2 elements removed



$\lambda_1 = 4329.04$   
120 x 2 elements removed



$\lambda_1 = 3640.02$   
126 x 2 elements removed

**Figure 9.31** - Evolving layouts and corresponding buckling load factors of the portal frame (continued)

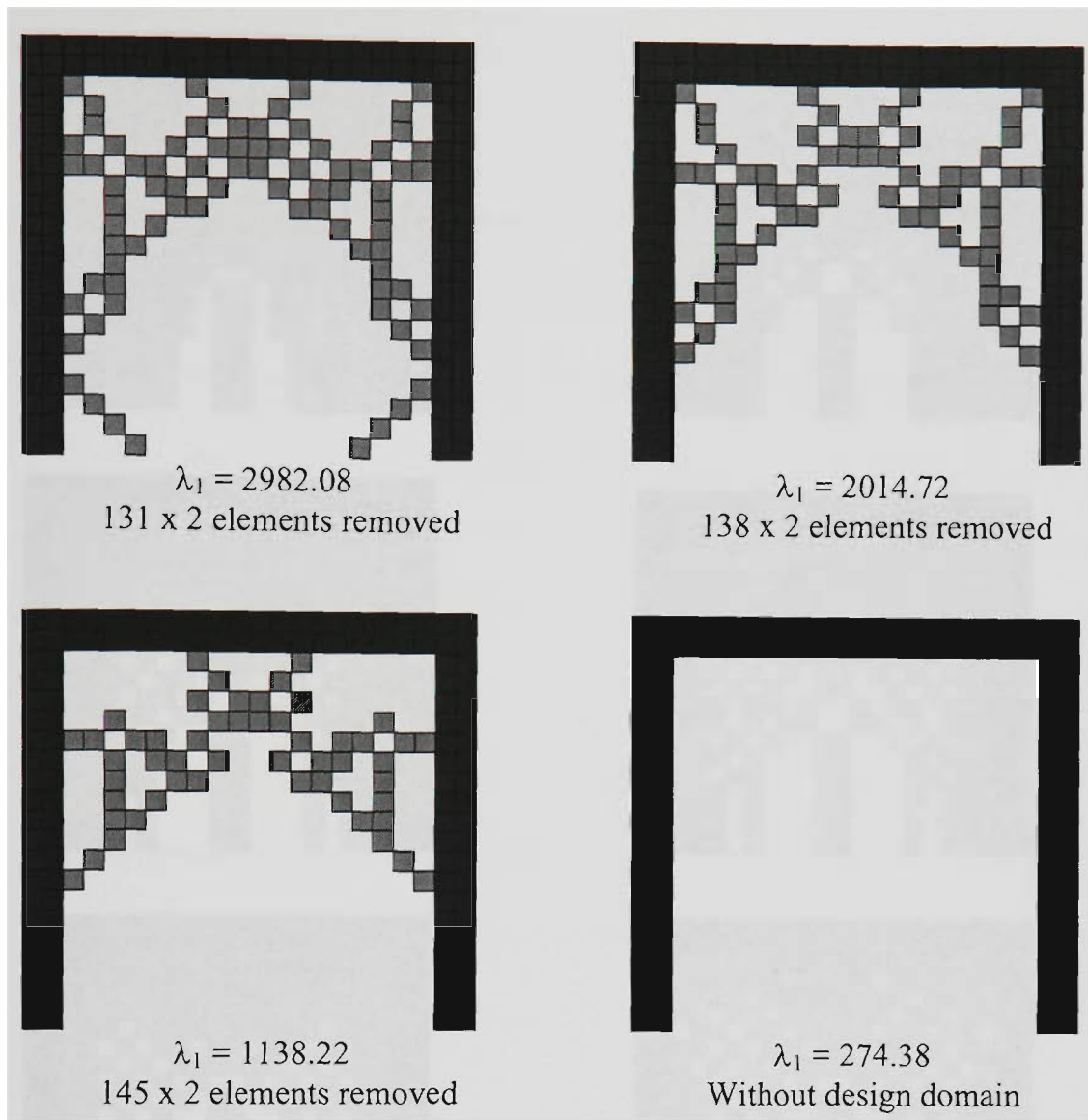


**Figure 9.31** - Evolving layouts and corresponding buckling load factors of the portal frame

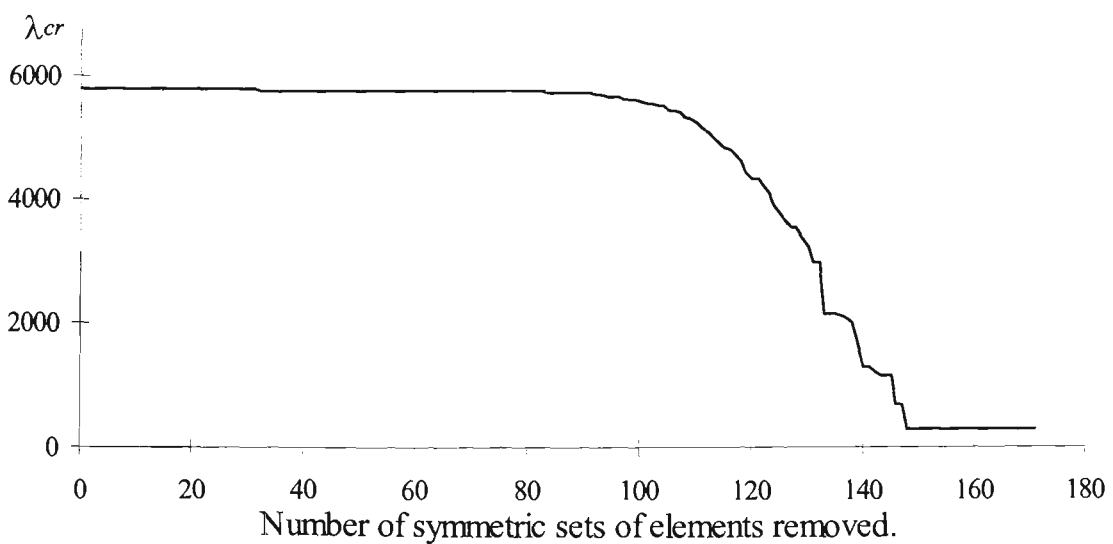


**Figure 9.32** - Evolutionary history of the layout optimisation of the portal frame

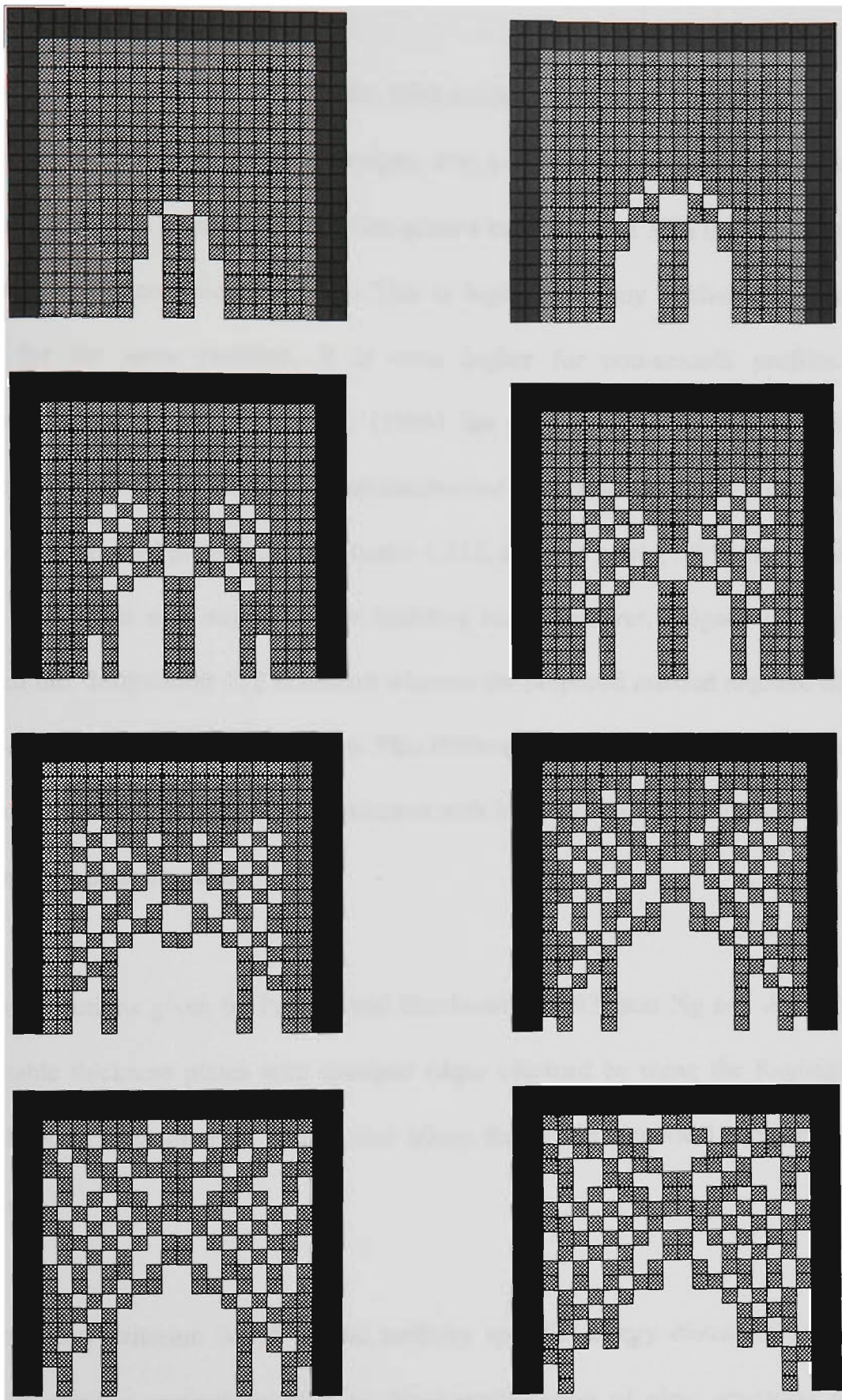


Figure 9.33 - Evolving shapes of the portal frame obtained with 4 node elements

## 9.9 Conclusions

The optimum designs obtained with the ESO method yield higher buckling loads than corresponding previously reported designs. For a simply supported square plate, an optimum design has been proposed which gives a buckling load 37% higher than that of a uniform equivalent thickness plate. This is higher than any published and correct results for the same problem. It is even higher for non-smooth profiles. The corresponding shape given by Levy (1996) has only a 29% increase in buckling resistance and that given by Pandey and Sherbourne (1992) has only a 24% increase. For the simply supported plate with aspect ratio 1.333, Folgado *et al.* (1995) also obtained a similar design but with slightly lower buckling load. However, Folgado *et al.* (1995) achieved this design after 112 iterations whereas the proposed method required only 30 iterations to attain the optimum design. This difference is important because the number of iterations is crucial in analysing structures with higher order elements such as 8-node isoparametric plate elements.

Buckling solutions given by Pandey and Sherbourne (1992) and Ng and Araar (1989) for variable thickness plates with clamped edges obtained by using the Rayleigh-Ritz method appear to be in error. It is unclear where they made numerical mistakes in their analysis.

The optimality criterion based on the uniform specific energy distribution does not appear to admit a general solution to shape optimisation of plate structures against buckling. The uniform strain energy concept may hold true for statically determinate structures, but not for variable-thickness plate structures.

Plate buckling optimum designs have been obtained with 8-node isoparametric elements. When 4-node linear elements are used, checkerboard-like patterns are observed in the optimum designs. The cause for this problem is numerical instability. A simple approach, element sensitivity number redistribution method, has been proposed to improve the use of 4-node elements in the plate optimisation process. This method works well for the problems with a small ratio between the maximum and minimum allowable thicknesses.

This chapter has also tried to address the layout optimisation of structures against buckling. It has been shown with a two-dimensional example that a significant weight reduction can be achieved by optimising the layout of the structure. However the approach used for the layout optimisation is not computationally efficient and further research needs to be done to find an efficient way to calculate the sensitivity numbers when an element is removed.

## CHAPTER 10 - CONCLUSIONS AND FUTURE RESEARCH

*"It is good to have an end journey towards,  
but it is the journey that matters, in the end."*

*- Ursula Le Guin*

### 10.1 Conclusions

The objective of the research presented in this thesis was to investigate and develop simple, mathematically less complex and computationally efficient optimisation methods based on Evolutionary Structural Optimisation (ESO) concept to enhance the buckling resistance of structures. This chapter summarises what have been achieved in this study and discusses the further developments required in these and related areas.

The capability of the ESO method for buckling optimisation was illustrated with various examples of single modal, multimodal, multiple load case and multiple constraint frame structures and plate structures. Critical buckling load factors were substantially increased and significant weight reductions were observed in these optimum designs. The results were compared with the exact solutions and with other published solutions. The optimum designs obtained with ESO methods for plate structures and for most frame structures yield higher, if not equal, buckling loads than corresponding previously reported results.

The change in critical buckling load factor due to structural modifications was derived from the discrete form of eigenvalue problem  $([K] + \lambda_j[K_g])\{u_j\} = 0$ . Sensitivity numbers for element resizing were obtained by ignoring the change in stress stiffness matrix due to element cross-sectional modifications. Since the change in stress matrix due to element removal cannot be ignored because of the significant changes in the membrane or axial stress resultants in its surrounding elements, buckling optimisation in this study has been restricted only to sizing optimisation. For repeated eigenvalue problems or multimodal structures, the effect of modal interaction associated with repeated eigenvalues was taken into account in a simple but very effective way by taking the average values of the individual sensitivity numbers of all participating buckling modes.

The resizing procedure used in the proposed method is much simpler than other resizing algorithms or the recurrence relations commonly used in optimality criteria methods. This resizing procedure does not require any arbitrary constants to control the convergence of the optimisation process as in other optimality criteria methods. Furthermore, in ESO method the elements are resized gradually by a small cross-sectional modification at each iteration. This gradual evolution treats the statically indeterminate structures more effectively than other optimality criteria methods. In addition, the sizing constraints can be easily included in the optimisation process and the non-design domain can also be specified. The influence of ESO parameters, the resizing ratio and the step size, was studied with several examples. In general the accuracy of the solution improves with a smaller resizing ratio and a smaller step size but at the expense of higher computational cost. These parameters need to be kept small for highly

statically indeterminate structures, for structures with complex buckling modes and for multimodal structures.

Initially the ESO method for buckling optimisation was formulated to maximise the critical buckling load of the structure while keeping its weight constant. Later this method was extended to the minimum weight design of frame structures with prescribed buckling load constraints. This was achieved with the introduction of uniform scaling which brings the critical buckling load factor equal to the factor of safety against buckling of the structure after each iteration. An empirical rule was proposed for the uniform scaling of nonlinear size-stiffness structures and space structures. This empirical rule greatly reduces the number of iterations required for uniform scaling and ensures convergence.

For multiple load case structures, element sensitivity numbers were calculated by considering the influence of all the load cases. The uniform scaling factor of each load case served as weighting parameter (which played a similar role as the Lagrangian multipliers in optimality criteria methods) when defining the sensitivity numbers and it was also used to identify the most critical load case. It was shown with the examples that optimising a structure under a single loading condition would violate the buckling constraints of the other load cases.

The ESO method for multiple constraints problem (including stress, stiffness and displacement constraints in addition to the stability constraint) systematically reduces the weight by uniform scaling and shifting the material from the strongest part to the

weakest part through the use of sensitivity numbers. Here again the uniform scaling factor of each constraint was used as weighting parameter when defining the element sensitivity numbers. Furthermore, the most active constraint was determined from the maximum of uniform scaling factors of all constraints and it was used to scale the design uniformly after each iteration. It was also shown with the examples that optimising a structure with a single constraint alone would significantly violate the other constraints.

Plate buckling optimum designs were obtained for uniaxial-compression-loaded rectangular plates with the use of 8-node isoparametric elements. The poor performance of low order finite elements such as 4-node linear elements in the optimisation process was clearly illustrated with examples. Since the computational time and the disk storage requirements were drastically increased with the use of higher order elements, a simple approach, element sensitivity number re-distribution method with 4-node elements was proposed.

It was also shown with an example that a significant weight reduction could be achieved by optimising the layout of the plate structure.

This section concludes emphasising the following positive points of ESO method for buckling optimisation.

- The concept of this method is easy to understand by practising engineers and scientists and it does not involve any complex mathematics.

- This method is suitable for designing practical structures with a large number of design variables.
- This method can be easily implemented with any of the commercially available finite element analysis software.
- This method allows the designer to know every stage of the optimisation process and lets him to consider intermediate designs as well.

## **10.2 Further Recommendations**

In addition to the work carried out in this study, recommendations for further research closely related to the buckling optimisation include the following:

- 1) Since a significant weight reduction can be achieved by optimising the layout of the structure by removing the inefficient elements from the design domain, it is important to find an efficient way to calculate the change in buckling load factor when an element is removed. Substructuring or any other approximate methods need to be investigated to obtain the approximate change in stress stiffness matrix due to the element removal.
- 2) The use of higher order elements in plate buckling optimisation process is very computationally expensive. Although the element sensitivity number re-distribution method with 4-node elements works well for the problems with a small ratio of maximum to minimum allowable thicknesses, it does not appear to work as well for problems with high thickness ratios. Furthermore, the plate problems often exhibit multimodal situations which require the solution of several buckling modes. For

example, uniaxially loaded CCCC square plate exhibits bimodality and the first three eigenvalues coincide for uniaxially loaded CCSS square plate and for biaxially loaded SSSS square plate. In a buckling analysis, the computational time increases exponentially with the number of eigenvalues requested. And also the buckling solution of multimodal problems may require very high accuracy (the tolerance of the eigenvalues need to be kept very small) in the calculation of eigenmodes to accurately take account of the modal interaction. All these factors make the buckling optimisation of plate structures very complicated. Therefore it is important to investigate and formulate numerically stable and computationally efficient finite element methods to be used in the plate buckling optimisation problems.

- 3) For plate structures, other constraints such as stress, stiffness and displacement constraints also need to be included in the optimisation problems.
  
- 4) Material and geometric nonlinearity may also need to be studied in the optimisation problems. The hypotheses behind the linearised buckling model limits its range of applicability. However, in spite of its limitations it should be noted that the results obtained with the linearised model give important information for optimisation purposes as an upper bound of the load capacity of the structure. Also if the nonlinear analysis model is solved iteratively by a set of linearised subproblems, the respective nonlinear model can be based on the developments presented for linear model. Optimisation with orthotropic and anisotropic material should also be investigated especially with plate problems.

## **PUBLICATIONS DURING THIS CANDIDATURE**

- 1) Manickarajah, D., Xie, Y.M. and Steven, G.P. 1995. A simple method for the optimisation of columns, frames, and plates against buckling. In: S. Kitipornchai, G.J. Hancock, and M.A. Bradford (eds.), *Structural Stability and Design*, ICSSD, (*Proceedings of the International Conference on Structural Stability and Design*, Sydney, Australia), Balkema, Rotterdam, pp. 175-180.
- 2) Manickarajah, D., Xie, Y.M. and Steven, G.P. 1997. Optimum design of discrete structures with stress, stiffness and stability constraints. In: R.H. Grzebieta, R. Al-Mahaidi and J.L. Wilson (eds.), *Mechanics of Structures and Materials*, 15ACMSM, (*Proceedings of the 15th Australasian Conference on The Mechanics of Structures and Materials*, Melbourne, Australia), Balkema, Rotterdam, pp. 411-417.
- 3) Manickarajah, D., Xie, Y.M. and Steven, G.P. 1998. Elimination of checkerboard patterns from plate buckling optimum designs. In: G.P. Steven, O.M. Querin, H. Guan and Y.M. Xie (eds.), *Structural Optimisation*, (*Proceedings of the Australasian Conference on Structural Optimisation*, Sydney, Australia), Oxbridge press, Victoria, Australia, pp. 525-532.
- 4) Xie, Y.M., Steven, G.P., Querin, O.M. and Manickarajah, D. 1998. Evolutionary structural optimisation: status and promise. In: Y.B. Yang and L.J. Leu (eds.), *Structural Engineering & Construction: Tradition, Present and Future*, (*Proceedings of the sixth east Asia-pacific conference on structural engineering & construction*, Taipei, Taiwan), Vol. 1, pp. 289-294.

- 5) Manickarajah, D., Xie, Y.M. and Steven, G.P. 1998, Evolutionary method for optimisation of plate buckling resistance. *Finite Element in Analysis and Design*, (accepted for publication).
- 6) Manickarajah, D., Xie, Y.M. and Steven, G.P. 1997. A simple method for the optimisation of columns and frames with stability constraints. *Computers and Structures*, (submitted).
- 7) Manickarajah, D., Xie, Y.M. and Steven, G.P. 1997. Optimum design of frames with multiple constraints using an evolutionary optimisation method. *Computers and Structures*, (submitted).

## REFERENCES

- 1) Barson, G.M. (1994), Optimal design of planar frames based on structural performance criteria. *Computers & Structures*, Vol. 53, No. 6, pp. 1395-1400.
- 2) Bendsoe, M.P. (1995), *Optimization of Structural Topology, Shape and Material*, Springer-Verlag, Berlin.
- 3) Bendsoe, M.P. and Kikuchi, N. (1988), Generating optimal topologies in structural design using a homogenization method. *Comp. Methods Appl. Mech. Eng.* Vol. 71, pp. 197-224.
- 4) Berke, L. and Khot, N. (1988), Performance characteristics of optimality criteria methods. In G.I.N. Rozvany and B.L. Karihaloo (eds.), *Structural Optimization*, Kluwer Academic Publishers, Dordrecht, pp. 31-37.
- 5) Bratus, A.S. and Seyranian, A.P. (1983), Bimodal solutions in eigenvalue optimization problems. *Appl. Math. mech.*, Vol. 47, pp. 451-457.
- 6) Canfield, R.A. (1993), Designs of frames against buckling using a Rayleigh quotient approximation. *AIAA Journal*, Vol. 31, No. 6, pp. 1143-1149.
- 7) Capey, E.C. (1956), The buckling under longitudinal compression of a simply supported panel that changes in thickness across the width. Paper 235, Aeronautical Research Council, London, U.K.
- 8) Chu, D.N., Xie, Y.M., Hira, A. and Steven, G.P. (1996), Evolutionary structural optimization for problems with stiffness constraints. *Finite Elements in Analysis and Design*, Vol. 21, pp. 239-251.

- 9) Chu, D.N., Xie, Y.M., Hira, A. and Steven, G.P. (1997a), On various aspects of evolutionary structural optimization for problems with stiffness constraints. *Finite Elements in Analysis and Design*, Vol. 27, pp. 197-212.
- 10) Chu, D.N., Xie, Y.M., Hira, A. and Steven, G.P. (1997b), Truss topology by an evolutionary structural optimization method. *Struct. Optim.* (submitted).
- 11) Clausen, T. (1849-1853), "Uber die Form Architektonischer Saulen" *Melanges Mathematiques et Astronomiques*, pp. 279-294.
- 12) Ding, Y. (1989), Multilevel optimization of frames with beams including buckling constraints. *Comput. Struct.* Vol. 32, No. 2, pp. 249-261.
- 13) Folgado, J., Rodrigues, H. and Guedes, J.M. (1995), Layout design of plate reinforcements with a buckling load criterion. In: N. Olhoff and G.I.N. Rozvany (eds.), *Proceedings of the First World Congress of Structural and Multidisciplinary Optimization*, Goslar, Germany, Pergamon, pp. 659-666.
- 14) Haftka R.T., Gurdal Z. and Kamat M.P. (1992), *Elements of Structural Optimization*. 3rd revised edition, Kluwer Academic Publishers, Dordrecht.
- 15) Harik, I.E. and Andrade, M.G. (1989), Stability of plates with step variation in thickness. *Comput. Struct.* Vol. 33, pp. 257-263.
- 16) Harik, I.E. and Liu, X. and Ekambaram, R. (1991), Elastic stability of plates with varying rigidities. *Comput. Struct.* Vol. 38, pp. 161-168.
- 17) Haug, E.J. and Rousselet, B. (1980), Design sensitivity analysis in structural mechanics. II: eigenvalue variations. *J. Struct. Mech.* Vol. 8, pp. 161-186.
- 18) Hjelmstad, K.D. and Pezeshk, S. (1991), Optimal design of frames to resist buckling under multiple load cases. *Journal of Structural Engineering*, ASCE, Vol. 117, No. 3, pp. 914-935.

- 19) Jenkins, W.M. (1991), Structural optimization with the genetic algorithm. *The Structural Engineer*, Vol. 69, NO. 24, pp. 418-422.
- 20) Jog, C.S. and Haber, R.B. (1995), Checkerboard and other spurious modes in solutions to distributed-parameter and topology design problems. In: N. Olhoff and G.I.N. Rozvany (eds.), *Proceedings of the First World Congress of Structural and Multidisciplinary Optimization*, Goslar, Germany, Pergamon, pp. 237-242.
- 21) Kamat, M.P. (1993), *Structural Optimization: Status and Promise*. AIAA, U.S.A.
- 22) Karihaloo, B.L. and Kanagasundaram, S. (1993), Optimum design of plane structural frames by non-linear programming. In G.I.N. Rozvany (ed.), *Optimization of Large Structural Systems*, Vol. II, Netherlands, Kluwer Academic Publishers, pp. 897-926.
- 23) Keller, J.B. (1960), The shape of the strongest column. *Archive of Rational Mechanical Analysis*, Vol. 5, pp. 275-285.
- 24) Khot N.S., Venkayya V.B and Berke L. (1976), Optimum structural design with stability constraints. *International Journal for Numerical Methods in Engineering*, Vol. 10, pp. 1097-1114.
- 25) Kirsch, U. (1992), Approximate reanalysis methods. In M.P. Kamat (ed.), *Structural optimization : Status and Promise*, AIAA, USA, pp. 103-121.
- 26) Kobayashi, H. and Sonoda, K. (1990), Buckling of rectangular plates with tapered thickness. *J. Struct. Engrg.* ASCE Vol. 116, pp. 1278-1289.
- 27) Lagrange, J.L. (1770-1773), "Sur la Figure des Colonnes" *Miscellanea Taurinensia*.  
p. 123
- 28) Levy, R and Ganz, A. (1991), Analysis of optimized plates for buckling. *Comput. Struct.* Vol. 41, pp. 1379-1385.

- 29) Levy, R. (1996), Rayleigh-Ritz optimal design orthotropic plates for buckling. *Struct. Engrg. Mech.* Vol. 4, No. 5, pp. 541-552.
- 30) Levy, R. and Sokolinsky, V. (1995), Prebuckling optimal design of orthotropic variable thickness plates for inplane loading. *Struct. Optim.* Vol. 9, pp. 96-104.
- 31) Lin, C.C. and Liu, I.W. (1989), Optimal design based on optimality criterion for frame structures including buckling constraint. *Computers & Structures*, Vol. 31, No. 4, pp. 535-544.
- 32) Liu, I.W. and Lin, C.C. (1992), Indeterminate approach to the optimization of frame structures with stability constraints. *Comput. Struct.* Vol. 44, No. 5, pp. 973-982.
- 33) Mansfield, E.H. (1973), Inverse methods in two dimensional elasticity. In: E. Becker and G. K. Mikhailov (eds.), *Proc. 13th Cong. of Theoretical and Appl. Mech.*, Springer-Verlag, Berlin, Germany, pp. 229-239.
- 34) Morris, A.J. (1982), *Foundations of Structural Optimization : A Unified Approach*. John Wiley & Sons, New York.
- 35) Murthy, K.N. and Christiano, P. (1973), Design of least weight structures for prescribed buckling load. *AIAA Journal*, Vol. 12, pp. 1773-1775.
- 36) Ng, S.F. and Araar, Y. (1989), Free vibration and buckling analysis of clamped rectangular plates of variable thickness by the Galerkin method. *J. Sound Vib.* Vol. 135, pp. 263-274.
- 37) Olhoff, N. and Rasmussen, S.H. (1977), On single and bimodal optimum buckling loads of clamped columns. *International Journal of Solids and Structures*, Vol. 13, pp. 605-614.

- 38) Pandey, M.D. and Sherbourne, A.N. (1992), Mechanics of shape optimization in plate buckling. *Journal of Engineering Mechanics*, ASCE, Vol. 118, No. 6, pp. 1249-1266.
- 39) Parsons, H.W. (1955), The buckling under compression of a thin rectangular plate of variable thickness. Paper 17231, Struct. 1759, Aeronautical Research Council, London, U.K.
- 40) Pezeshk, S. and Hjelmstad, K.D. (1991), Optimal design of planar frames based on stability criterion. *Journal of Structural Engineering*, ASCE, Vol. 117, No. 3, pp. 896-913.
- 41) Prager W. and Taylor J.E. (1968), Problems of optimal structural designs. *Journal of Applied Mechanics*. Vol. 35, pp. 602-606.
- 42) Rozvany, G.I.N. (1989), *Structural Design Via Optimality Criteria*, Kluwer Academic Publishers, Dordrecht.
- 43) Rozvany, G.I.N. and Karihaloo, B.L. (1988), *Structural Optimization*, Kluwer Academic Publishers, Dordrecht.
- 44) Seyranian, A.P. (1987), Multiple eigenvalues in optimization problems. *Appl. Math. Mech.*, Vol. 51, pp. 272-275.
- 45) Seyranian, A.P., Lund, E. and Olhoff, N. (1994), Multiple eigenvalues in structural optimization problems. *Struct. Optim.* Vol. 8, pp. 207-227.
- 46) Simites, G.J., Kamat, M.P. and Smith, C.V. (1973), Strongest column by the finite element displacement method. *AIAA Journal*, Vol. 11, No. 9, pp. 1231-1232.
- 47) Spillers, W.R. and Levy, R. (1990), Optimal design for plate buckling. *Journal of Structural Engineering*, ASCE, Vol. 116, No. 3, pp. 850-858.

- 48) Szyszkowski, W. (1992), Multimodal optimality criterion for maximum stability. *Int. J. Non-Linear Mech.* Vol. 27, pp. 623-633.
- 49) Szyszkowski, W. and Watson, L.G. (1988), Optimization of the buckling load of columns and frames. *Engineering Structures*, Vol. 10, pp. 249-256.
- 50) Szyszkowski, W., Watson, L.G. and Fietkiewicz, B. (1989), Bimodal optimization of frames for maximum stability. *Comput. Struct.* Vol. 32, No. 5, pp. 1093-1104.
- 51) Tada, Y. and Wang, L. (1995), Reinvestigation on optimization of clamped-clamped columns and symmetry of corresponding eigenfunctions. *JSME Int. J.*, Vol. 38, No. 1, pp. 38-43.
- 52) Tadjbakhsh, I. and Keller, J.B. (1962), Strongest columns and isoperimetric inequalities for eigenvalues. *Journal of Applied Mechanics*, Vol. 9, pp. 159-164.
- 53) Taylor, J.E. (1967), The strongest column : An energy approach. *Journal of Applied Mechanics*. Vol. 34, pp. 486-487.
- 54) Taylor, J.E. and Prager, W. (1968), Problems of optimal structural design. *Journal of Applied Mechanics*. Vol. 35, pp. 102-106.
- 55) Trahair, N.S. and Booker, J.R. (1970), Optimum elastic columns. *International Journal of Mechanical Science*. Vol. 12, pp. 973-983.
- 56) Turner, H.K and Plaut, R.H. (1981), Optimal design for stability under multiple loads. *Journal of Engineering Mechanics*, ASCE, Vol. 106, No. 6, pp. 1365-1382.
- 57) Vanderplaats, G.N. (1993), Thirty years of modern structural optimization. *Advances in Engineering Software*, Vol. 16, pp. 81-88.
- 58) Vanderplaats, G.N. and Salajegheh, E. (1987), New approximation method for stress constraints in structural synthesis. *AIAA Journal*, Vol. 27, No. 3, pp. 352-360.

- 59) Venkayya, V.B., Khot, N.S. and Berke, L. (1973), Application of optimality criteria approaches to automated design of large practical structures. Presented at the AGARD Second Symposium on Structural Optimization, Milan, Italy.
- 60) Wittrick, W.H. and Ellen, C.H. (1962), Buckling of tapered rectangular plates in compression. *Aero. Quart.* Vol.13, pp. 308-326.
- 61) Xie, Y.M. and Steven, G.P. (1993), A simple evolutionary procedure for structural optimization. *Comput. Struct.* Vol. 49, No. 5, pp. 885-896.
- 62) Xie, Y.M. and Steven, G.P. (1994a), Optimal design of multiple load case structures using an evolutionary procedure. *Engineering Computations*, Vol. 11, pp. 295-302.
- 63) Xie, Y.M. and Steven, G.P. (1994b), A simple approach to structural frequency optimization. *Comput. Struct.* Vol. 53, No. 6, pp. 1487-1491.
- 64) Xie, Y.M. and Steven, G.P. (1996), Evolutionary structural optimization for dynamic problems. *Comput. Struct.* Vol. 58, pp. 1067-1073.
- 65) Xie, Y.M. and Steven, G.P. (1997), *Evolutionary Structural Optimization*, Springer-Verlag, Berlin.
- 66) Zhao, C., Steven, G.P. and Xie, Y.M. (1996a), Evolutionary natural frequency optimization of thin plate bending vibration problems. *Struct. Optim.* Vol. 11, pp. 244-251.
- 67) Zhao, C., Steven, G.P. and Xie, Y.M. (1996b), General evolutionary path for fundamental natural frequencies of structural vibration problems: towards optimum from below. *Structural Engineering and Mechanics*, Vol. 4, No. 5, pp. 513-527.



